

MMS Project
Long-Term Integrity of Deepwater Cement
Systems Under Stress/Compaction Conditions

Summary Report

Issued September 3, 2004

Fred Sabins
fsabins@csi-tech.net

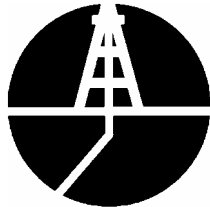




Table of Contents

Objectives.....	1
Observations and Conclusions	1
Total Energy Scale-Up Method	3
Analysis Methodology	4
Spreadsheet Operation and Scaleup	5
Example Analysis	6
Appendix I	10
Appendix II	11
Appendix III	12
Appendix IV	13
Appendix V	14
Appendix VI	15



Objectives

The overall objective of this project is to determine the properties that affect cement's capability to produce a fluid-tight seal in an annulus. The project primarily focused on deepwater applications, but general applications were also examined. The research conducted focused on the measurement and correlation of cement's mechanical properties to the cement's performance. Also, research was conducted to determine which laboratory methods should be used to establish the cement's key properties.

Finally, a method of quantifying laboratory test results and scaling them to field conditions was developed. This method, contained in a spread sheet, can be used to estimate cement seal performance in actual well operations.

This report includes a summary of all results obtained throughout the project as well as copies of all previous reports.

Observations and Conclusions

The following conclusions and observations are based on the results of this project:

1. A literature review was conducted and gave the following points
 - a. Gas leaks in wells have also been attributed to cement shrinkage, which creates circumferential fractures that become paths for gas flow.
 - b. Expanding cement can lead to a microannulus between the casing and cement when it is placed in soft formations.
 - c. Other experiments have shown that pressure testing can cause a loss in cement integrity and create a path for gas flow.
2. Results of numerical modeling of stresses and strains indicated that significant strain resulted from stress applied in the soft-formation case. Material properties of the cement become much more significant as formation strength becomes less. With strong formation backing, stress in the cemented annulus is greatly reduced.
3. New testing methods for measuring shear bond strengths and shrinkage were developed.
4. Shear bond strengths are higher for samples cured in a high restraint environment (pipe-in-pipe) compared to lower shear bond strength values for samples cured in a low restraint environment (pipe-in-soft).
5. Both temperature and pressure cycling of cement samples are detrimental to shear bond strengths in both low and high restraint simulations.



6. Cement formulations conditioned in high restraint simulations resulted in higher shear bond strengths and withheld annular seals more successfully as compared to formulations conditioned in low restraint simulations.
7. Shear bond testing was repeated for soft, intermediate, and hard formations with the four main cement systems and a modified testing procedure. All results indicated that bond is degraded extensively both by pressure and temperature cycling.
8. Shrinkage of a typical class A neat design occurs with a measured volume decrease of 6.8%.
9. Hydrostatic cycling of cement samples deforms the cement over time.
10. Great improvements in tensile strengths were observed with the addition of carbon fibers
11. A significant increase in compressive strength with increasing confining stress in lower-strength compositions was observed.
12. Anelastic strain testing, a variation of hydrostatic testing, was designed to allow a more accurate evaluation of permanent strain resulting from stressing different test compositions. Anelastic strain determines strain and cyclic loading effects under similar conditions with respect to each composition's ultimate strength. Based on the systems tested, indications that each specimen would undergo additional anelastic strains with increase cycles were observed. Comparison of the data sets indicates larger strains for low density compositions than for normal density cements. Results of strain versus time indicate that both foam and bead cement exhibit larger increasing strain with time under stress. Foam cement's level of strain with increasing stress was slightly more than bead cement. Cyclic strain comparison of Bead, Foam, Neat and Latex systems indicate significant increases in cycling effect for foam compared to the other three compositions
13. A new test method for testing cement column seals, 8-foot Column Seal Testing, was developed. A number of systems were tested throughout the project to compare a cement's capacity to isolate gas pressure across an enclosed column.
14. TXI Lightweight cement performed well in the 8-foot Column Seal model testing.
15. A test method for determining cement's capability to maintain its seal under downhole conditions, mechanical integrity testing, was successfully developed. Low, intermediate, and high restraints simulate the soft, intermediate, and hard formations encountered in a well.
16. Thermal cycling appears to negatively affect foam cement's sealing ability to a greater degree than pressure cycling.



17. A modified annular seal testing method was employed on all formations and the failures of annular seals was achieved in all formations by increasing cycling until achieving flow. The general trend was that hard formations needed the greatest amount of cycling to achieve failure. Intermediate formations required less cycling to achieve failure and soft formations required the least amount of cycling to achieve failure.
18. With only two exceptions, the amount of energy (pressure or temperature) required to induce cement sheath failure increases with the competence of the formation. The stronger the formation, the more support it lends to the cement sheath so that it can withstand the imposed loads.
19. Bead cements performed very well in all the testing, as evidenced in the cases of weaker formations. The stronger encapsulation of the air pocket in bead vs foam may mean that bead cements will withstand heat better than foam systems. In the case of pressure energy, foam also performed better than Type 1 and Latex slurries with weaker formation support. This may be due to better anelastic behavior, in which the cement is more ductile than the higher-strength systems.
20. In all cases, the amount of temperature energy required to initiate failure is much lower than the pressure energy to failure. This may be due the destructive effects of matrix water expansion with temperature.
21. Analysis of all annular seal data via total energy calculations produced an acceptable method of quantifying the test results.
22. The analysis shows promising trends in dimensionless analysis of cement sheath loading, but is based on very few data points. The same correlation described here and presented in the spreadsheet is valid for energy input in the form of temperature, but more precise measurements and additional data points are required for confirmation. Additional cement and formation types will also verify and extend the analysis to a broader range of real-well conditions.
23. More work is required to understand the energy absorption of the various wellbore components, so that the energy applied to the slurry itself is isolated and understood. As a qualitative example, heavier wall internal pipe will absorb more energy, thereby reducing the energy input to the slurry. More testing will allow in-depth understanding of energy distribution in the wellbore.

Total Energy Scale-Up Method

The data from this project were used to create a method of estimating a particular cement composition's ability to maintain annular seal under conditions of actual well operation. This method of scale-up from laboratory mechanical property and performance data to



estimation of full scale performance is presented in spreadsheet MMS Ph 1 Energy Analysis.xls. The results of the Annular Seal testing were analyzed by utilizing an energy approach, in which the energy applied to the pipe / cement / formation system constitutes the mechanism of failure. Resisting the applied energy are the mechanical properties of pipe, cement, and formation, operating as a system. This methodology is essentially a macro approach, intended to eventually understand the relative effects of both production heat up as well as pressure application on the integrity of the cement sheath. By analyzing the data in terms of energy applied to the system verses the cement’s mechanical properties and ability to resist seal failure, disparate forms of energy application and their effects on cement seal can be correlated and understood.

Analysis Methodology

Test methodology is fully explained in the various MMS Reports previously published and contained herein as appendices. For the purpose of analysis, two dimensionless variables are defined to quantify the energy applied to the system as well as how the system resists the energy input. When plotted against each other, calculated laboratory Energy Application factor (E1A) and Energy Resistance factor (E1R) correlate to a power equation ($E1R = X * E1A^Y$). The values constitute a failure curve; E1A:E1R values below the curve are more likely to fail due to the energy application, and values above the curve are less likely to fail. A point is also plotted for a field condition to show the relationship between the field condition and the lab-generated cement failure.

Discussion and rationale for the dimensionless variables E1A and E1R are as follows. It is important to note that these factors were generated with a very limited number of data points. Further refinement is possible in the future as Phase 2 of this project progresses and more data are generated.

$$E1A = \frac{\text{Energy} * \text{Hole Radius}}{\text{Mass cmt} * \text{Pipe Steel Area}}$$

E1A is a measure of the intensity of the loading on the cement sheath. The factor is directly proportional to the Energy applied to the system as well as the Hole Radius, so those variables appear in the numerator. The loading intensity is inversely proportional to the mass of the cement as well as the Cross-Sectional area of the steel in the pipe. The Hole Radius seeks to quantify the effect of larger-diameter wells in terms of the increased loading associated with the pressure inside the pipe. On the other hand, some of the energy is consumed by the steel pipe before it can transfer load to the cement, so the amount of steel is located in the denominator.

$$E1R = \frac{Ff * \text{Volume cmt} * \text{Tensile Strength cmt}}{\text{Energy} * \text{Young's Modulus cmt} * \text{Anelastic Strain}}$$

E1R is a measurement of the ability of the cement and formation system to resist the applied energy. Terms in the variable include:



- Ff: Formation Factor, defined by Formation Young's Modulus / 2,000,000. This is a measure of the competence of the formation. The harder the formation, the better "backup" it lends to the cement sheath, and the less likely the cement is to fail under applied energy.
- Cement Characteristics:
 - Volume: As the volume of cement is increased, the ability of the sheath to resist failure increases.
 - Tensile Strength: The higher the tensile strength, the more it is able to resist hoop stresses imposed by internal pipe loading
 - Young's Modulus: The more brittle the cement (higher Young's Modulus), the more likely it is to crack under internal pipe loading. For this reason, this factor is contained in the denominator.
 - Anelastic Strain: This factor constitutes permanent deformation under cycling stress well below ultimate strength. The slope of the linear fit is used as opposed to a discrete value, because the Anelastic Strain value varies with the number of cycles. The factor is in the denominator because a zero slope would be consistent with a material that does not exhibit this behavior, such as steel. The higher the slope of the linear regression line, the less the ability of the cement to resist repeated load applications.
- Energy: Energy applied to the system is located in the denominator because higher energy levels decrease the ability of the system to remain intact over time

For the lab data, the correlation between E1A and E1R, using the energy at which failure of the cement sheath is detected by the presence of gas flow, is:

$$E1R = 8.02 * 10^6 * E1A^{2.1304}$$

This line constitutes the failure line, because it was created by E1A and E1R pairs generated at the point of failure. E1A and E1R points for a given situation that fall below the line indicate a likely failure of the cement sheath; points above the line indicate cement sheath integrity. As the number of data points that were generated is relatively low, the line does not represent an absolute failure / non-failure demarcation. Confidence increases with distance from the line, either above or below.

Spreadsheet Operation and Scaleup

The spreadsheet allows the user to input actual well conditions (hole size, pipe OD and ID, and cemented interval), as well as cement and formation qualitative identifiers. The cements tested included Type 1 and Latex slurries mixed at 15.6 lb/gal, and Bead and Foam slurries mixed at 12.0 lb/gal. Formation types include Hard (represented in the test by steel pipe, YM > 2,000,000 psi), Intermediate (represented by PVC pipe, YM approximately 500,000 psi), and Soft (unconsolidated sand pack, YM approx 200 psi). Additional user inputs include a pressure application schedule, in which the user selects



the number of times that the well is subjected to various levels of internal pressure.

All user-input cells are denoted by **Bold Red** font, and only those cells may be altered. The spreadsheet calculates E1A and E1B for the field condition, and plots the single field point on a graph with the curve fit lab failure line.

Example Analysis

The following example presents data input, calculation results, and presentations from the MMS Annular Seal Energy Analysis Spreadsheet. All members have receives the operational spreadsheet under separate cover. Background calculation data are included after the plot of E1R vs. E1A.

MMS Annular Seal Energy Analysis Pressure Analysis

Spreadsheet Annotation:

- 1) Change only **Bold Red** cells on Input_Output Tab
- 2) Spreadsheet estimates field scale cement annular seal failure
 - by comparing calculated energy application and energy resistance factors with laboratory data.

Input Data	Field Scale	Lab Data	
<i>Geometry Data</i>			
Hole Dia	10.00	3.000	in
Pipe OD	8.50	1.063	in
Pipe ID	7.80	0.450	in
Cemented Interval	1,000	0.333	ft
<i>Cement Data</i>			
Cement	Type 1		
Formation	Hard		
Density	15.6	15.6	lb/gal
Tensile Strength	394	394	psi
Young's Modulus	81,600	81,600	psi
Anelastic Strain slope	4.95E-08	4.95E-08	
<i>Formation Data</i>			
Young's Modulus	2,000,000	2,000,000	psi
<i>Calculated Data</i>			
Hole Radius	5.000	1.500	in
Pipe OR	4.250	0.531	in
Pipe IR	3.900	0.225	in
Pipe Steel CS	8.961	0.728	sq in



Pipe Internal CS Area	47.784	0.159	sq in
Pipe Internal Volume	573,403.491	0.636	cu in
Formation Factor	1.000	1.000	
Annular Radius	0.750	0.969	in
Annular CS Area	21.795	6.182	sq in
Annular (Cement) Volume	261,537.59	24.73	cu in
Cement Mass	17,662.28	1.67	lbm

Failure Energy, Lab		222,660	in-lb
E1A Lab		275	
E1R Lab		1,083.29	

Applied Energy, Field	2.52E+10		in-lb
E1A Field	797.0		
E1R Field	101.12		

Pressure Loading Schedule

Pressure	Applications	Applied Energy in - lbs
1,000	-	0.00E+00
2,000	-	0.00E+00
3,000	-	0.00E+00
4,000	-	0.00E+00
5,000	4	1.15E+10
6,000	4	1.38E+10
7,000	-	0.00E+00
8,000	-	0.00E+00
9,000	-	0.00E+00
10,000	-	0.00E+00

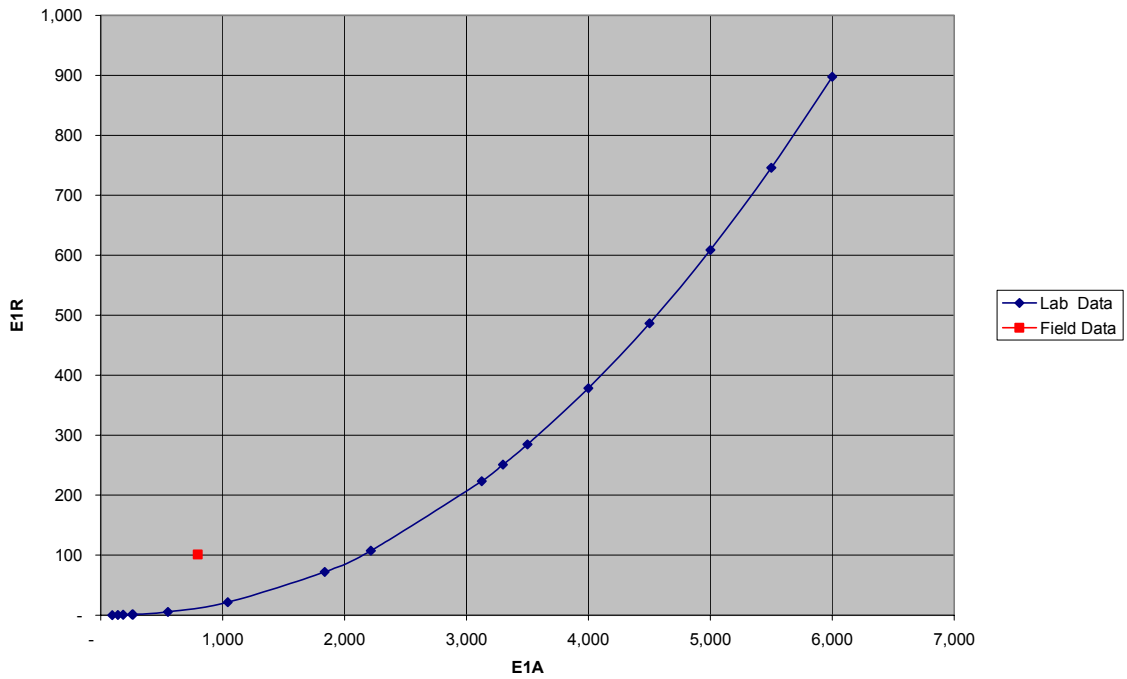


Output Data

Cement Type Type 1

Formation Type Hard

E1R vs E1A



Cement Properties				
	Ten Str	Tens YM	AS Slope	AS Intercept
Bead			1.46E-07	3.53E-08
	400	60,000		
Foam			1.08E-07	3.94E-08
	253	32,300		
Latex			6.44E-08	6.28E-08
	539	53,200		
Type 1			4.95E-08	7.85E-09
	394	81,600		



<i>Formation Properties</i>		
	<i>Tens YM</i>	<i>Form Factor</i>
Hard	2,000,000	1.0000
Intermediate	500,000	0.2500
Soft	200	0.0001

<i>Lab Data</i>				
<i>Energy at Failure, in-lbs</i>				
	Hard	Intermediate	Soft	Density
Bead	162,224	28,628	13,360	12
Foam	95,426	54,075	9,543	12
Latex	149,501	17,813	6,362	15.6
Type 1	222,660	17,813	9,543	15.6

<i>Lab Data Failure Control Curve</i>		
Multiplier	8.02E-06	
Power	2.1304	
E1A calc	E1R Fit	
94	0.13	
141	0.31	
184	0.53	
257	1.09	
264	1.16	
264	1.16	
551	5.55	
1,041	21.52	
1,838	72.18	
2,215	107.41	
3,124	223.55	
3,299	250.97	
3500	284.75	
4000	378.45	
4500	486.38	
5000	608.78	
5500	745.84	
6000	897.73	
797	101	<-- Fld Data Pt



CSI Technologies

Appendix I

Report 1

MMS Project

Long-Term Integrity of Deepwater Cement Systems Under Stress/Compaction Conditions

Report 1

Issued April 8, 2002



CEMENTING SOLUTIONS, INC.

Table of Contents

Introduction	3
Thickening-Time Test.....	3
Free-Fluid Test.....	3
Compressive Strength.....	3
Tensile Strength and Tensile Young’s Modulus	4
Young’s Modulus	5
Shear Bond Strength.....	11
Shrinkage Testing	14
Literature Review	16
Participants’ Responses	17
Future Testing	18
References	22

Introduction

This project is conducting research to determine the properties that affect cement's capability to seal fluids and to develop correlations between cement properties and sealing performance under downhole conditions. Testing to this point has been performed on neat Class A cement. The testing has helped to refine and confirm the test procedures that will be used for the remainder of the project.

Thickening-Time Test

Following the procedures set forth in API RP 10B¹, a thickening-time test was performed on the neat Class A slurry. The test conditions started at 80°F and 600 psi, and were ramped to 65°F and 5,300 psi in 48 minutes. Data from the thickening time test can be seen in **Table 1**.

Table 1—Results from Thickening-Time Test

Time (hr:min)	Consistency (Bc)
3:05	40
3:58	70
4:38	100

Free-Fluid Test

The free-fluid testing that was performed on the Class A slurry came from API RP 10B¹. The free-fluid procedure, also referred to as operating free water, uses a graduated cylinder that is oriented vertically. The free fluid for the slurry maintained at 65°F was measured to be 0.80% (by volume).

Compressive Strength

Table 2 presents compressive strength data for neat Class A cement. The compressive strengths were derived using the 2-in. cube crush method specified in API RP 10B¹. The samples were cured in an atmospheric water bath at 45°F. The reported values were taken from the average of three samples.

Table 2—Crush Compressive Strength

Cure Time (days)	Crush Compressive Strength (psi)
7	2,735
10	4,065
12	4,385
14	4,035
17	4,470

Tensile Strength and Tensile Young's Modulus

Mechanical properties of the neat Class A cement were tested. Tensile strength was tested using ASTM C496² (Standard Test Method for Splitting Tensile Strength of Cylindrical Concrete Specimens). For this testing, the specimen dimensions were 1.5 in. diameter by 1 in. long. **Figure 1** shows a general schematic of how each specimen is oriented on its side when tested. The force was applied by constant displacement of the bottom plate at a rate of 1 mm every 10 minutes. Change in the specimen diameter can be calculated from the test plate displacement. The (compressive) strength of the specimen during the test can be graphed along with the diametric strain (change in diameter/original diameter) to generate the tensile Young's modulus.

Figure 1—Sample Orientation for ASTM C496-90 Testing

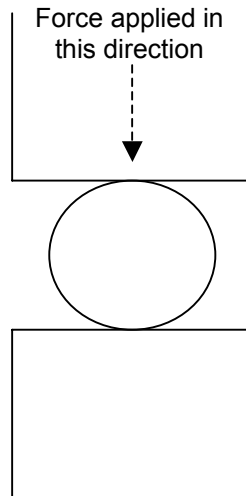


Table 3 shows the 14-day tensile strength and tensile Young's modulus of the cement. The samples were cured at atmospheric pressure in a water bath maintained at 45°F. The samples were cured under confined conditions (in the mold for the entire 14 days) and unconfined conditions (removed from mold after 24 hours and allowed to cure the remainder of the time outside of the mold).

Table 3—Splitting Tensile Strength and Tensile Young’s Modulus Data

Curing Condition	Splitting Tensile Strength (psi)				Tensile Young's Modulus (10^4 psi)			
	Sample			Average	Sample			Average
	1	2	3		1	2	3	
Confined	409	406	368	394	20.43	19.20	17.83	19.15
Unconfined	163	278	198	213	7.88	8.35	8.25	8.16

For this project, rock mechanics personnel from Westport and Conoco will be discussing incorporation of a test method³ from the International Society for Rock Mechanics (ISRM). The ISRM method calls for testing with a curved adapter that gives more contact area between the testing surface and the test specimen and results in less variation in results.

Some of the variation in the data could be attributed to settling of the cement slurry. The samples were cured in molds that were 5 in. long, and the individual 1-in. samples were then cut from the 5-in. specimen. For future testing, to avoid potential slurry settling, the slurry will be preconditioned for 20 minutes in an atmospheric consistometer and then be poured into individual, shorter molds so only one individual test sample will come from each mold.

Young’s Modulus

Traditional Young’s modulus testing was also performed using ASTM C469⁴, Standard Test Method for Static Modulus of Elasticity (Young’s Modulus) and Poisson’s Ratio of Concrete in Compression. Young’s modulus and effective compressive-strength were tested. The effective compressive strength is the equivalent unconfined compressive strength, which eliminates the effect of confining pressure. The diameter of each test specimen was 1.5 in., and the length was 3.0 in.

The following procedure is used for the Young’s modulus testing.

1. Each sample is inspected for cracks and defects.
2. The sample is cut to a length of 3.0 in.
3. The sample’s end surfaces are then ground to get a flat, polished surface with perpendicular ends.
4. The sample’s physical dimensions (length, diameter, weight) are measured.
5. The sample is placed in a Viton jacket.
6. The sample is mounted in the Young’s modulus testing apparatus.
7. The sample is brought to 100-psi confining pressure and axial pressure. The sample is allowed to stand for 15 to 30 min until stress and strain are at equilibrium. (In case of an unconfined test, only axial load is applied.)
8. The axial and confining stress are then increased at a rate of 25 to 50 psi/min to bring the sample to the desired confining stress condition. The sample is allowed to stand until stress and strain reach equilibrium.
9. The sample is subjected to a constant strain rate of 2.5 mm/hr.

10. During the test, the pore-lines on the end-cups of the piston are open to atmosphere to prevent pore-pressure buildup.
11. After the sample fails, the system is brought back to the atmospheric stress condition. The sample is removed from the cell and stored.

Samples that were cured in an unconfined condition (removed from mold after 24 hours and allowed to cure the remainder of the time outside of the mold) were tested at confining pressures of 0; 1,500; and 5,000 psi. Data from these tests are presented in **Table 4**. Testing at 0 confining pressure was also performed on samples that were cured in a confined condition (in the mold for the entire 14 days). Results from testing on the confined samples are presented in **Table 5**. All samples were cured for 14 days at atmospheric pressure in a water bath maintained at 45°F.

Table 4—Young’s modulus data for samples cured in an unconfined condition

Confining Pressure (psi)	Young's Modulus (10^5 psi)	Effective Compressive Strength (psi)
0	8.13	4,118
	17.37	8,125
	15.99	9,166
1,500	12.39	7,912
	8.23	7,526
	12.59	9,046
5,000	8.22	8,553
	9.31	9,133
	9.67	9,007

Table 5—Young’s modulus data for samples cured in a confined condition

Confining Pressure (psi)	Young's Modulus (10^5 psi)	Effective Compressive Strength (psi)
0	15.80	7,330
	17.50	6,823
	9.35	4,000

Figures 2 through 5 show Young’s modulus plots for the different curing and testing conditions presented above. Young’s modulus is the slope of the stress-strain curve. The highlighted portion of each curve shows the most linear segment where the Young’s modulus is derived.

Figure 2—Young’s modulus testing for samples cured in an unconfined condition and tested at a zero confining pressure

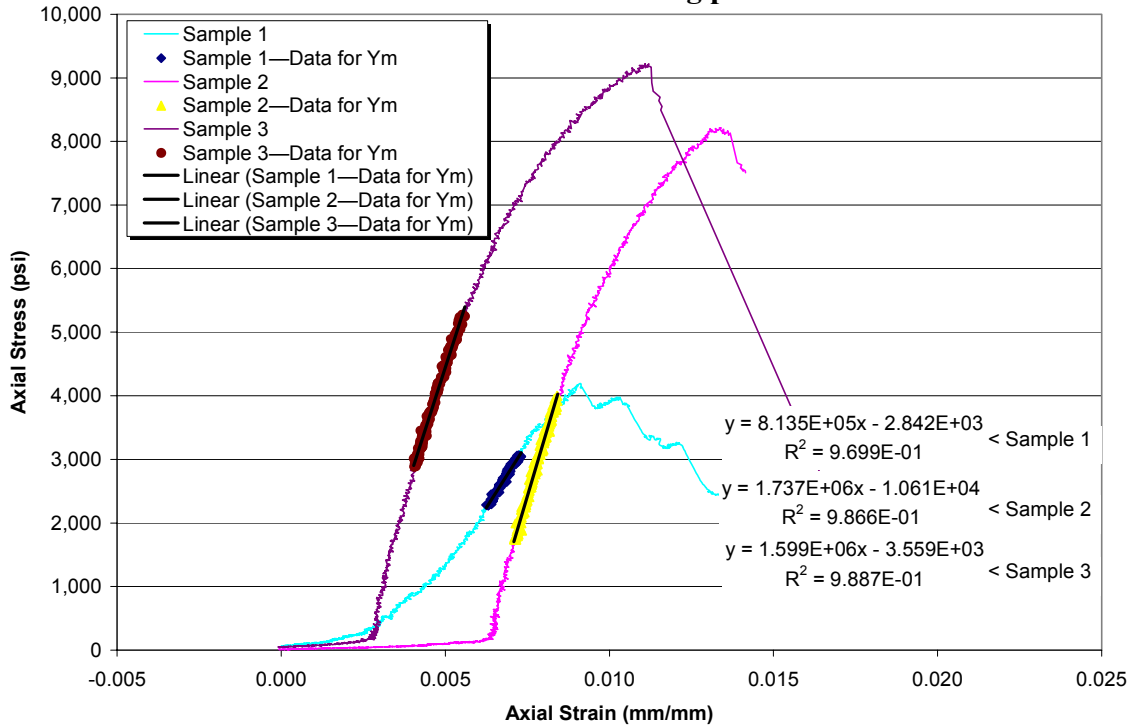


Figure 3—Young’s modulus testing for samples cured in an unconfined condition and tested at a confining pressure of 1,500 psi

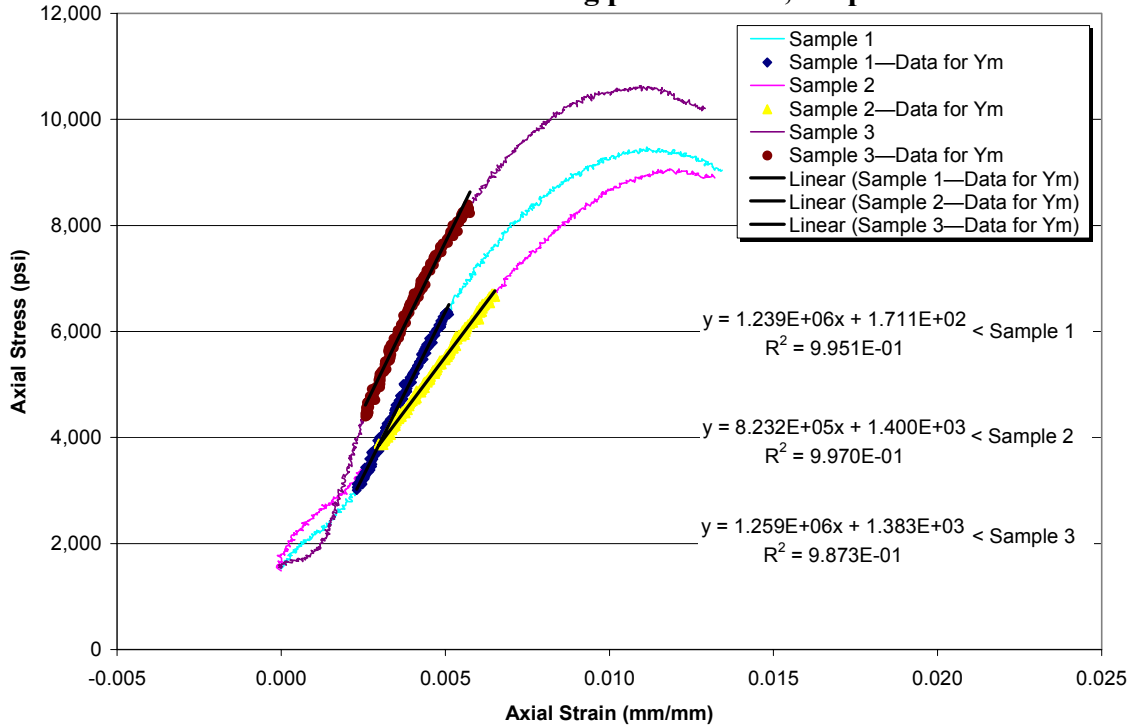


Figure 4—Young’s modulus testing for samples cured in an unconfined condition and tested at a confining pressure of 5,000 psi

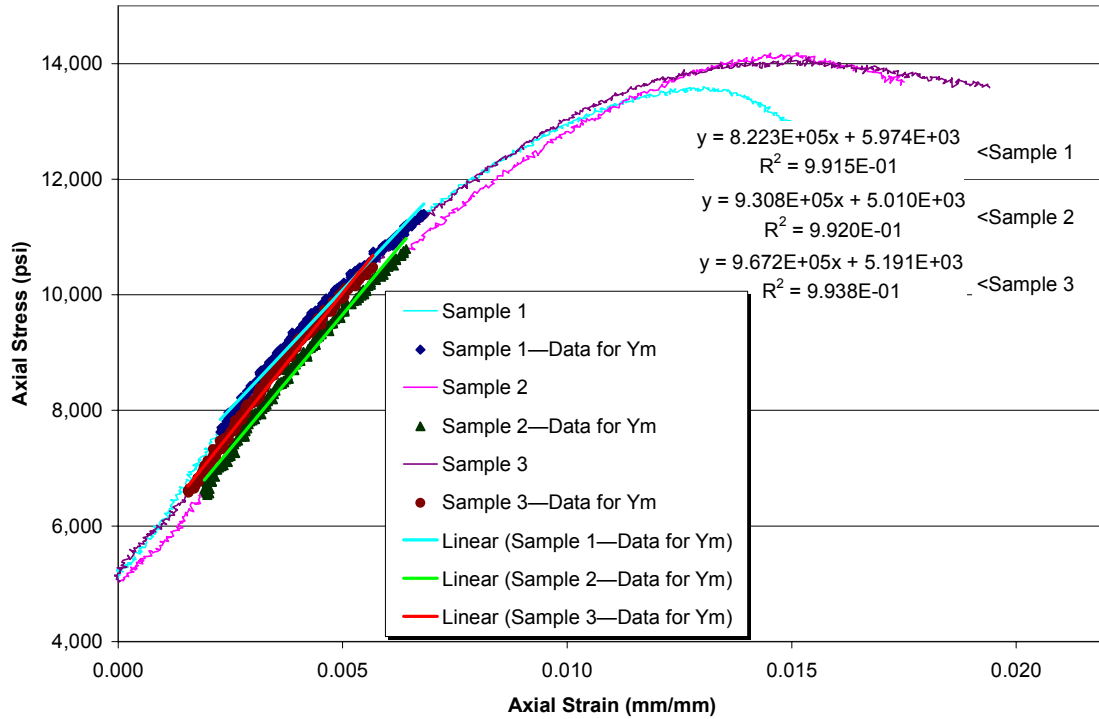
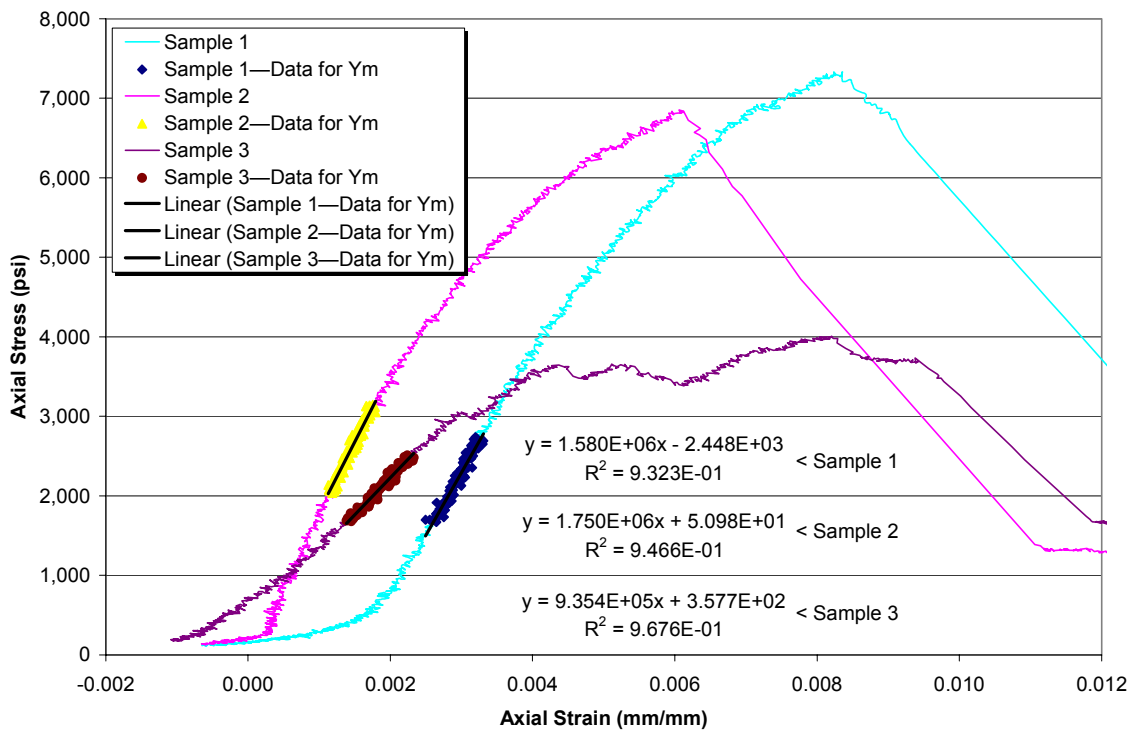


Figure 5—Young’s modulus testing for samples cured in a confined condition and tested at zero confining pressure



Tests were also conducted to determine the effect that temperature cycling has on Young's modulus. The temperature cycling procedure was designed to simulate temperature conditions that might be encountered during production of a well. The samples are first cured for 14 days in a 45°F water bath at atmospheric pressure. They are then subjected to five days of temperature cycling. During each of these five days of temperature cycling, the cured samples are cycled as follows.

1. Samples are removed from 45°F water bath and placed in 96°F water bath for one hour.
2. Samples are placed in 180°F water bath for four hours.
3. Samples are placed in 96°F water bath for one hour.
4. Samples are placed back in 45°F water bath.

Table 6 presents samples that were cured at 45°F in an unconfined condition (removed from mold after one day and allowed to cure the remaining 13 days outside of the mold) and that were then temperature-cycled for five days. **Figures 6** and **7** graphically present the Young's modulus data.

Table 6— Young's modulus data for samples cured in an unconfined condition and then temperature-cycled for five days

Confining Pressure (psi)	Young's Modulus (10 ⁵ psi)	Effective Compressive Strength (psi)
0	11.59	5,014
	5.48	4,084
	12.45	5,243
1,500	8.92	6,975
	10.48	6,642
	11.09	7,022

Figure 6—Young’s modulus testing for samples cured in an unconfined condition and then temperature-cycled for five days and tested at zero confining pressure

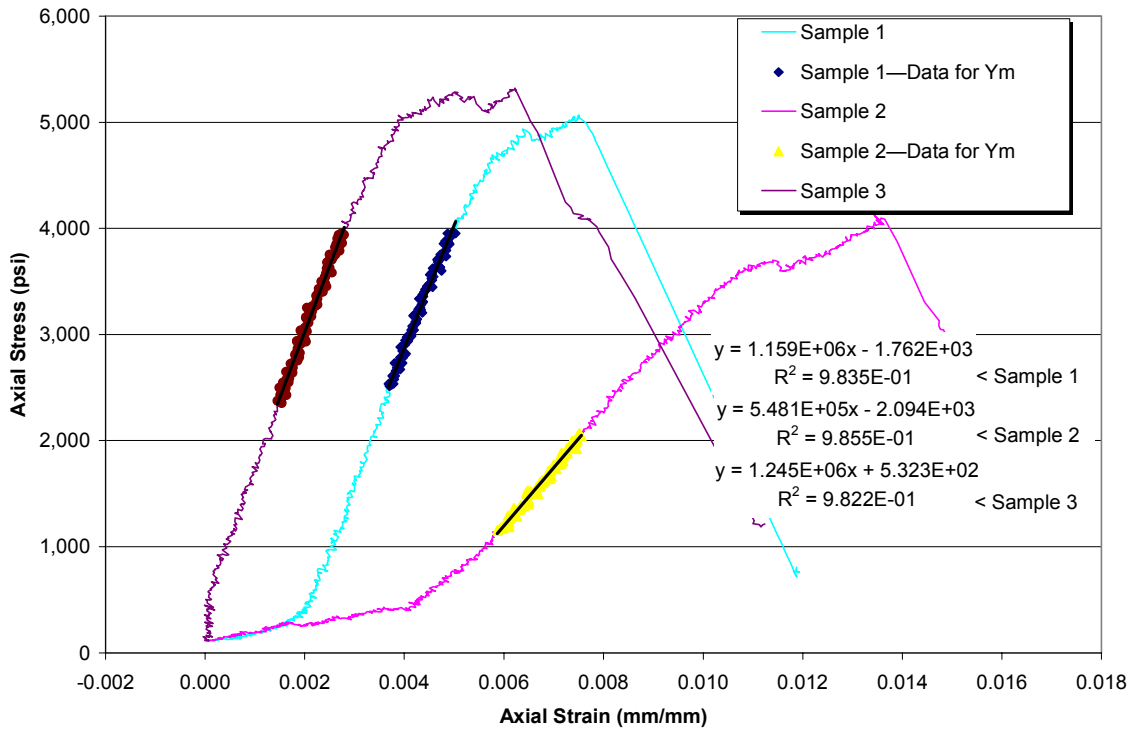
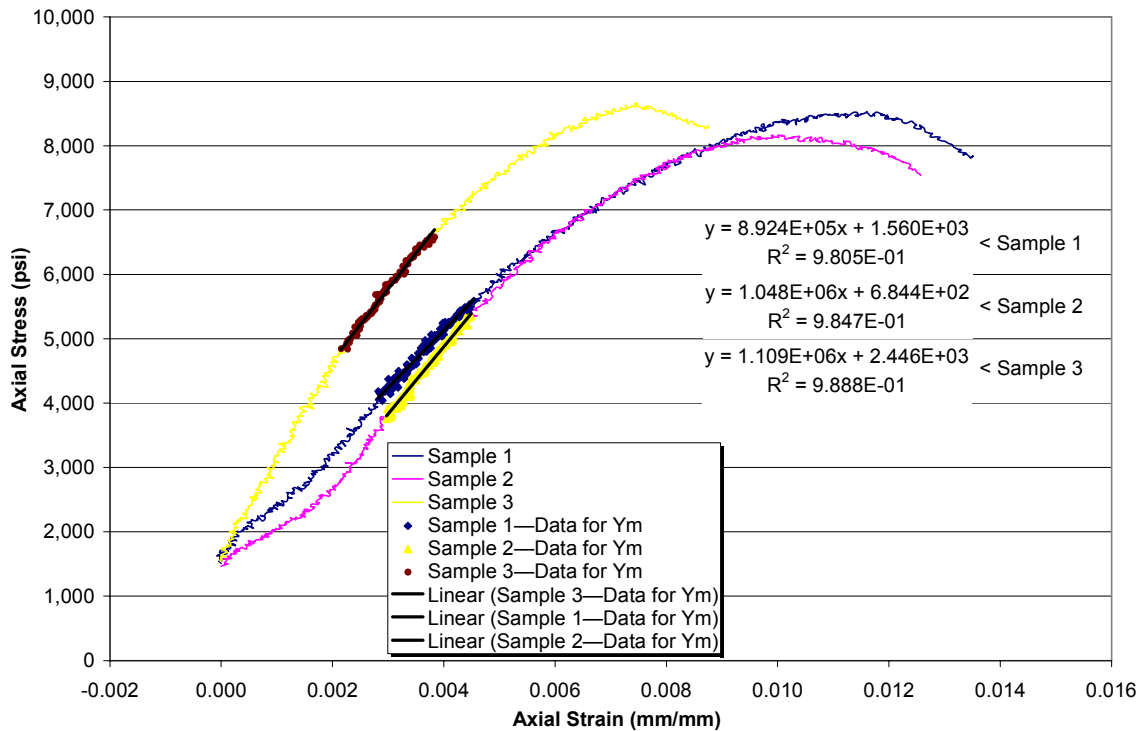


Figure 7—Young’s modulus testing for samples cured in an unconfined condition and then temperature-cycled for five days and tested at a confining pressure of 1,500 psi



Some of the variation in the Young's modulus data could be attributed to settling of the cement slurry. The samples were cured in molds that were 10 in. long, and the individual 3-in. samples were then cut from the 10-in. specimens. For future testing, to avoid potential slurry settling, the slurry will be preconditioned for 20 minutes in an atmospheric consistometer and then poured into individual, shorter molds so only one individual test sample will come from each mold.

For future Young's modulus testing, it has been recommended to maintain a pore pressure that is 80% of the testing (final) confining load. The pore pressure will be ramped up at the same rate as the confining load and the pore pressure will be held and maintained once it reaches 80% of the testing confining load. This is believed to be a better simulation of the conditions that are experienced downhole.

Shear Bond Strength

Testing was also performed to evaluate shear bond strength of neat Class A cement. These studies investigate the effect that restraining force has on shear bond. Samples were cured in a pipe-in-pipe configuration (**Figure 8**) and in a pipe-in-soft configuration (**Figure 9**). The pipe-in-pipe configuration consists of a sandblasted internal pipe with an outer diameter (OD) of $1 \frac{1}{16}$ in. and a sandblasted external pipe with an internal diameter (ID) of 3 in. and lengths of 6 in. A contoured base and top are used to center the internal pipe within the external pipe. The base extends into the annulus 1 in. and cement fills the annulus to a length of 4 in. The top 1 in. of annulus contains water.

For the pipe-in-soft shear bonds, plastisol is used to allow the cement to cure in a less-rigid, lower-restraint environment. Plastisol is a mixture of a resin and a plasticizer that creates a soft, flexible substance. This particular plastisol blend (PolyOne's Denflex PX-10510-A) creates a substance with a hardness of 40 duro.

The pipe-in-soft configuration contains a sandblasted external pipe with an ID of 4 in. A molded plastisol sleeve with an ID of 3.0 in. and uniform thickness of 0.5 in. fits inside this external pipe. With the aid of a contoured base and top, a sandblasted internal pipe with an OD of $1 \frac{1}{16}$ in. is then centered within the plastisol sleeve. The pipes and sleeve are 6 in. long. The base extends into the annulus 1 in. and cement fills the annulus to a length of 4 in. between the plastisol sleeve and the inner $1 \frac{1}{16}$ -in. pipe. The top inch of annulus is filled with water.

Figure 8—Cross-Section of Pipe-in-Pipe Configuration for Shear Bond Tests

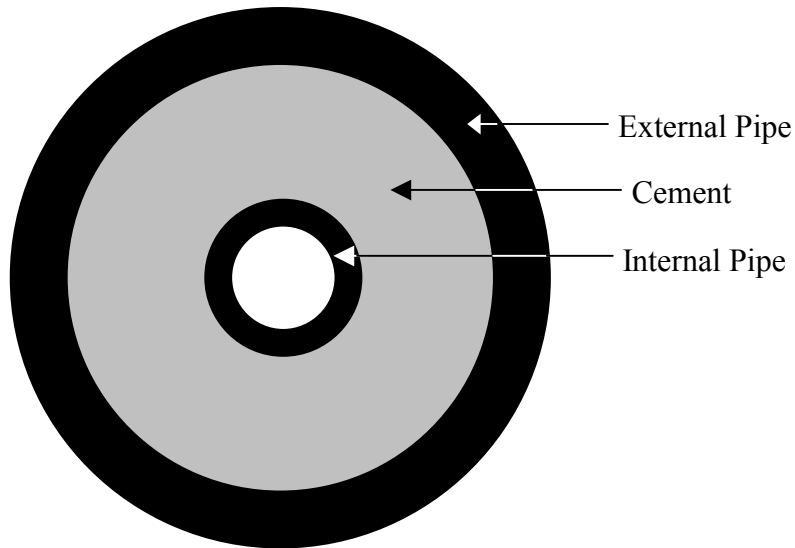
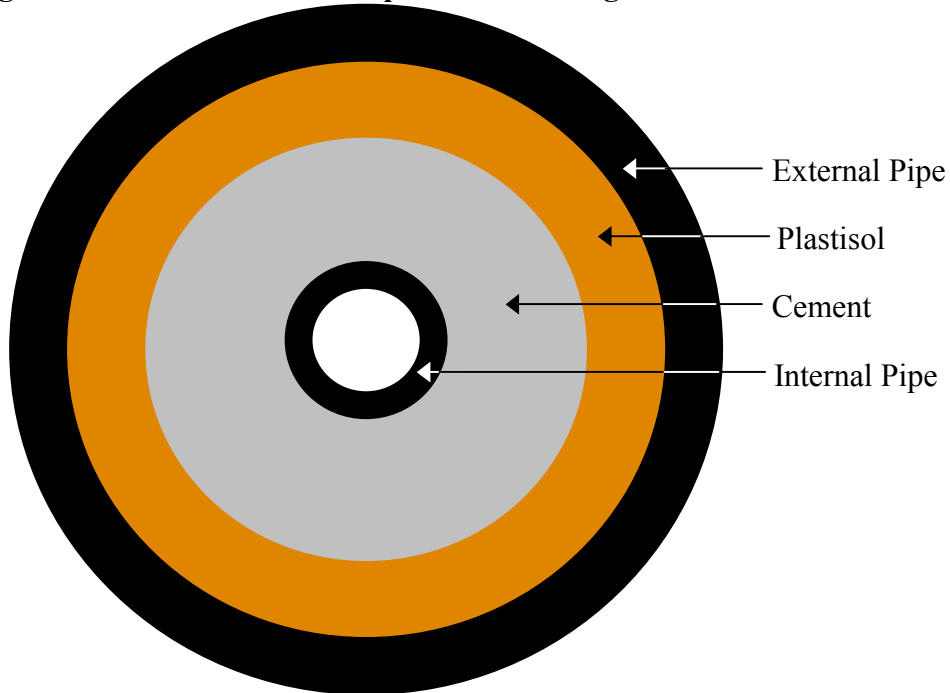


Figure 9— Cross-Section of Pipe-in-Soft Configuration for Shear Bond Tests



The shear bond measures the stress necessary to break the bond between the cement and the internal pipe. This was measured with the aid of a test jig that provides a platform for the base of the cement to rest against as force is applied to the internal pipe to press it through. (Figure 10) The shear bond force is the force required to move the internal pipe. The pipe is pressed only to the point that the bond is broken; the pipe is not pushed out of

the cement. The shear bond strength is the force required to break the bond (move the pipe) divided by the surface area between the internal pipe and the cement. Future testing will also look at some other testing alternatives: (1) greasing the interior of the external pipe and (2) pressing out the external pipe first. These would help avoid the potential effects that the cement bond to the external pipe has on the measurement of shear bond of the cement to the internal pipe.

**Figure 10—Configuration for Testing Shear Bond Strength
Force Applied Here**

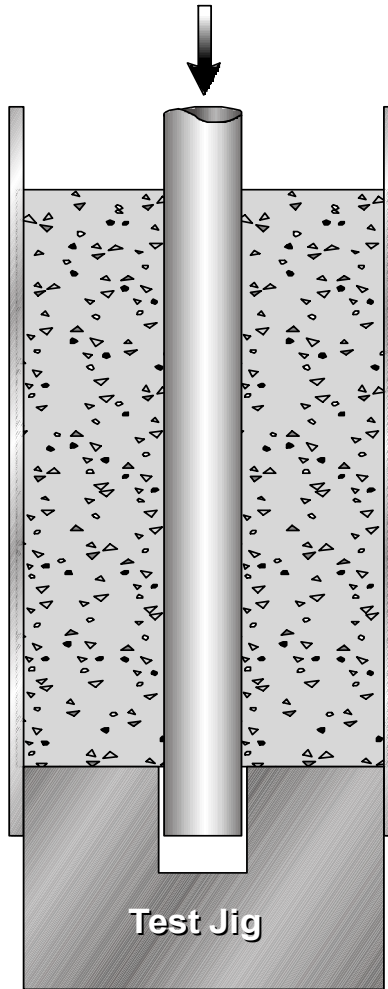


Table 7 presents the 14-day shear bond strengths of the cement samples in the pipe-in-pipe and pipe-in-soft configurations. They were cured at atmospheric pressure in a water bath maintained at 45°F.

Table 7—Shear bond strengths

Configuration	Shear Bond Strength (psi)			
	Sample			Average
	1	2	3	
Pipe-in-Pipe	1,200	1,233	945	1,126
Pipe-in-Soft	128	190	275	198

The effect that temperature cycling has on shear bond was also tested. The temperature cycling procedure was designed to simulate temperature conditions that might be encountered during production of a well. The samples are first cured for 14 days in a 45°F water bath at atmospheric pressure. They are then subjected to five days of temperature cycling. During each of these five days of temperature cycling, the cured samples are cycled as follows.

1. Samples are removed from 45°F water bath and placed in 96°F water bath for one hour.
2. Samples are placed in 180°F water bath for four hours.
3. Samples are placed in 96°F water bath for one hour.
4. Samples are placed back in 45°F water bath.

The results for the temperature-cycled shear bonds are presented in **Table 8**.

Table 8—Shear bond strengths for temperature-cycled samples

Configuration	Shear Bond Strength (psi)			
	Sample			Average
	1	2	3	
Pipe-in-Pipe	167	167	161	165
Pipe-in-Soft	68	65	82	72

Some variation in test results with the Young's modulus and tensile strength testing could be potentially attributed to settling of the cement slurry. For future testing, to avoid potential slurry settling with shear bond and other tests, the slurry will be preconditioned for 20 minutes in an atmospheric consistometer and then poured into individual, shorter molds so only one individual test sample will come from each mold.

Shrinkage Testing

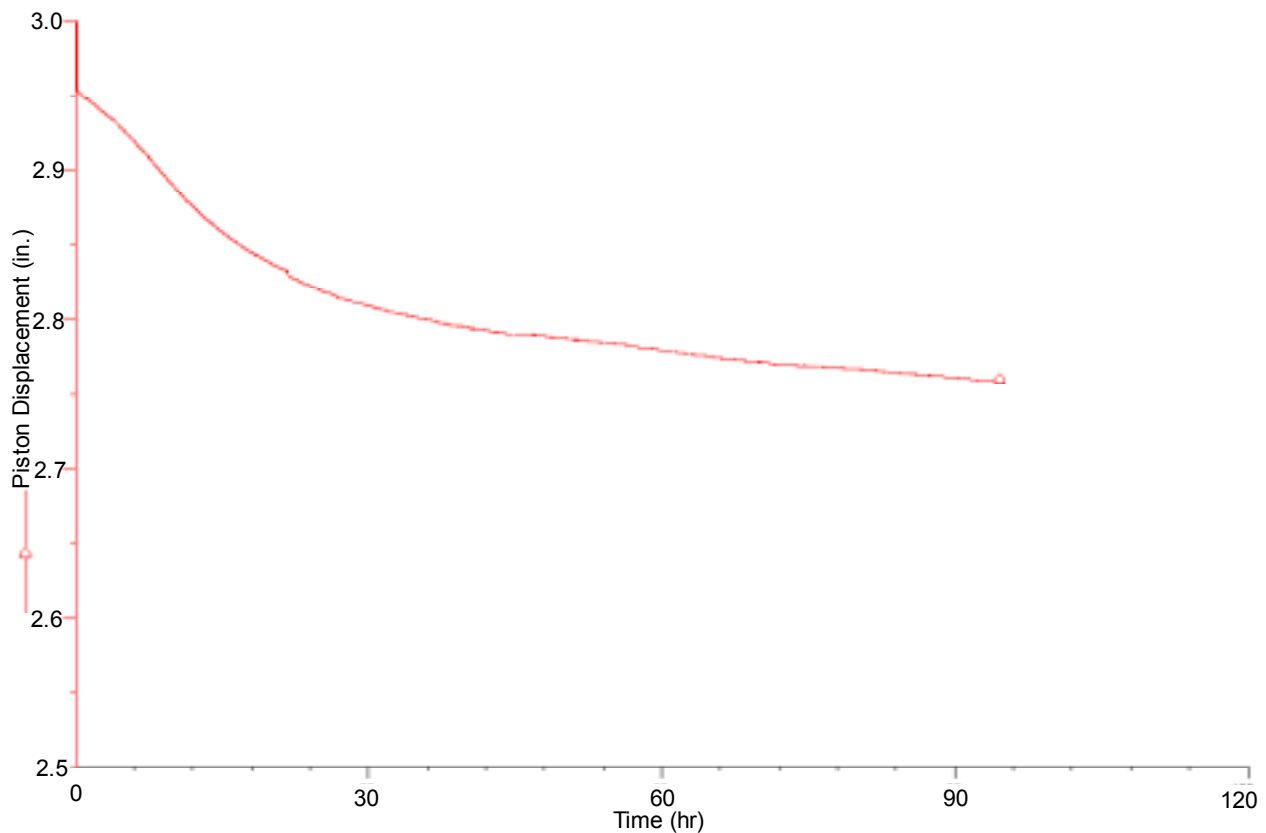
Using a modified Chandler Model 7150 Fluid Migration Analyzer, tests were performed to determine shrinkage of the neat Class A cement. The following procedures were used for performing the shrinkage testing.

1. Fill the test cell with 180 cm³ of the cement slurry.
2. Place 40 mL of water on top of cement slurry.
3. Place the hollow hydraulic piston into the test cell and on top of the water.

4. Close off the test cell and attach the pressure lines and piston displacement analyzer.
5. Close all valves except valve on top of test cell cap. Purge air out of system.
6. Apply 1,000-psi hydrostatic piston pressure to the test cell and begin recording data (time, piston displacement, and pressure).
7. Run test and gather data for desired amount of time.

Figure 11 is a chart of the piston displacement that was recorded during the inner shrinkage testing. The piston displacement indicates the inner shrinkage of the cement.

Figure 11—Piston displacement during inner shrinkage testing of Class A cement



Changes in the cement volume are assumed to be overwhelmingly dominated by inner shrinkage, although any bulk shrinkage would also affect the volume. From the piston displacement data, the cement volume shrank by 6.8%.

Future testing will test for bulk (plastic state) shrinkage, which measures the external volume change of the cement. The Chandler Model 7150 Fluid Migration Analyzer can also be used for the plastic-state shrinkage testing. The procedures for the testing are as follows.

1. Grease the interior of the test cell for ease of piston movement.
2. Fill the test cell approximately halfway with cement slurry.
3. Place the hollow hydraulic piston into the cell and on top of the cement slurry.

4. Close off the test cell and attach the pressure lines and piston displacement analyzer.
5. Close all valves except valve on top of test cell cap. Purge the air above the piston with water until water passes through the release valve and then close the valve.
6. Apply 1,000-psi hydrostatic piston pressure to test cell and begin recording data (time, piston displacement, and pressure).
7. Run test and gather data for desired length of time.

Literature Review

A literature review is being conducted that is looking at some of the potential stressors on casing and cement such as compaction, temperature cycling, and pressure cycling. The literature discusses some of the resulting damage that can occur from the stressors, ways to model the stressors, and guidelines for minimizing or preventing the damage. The literature review is ongoing. Here is what has been done to date.

Production of a well leads to a decrease in downhole fluid pressure. With the pressure decrease, more of the weight of the overburden sediments must be supported by the rock matrix, which can lead to compaction. This subsurface compaction can also result in surface subsidence.⁵

Compacted reservoirs can lead to casing compression, buckling, shear, and bending.^{5, 6} Companies have performed straightforward mathematical analysis and finite element modeling to determine the casing characteristics that best withstand the different aspects of compaction.^{7, 8, 9, 10} Cement designs have also been based off of finite element modeling that was performed to simulate various stressors that can be seen by the cement.^{11, 12, 13, 14}

Gas leaks in wells have also been attributed to cement shrinkage, which creates circumferential fractures that become paths for gas flow.¹⁵ Baumgarte *et al.* looked at expanding cement (which is used to prevent some gas flow problems) and found that, although helpful in many situations, expanding cement can actually lead to a microannulus between the casing and cement when it is placed in soft formations.¹⁶

Jackson and Murphey examined the effect of casing pressure on annular cement seal. They used near-full-scale laboratory simulation and found that 5-in. casing that is pressure tested to 70% of its burst pressure could potentially lead to a loss of cement integrity and create a path for gas flow. They also tested for a reduced hydrostatic situation where the casing was pressured to 10,000 psi while the cement set and then the pressure was released; this situation also created a path for gas flow.¹⁷

Participants' Responses

Participants were asked to provide ideas on the factors that affect the integrity of the annular seal and flow of fluids. The following responses were received from the participants.

- Condition of the surface of the casing(s) – sandblasted, rusted, mill varnish, rough coat material, etc.
- Cement pumping rate – plug, laminar, or turbulent flow regime
- Hole cleaning spacer – type and volume
- Open hole lithology
- Fluid in hole before cement – water-based mud, oil-based mud, synthetic mud, clear fluid, water, liquid hydrocarbons, gas, etc.
- Wall cake – integrity, thickness, composition, etc.
- Borehole rugosity and tortuosity
- Pipe movement during cementing – rotation or reciprocation
- Casing jewelry – turbulators; wall scratchers; centralizer design, effectiveness, and spacing; etc.
- Cement sheath thickness/casing stand-off from hole wall
- Composition/type of cement slurry – neat, lightweight, foam, additives, gel and setting times, permeability of set cement, etc.
- Pore pressure in the cement and in the formation as a function of time. Maybe permeability, too.
- Shrinkage in the paste with increasing hydration - in the case where extra fluid is available and in the case where it is not (casing/permeable formation v. casing in casing or long liner lap)
- Decay in the hydrostatic pressure transmitted by the cement column with time
- Water/cement ratio
- Initial stress state in the cement
- Thermal expansion coefficients of formation, cement, casing
- Cement failure strain, cement failure envelope under triaxial conditions at widely different strain rates
- Cement work of fracture, fracture toughness
- Cement creep under complex stress and at temperature
- An oversimplistic belief that a 2-in. cube crush test tells anything about the cement mechanical properties in the annulus
- Inability to model (by FEA) the behavior of the sandwich of formation>mud cake>cement>microannulus>casing under complex stress from (say) compaction, tectonic displacements, fault movement, etc.
- Influence of temperature on all the above - on the property measurement and on the chemistry of the cement over time - years rather than hours
- Annular geometry and eccentricity
- Mud cake properties - formation>mud cake>cement>microannulus>casing
- Mud displacement efficiency % and geometry/extent of anything less than 100%
- Induced changes - thermal (e.g., production or cold completion brine)

- Induced changes - mechanical (e.g., pressure testing casing maybe at early age)
- Setting of pack-offs in wellheads, setting of integral liner top packers
- Inability to mix and pump the job as designed
- Cement
- Mud
- Formation fluids
- Cement slurry design
- Sheer incompetence
- Temperature cycling
- Out-of-gauge openhole large washouts
- Pipe centralization
- Cement slurry density variations
- Downhole fluid movements while cement sets
- Cement ability to develop gel strength rapidly
- Pressure cycling
- Positive pressure tests on casing after cement set
- Ineffective packer element design. (DV packer collars are not effective in sealing off gas)

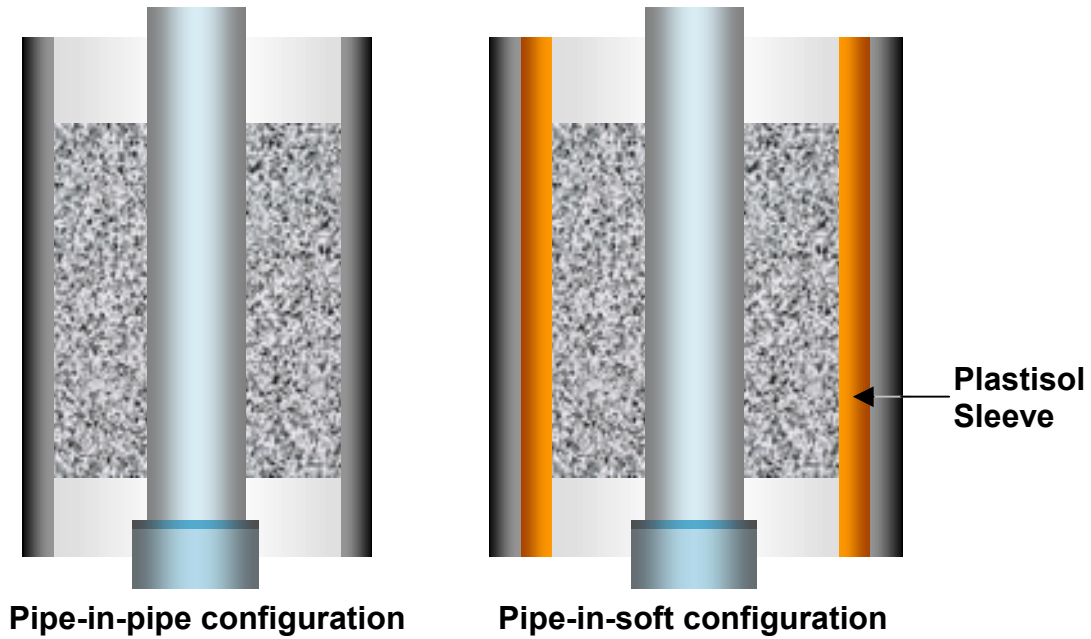
Future Testing

Casing Pressure Test

Future studies will investigate the effect that casing pressure tests have on annular seal. Many people feel that casing pressure tests expand the casing and create pressures on and increase the inner diameter of the surrounding cement. The stresses and physical changes can adversely strain the cement and potentially deform the cement irrecoverably.

A laboratory model has been developed to simulate casing pressure tests (**Figure 12**). The model can be made in two different configurations— pipe-in-pipe and pipe-in-soft. This is to simulate high-restraint and low-restraint formations. This can help to identify differences between hard formation and loosely consolidated formation. The pressure testing will be initiated after different times of cement curing to determine the effects of curing time before pressure testing. Multiple cycles of pressure testing will be performed.

Figure 12—The two different configurations for the casing pressure test

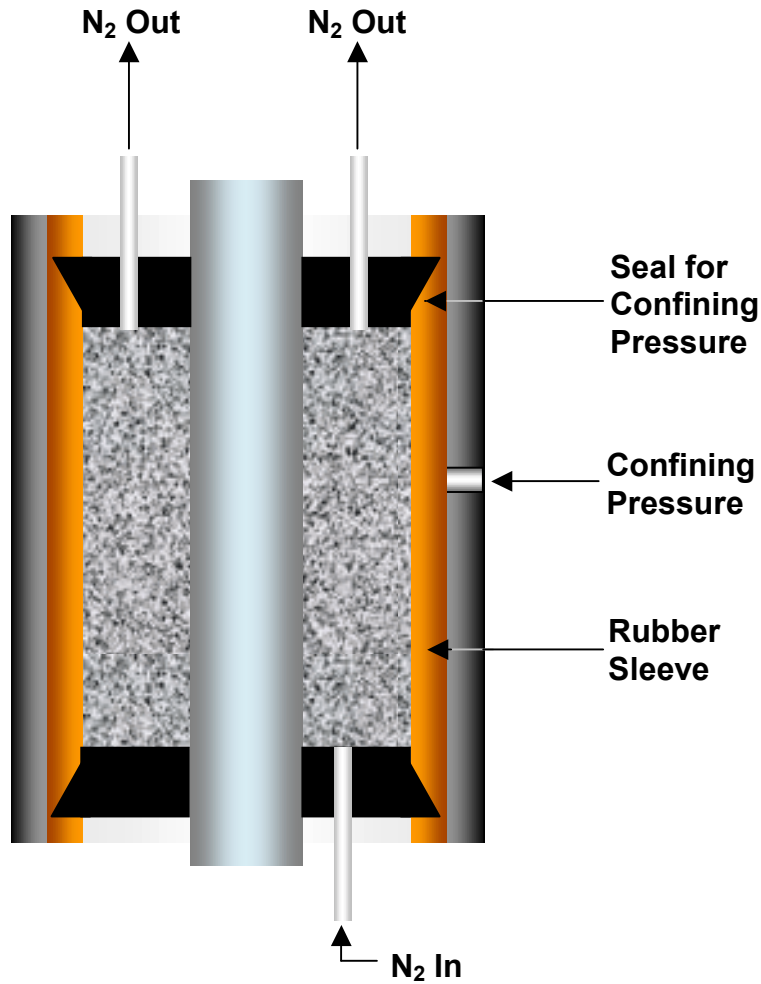


Annular Seal Test

A key factor of this project is investigating cement’s capability to maintain its seal under downhole stresses. An annular seal model is being developed that can measure bulk permeability across a cement system that has been stressed from temperature or pressure cycling. As with some of the other testing, the annular seal test model will have pipe-in-pipe and pipe-in-soft configurations to simulate high and low restraints, respectively.

Figure 13 is a schematic of the pipe-in-soft configuration of the annular seal model.

Figure 13—Cross section of annular seal model for pipe-in-soft configuration



The inner pipe of the model will be the main conduit for the stressing medium. For instance, the inner pipe can contain heated fluids while the remainder of the system is at a different temperature; this simulates the hotter formation fluids that can be experienced during production. The inner pipe of the model can also be pressurized up to 5,000 psi, simulating casing pressure testing which is believed by many to lead to loss of annular seal because of the expanding and contracting casing.

The annular seal testing will be performed after each time the interior conduit pipe is pressurized. For the temperature cycling, the model will be subjected to five complete temperature cycles and then annular seal testing will be done. The model will again be temperature cycled five times and then annular seal testing performed. This will continue with annular seal testing after every fifth temperature cycle until annular flow is detected or after 20 temperature cycles, whichever comes first.

In the pipe-in-soft configuration, the rubber sleeve surrounding the cement is able to withstand 25 psi. During the annular seal test, pressure can then be applied to the outside

of the rubber sleeve, allowing the sleeve to make a fluid-tight seal on the outside of the cement. Pressurized nitrogen gas (<25 psi) can then be applied axially across the cement and the only paths for fluid flow is through cement or along the interface between the cement and the inner pipe. Any exiting nitrogen flow rate can be monitored and measured. There is no need for the rubber sleeve or the exterior confining pressure in the pipe-in-pipe configuration.

Testing on Other Cement Designs

After finalizing some of the test procedures, testing will be started on specific cement slurries. The first four slurries to test after the Class A cement slurry include foamed cement (20 to 25% foam quality), latex cement (1 gal/sk), high-strength fumed silica cement (with carbon fibers), and cement with lightweight hollow spheres.

Mathematical Modeling

Progress is also being made to contract with the University of Houston to perform finite element analysis (FEA) of the laboratory models being used in the project (temperature and pressure cycling models). The results from the laboratory experiments will be compared to the mathematical modeling. These studies will then be compared with other FEA work that has been presented in the literature.

The mathematical modeling will be analyzed to determine if the stresses associated with the temperature and pressure cycling will result in loss of annular seal. This can be compared with the annular-seal testing that will physically test the cement systems for annular seal.

References

- ¹ API Recommended Practice 10B: “Recommended Practice for Testing Well Cements,” 22nd Edition, American Petroleum Institute, Washington, D.C., December 1997.
- ² “Standard Test Method for Splitting Tensile Strength of Cylindrical Concrete Specimens,” ASTM C496-96, West Conshohocken, PA, 1996.
- ³ International Society for Rock Mechanics, “Suggested Methods for Determining Tensile Strength of Rock Materials—Part 2: Suggested Method for Determining Indirect Tensile Strength by the Brazil Test,” March 1977.
- ⁴ “Standard Test Method for Static Modulus of Elasticity and Poisson’s Ratio of Concrete in Compression,” ASTM C469-94, West Conshohocken, PA, 1994.
- ⁵ Bruno, M.S., “Subsidence-Induced Well Failure,” SPE Paper 20058, June 1992.
- ⁶ Dusseault, M.B. and Bruno, M.S., “Casing Shear: Causes, Cases, Cures,” SPE Paper 48864, November 6, 1998.
- ⁷ Jellison, M.J. and Brock, J.N., “The Impact of Compression Forces on Casing-String Designs and Connectors,” SPE Paper 67608, December 2000.
- ⁸ Cernocky, E.P. and Scholibo, F.C., “Approach to Casing Design for Service in Compacting Reservoirs,” SPE Paper 30522, October 25, 1995.
- ⁹ Fredrich, J.T.; Arguello, B.J.; Wawersik, W.R.; Deitrick, G.L.; de Rouffignac, E.P.; Myer, L.R.; and Bruno, M.S., “Three-Dimensional Geomechanical Simulation of Reservoir Compaction and Implications for Well Failures in the Belridge Diatomite,” SPE Paper 36698, October 9, 1996.
- ¹⁰ Bruno, M.S., “Geomechanical Analysis and Decision Analysis for Mitigating Compaction Related Casing Damage,” SPE Paper 71695, October 3, 2001.
- ¹¹ Thiercelin, M.J.; Dargaud, B.; Baret, J.F.; and Rodriguez, W.J., “Cement Design based on Cement Mechanical Response,” October 8, 1997.
- ¹² Bosma, M.; Ravi, K.; van Driel, W.; and Schreppers, G. J., “Design Approach to Sealant Selection for the Life of the Well,” SPE Paper 56536, October 3, 1999.
- ¹³ Di Lullo, G. and Rae, O., “Cement for Long Term Isolation—Design Optimization by Computer Modeling and Prediction,” IADC/SPE 62745, September 13, 2000.
- ¹⁴ Bosma, M.G.R.; Cornelissen, E.K.; and Schwing, A., “Improved Experimental Characterization of Cement/Rubber Zonal Isolation Materials,” SPE Paper 64762, November 10, 2000.

¹⁵ Dusseault, M.B.; Gray, M.N.; and Nawrocki, P.A., “Why Oilwells Leak: cement Behavior and Long-Term Consequences,” November 10, 2000.

¹⁶ Baumgarte, C.; Thiercelin, M.; and Klaus, D., “Case Studies of Expanding Cement to Prevent Microannular Formation,” SPE Paper 56535, October 6, 1999.

¹⁷ Jackson, P.B. and Murphey, C.E., “Effect of Casing Pressure on Gas Flow Through a Sheath of Set Cement,” SPE/IADC Paper 25698, February 25, 1993.



CSI Technologies

Appendix II

Report 2

MMS Project
Long-Term Integrity of Deepwater Cement
Systems Under Stress/Compaction Conditions

Report 2

Issued July 31, 2002



CEMENTING SOLUTIONS, INC.



Table of Contents

Executive Summary	3
Background	3
The MMS Project.....	3
Project Progress	4
Introduction.....	5
Conventional Testing	6
Thickening-Time Test.....	6
Free-Fluid Test.....	6
Compressive Strength	7
Rock Properties Testing.....	8
Tensile Strength and Tensile Young's Modulus.....	8
Compressive Young's Modulus.....	11
Hydrostatic Cycling Tests.....	22
Unconventional Performance Testing.....	26
Shear Bond Strength	26
Shrinkage Testing	30
Annular Seal Testing.....	31
Casing Pressure Test	31
Annular Seal Testing Procedure	33
Mathematical Modeling	35
Appendix: Mathematical Modeling	36
Introduction.....	36
Mathematical Model	37
Stress Conditions	39
Parametric Studies	40
Results and Discussion	40
Casing Pressure.....	41
Confining Pressure.....	41
Young's Modulus and Poisson Ratio.....	41
Cement Thickness.....	42
Temperature Gradient	42
Conclusions.....	43



Cementing Solutions, Inc.

Executive Summary

Background

The U.S. Department of the Interior, Minerals Management Service (MMS) has stated that, of the 14,000 producing wells offshore; some 11,000 exhibit sustained annular casing pressure. This annular pressure can be the result of a number of factors, some related to cement composition and some related to the downhole environment. The lithology of offshore formations (particularly in drilling deepwater wells) has recently been identified as the key element in well integrity. One of the most important factors when considering lithology of offshore formations in general is the stress exerted on the cement column during the life of the well. This stress can be thermally or hydraulically induced due to well intervention operations, or result from compaction. Stress gradients can be sufficiently large to cause mechanical failure of the cement.

Shallow formations penetrated in drilling deepwater wells often require extraordinary zonal isolation procedures to prevent shallow water flows. Severe operational and economic consequences resulting from the immediate flow of water from these shallow formations up to the sea floor demand that the surface casings penetrating these zones be adequately sealed. Significant effort has been devoted to development of cement compositions to alleviate shallow water flow. However, the long-term integrity of the seal provided by these special compositions has not been evaluated. Additionally, the lithology of deeper strata may increase the potential of subsidence at any depth as pore pressure is reduced with geopressured drawdown. Cement compositions used throughout construction of these wells must be able to withstand stresses exerted by subsidence while still providing an annular seal.

The MMS Project

The MMS, in collaboration with representatives from AGIP, Anadarko, ARAMCO, BP Exploration, Conoco, DOE, ExxonMobil, ONGA, Petrobras, Saudi Aramco, and Unocal, is performing the MMS Project (Long-term Integrity of Deepwater Cement Systems Under Stress/Compaction Conditions) to evaluate the ability of cement compositions to provide well integrity and zonal isolation through zones in which subsidence, compaction, and excessive stresses can be long-term problems. Though the project's focus is on deepwater conditions, the well integrity issues hold for cementing in a variety of conditions, so the study has wide applicability. A significant number of wells drilled in deep water and other high-stress environments may not have adequate long-term zone isolation.

The MMS Project is challenging. A significant aspect of this project is to develop a correlation of the conventional cement tests with rock properties tests in conjunction with realistic annular seal model studies. This correlation will allow the prediction of the ability of various cement systems to seal under downhole stress conditions.



Cementing Solutions, Inc.

A series of cement seal evaluation tests will be conducted in an apparatus designed to approximate the various stresses applied to the cemented annulus throughout the well's operating life. This apparatus (called an annular seal device) was developed as a standard means to measure the ability of a cementing system to provide sealing to water or gas in realistic *in-situ* conditions. The annular configuration allows realistic geometries and sealing conditions. Following are test parameters that will be evaluated:

- Cement compositions of varying densities from conventional normal weights to foamed cements
- Thermal cycling induced stress
- Pressure cycling induced stress
- Multiple cycles over six months duration
- Compaction conditions varying from no compaction to soft formations with significant compaction
- Mechanical properties of the cements

By rigorously and thoroughly applying these parameters to cement compositions, and by comparing the laboratory results to mathematical models developed by the University of Houston, the MMS Project team is confident of success in designing cement materials and systems that will withstand the extreme stress/compaction conditions that threaten well integrity.

Project Progress

Thus far, Phase I of the project has yielded significant data to help address the well integrity issue. Data from the conventional, rock properties, and unconventional performance tests performed in Cementing Solutions, Inc.'s laboratory are provided in this paper. The mathematical modeling performed by the University of Houston revealed the cement material properties and cement thickness have negligible effect on the overall stress distribution in the Pipe-in-Pipe configuration, but that the material properties become significant for the Pipe-in-Soft configuration. In the Pipe-in-Soft configuration, thermal stresses lead to tensile stresses, which can result in tensile failures at high temperature variations. A very sharp stress contrast was observed in all cases at the casing-cement interface.

The project will continue with additional testing. Ongoing status reports will be provided to project participants. The final project report will summarize the project work and the test results. The final report will also present the decision matrix that will help guide the industry in how to design cement slurries that are best suited to withstand the problematic stress/compaction situations with deepwater and other high-stress environments and operations.



Cementing Solutions, Inc.

Introduction

The MMS Project pools the expertise of the United States Federal Government's Mineral Management Service (MMS) and several of the world's leading Oil & Gas production companies to investigate the long-term integrity of deepwater and other high-stress cement systems under stress/compaction conditions. The project's research will develop correlations between cement properties and seal performance under stress gradients that can be sufficiently large to cause mechanical failure of the cement.

The MMS Project consists of nine tasks:

1. Problem analysis
2. Property determination and test design
3. Mathematical analysis of stress
4. Testing baseline cement composition
5. Refine test procedure
6. Develop composition matrix
7. Conduct tests
8. Analyze results
9. Develop decision matrix

The University of Houston performed finite element analysis (FEA) of the laboratory models used in the project so the laboratory results can be compared to the mathematical modeling. The mathematical modeling was analyzed to determine if the stresses associated with the temperature and pressure cycling result in loss of annular seal.

Laboratory testing was performed on neat Type I cement at 15.6 lb/gal, foamed Type I cement, and Type I cement with lightweight beads. The neat Type I cement contains water at 5.2 gal/sk. The slurry with lightweight beads contains 13.2% BWOC 3M™ Scotchlite™ K46 Glass Bubbles and water at 6.9 gal/sk for a density of 12.0 lb/gal. The foamed cement contains Witcolate® 7093 (a foaming agent) at 0.03 gal/sk, Aromox® C/12 (a foam stabilizer) at 0.01 gal/sk, 1.0% BWOC calcium chloride, and water at 5.2 gal/sk for an unfoamed slurry density of 15.6 lb/gal; the slurry is then foamed to 12.0 lb/gal. The testing has helped to refine and confirm the test procedures that will be used for the remainder of the project

The following sections of this report provide data from the conventional testing, rock properties testing, and unconventional performance testing completed so far. The report concludes with a detailed explanation of the mathematical modeling procedures used in this project and the preliminary conclusions based on that modeling.



Conventional Testing

Thickening-Time Test

Following the procedures (set forth in API RP 10B) thickening-time tests were performed on the three cement systems. The test conditions started at 80°F and 600 psi, and were ramped to 65°F and 5,300 psi in 48 minutes.

Some preparation and testing methods were modified to adapt for the lightweight bead and foamed slurries. The mixing procedures were modified for the bead slurry to minimize bead breakage that can occur because of high shear from API blending procedures. The following blending procedure was used for the bead slurry.

1. Weigh out the appropriate amounts of the cement, water, and beads into separate containers.
2. Mix the cement slurry (without beads) according to Section 5.3.5 of API RP 10B.
3. Pour the slurry into a metal mixing bowl and slowly add beads while continuously mixing by hand with a spatula. Mix thoroughly.
4. Pour this slurry back into the Waring blender and mix at 4,000 rev/min for 35 seconds to mix and evenly distribute the contents.

Testing methods for the foamed slurries were also modified. For example, thickening time is performed on unfoamed slurries only. Because the air in the foam does not affect the hydration rate, the slurry is prepared as usual per API RP 10B and then the foaming surfactants are mixed into the slurry by hand without foaming the slurry.

Table 1 provides data from the thickening-time test.

Free-Fluid Test

The free-fluid testing that was performed on the Type I, Foamed Cement and Bead Slurries came from API RP 10B. The free-fluid procedure, also referred to as operating free water, uses a graduated cylinder that is oriented vertically. The free fluid for the slurry maintained at 65°F was measured by volume as shown in **Table 1**.



Cementing Solutions, Inc.

Table 1—Results from Thickening-Time and Free-Fluid Tests

Slurry System	Thickening Time to 100 Bc (Hr:Min)	Percent Free Fluid
Neat	4:38	0.8
Foamed	3.42	0.0
Bead	5:04	0.8

Compressive Strength

Table 2 presents compressive strength data for neat Type I, Foamed Cement, and Bead Cement. The compressive strengths were derived using the 2-in. cube crush method specified in API RP 10B. The samples were cured in an atmospheric water bath at 45°F. The reported values were taken from the average of three samples. Cells in Table 2 marked with “—” indicate that no compressive strength tests were performed for that time period.

Table 2—Crush Compressive Strength

Slurry System	Compressive Strength (psi) at Specified Number of Days							
	7	10	12	14	16	17	18	19
Neat	2735	4065	4385	4034	—	4471	—	—
Foamed	339	—	446	455	500	—	—	478
Bead	352	—	511	526	527	—	602	—



Rock Properties Testing

Tensile Strength and Tensile Young's Modulus

Mechanical properties of the neat Type I, Foamed Cement and Bead Cement were tested. Tensile strength was tested using ASTM C496 (Standard Test Method for Splitting Tensile Strength of Cylindrical Concrete Specimens). For this testing, the specimen dimensions were 1.5 in. diameter by 1 in. long. **Figure 1** shows how each specimen is oriented on its side when tested. The force was applied by constant displacement of the bottom plate at a rate of 1 mm every 10 minutes. Change in the specimen diameter can be calculated from the test plate displacement. The (compressive) strength of the specimen during the test can be graphed along with the diametric strain (change in diameter/original diameter) to generate the tensile Young's modulus.

Figure 1—Sample Orientation for ASTM C496-90 Testing

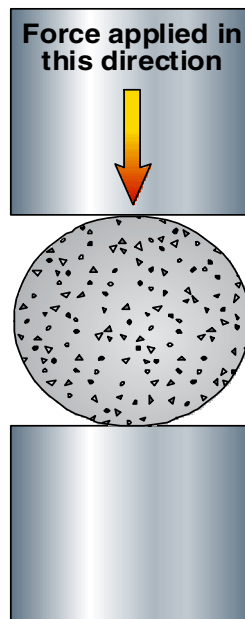


Table 3 shows the 14-day tensile strength and tensile Young's modulus of the neat Type I cement. The samples were cured at atmospheric pressure in a water bath maintained at 45°F. The samples were cured under confined conditions (in the mold for the entire 14 days) and unconfined conditions (removed from mold after 24 hours and allowed to cure the remainder of the time outside of the mold). These were cured vertically with optimal conditioning time, and the top and bottom sections were removed. The tests were performed using a flat plate.



Cementing Solutions, Inc.

Table 3—Splitting Tensile Strength and Tensile Young’s Modulus Data

Curing Condition	Splitting Tensile Strength (psi)				Tensile Young’s Modulus (10 ⁴ psi)			
	Sample			Average	Sample			Average
	1	2	3		1	2	3	
Confined	409	406	368	394	20.43	19.20	17.83	19.15
Unconfined	163	278	198	213	7.88	8.35	8.25	8.16

For this project, rock mechanics personnel from Westport and Conoco also incorporated the use of a test method from the International Society for Rock Mechanics (ISRM). The ISRM method calls for testing with a curved adapter or plate that gives more contact area between the testing surface and the test specimen and results in less variation in results.

Table 4 presents data from tests using the traditional flat plates of ASTM C496 and tests using the curved plates from the ISRM test method. These tests were run with samples cured “in the mold” or confined. **Figures 2** and **3** show the data gathered during testing.

Table 4—Splitting Tensile Strength and Tensile Young’s Modulus of 12.0 lb/gal Foamed Cement

Plate Type	Failure Strength (psi)	Young’s Modulus (10 ⁴ psi)
Flat plate per ASTM	304	2.85
	276	3.99
	321	3.35
Curved plate per ISRM	206	3.66
	348	5.78
	204	3.26



Figure 2—Tensile Young’s Modulus (Using Flat Plates) of 12.0 lb/gal Foamed Cement

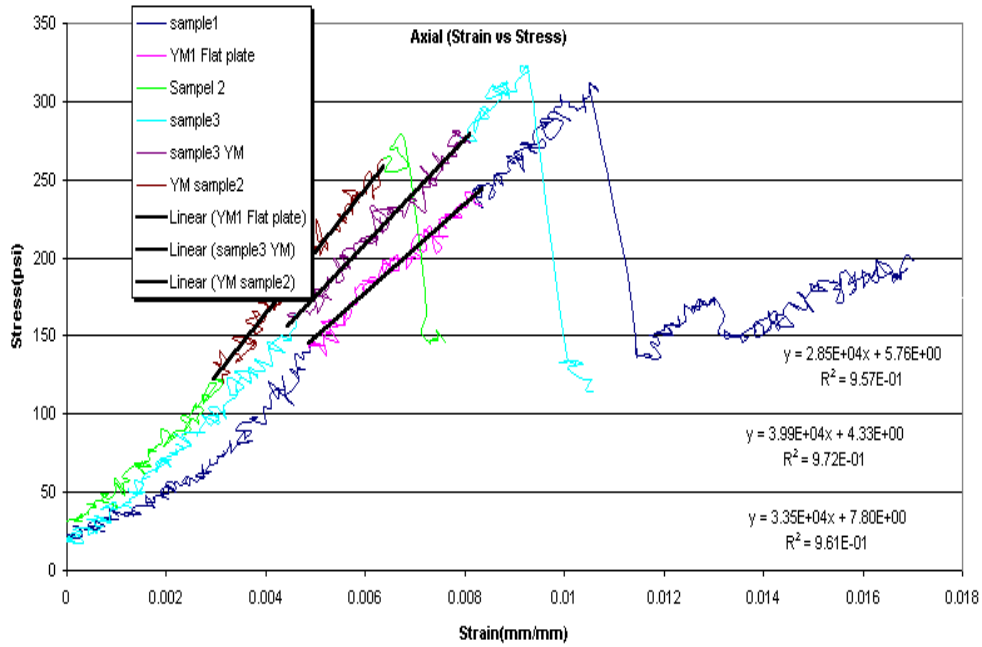
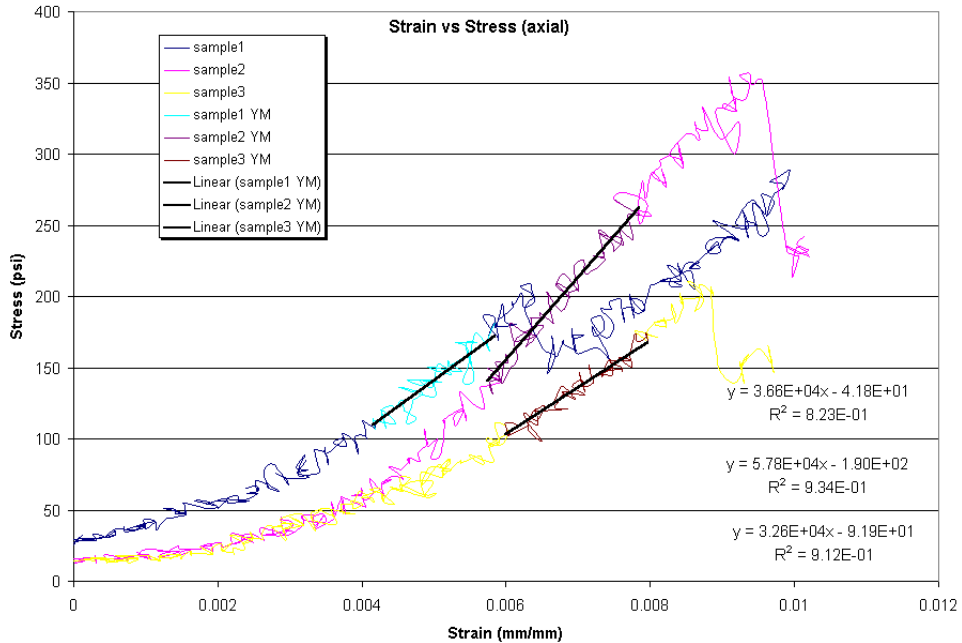


Figure 3—Tensile Young’s Modulus (Using Curved Plates) of 12.0 lb/gal Foamed Cement





Compressive Young's Modulus

Traditional Young's Modulus testing was also performed using ASTM C469, the Standard Test Method for Static Modulus of Elasticity (Young's Modulus) and Poisson's Ratio of Concrete in Compression. Young's Modulus and effective compressive-strength were tested. The effective compressive strength is the equivalent unconfined compressive strength, which eliminates the effect of confining pressure. The diameter of each test specimen was 1.5 in., and the length was 3.0 in.

The following procedure is used for the Young's Modulus testing.

1. Each sample is inspected for cracks and defects.
2. The sample is cut to a length of 3.0 in.
3. The sample's end surfaces are then ground to get a flat, polished surface with perpendicular ends.
4. The sample's physical dimensions (length, diameter, weight) are measured.
5. The sample is placed in a Viton jacket.
6. The sample is mounted in the Young's Modulus testing apparatus.
7. The sample is brought to 100-psi confining pressure and axial pressure. The sample is allowed to stand for 15 to 30 minutes until stress and strain are at equilibrium. (In case of an unconfined test, only axial load is applied.)
8. The axial and confining stresses are then increased at a rate of 25 to 50 psi/min to bring the sample to the desired confining stress condition. The sample is allowed to stand until stress and strain reach equilibrium.
9. The sample is subjected to a constant strain rate of 2.5 mm/hr.
10. During the test, the pore-lines on the end-cups of the piston are open to the atmosphere to prevent pore-pressure buildup.
11. After the sample fails, the system is brought back to the atmospheric stress condition. The sample is removed from the cell and stored.

Samples that were cured in an unconfined condition (removed from mold after 24 hours and allowed to cure the remainder of the time outside of the mold) were tested at confining pressures of 0 (zero); 1,500; and 5,000 psi. Young's modulus data for neat Type I samples are presented in **Table 5**. Testing at 0 (zero) confining pressure was also performed on samples that were cured in a confined condition (in the mold for the entire 14 days). Results from testing on the confined, neat Type I samples are presented in **Table 6**. All samples were cured for 14 days at atmospheric pressure in a water bath maintained at 45°F.



Table 5—Young’s Modulus Data for Neat Type I Samples Cured “Out of the Mold”

Confining Pressure (psi)	Young’s Modulus (10 ⁵ psi)	Effective Compressive Strength (psi)
0	8.13	4,118
	17.37	8,125
	15.99	9,166
1,500	12.39	7,912
	8.23	7,526
	12.59	9,046
5,000	8.22	8,553
	9.31	9,133
	9.67	9,007

Figure 4—Young’s Modulus Testing for Neat Type I Samples Cured “Out of the Mold” and Tested at a Zero Confining Pressure

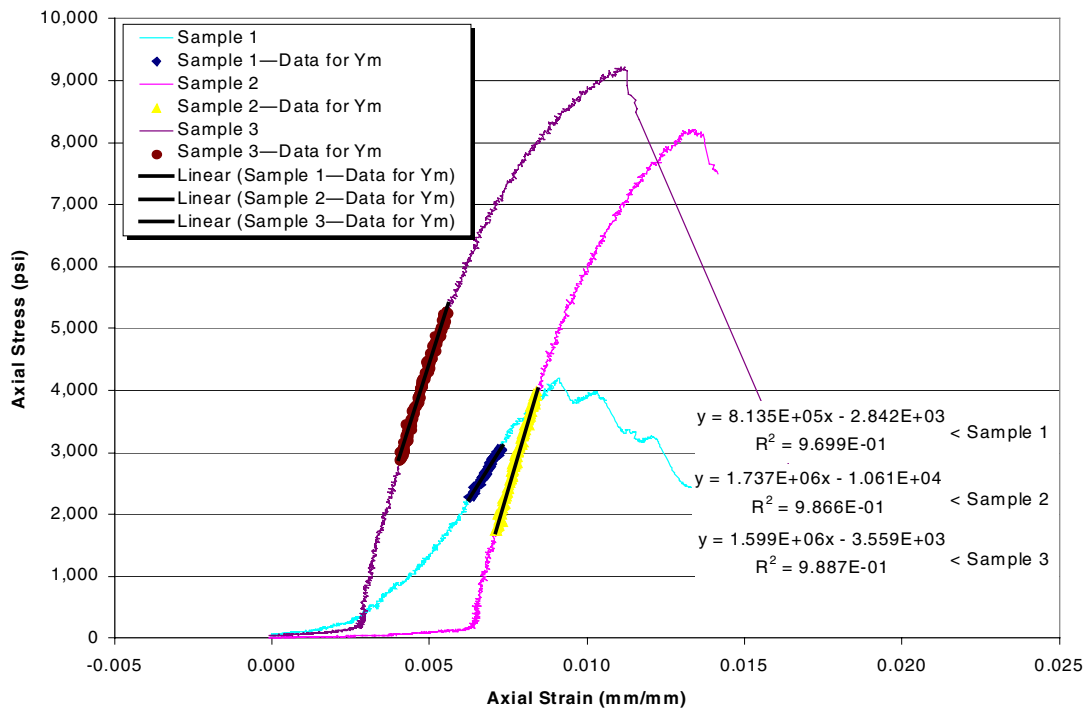




Figure 5—Young’s Modulus Testing for Neat Type I Samples Cured “Out of the Mold” and Tested at a Confining Pressure of 1,500 psi

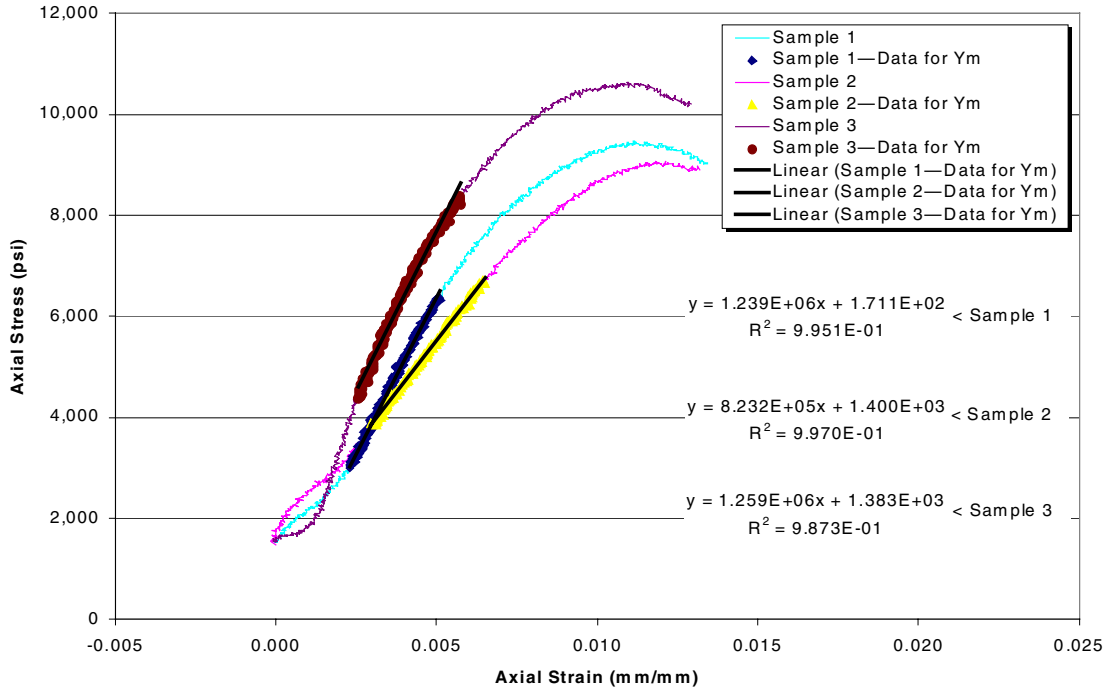




Figure 6—Young’s Modulus Testing for Neat Type I Samples Cured “Out of the Mold” and Tested at a Confining Pressure of 5,000 psi

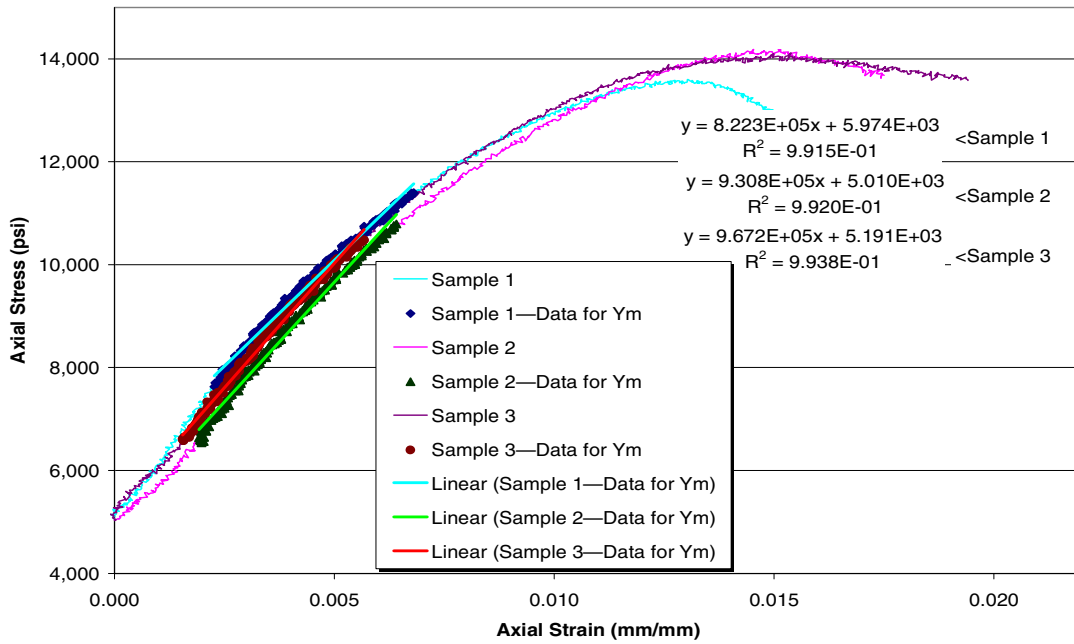
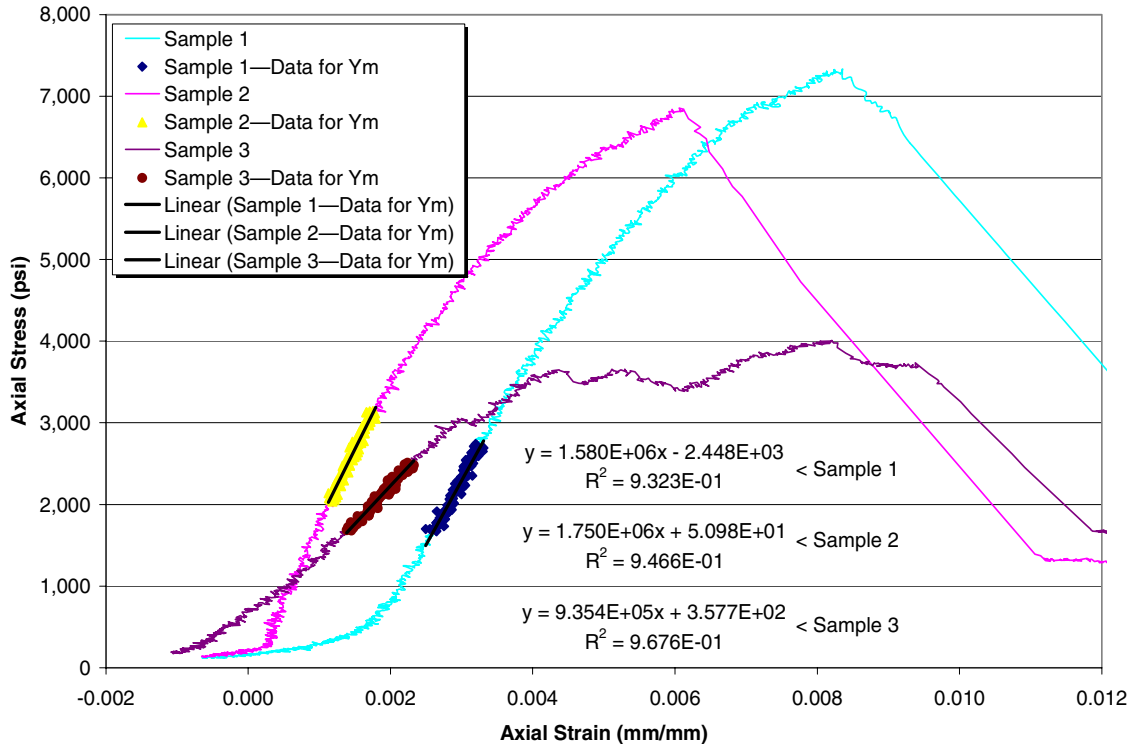


Table 6—Young’s Modulus Data for Neat Type I Samples Cured “In the Mold”

Confining Pressure (psi)	Young’s Modulus (10 ⁵ psi)	Effective Compressive Strength (psi)
0	15.80	7,330
	17.50	6,823
	9.35	4,000



Figure 7—Young’s Modulus Testing for Neat Type I Samples Cured “In the Mold” and Tested at Zero Confining Pressure



Tests were also conducted to determine the effect that temperature cycling has on Young’s Modulus. The temperature cycling procedure was designed to simulate temperature conditions that might be encountered during production of a well. The samples are first cured for 14 days in a 45°F water bath at atmospheric pressure. They are then subjected to five days of temperature cycling. During each of these five days of temperature cycling, the cured samples are cycled as follows.

1. Samples are removed from 45°F water bath and placed in 96°F water bath for 1 hour.
2. Samples are placed in 180°F water bath for 4 hours.
3. Samples are placed in 96°F water bath for 1 hour.
4. Samples are placed back in 45°F water bath.



Cementing Solutions, Inc.

Table 7 presents data from neat Type I samples that were cured at 45°F in an unconfined condition (removed from mold after one day and allowed to cure the remaining 13 days outside of the mold) and that were then temperature-cycled for five days. **Figures 6** and **7** present the Young's Modulus data.

Table 7— Young's Modulus Data for Neat Type I Samples Cured in an Unconfined Condition and Then Temperature-Cycled for Five Days

Confining Pressure (psi)	Young's Modulus (10^5 psi)	Effective Compressive Strength (psi)
0	11.59	5,014
	5.48	4,084
	12.45	5,243
1,500	8.92	6,975
	10.48	6,642
	11.09	7,022



Figure 8—Young’s Modulus Testing for Neat Type I Samples Cured in an Unconfined Condition

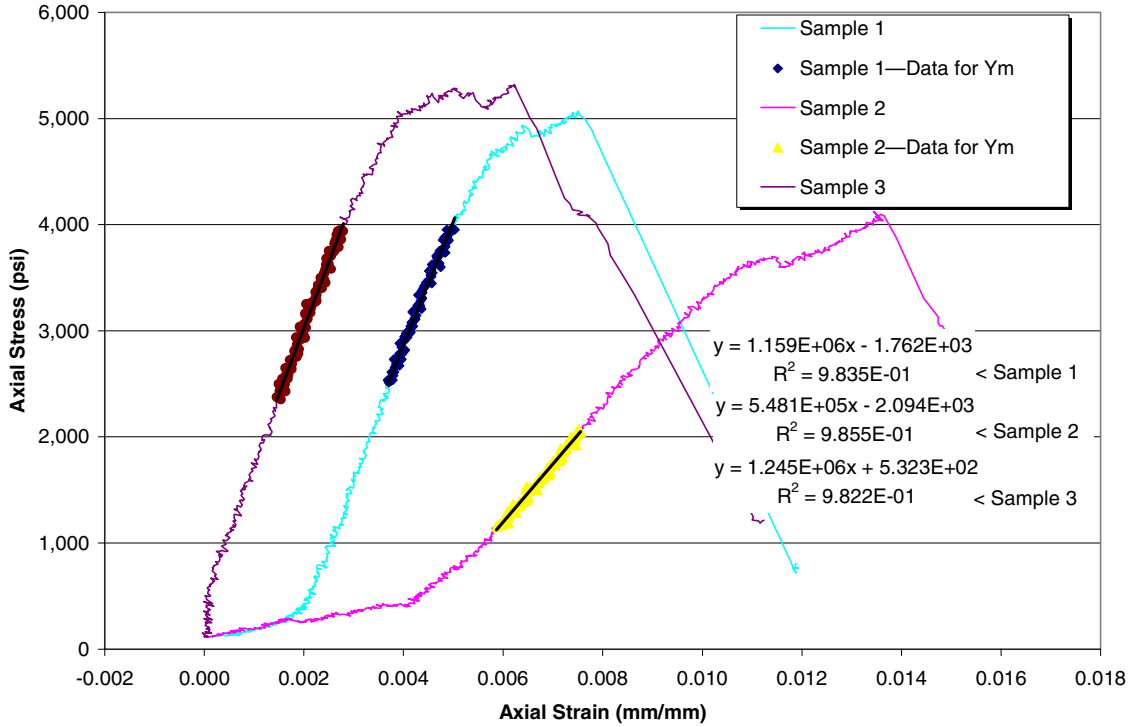
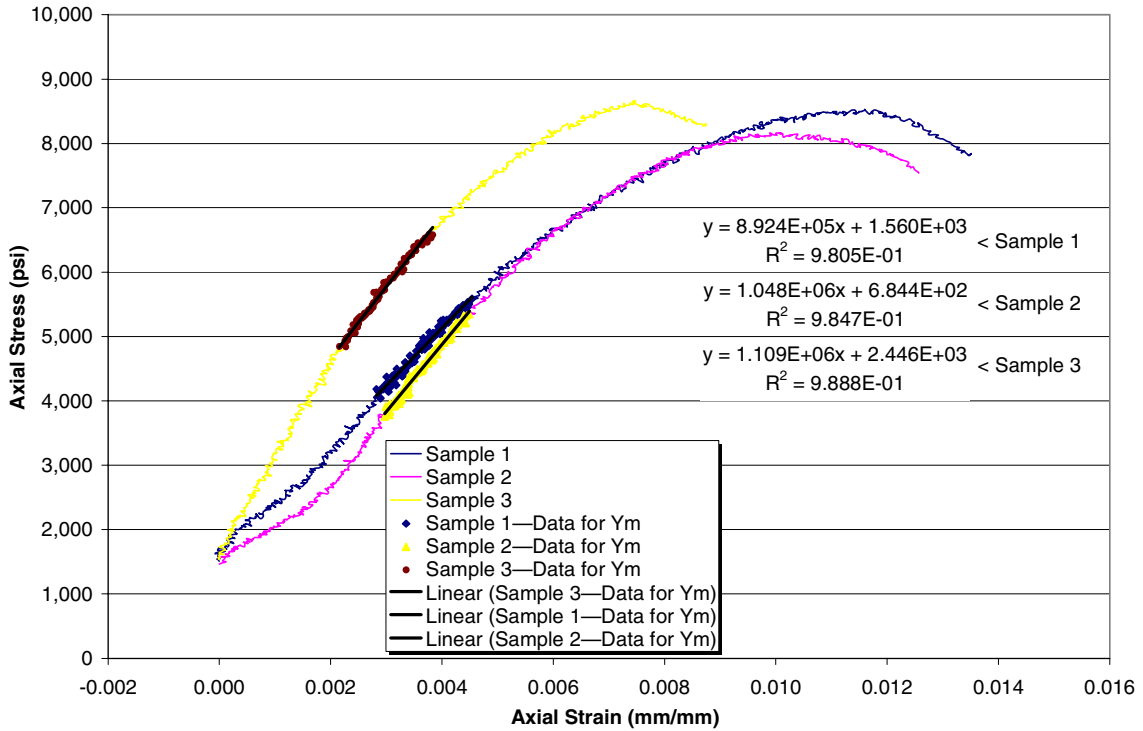




Figure 9—Young’s Modulus Testing for Neat Type I Samples Cured in an Unconfined Condition and Then Temperature Cycled for Five Days and Tested at a Confining Pressure of 1,500 psi



Some of the variation in the Young’s Modulus data could be attributed to settling of the cement slurry. The samples were cured in molds that were 10 in. long, and the individual 3-in. samples were then cut from the 10-in. specimens. For future testing, to avoid potential slurry settling, the slurry will be preconditioned for 20 minutes in an atmospheric consistometer and then poured into individual, shorter molds so only one individual test sample will come from each mold.

Table 8 and **Figures 10, 11, and 12** present Young’s Modulus and Poisson’s Ratio data for a 12 lb/gal foamed cement.

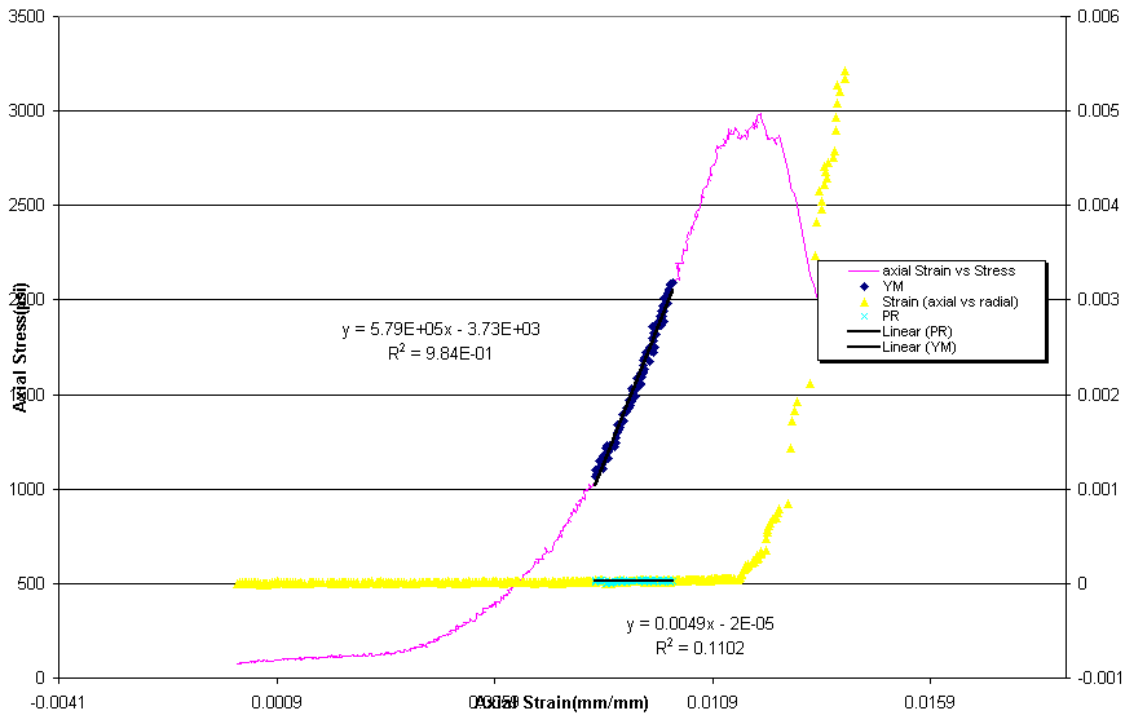
Table 8—Young’s Modulus and Poisson’s Ratio for 12 lb/gal Foamed Cement

Sample ID	Confining Stress (psi)	Failure Stress (psi)	Effective Failure Stress (psi)	Young’s Modulus (10 ⁵ psi)	Poisson’s Ratio (mm/mm)
1	0	2,885	2,885	5.79	0.0049
2	500	4,448	3,948	6.80	-0.0396
3	1,000	5,506	4,506	6.06	-0.0382



Cementing Solutions, Inc.

Figure 10—Young's Modulus and Poisson's Ratio Testing for 12 lb/gal Foamed Cement Tested at Zero Confining Pressure





Cementing Solutions, Inc.

Figure 11—Young's Modulus and Poisson's Ratio Testing for 12 lb/gal Foamed Cement Tested at 500 psi Confining Pressure

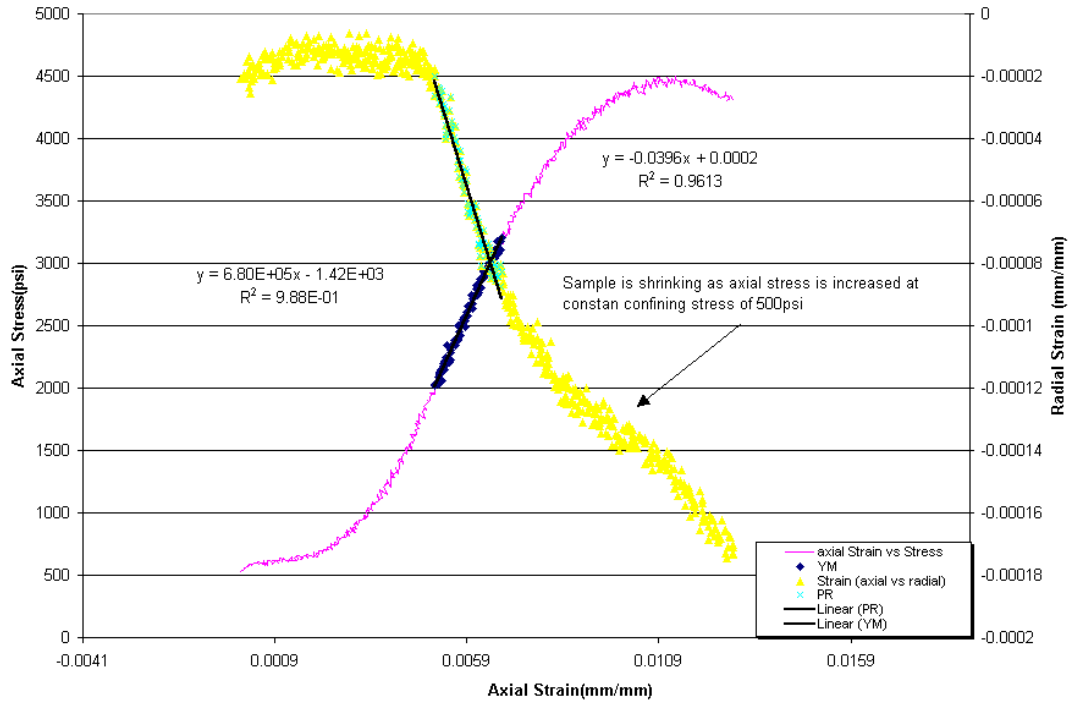
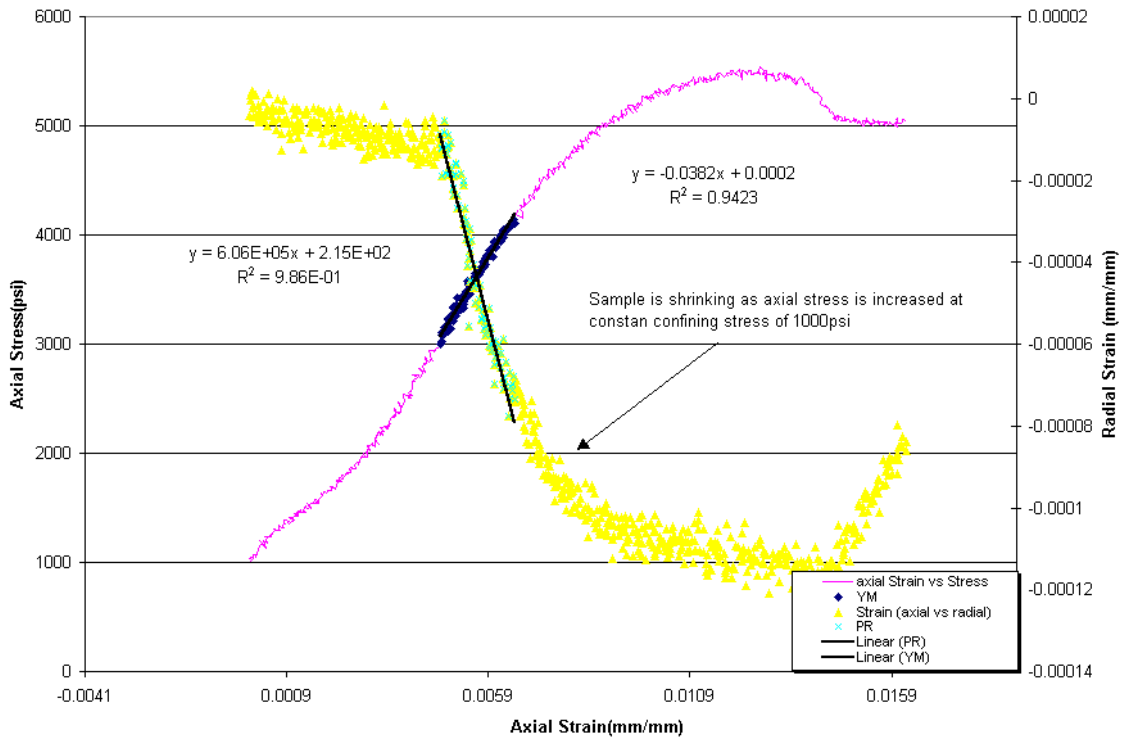




Figure 12—Young's Modulus and Poisson's Ratio Testing for 12 lb/gal Foamed Cement Testing at 1,000 psi Confining Pressure



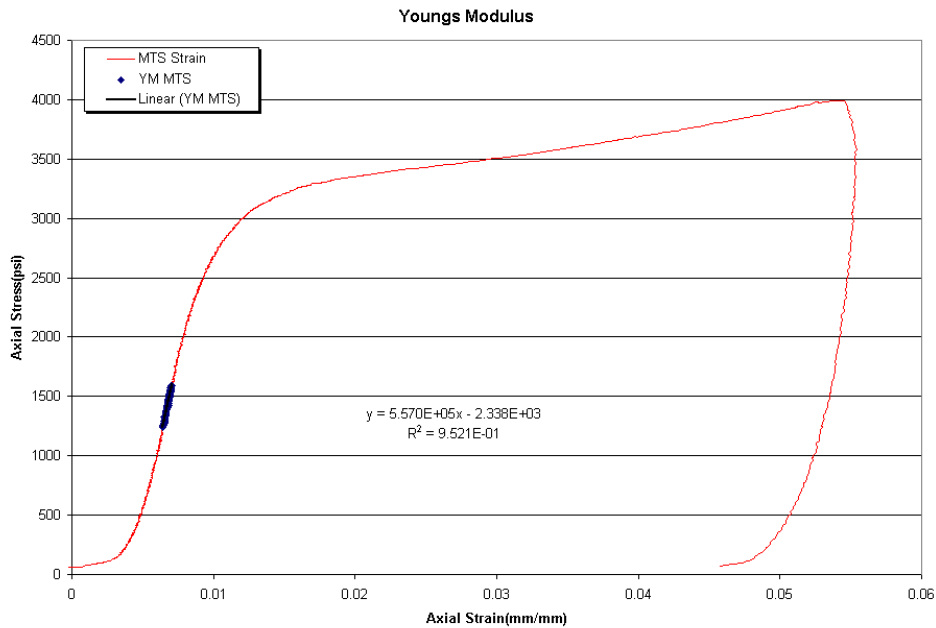


Hydrostatic Cycling Tests

Additional Young's modulus testing was done to get a better understanding how cement responds to downhole pressure cycling. In this testing, a 10-lb/gal, Type I foamed cement was subjected to hydrostatic cycling.

Figure 13 shows the hydrostatic Young's Modulus testing performed on the 10 lb/gal foamed cement. This testing was done to get an idea of how the cement sample responds under hydrostatic pressure conditions. It also gives an indication that other samples should be able to withstand at least 3,500-psi hydrostatic pressure. The last portion of the curve of **Figure 13**, where the curve is at a negative slope, is a misleading artifact associated with the ending of the test.

Figure 13—Young's Modulus Testing of 10 lb/gal Foamed Cement





Cementing Solutions, Inc.

Hydrostatic cycling testing was then done on a different sample of the same 10 lb/gal foamed cement. For that testing, the hydrostatic pressure is cycled through the following ramping procedures.

- (1) Ramp up to 1,000 psi.
- (2) Ramp down to 100 psi.
- (3) Ramp up to 1,500 psi.
- (4) Ramp down to 100 psi.
- (5) Ramp up to 2,000 psi.
- (6) Ramp down to 100 psi.

Each ramp was conducted at a rate of 16.7 psi/min and the sample was held at the destination hydrostatic pressures (i.e., 100; 1,000; 1,500; and 2,000 psi) for no longer than two minutes before proceeding to the next ramp step. **Table 9** shows the Young's Modulus value for each ramp procedure. **Figure 14** shows the results of the hydrostatic cycling.

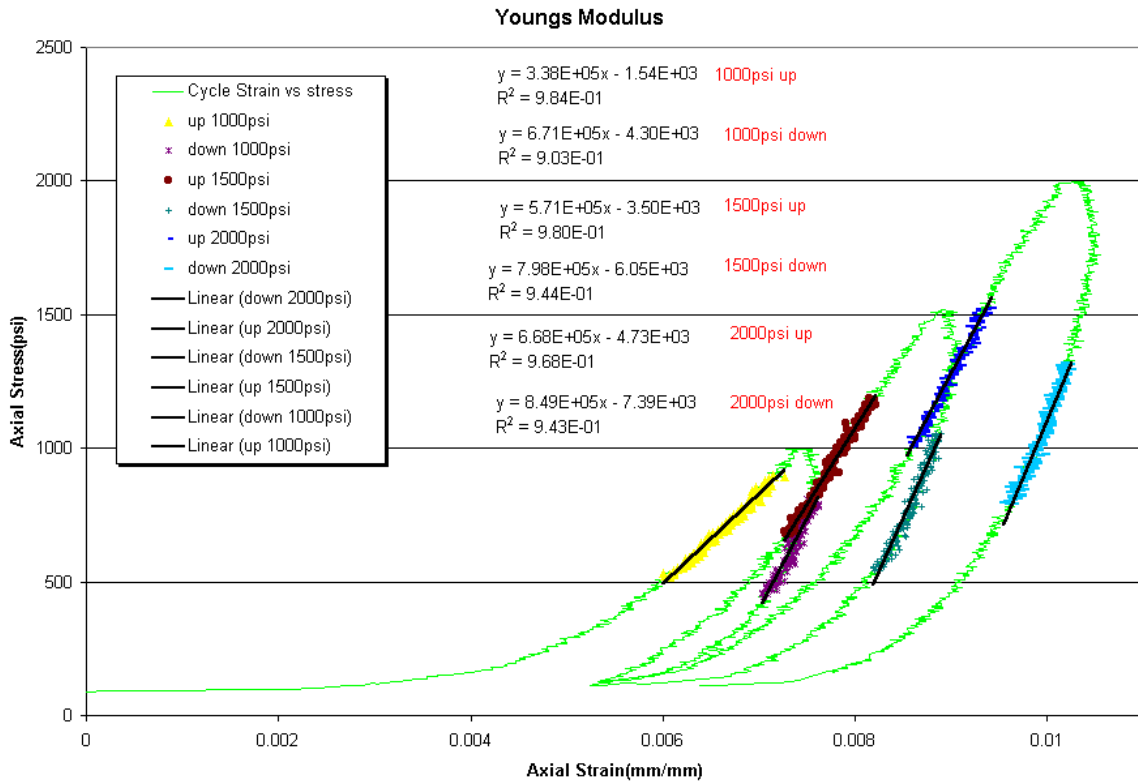
Table 9—Young's Modulus Data for 10 lb/gal Foamed Cement Exposed to Hydrostatic Cycling

Cycle #	Destination Hydrostatic Pressure (psi)	Young's Modulus (10^5 psi)
1	1,000	3.38
1	100	6.71
2	1,500	5.71
2	100	7.98
3	2,000	6.68
3	100	8.49



Cementing Solutions, Inc.

Figure 14—Young’s Modulus Testing of 10 lb/gal Foamed Cement During Hydrostatic Cycling

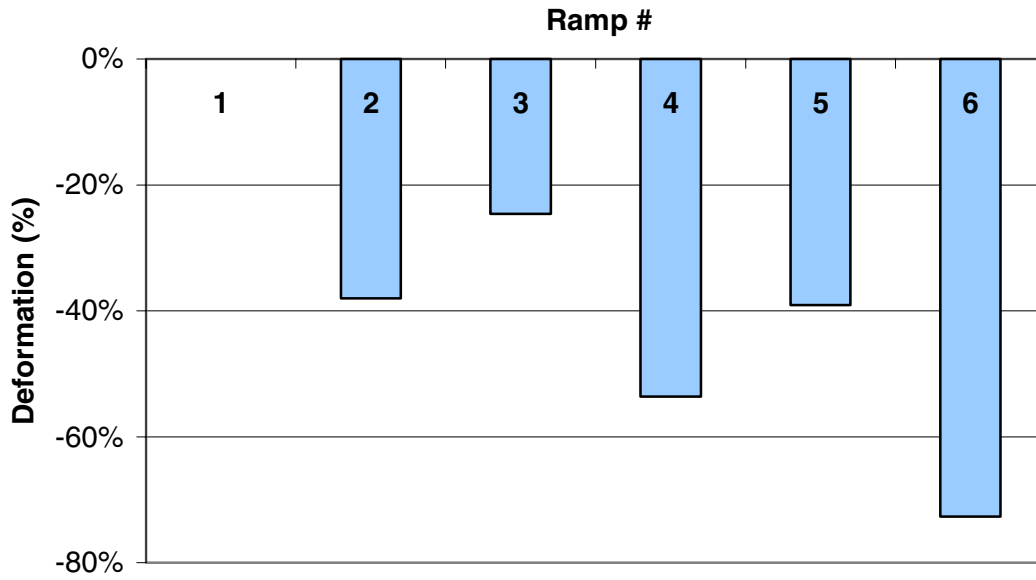


Further study of the hydrostatic cycling was done to examine the deformation that occurs during each of the ramps. **Figure 15** depicts the percentile deformation of each step of the ramps. The value (size) of the sample at 250 psi during the first ramp up to 1,000 psi is taken as the reference value for determining the percentile deformation. This size at 250 psi during Ramp 1 is compared to the sample size at 250 psi during each ramp step.



Cementing Solutions, Inc.

Figure 15—Deformation of 10 lb/gal Foamed Cement during Hydrostatic Cycling





Unconventional Performance Testing

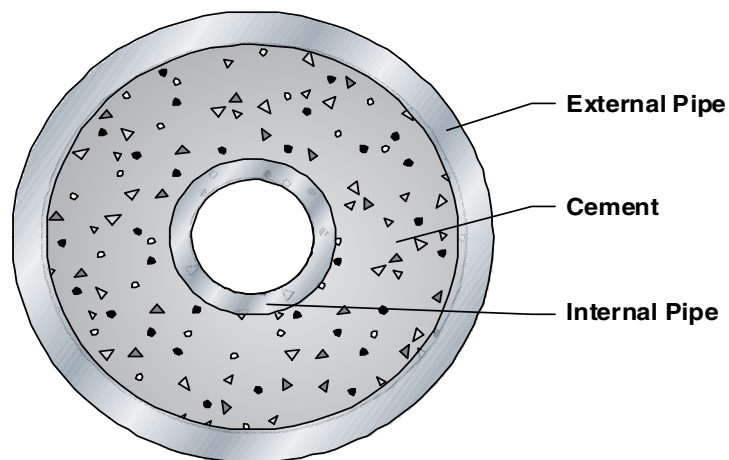
Shear Bond Strength

Testing was also performed to evaluate shear bond strength of neat Type I cement, foamed cement and bead cement. These studies investigate the effect that restraining force has on shear bond. Samples were cured in a pipe-in-pipe configuration (**Figure 16**) and in a pipe-in-soft configuration (**Figure 17**). The pipe-in-pipe configuration consists of a sandblasted internal pipe with an outer diameter (OD) of $1\frac{1}{16}$ in. and a sandblasted external pipe with an internal diameter (ID) of 3 in. and lengths of 6 in. A contoured base and top are used to center the internal pipe within the external pipe. The base extends into the annulus 1 in. and cement fills the annulus to a length of 4 in. The top 1 in. of annulus contains water.

For the pipe-in-soft shear bonds, plastisol is used to allow the cement to cure in a less-rigid, lower-restraint environment. Plastisol is a mixture of a resin and a plasticizer that creates a soft, flexible substance. This particular plastisol blend (PolyOne's Denflex PX-10510-A) creates a substance with a hardness of 40 duro.

The pipe-in-soft configuration contains a sandblasted external pipe with an ID of 4 in. A molded plastisol sleeve with an ID of 3.0 in. and uniform thickness of 0.5 in. fits inside this external pipe. With the aid of a contoured base and top, a sandblasted internal pipe with an OD of $1\frac{1}{16}$ in. is then centered within the plastisol sleeve. The pipes and sleeve are 6 in. long. The base extends into the annulus 1 in. and cement fills the annulus to a length of 4 in. between the plastisol sleeve and the inner $1\frac{1}{16}$ -in. pipe. The top inch of annulus is filled with water.

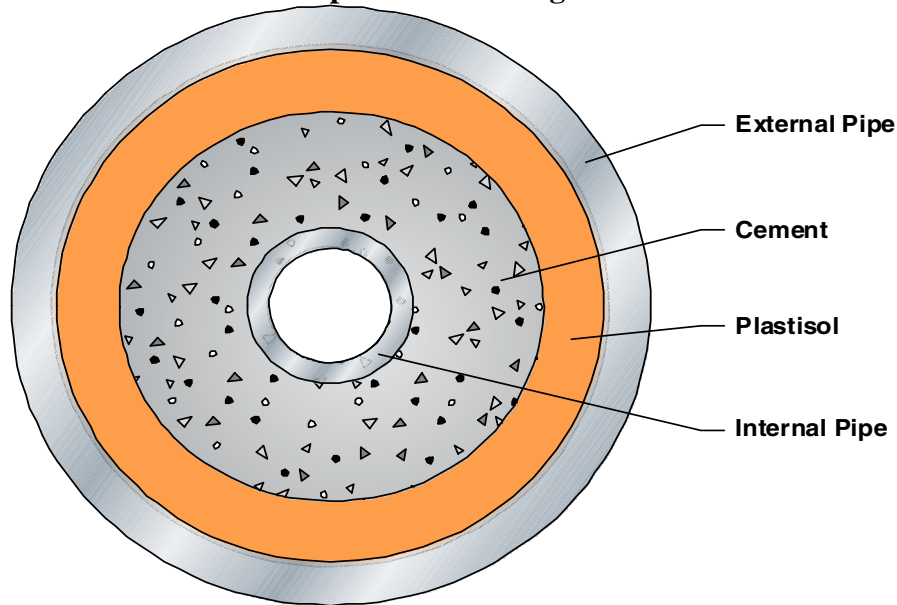
Figure 16—Cross-Section of Pipe-in-Pipe Configuration for Shear Bond Tests





Cementing Solutions, Inc.

Figure 17— Cross-Section of Pipe-in-Soft Configuration for Shear Bond Tests



The shear bond measures the stress necessary to break the bond between the cement and the internal pipe. This was measured with the aid of a test jig that provides a platform for the base of the cement to rest against as force is applied to the internal pipe to press it through (**Figure 18**). The shear bond force is the force required to move the internal pipe. The pipe is pressed only to the point that the bond is broken; the pipe is not pushed out of the cement. The shear bond strength is the force required to break the bond (move the pipe) divided by the surface area between the internal pipe and the cement.



Cementing Solutions, Inc.

Figure 18—Configuration for Testing Shear Bond Strength

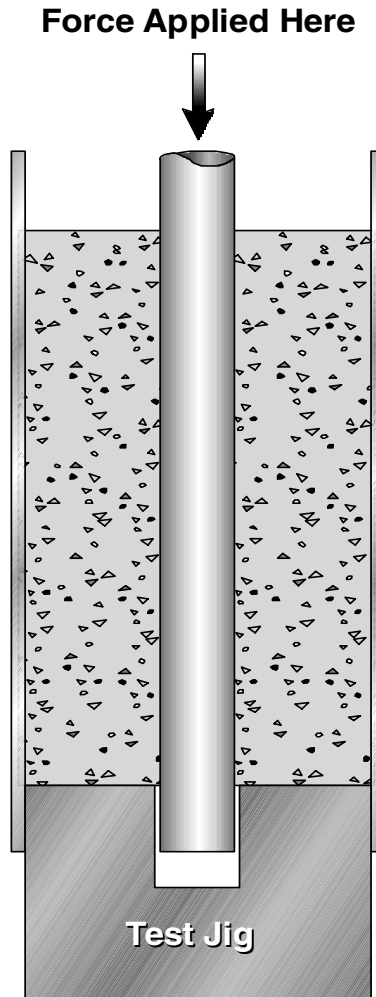


Table 10 presents the 14-day shear bond strengths of the cement samples in the pipe-in-pipe and pipe-in-soft configurations. They were cured at atmospheric pressure in a water bath maintained at 45°F. The † is used in the table to indicate samples that cracked during the pressure cycling. The ‡ is used in the table to indicate samples that were cured for some time other than 14 days; the number following the ‡ indicated the number of days the sample was cured.



Table 10—Shear Bond Strengths

Slurry System	Shear Bond Strength (psi) at Different Conditions					
	Baseline		Temperature Cycled		Pressure Cycled	
	Pipe-in-Pipe	Pipe-in-Soft	Pipe-in-Pipe	Pipe-in-Soft	Pipe-in-Pipe	Pipe-in-Soft
Neat	1194	198	165	72	194/106	23
Foamed	127/98	233	299/215 ^{‡26}	7	276/228 ^{‡24}	22 [†]
Bead	109/78	143	191/269 ^{‡27}	56	294/170 ^{‡24}	23 [†]

[†] indicates cement cracked during pressure cycling.

[‡] indicates sample was cured for the number of days specified after the [‡].

The effect that temperature cycling has on shear bond was tested. The temperature cycling procedure was designed to simulate temperature conditions that might be encountered during production of a well. The samples are first cured for 14 days in a 45°F water bath at atmospheric pressure. They are then subjected to five days of temperature cycling. During each of these five days of temperature cycling, the cured samples are cycled as follows.

1. Samples are removed from 45°F water bath and placed in 96°F water bath for 1 hour.
2. Samples are placed in 180°F water bath for 4 hours.
3. Samples are placed in 96°F water bath for 1 hour.
4. Samples are placed back in 45°F water bath.
5. Samples are conditioned for 20 minutes.

The effect that pressure cycling has on shear bond was also tested. The pressure cycling procedure was designed to simulate pressure conditions that might be encountered during production of a well. Because these samples will undergo high pressures, the interior pipe of each sample was made from 1-in. diameter, 40/41 coiled tubing pipe that can withstand 10,000 psi. Each end of the pipe is threaded. One end will have a pressure-tight cap on it during pressure cycling and the other end of the pipe will be connected to the pressure source.

The samples are first cured for 14 days in a 45°F water bath at atmospheric pressure. They are then subjected to five periods of pressure cycling in which the interior pipe is pressured to 5,000 psi for 10 minutes and then allowed to rest at 0 (zero) psi for 10 minutes.



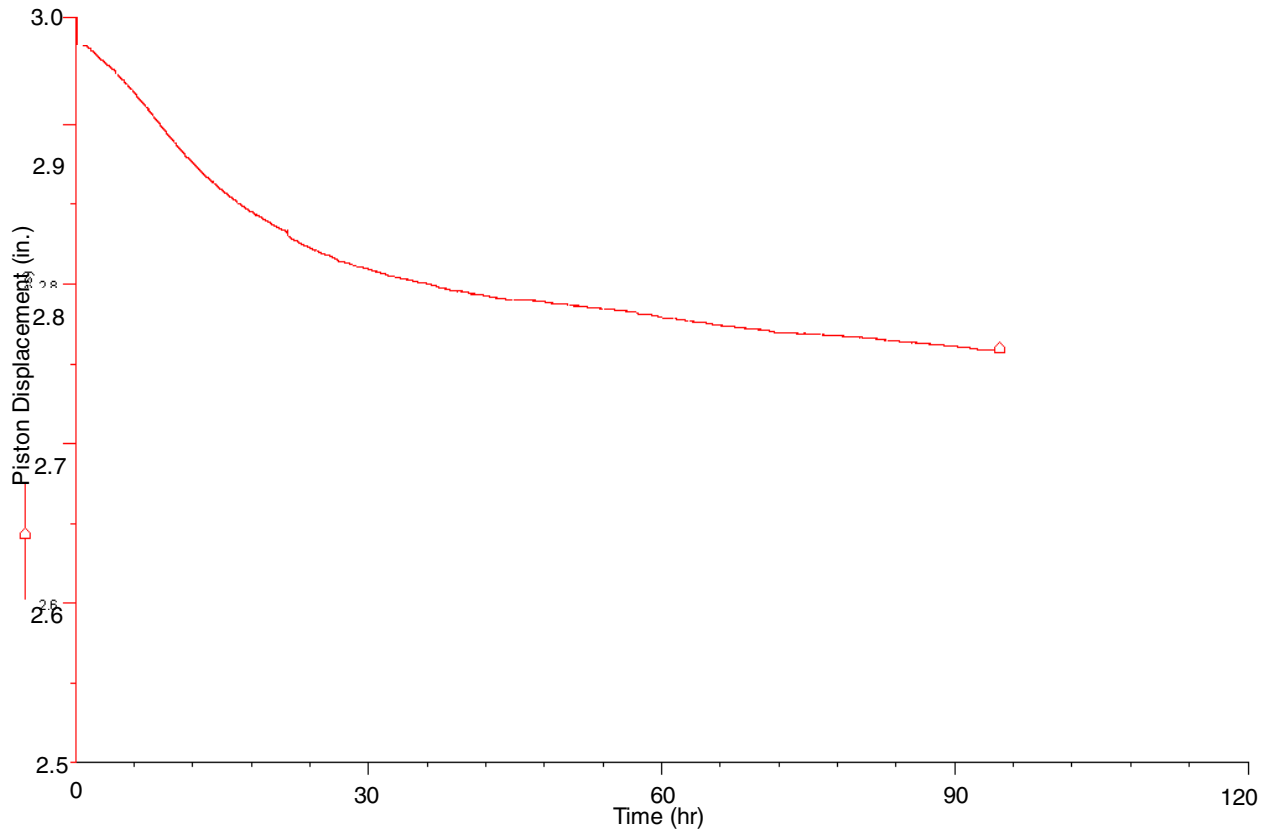
Shrinkage Testing

Using a modified Chandler Model 7150 Fluid Migration Analyzer, tests were performed to determine shrinkage of the neat Type I cement. The following procedures were used for performing the shrinkage testing.

1. Fill the test cell with 180 cm³ of the cement slurry.
2. Place 40 mL of water on top of cement slurry.
3. Place the hollow hydraulic piston into the test cell and on top of the water.
4. Close off the test cell and attach the pressure lines and piston displacement analyzer.
5. Close all valves except the valve on top of the test cell cap. Purge the air out of the system.
6. Apply 1,000-psi hydrostatic piston pressure to the test cell and begin recording data (time, piston displacement, and pressure).
7. Run the test and gather data for the desired amount of time.

Figure 19 shows the piston displacement recorded during the inner shrinkage testing. The piston displacement indicates the inner shrinkage of the cement.

Figure 19—Piston Displacement during Inner Shrinkage Testing of Type I Cement





Cementing Solutions, Inc.

Changes in the cement volume are assumed to be overwhelmingly dominated by inner shrinkage, although any bulk shrinkage would also affect the volume. From the piston displacement data, the cement volume shrank by 6.8%.

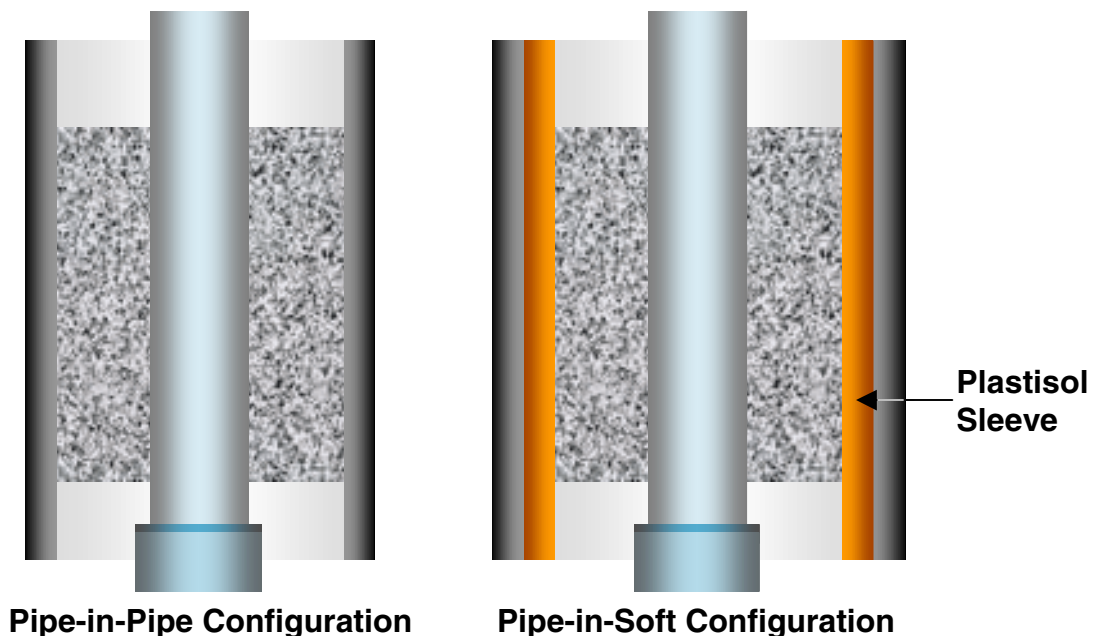
Annular Seal Testing

Casing Pressure Test

These studies investigate the effect that casing pressure tests have on annular seal. Many people think that casing pressure tests expand the casing and create pressures on and increase the inner diameter of the surrounding cement. The stresses and physical changes can adversely strain the cement and potentially deform the cement irrecoverably.

A laboratory model has been developed to simulate casing pressure tests (**Figure 20**). The model can be made in two different configurations— pipe-in-pipe and pipe-in-soft. This is to simulate high-restraint and low-restraint formations. This can help identify differences between a hard formation and a loosely consolidated formation. The pressure testing will be initiated after different times of cement curing to determine the effects of curing time before pressure testing. Multiple cycles of pressure testing will be performed.

Figure 20—The Two Configurations for the Casing Pressure Test

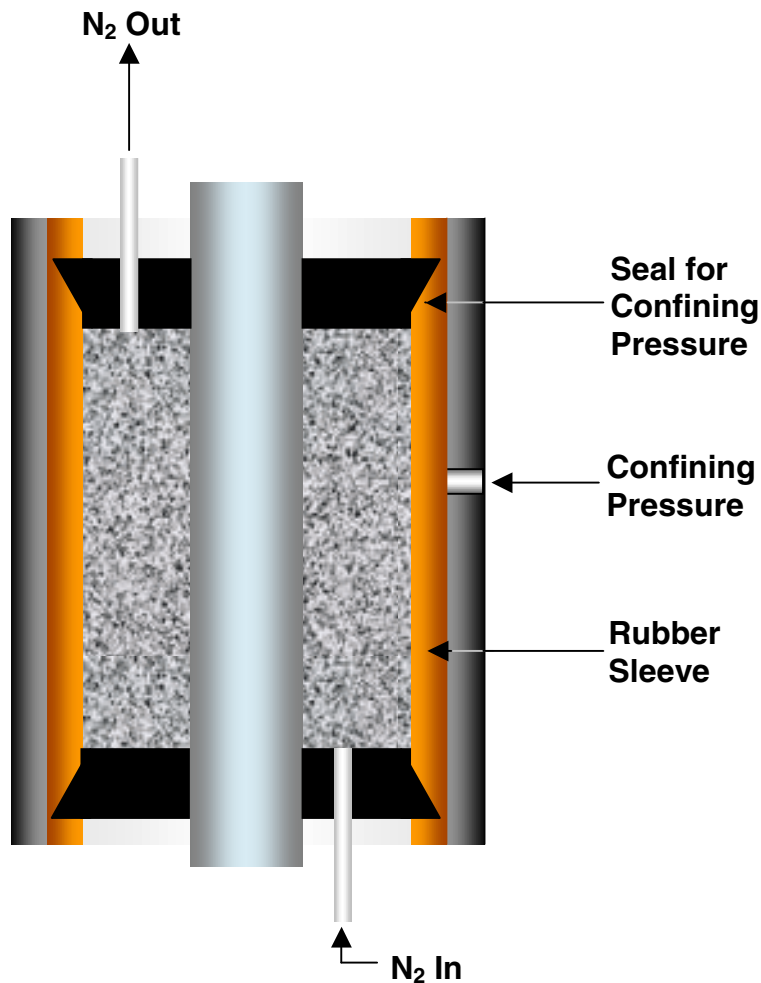




Cementing Solutions, Inc.

A key component of this project is investigating cement's capability to maintain its seal under downhole stresses. An annular seal model has been developed that can measure bulk permeability across a cement system that has been stressed from temperature or pressure cycling. As with some of the other testing, the annular seal test model will have pipe-in-pipe and pipe-in-soft configurations to simulate high and low restraints, respectively. **Figure 21** shows the pipe-in-soft configuration of the annular seal model.

Figure 21—Cross-Section of Annular Seal Model for Pipe-in-Soft Configuration



The inner pipe of the model will be the main conduit for the stressing medium. For instance, the inner pipe can contain heated fluids while the remainder of the system is at a different temperature; this simulates the hotter formation fluids that can be experienced during production. The inner pipe of the model can also be pressured up to 5,000 psi, simulating casing pressure testing which is believed by many to lead to loss of annular seal because of the expanding and contracting casing.



Cementing Solutions, Inc.

For the temperature and pressure cycling, the model will be subjected to five complete temperature and pressure cycles and then annular seal testing will be done.

In the pipe-in-soft configuration, the rubber sleeve surrounding the cement is able to withstand 25 psi. During the annular seal test, pressure can then be applied to the outside of the rubber sleeve, allowing the sleeve to make a fluid-tight seal on the outside of the cement. Pressurized nitrogen gas (<25 psi) can then be applied axially across the cement and the only paths for fluid flow is through cement or along the interface between the cement and the inner pipe. Any exiting nitrogen flow rate can be monitored and measured. In the pipe-in-pipe configuration, there is no need for the rubber sleeve or the exterior confining pressure.

Annular Seal Testing Procedure

These procedures are for the use of the Pipe-in-Soft annular seal apparatus and the Pipe-in-Pipe annular seal apparatus. These procedures are organized by apparatus and are to be used specifically for that type of apparatus. The Pipe-in-Soft apparatus is to be used with cores that were formed using a soft gel mold surrounding the cement slurry to form a core that was cured to set by using a semi-restricting force on the outside of the core. The Pipe-in-Pipe apparatus is to be used with those cores that were made inside iron pipes, giving the cement slurry a restricting force outside of the core.

Testing Procedure for Pipe-in-Soft:

1. After the core is cured, place the core inside the gel mold sleeve.
2. Place the core and sleeve inside the Pipe-in-Soft steel cell.
3. Once inside, both ends of the core are supported with O-rings.
4. The O-rings are then tightened to close off air-leaks that might be present.
5. Using water, pressurize the exterior circumference of the sleeve to 25 psi. Once the pressurized water is applied to the cell, check for leaks on the ends of the cell.
6. Using the cell's end caps, cap off both ends of the steel cell. One end cap has a fitting that allows for N₂ gas to be applied into the cell, and the other end cap allows for the gas to exit the cell.
7. Attach the pressure in-line to one end and then attach the pressure out-line to the other end.
8. Apply pressure to the in-line. (Do not exceed 20 psig.) Measure the out of the out-line using flowmeters.



Cementing Solutions, Inc.

Testing Procedure for Pipe-in-Pipe:

1. After the core is cured inside the iron pipe, using iron end caps, cap off each end of the pipe. Each end cap has a fitting that allows for gas to be applied into the pipe on one end, and also allows for the gas to exit the pipe on the other end.
2. Attach the pressure in-line to one end, and then attach the pressure out-line to the other end.
3. Apply pressure to the in-line. (Do not exceed 20 psig.) Measure the pressure out of the out-line using flowmeters.

As with the shear bond tests, temperature and pressure cycling were also performed with the annular seal tests. **Table 11** shows the results of the annular seal testing.

Table 11—Annular Seal Tests

Annular Seal	Type I	Foamed
Initial Flow — Pipe-in-Pipe	0 Flow	0 Flow
Initial Flow — Pipe-in-Soft	0 Flow	0.9K(md)Liquid(retesting)
Temperature Cycled — Pipe-in-Pipe	0 Flow	0 Flow
Temperature Cycled — Pipe-in-Soft	0 Flow	123K(md)(retesting)
Pressure Cycled — Pipe-in-Pipe	0 Flow	0 Flow
Pressure Cycled — Pipe-in-Soft	27K(md)	0.19K(md)(cracked during cycling)



Cementing Solutions, Inc.

Mathematical Modeling

The University of Houston performed finite element analysis (FEA) of the laboratory models used in the project (temperature and pressure cycling models) so the laboratory results can be compared to the mathematical modeling. The mathematical modeling was analyzed to determine if the stresses associated with the temperature and pressure cycling result in loss of annular seal. These studies will then be compared with other FEA work.

The mathematical simulations reveal that the Pipe-in-Pipe configuration is very stable and retains its integrity even at sufficiently large loading conditions. This is mainly due to the order of magnitude difference in the Young's Modulus of the steel pipe and the cement sheath. However, for the Pipe-in-Soft configuration, large deformations are observed in the cement and the plastisol layer, which suggests potential loss in integrity of cement-casing bonding and hence the annular seal. This result must be confirmed by experiments and further analysis to account for the interfacial bonding.

The cement material properties and cement thickness have negligible effect on the overall stress distribution in the Pipe-in-Pipe configuration. However, for the Pipe-in-Soft configuration, the material properties become significant. Thermal stresses lead to tensile stresses, which can result eventually in tensile failures at high temperatures. A very sharp stress contrast is observed in all cases at the casing-cement interface.

Details of the mathematical modeling procedure, results, and conclusions are contained in the Mathematical Modeling appendix to this report.



Appendix: Mathematical Modeling

Introduction

In understanding the long-term integrity of cement in deepwater systems and determining the properties that affect the ability of cement to seal fluids, a principal step is to mathematically model the system to study different stress-causing phenomena. Besides enabling researchers to theoretically predict the effect of various stress conditions such as temperature cycling, pressure cycling, etc., mathematical modeling will also provide a means of justification to test the designs and steer the direction of laboratory testing. The results of these models will be analyzed to determine if the stresses associated with the stress-causing conditions will result in loss of annular seal of cement.

Further, in the presence of asymmetrical far-field stresses, internally pressurized and cemented wells can experience both tensile and compressive stresses. As a result, fracture initiation (if the internal pressure is sufficiently high) is a function of the cement's tensile strength and the tensile stresses induced within the cement sheath. This makes some portions of the cement sheath particularly vulnerable to fracture initiation. The stress distribution in casing-cement-rock system needs to be estimated as a single continuous problem over disjointed domains. It is presumed that a fundamental study of such systems will provide valuable clues on the selection of choice of well completion and appropriate cement properties.

Two main configurations have been considered for modeling purposes: Pipe-in-Pipe and Pipe-in-Soft (see **Figure 1**). The focus will be on establishing a mathematical framework for analysis of different loading conditions, temperature gradients and material properties and their effect on the induced stress distribution. Long term effects such as subsidence and compaction may also be interpreted and incorporated through appropriate changes to loading conditions. A parametric variation of cement's material properties and thickness has been studied to determine the role of each variable toward the overall stress and strain distributions.

The following sections describe briefly the mathematical model and discuss the main results of the analysis.



Mathematical Model

In practice, the magnitude and orientation of the *in situ* stress field is altered locally, as a result of the drilling of a well. In addition, when internal wellbore pressure and temperature gradients are present, the pre-existing stress fields are distorted significantly to give rise to new induced stresses. The following equation summarizes the regular elasticity problem, with internal wellbore pressure and far-field boundary conditions:

$$\begin{aligned}\nabla \cdot \sigma &= 0 && \text{on } B \\ \varepsilon &= \frac{1}{2}(\nabla u + \nabla u^T) \\ \sigma &= L\varepsilon \\ e_i \cdot (\sigma \cdot n) &= \hat{\sigma}_1 && \text{on } \partial B_{1i}\end{aligned}\tag{1}$$

where σ is the stress tensor, ε is the strain tensor, u is the displacement vector and L is the elasticity tensor. Equation 1 represents the traction boundary condition specified on the internal and external boundary.

In deepwater conditions, the subsea temperature will be lower ($< 5^\circ\text{C}$) than the surface temperature. However, after prolonged production, the pipelines can reach much higher temperature (about 100°C). As a result, there is a temperature gradient present across the annular cylinders (casing and cement sheath).

When the temperature rise in a homogeneous body is not uniform, different elements of the body tend to expand at different rates, and the requirement that the body remain continuous conflicts with the requirement that each element expand by an amount proportional to the local temperature rise. Thus the various elements exert upon each other a restraining action resulting in continuous unique displacements at every point. The system of strains produced by this restraining action cancels out all, or part of, the free thermal expansions at every point so as to ensure continuity of displacement. This system of strains must be accompanied by a corresponding system of self-equilibrating stresses. These stresses are known as thermal stresses. A similar system of stresses may be induced in a structure made of dissimilar materials even when the temperature change throughout the structure is uniform. Also, if the temperature change in a homogeneous body is uniform and external restraints limit the amount of expansion or contraction, the stresses produced in the body are termed as thermal stresses.

In a completed wellbore system, all these three conditions are present and contribute toward thermal stresses, namely non-uniform temperature distribution, dissimilar materials (casing, cement, etc.), and external restraints.



Cementing Solutions, Inc.

The desired energy equation for an isotropic, elastic solid is

$$k\nabla^2 T = C_{e=0} \frac{\partial T}{\partial t} + \beta T_0 \frac{\partial e'}{\partial t} \quad (2)$$

where k is the thermal conductivity, T is the temperature rise from the initial uniform temperature T_0 , of the stress-free state, $\beta = E\alpha/(1-2\nu)$, $C_{e=0}$ is the heat capacity per unit volume at zero strain and e' is the dilatation.

This equation is based on the Fourier law of heat condition and the linear thermoelastic stress-strain relations, and it shows that the temperature distribution in a body depends upon the dilatations through out the body. Thus, the temperature and strain (and hence, stress) distributions are coupled and an exact analysis would require the simultaneous determination of the stress and temperature profiles.

For numerical modeling purposes, the casing-cement-rock system is considered as concentric cylindrical structures, in continuous contact with each other. The Pipe-in-Pipe configuration represents a hard formation, while the Pipe-in-Soft configuration represents a soft formation. A generic, 3D finite element model is developed for this composite system using Abaqus 5.7 and Matlab 6.0 (see **Figure 2**). Pure elastic stress-strain analysis is performed using customized Matlab programs, while thermal stress analysis is handled using Abaqus. For laboratory tests involving homogeneous casing and confining pressures, the system is axi-symmetric and hence only a quadrant of the annular structure is studied.

Assumptions

1. The system can be modeled using linear elastic theory.
2. The composite system retains continuity at the interfaces.
3. The system is axi-symmetric because of the boundary conditions.
4. All materials are homogeneous and continuous.
5. Plastisol has the same material properties as that of rubber.
6. Plane stress condition is valid.



Cementing Solutions, Inc.

Stress Conditions

The following stress-causing conditions have been considered for mathematical modeling purposes:

- Normal production operation
- Pressure cycling (casing pressure)
- Subsidence, compaction (confining pressure)
- Temperature cycling (thermal stress)

The normal production operation includes an operating casing pressure and an external confining pressure (*in situ* stresses), along with a steady thermal gradient. All elastic and thermoelastic simulations represent steady state conditions. A fully rigorous coupled thermoelastic equation is considered for numerical modeling purposes. However, the effect of dilatation is negligible when the system is allowed to evolve up to steady state.



Parametric Studies

The following parameters and cement properties have been varied to study their influence on stress distribution in the cement:

- Casing pressure (100 to 10,000 psi)
- Confining pressure (100 to 1000 psi)
- Temperature gradient (80 to 180° F)
- Young's modulus (1000 to 7000 psi)
- Poisson ratio (0.15 to 0.45)
- Cement thickness (1 to 7 inches)

All numerical simulations are representative of the laboratory testing conditions, with the parameter ranges provided by CSI from their experimental results. All parametric studies are with respect to the following reference case:

Parameter	Value
Casing pressure	500 psi
Confining pressure	500 psi
Young's modulus	5000 psi
Poisson ratio	0.35
Cement thickness	1 inch
No thermal gradient	

Results and Discussion

Stress, displacement and temperature profiles for both the configurations are computed using a 3D finite element model, with quadratic elements. **Figure 3** shows the first principal stress and horizontal displacement profiles for a representative case (Pipe-in-Pipe), with an internal casing pressure of 500 psi and no confining pressure or thermal gradient. A Young's Modulus of 5,000 psi and a Poisson ratio of 0.35 were used for the cement sheath. It may be observed that most of the stress variation is arrested within the inner pipe (made of steel), with a relatively high Young's Modulus (3.05×10^7 psi). As a result, very little stress is transferred across to the cement sheath. The outer pipe experiences hardly any load in the absence of a direct confining pressure, as is evident from the negligible stresses and displacements.



Cementing Solutions, Inc.

Casing Pressure

The casing pressure is varied from 100 to 10,000 psi for the Pipe-in-Pipe configuration, in the absence of any confining pressure or thermal gradient. The first principal stress and horizontal displacement along the x-axis is plotted in **Figure 4**. Clearly, the inner steel pipe limits the transfer of any load across to the cement sheath, because of its high Young's Modulus. A sharp stress contrast is observed at the casing-cement interface, while the continuity requirement of displacement at the interface manifests itself as differing gradients in the two materials and reaching zero at the external boundary. Since the inner steel pipe is the dominant material as far as the load distribution is concerned, very little effect is felt by the cement sheath.

The same result is observed for the stress distribution, even more pronounced, in the Pipe-in-Soft configuration (see **Figure 5**) in the absence of confining pressure. However, larger displacements are observed in comparison to the Pipe-in-Pipe case. This suggests that the cement sheath can displace more from its set position and can potentially lose its annular seal in a soft formation.

Confining Pressure

In addition to base casing pressure of 500 psi, a confining pressure is applied on the outside ranging from 100 to 1000 psi. All other conditions are held constant as before. The stress profile (shown in **Figure 6**) shows a similar result as before, since both the inner and outer pipes are assumed to be of the same material (steel). The cement sheath has a reduced and almost uniform stress distribution, while the steel pipes arrest most of the variation.

For the Pipe-in-Soft configuration, when a confining pressure is present, both the cement and the plastisol layer undergo relatively larger deformations. However, increasing the confining pressure from 100 to 1000 psi has little effect on the magnitude of displacements in all the three materials (see **Figure 7**).

Young's Modulus and Poisson Ratio

The cement material properties (Young's Modulus and Poisson Ratio) are varied to study their effect on stress distribution in the Pipe-in-Pipe configuration. The Young's modulus is varied between 1000 and 7000 psi, and the Poisson ratio is varied from 0.15 to 0.45. Since the steel pipe transfers very little stress to the cement sheath, there is a negligible influence on the stress and strain distribution in the cement sheath (see **Figure 8** and **Figure 9**).



Cementing Solutions, Inc.

Cement Thickness

The thickness of the cement layer is varied between 1 to 7 inches for the Pipe-in-Pipe configuration. As the thickness increases, a larger portion of the cement is under compression, which results in an increased horizontal displacement for the same casing and confining pressure, as shown in **Figure 10**. It may be observed that the same amount of net displacement is experienced by the inner and outer steel pipes, in comparison to the more flexible cement sheath.

Temperature Gradient

In addition to a casing pressure of 500 psi and a confining pressure of 500 psi, a thermal gradient is applied across the concentric cylinders for the Pipe-in-Pipe configuration. The external temperature on the outer pipe is held constant at 68°F, and the temperature at the inner surface of the inner pipe is varied between 80°F and 180°F. The temperature profile is symmetric, and varies only along the radial direction (shown in **Figure 11**). While the elastic stress acts in compression, the thermal stress arising due to non-uniform and dissimilar expansion of the composite system can lead to tensile stresses. As a result, the net stress experienced by the system is controlled by the dominant stress source. It may be observed from the displacement profile (**Figure 12**) that the thermal stresses tend to expand the concentric cylinders. At high temperatures and low external loads, the thermal stress can be controlling the net displacement and vice versa at low temperatures and high external loads.



Cementing Solutions, Inc.

Conclusions

In summary, from the above simulations performed to verify and complement the laboratory testing, it is observed that the Pipe-in-Pipe configuration is very stable and retains its integrity even at sufficiently large loading conditions. This is mainly due to the order of magnitude difference in the Young's Modulus of the steel pipe and the cement sheath. It is suggested to study the behavior of these systems at higher cement Young's Modulus. However, for the Pipe-in-Soft configuration, large deformations are observed in the cement and the plastisol layer, which suggests potential loss in integrity of cement-casing bonding and hence the annular seal. This, however, must be confirmed by experiments and further analysis to account for the interfacial bonding.

The cement material properties and cement thickness have negligible effect on the overall stress distribution in the Pipe-in-Pipe configuration. However, for the Pipe-in-Soft configuration, the material properties become significant. Thermal stresses lead to tensile stresses, which can result eventually in tensile failures at high temperatures. A very sharp stress contrast is observed in all cases at the casing-cement interface.

The mathematical model framework is generic and can be easily extended to include several other scenarios such as heat generation (due to heat of hydration) in the cement layer, multi-layered formation, pressure transmission of gas flow, etc.



Cementing Solutions, Inc.

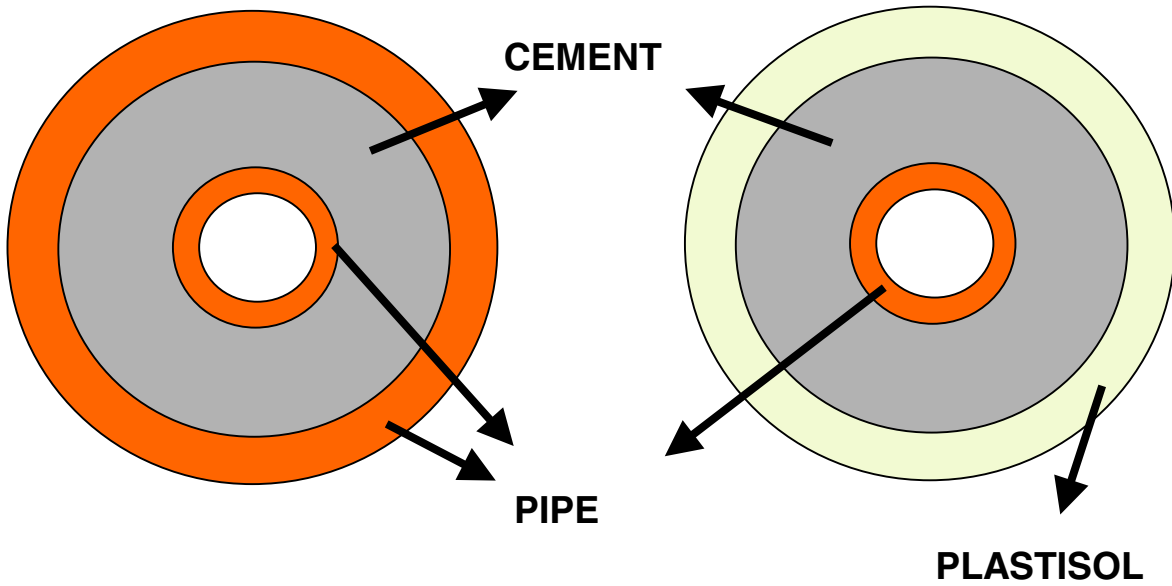


Figure 1 — Pipe-in-Pipe and Pipe-in-Soft Configurations

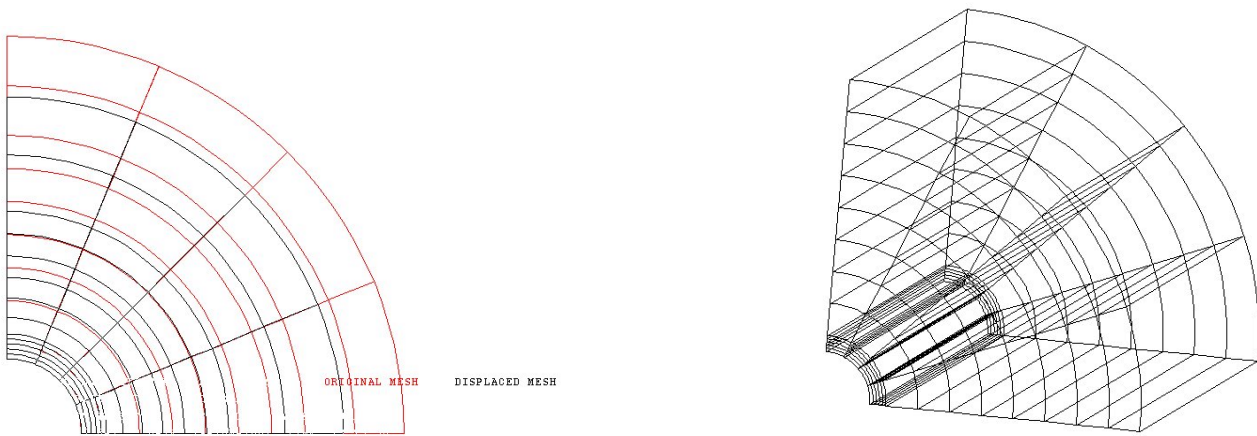


Figure 2—3D Finite Element Model Grid



Cementing Solutions, Inc.

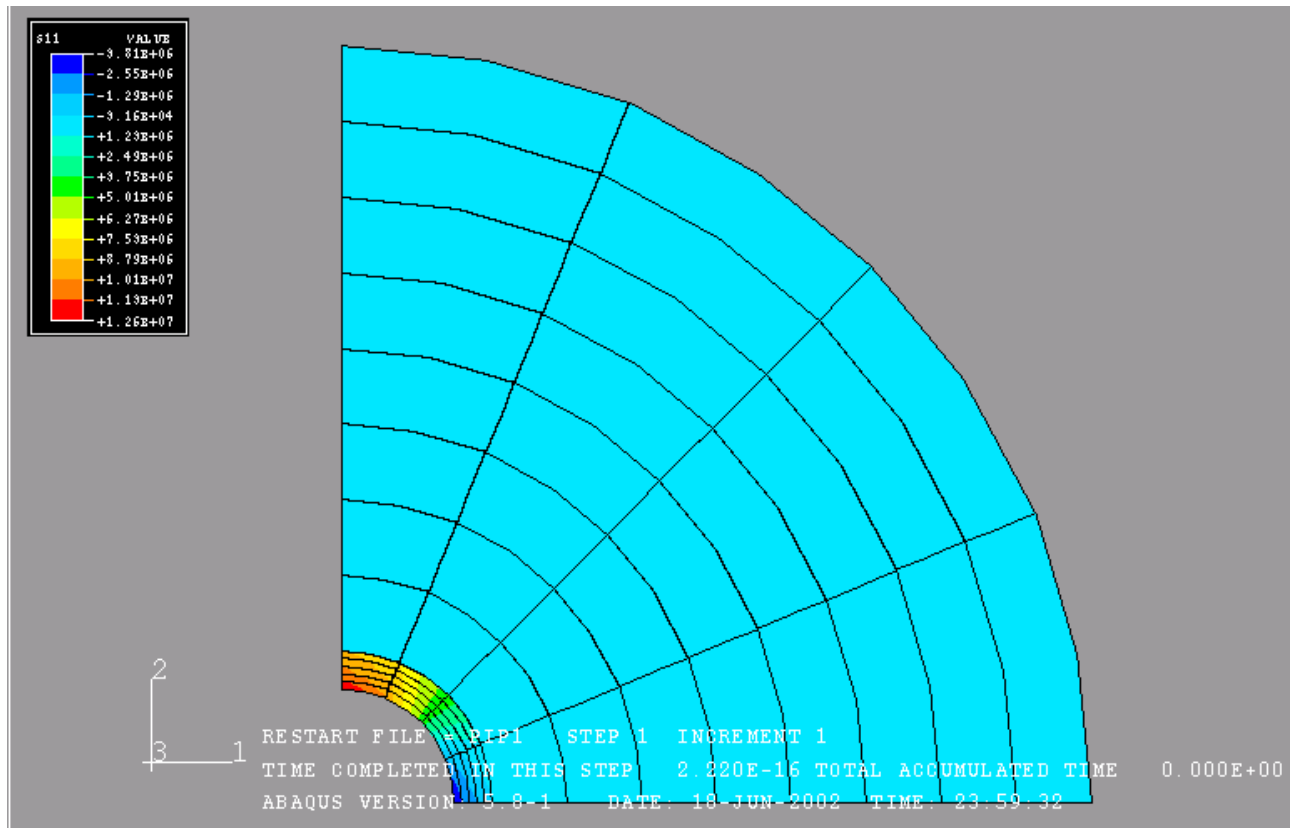


Figure 3a—First Principal Stress Profile (PIP; No Confining Pressure)



Cementing Solutions, Inc.

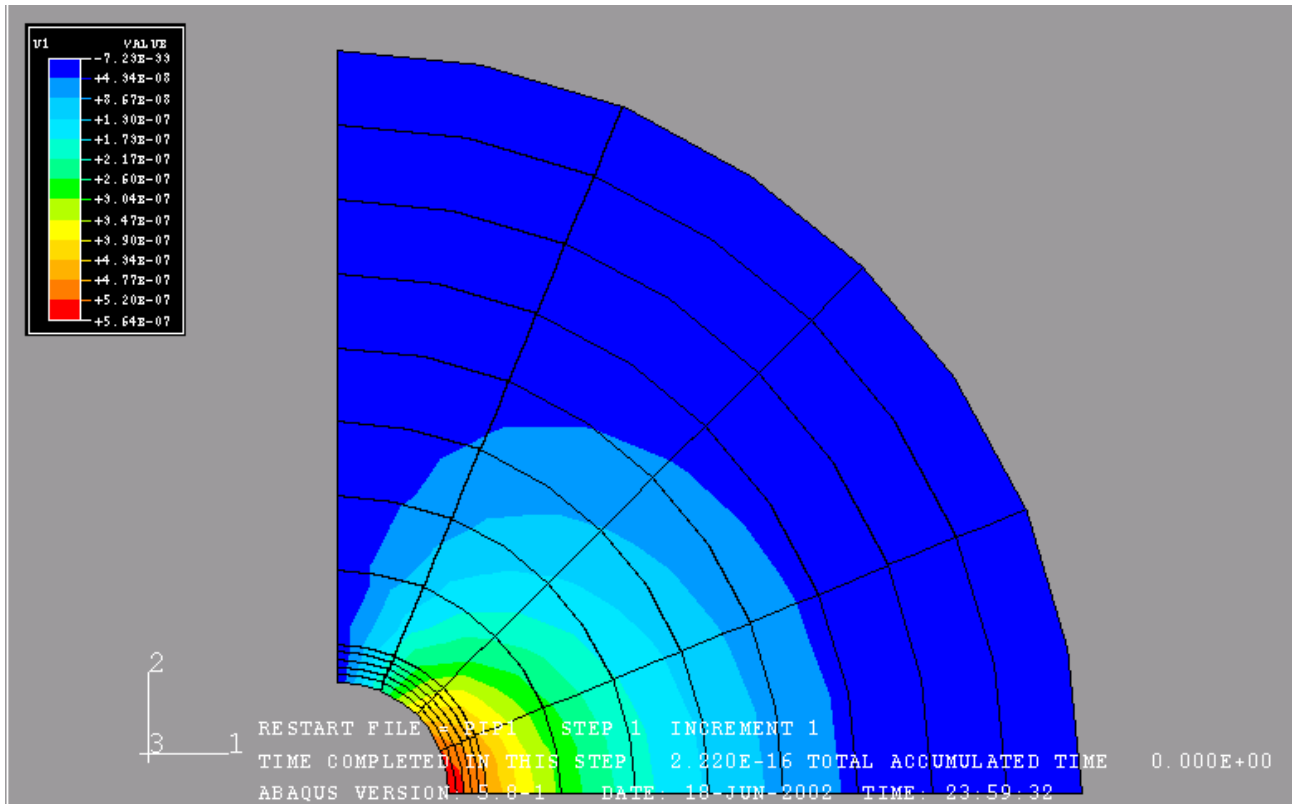


Figure 3b—Horizontal Displacement Profile (PIP; No Confining Pressure)



Cementing Solutions, Inc.

Young's Modulus **5000 psi**
Poisson Ratio **0.35**
Confining Pressure **None**
Cement Thickness **1 inch**
Temperature Gradient **None**

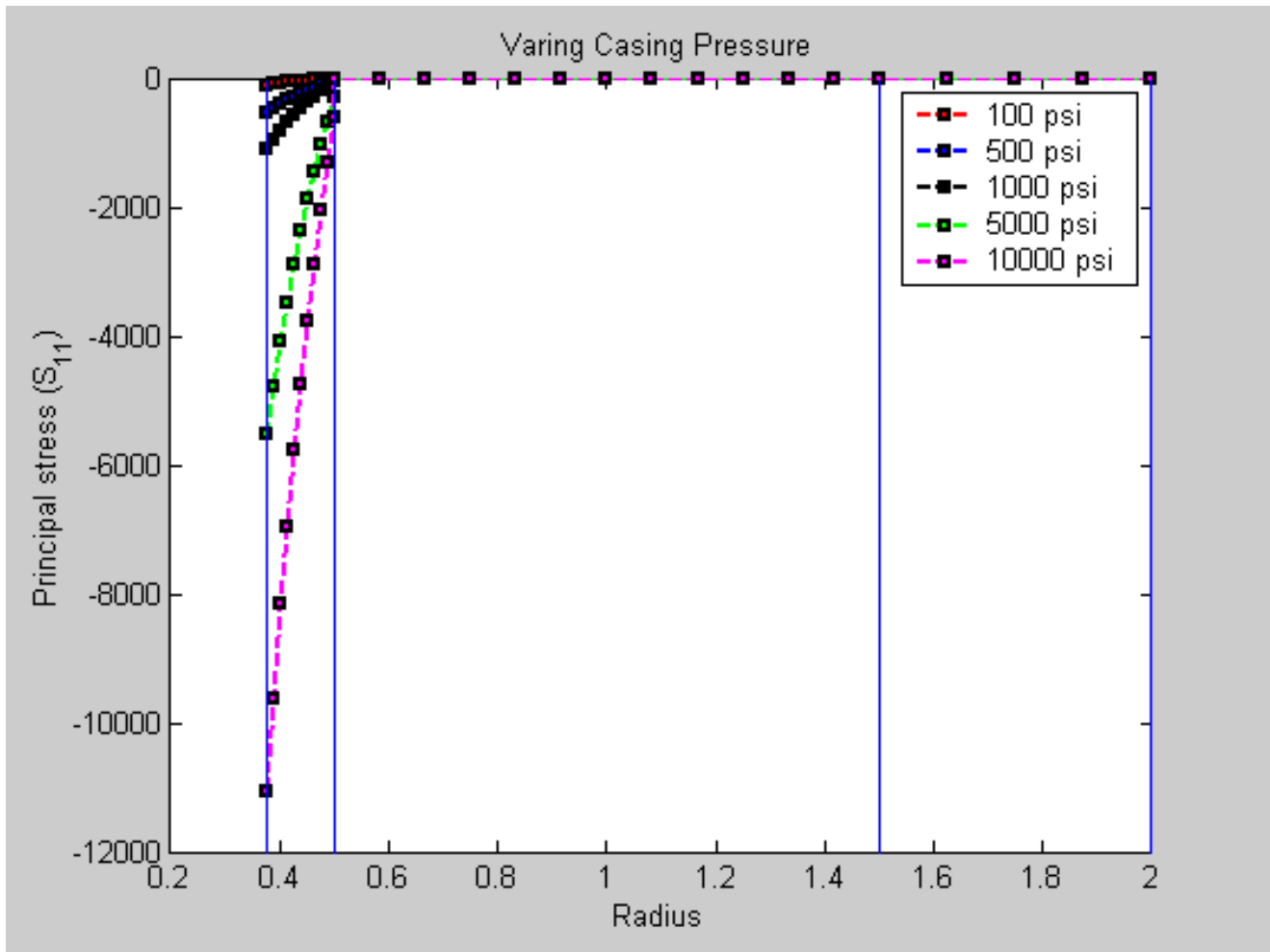


Figure 4a—First Principal Stress Profile along X-Axis (PIP)



Cementing Solutions, Inc.

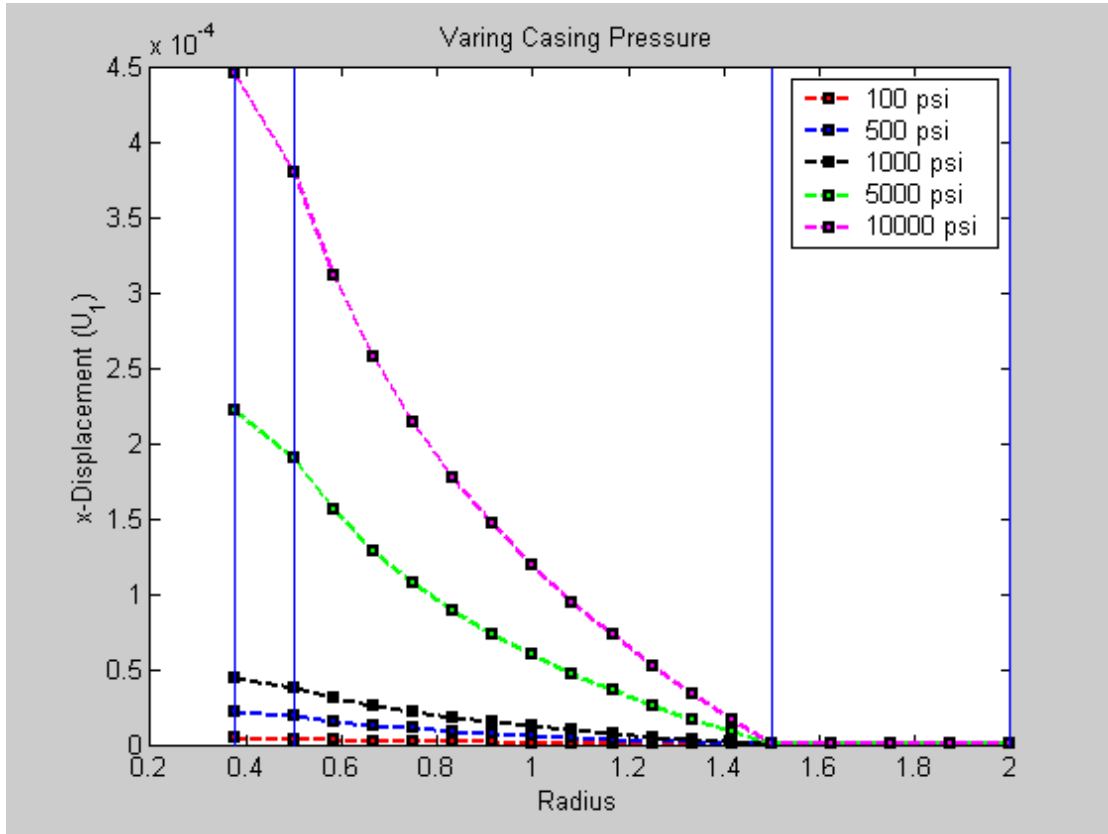


Figure 4b—Horizontal Displacement Profile along X-Axis (PIP)



Cementing Solutions, Inc.

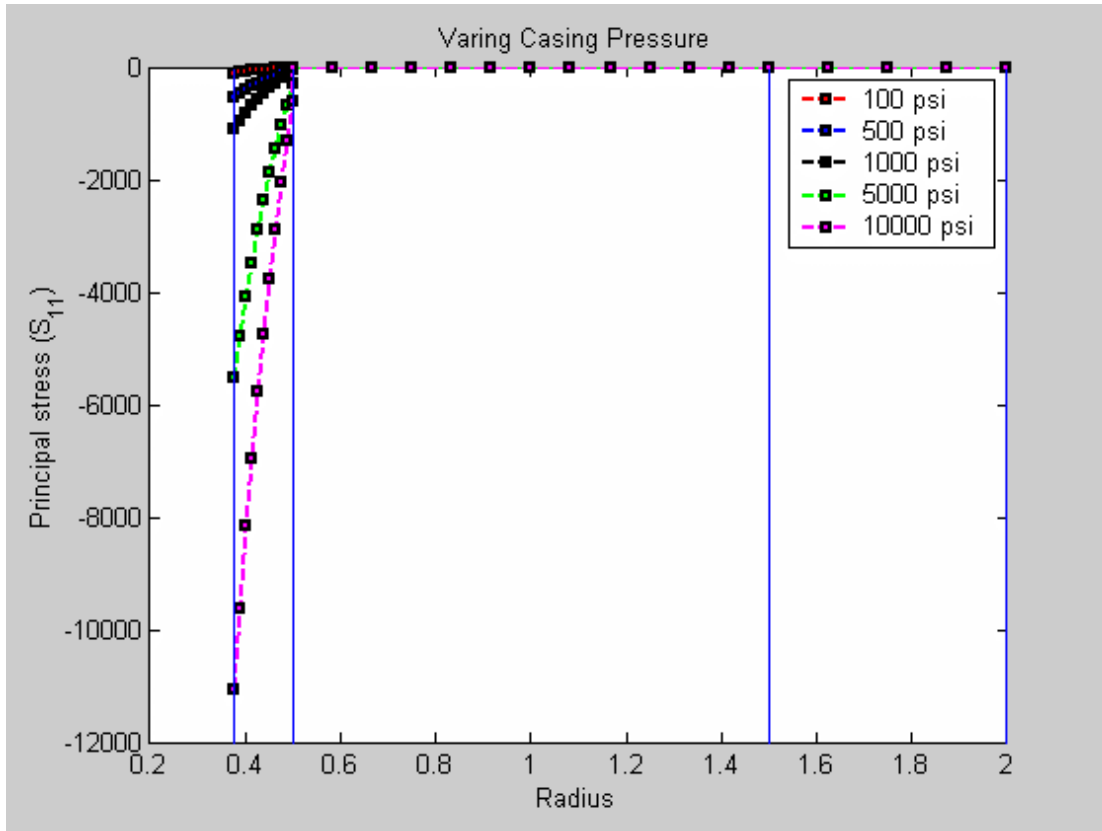


Figure 5a—First Principal Stress Profile along X-Axis (PIS)



Cementing Solutions, Inc.

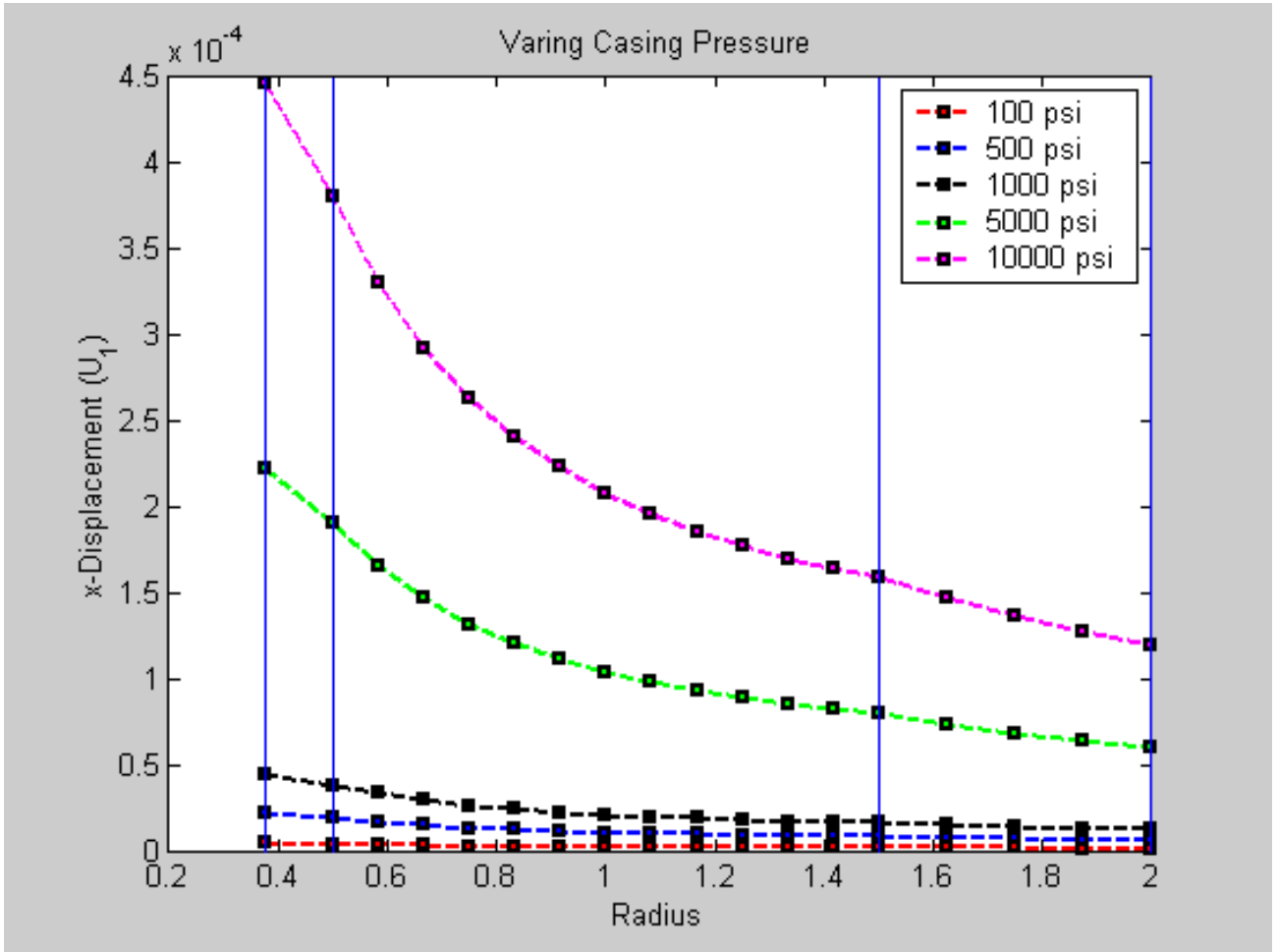


Figure 5b—Horizontal Displacement Profile along X-Axis (PIP)



Cementing Solutions, Inc.

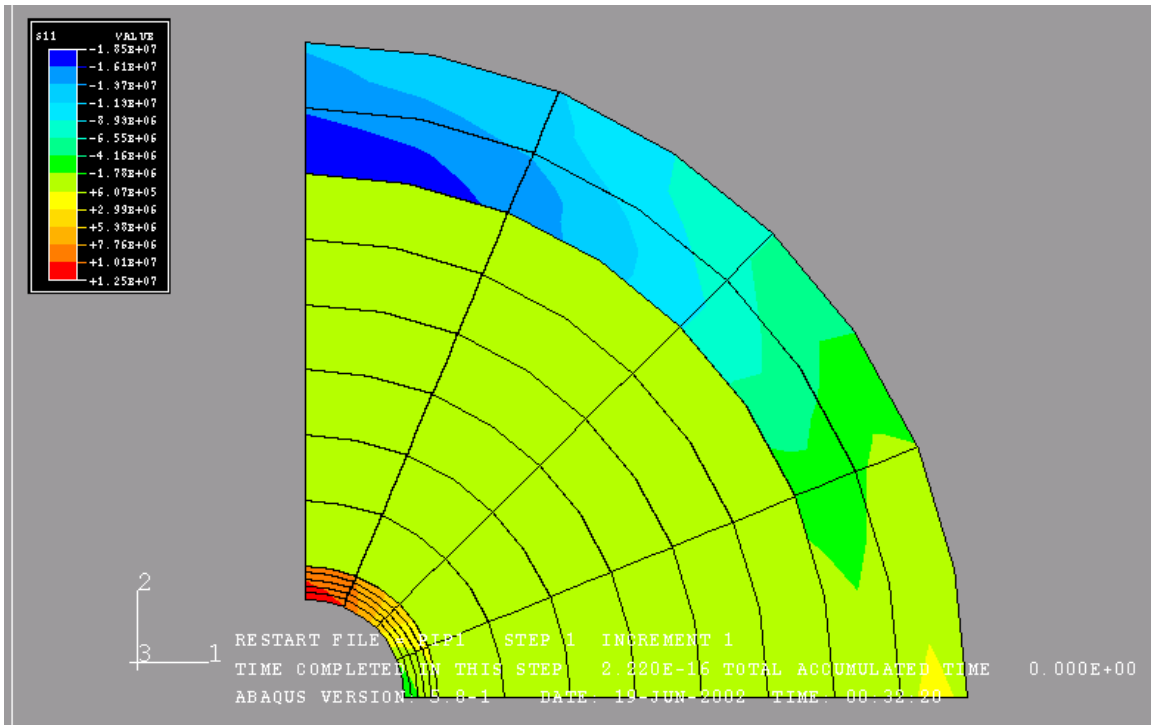


Figure 6a—First Principal Stress Profile (PIP; with Confining Pressure)



Cementing Solutions, Inc.

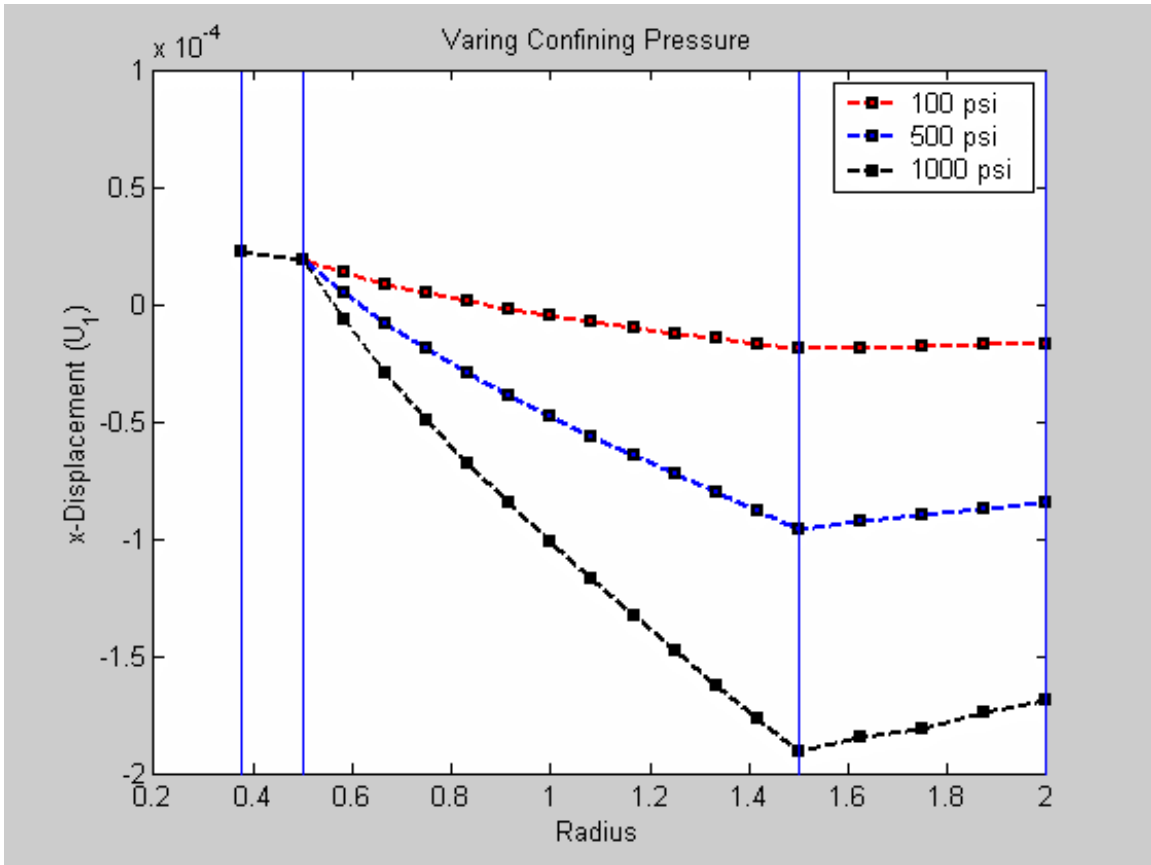


Figure 6b—Horizontal Displacement Profile (PIP; with Confining Pressure)



Cementing Solutions, Inc.

Young's Modulus **5000 psi**
Poisson Ratio **0.35**
Confining Pressure **500 psi**
Cement Thickness **1 inch**
Temperature Gradient **None**

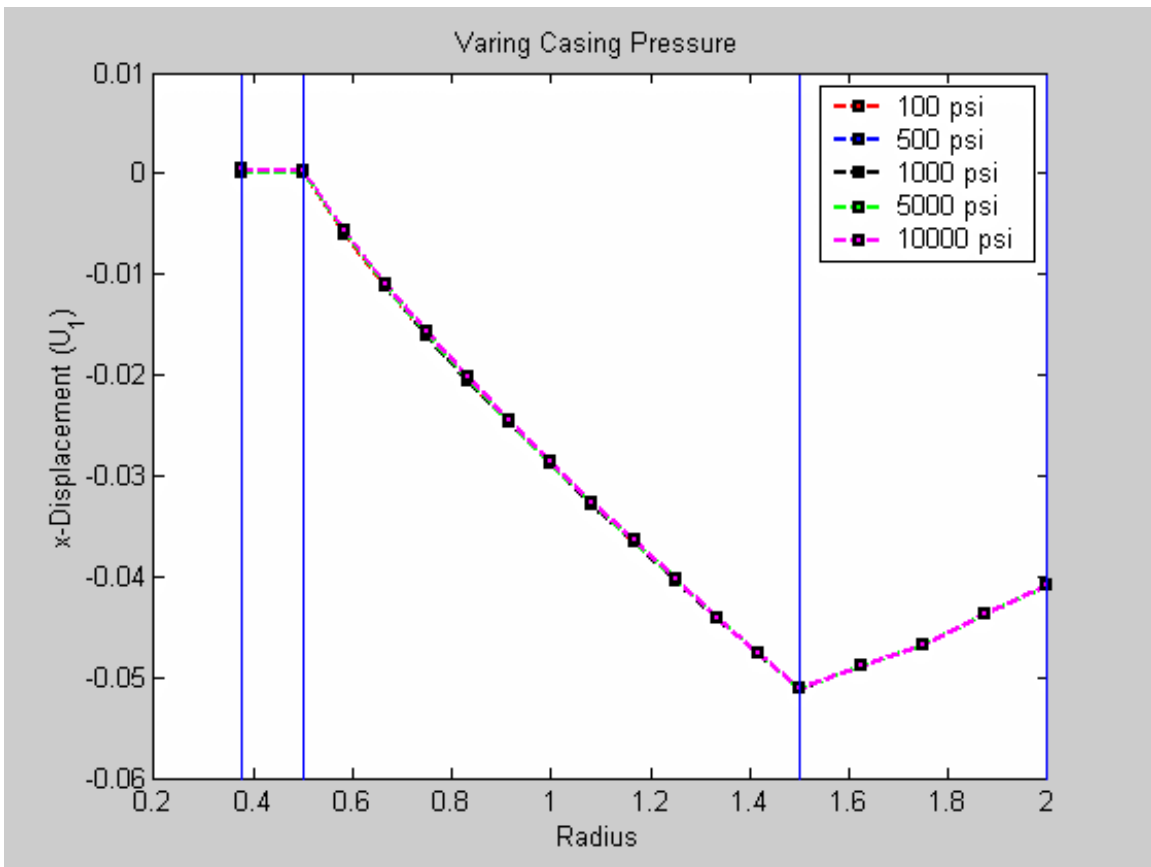


Figure 7—Horizontal Displacement Profile (PIS; with Confining Pressure)



Cementing Solutions, Inc.

Confining Pressure	500 psi
Poisson Ratio	0.35
Casing Pressure	500 psi
Cement Thickness	1 inch
Temperature Gradient	None

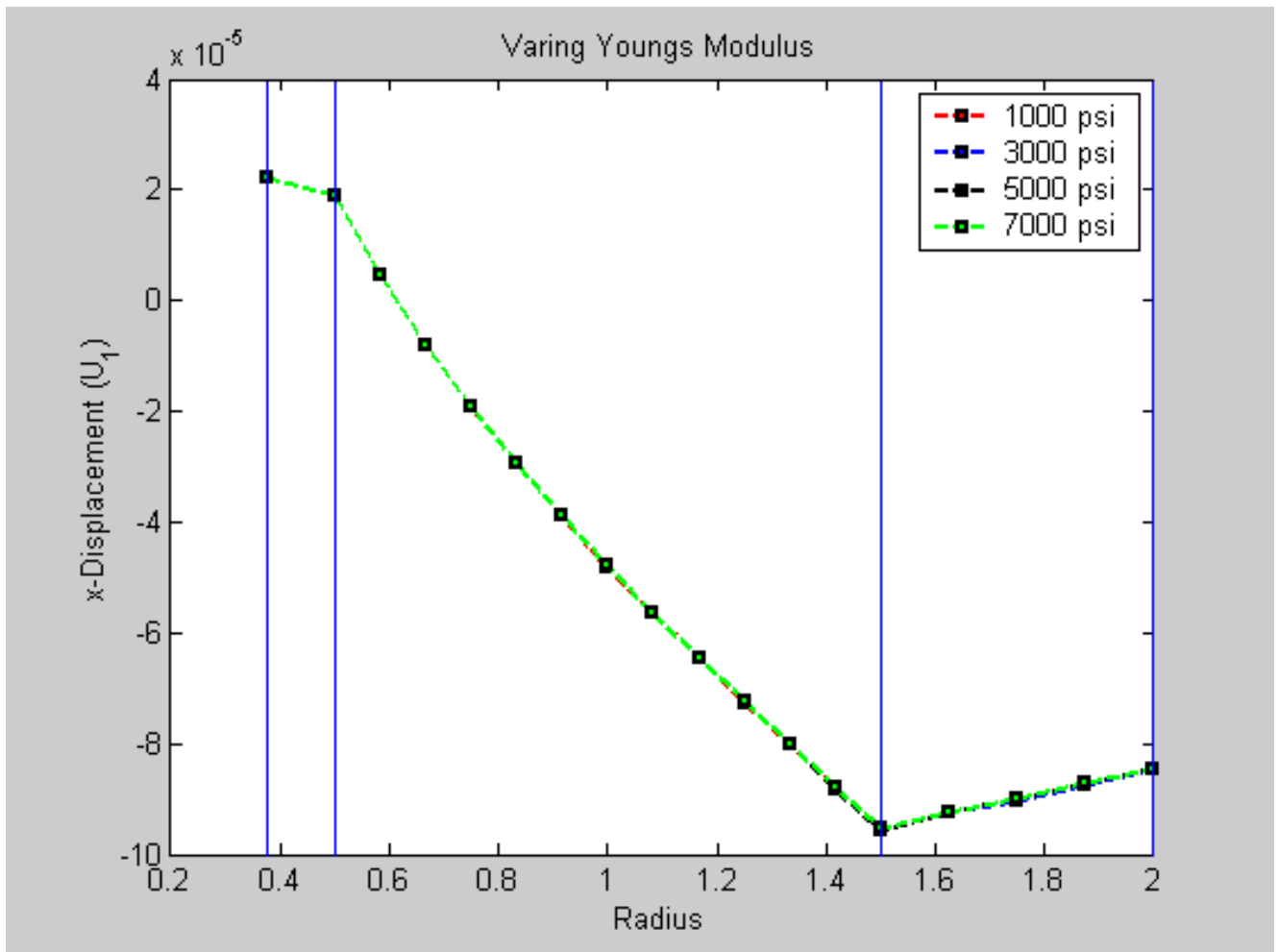


Figure 8—Horizontal Displacement Profile (PIP; Varying Young's Modulus)



Cementing Solutions, Inc.

Confining Pressure	500 psi
Young's Modulus	5000 psi
Casing Pressure	500 psi
Cement Thickness	1 inch
Temperature Gradient	None

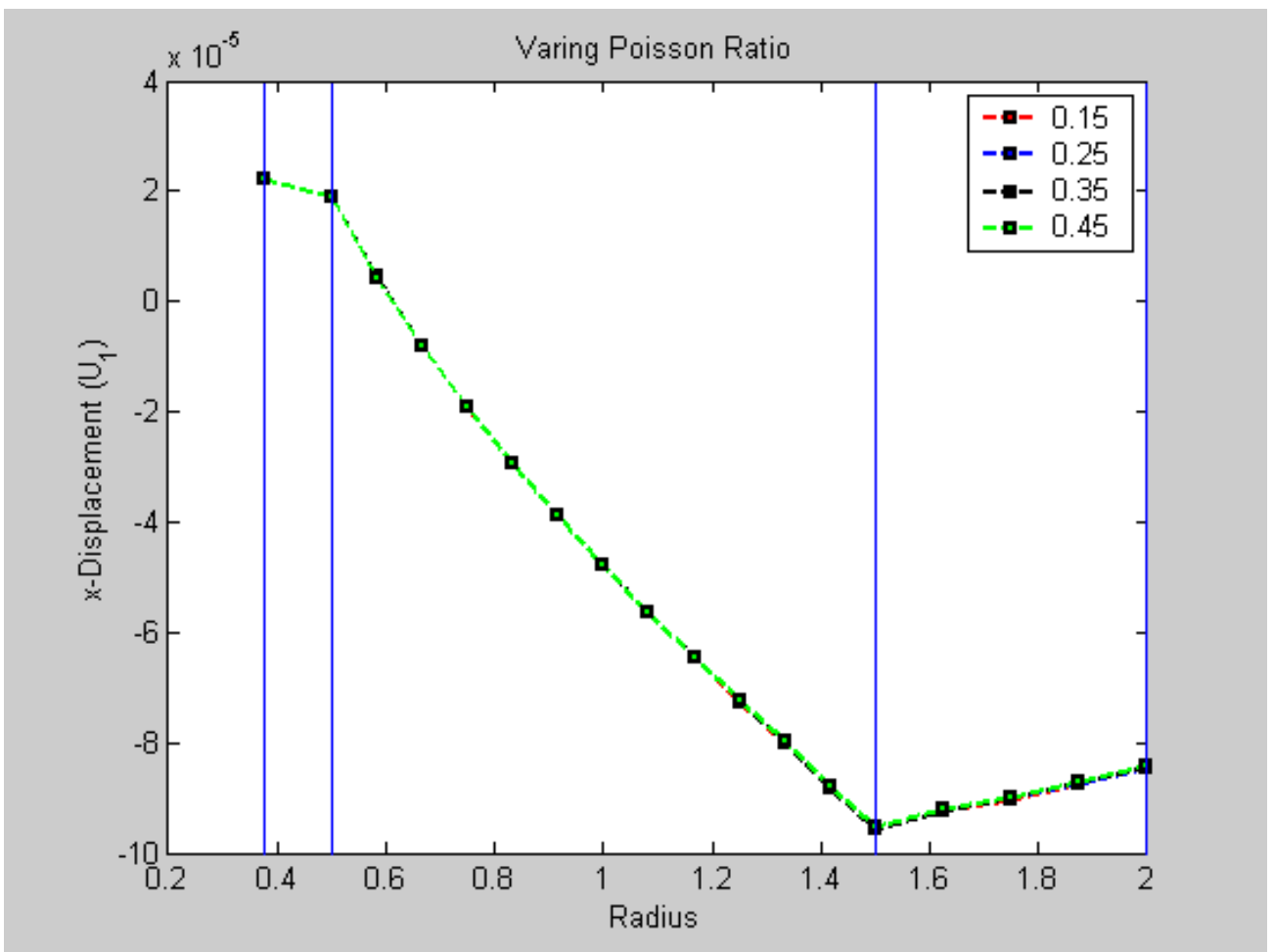


Figure 9—Horizontal Displacement Profile (PIP; Varying Poisson Ratio)



Cementing Solutions, Inc.

Confining Pressure	500 psi
Young's Modulus	5000 psi
Casing Pressure	500 psi
Poisson Ratio	0.35
Temperature Gradient	None

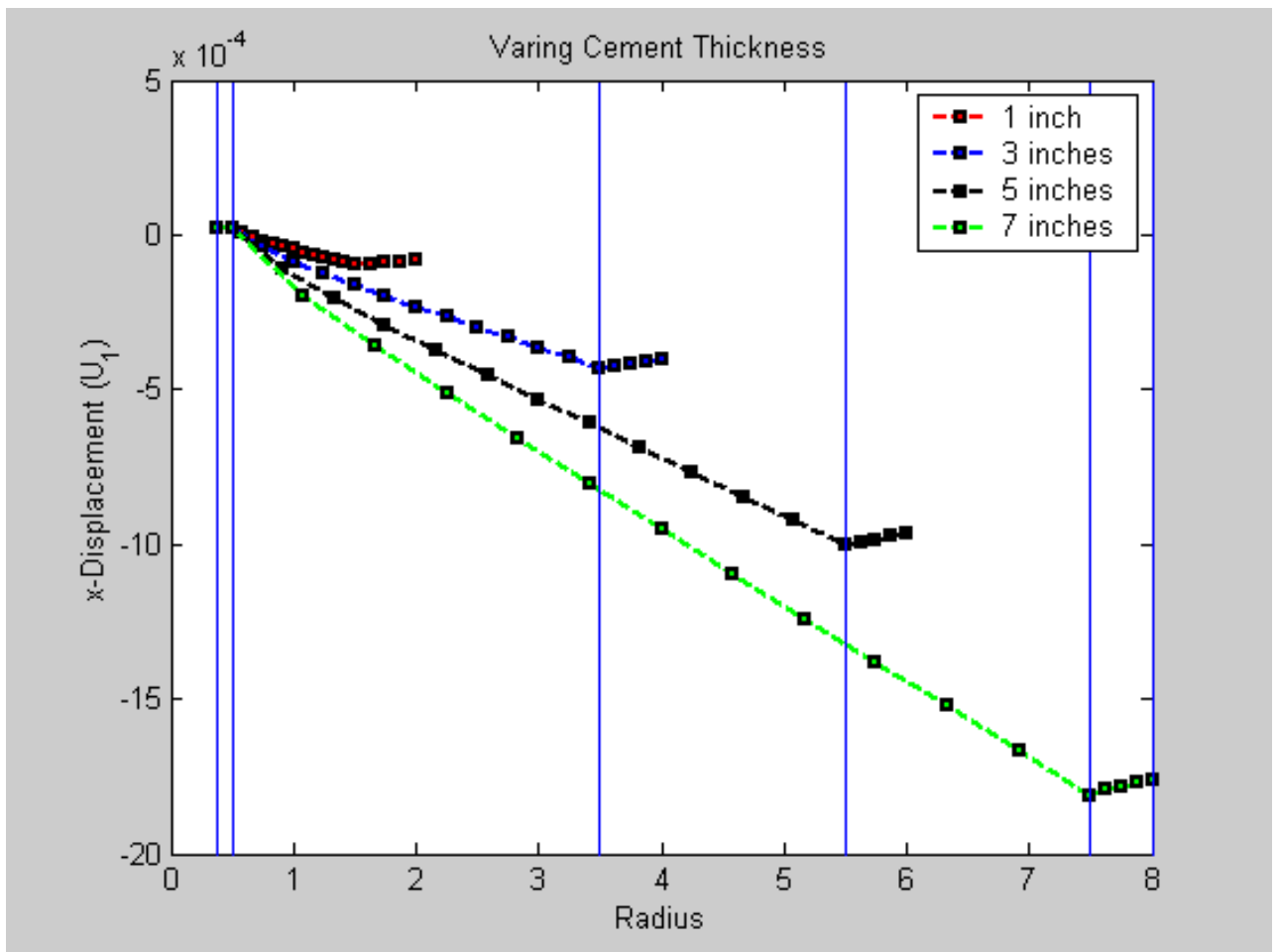


Figure 10—Horizontal Displacement Profile(PIP; Varying Cement Thickness)

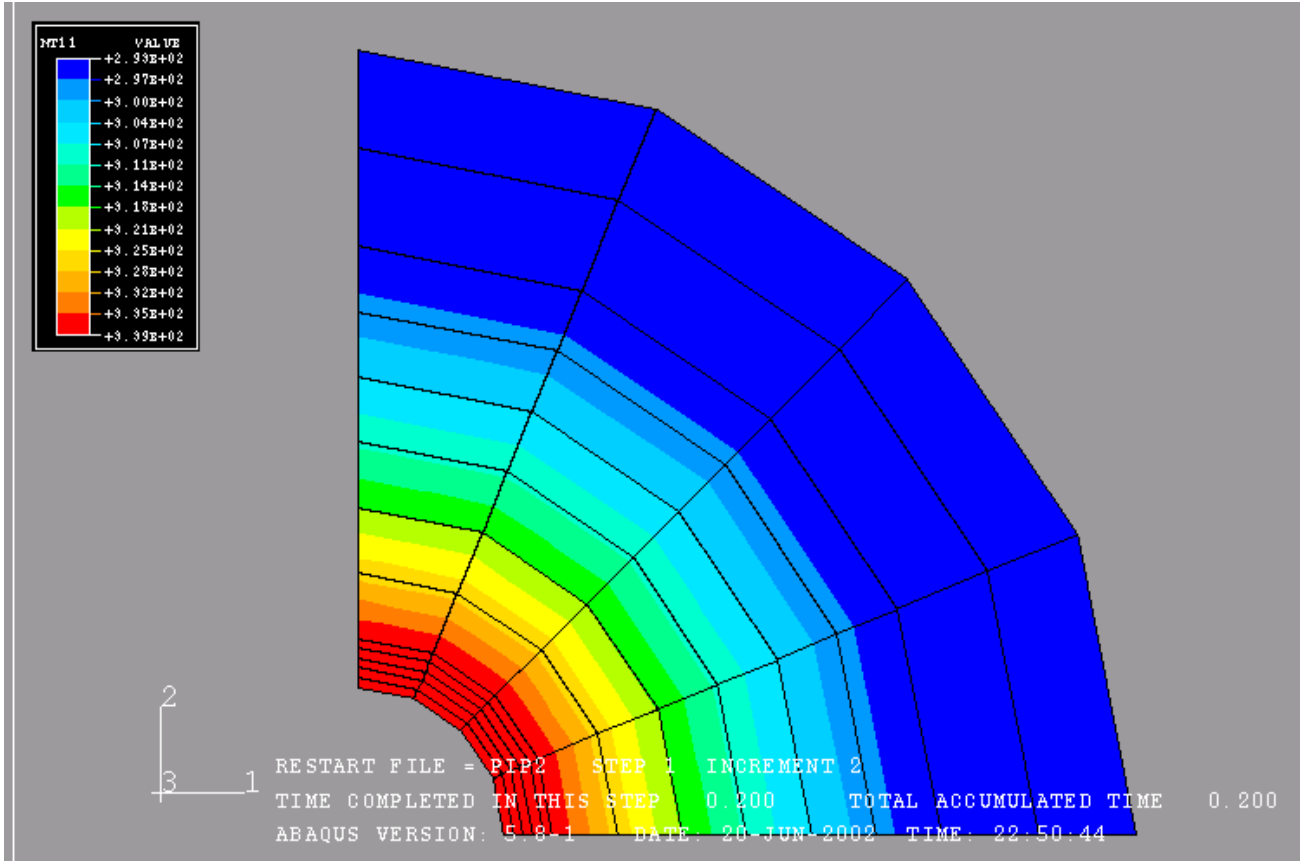


Figure 11—Temperature Profile (PIP)



Cementing Solutions, Inc.

Young's Modulus	5000 psi
Poisson Ratio	0.35
Confining Pressure	None
Cement Thickness	1 inch
Casing Pressure	500 psi

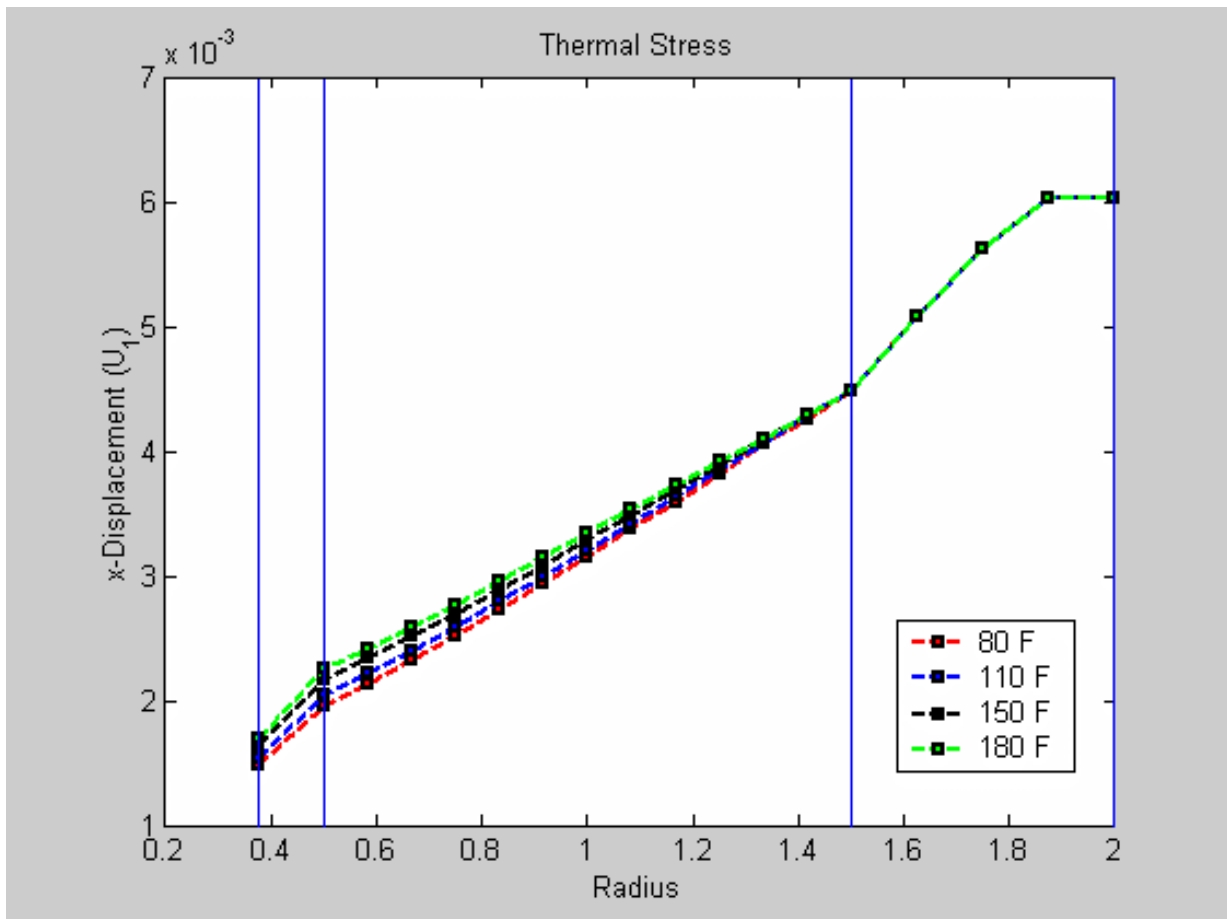


Figure 12—Horizontal Displacement Profile (PIP; Varying Internal Temperature)



CSI Technologies

Appendix III

Report 3

MMS Project

Long-Term Integrity of Deepwater Cement Systems Under Stress/Compaction Conditions

Report 3

Issued November 19, 2002



CEMENTING SOLUTIONS, INC.



Table of Contents

Objectives	1
Conventional Performance Testing	1
<i>Composition.....</i>	<i>1</i>
<i>Compressive Strength Testing.....</i>	<i>2</i>
<i>Rock Properties Testing.....</i>	<i>2</i>
Young's Modulus Testing	2
<i>Tensile Strength Testing.....</i>	<i>5</i>
<i>Hydrostatic Pressure Testing.....</i>	<i>6</i>
Chandler Engineering, Inc. Mechanical Properties Device	11
Unconventional Performance Testing	12
<i>Shear Bond Testing.....</i>	<i>12</i>
<i>Shrinkage Testing.....</i>	<i>13</i>
<i>Annular Seal Testing.....</i>	<i>13</i>
Pipe-in-Pipe Testing	13
<i>Mathematical Modeling.....</i>	<i>13</i>
Compressive Failure	14
Shear Failure (Hoop Stress).....	17
Heat of Hydration.....	19
Thermal Stress	23
Hoop Stress (Tensile) without Confining Pressure	24
Displacement (No Confining Pressure).....	26
Hoop Stress (Tensile) with Confining Pressure	28
Displacement with Confining Pressure	29
Appendix A—Young's Modulus Testing	32
Appendix B—Tensile Strength Testing	33
Appendix C—Shear Bond Strength Testing	34
<i>Temperature Cycling.....</i>	<i>36</i>
<i>Pressure Cycling.....</i>	<i>37</i>



Cementing Solutions, Inc.

Appendix D—Shrinkage Testing	38
Appendix E—Annular Seal Testing	39
<i>Simulated Soft Formation Test Procedure</i>	<i>39</i>
<i>Simulated Hard Formation Test Procedure.....</i>	<i>39</i>
Appendix F—Chandler Engineering Mechanical Properties Analyzer	40



Objectives

The overall objective of this research project is to determine the properties that affect cement’s capability to produce a fluid-tight seal in an annulus and to develop correlations between cement properties and sealing performance under downhole conditions. The testing reported previously in progress reports 1 and 2 has helped to refine and confirm the test procedures that will be used for the remainder of the project.

Research conducted during this project period focused on continued measurement and correlation of cement mechanical properties, mechanical bond integrity of a cemented annulus, and mathematical simulation of stresses induced in a cemented annulus. Mechanical property testing included measurement of tensile strength and Young’s Modulus measurements under various confining loads. Mechanical integrity testing included shear bond and annular seal testing on specimens cured under various cyclic curing schedules. Mathematical simulation of casing and cement stress and strain induced by thermal and pressure cycling was also performed during this project period.

Conventional Performance Testing

Composition

The compositions tested in this project are detailed in **Table 1** below.

Table 1—Cement Compositions for Testing

Comp. No.	Description	Cement	Additives	Water Requirement (gal/sk)	Density (lb/gal)	Yield (ft ³ /sk)
1	Neat slurry	TXI Type 1	—	5.23	15.6	1.18
2	Neat slurry with fibers					
3	Foam slurry	TXI Type 1	0.03 gal/sk Witcolate 0.01 gal/sk Aromox C-12 1% CaCl	5.2	12.0	1.19
4	Bead slurry	TXI Type 1	13.19% K-46 beads	6.69	12.0	1.81
5	Latex slurry	TXI Type 1	1.0 gal/sk LT-D500	4.2	15.63	1.17
6	Latex fiber slurry	TXI Type 1	1.0 gal/sk LT-D500 3.5% carbon milled fibers 0.50% Melkrete	4.09	15.63	1.20
7	Class H with silica	Class H	35% coarse silica 0.6% retarding fluid loss additive	5.38	16.4	1.40
8	Class H with silica and fibers	Class H	35% coarse silica 0.6% retarding fluid loss additive 3.2% milled fibers	5.38	16.4	1.43



Compressive Strength Testing

A summary of the compressive strength tests conducted was included in Report 2, and will not be repeated in this report. Please see Report 2 for a detailed description of these tests.

Report 2 discussed concerns about a possible discrepancy in compressive strength data provided by Westport and CSI. Compressive strength testing of representative compositions was conducted at Westport Laboratory to check the accuracy of CSI's test procedure. The results presented in **Table 2**, which represent the averages of three samples tested, indicate that data from the outside laboratory tracks closely with that of CSI.

Table 2—Comparison of Compressive Strengths

Location	Compressive Strength (psi) at 45°F	Compressive Strength (psi) at 80°F
Westport	1400	2015
CSI	1455	1920

Rock Properties Testing

Young's Modulus Testing

Composition 1 samples were cured in an unconfined condition (removed from mold after 24 hours and allowed to cure the remainder of the time outside of the mold) and tested at confining pressures of 0; 1,500; and 5,000 psi. The results are presented in **Table 3**.

Similar tests were conducted for Compositions 3 and 4 at confining pressures of 0, 500, and 1,000 psi, and for Composition 5 at confining pressures of 0, 250, and 500 psi. The results are presented in **Tables 4 through 6**.

Table 3—Composition 1, Compressive Young's Modulus

Confining Pressure (psi)	Effective Strength (psi)	Young's Modulus (psi)
0	8645	16.7 E 5
1500	8160	11.1 E 5
5000	8900	9.1 E 5

Table 4—Composition 3, Compressive Young's Modulus

Confining Pressure (psi)	Effective Strength (psi)	Young's Modulus (psi)
0	2885	5.8 E 5
500	3950	6.8 E 5
1000	4510	6.1 E 5



Table 5—Composition 4, Compressive Young's Modulus

Confining Pressure (psi)	Effective Strength (psi)	Young's Modulus (psi)
0	5150	9.5 E 5
500	6000	8.1 E 5
1000	6150	1 E 5

Table 6—Composition 5, Compressive Young's Modulus

Confining Pressure (psi)	Effective Strength (psi)	Young's Modulus (psi)
0	3500	5.6 E 5
250	5250	8.9 E 5
500	6000	9.4 E 5

Figure 1—Young's modulus testing of Composition 2 (neat Type 1 with fibers)

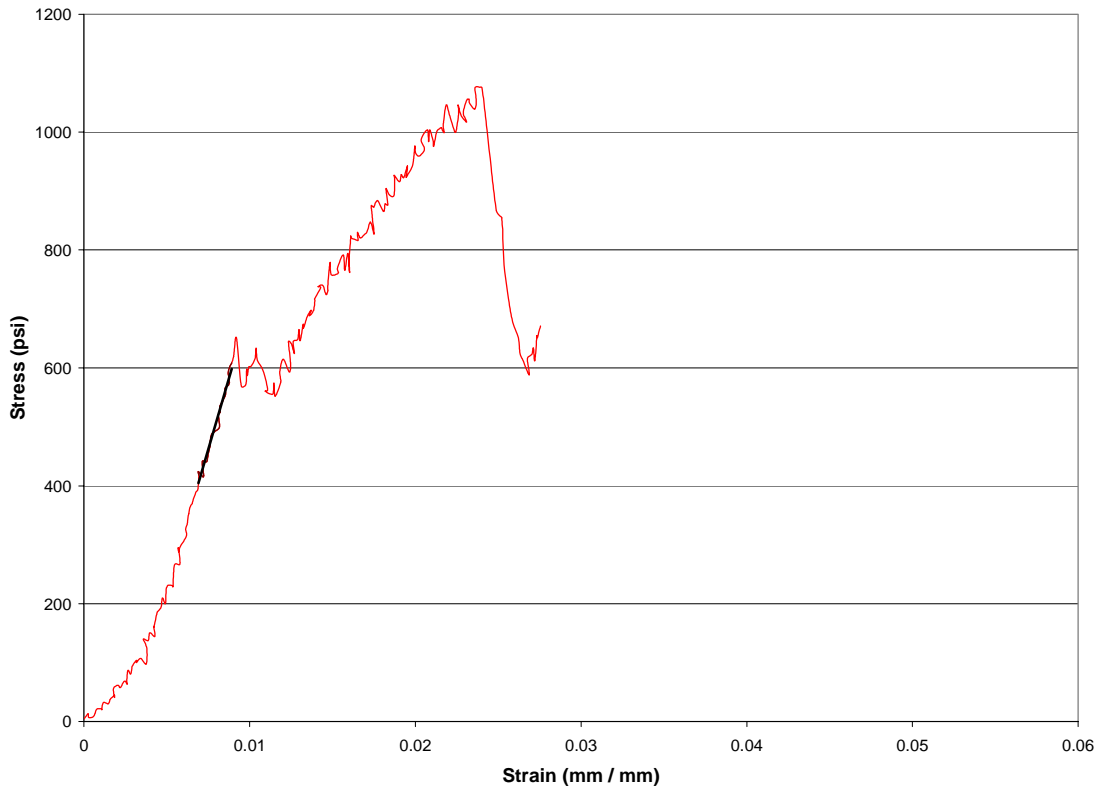
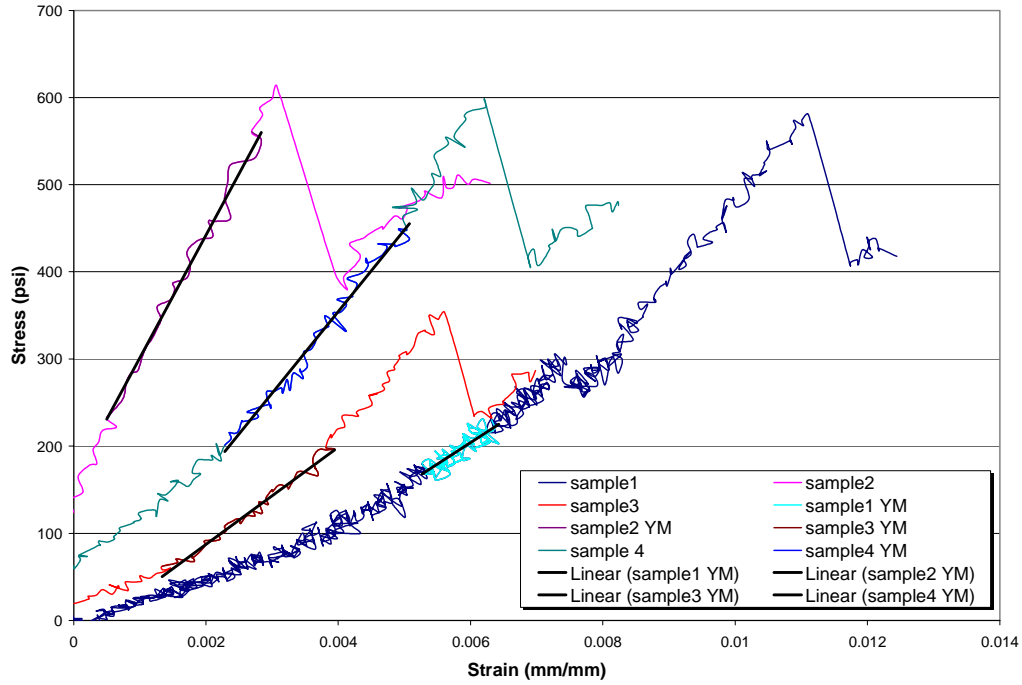


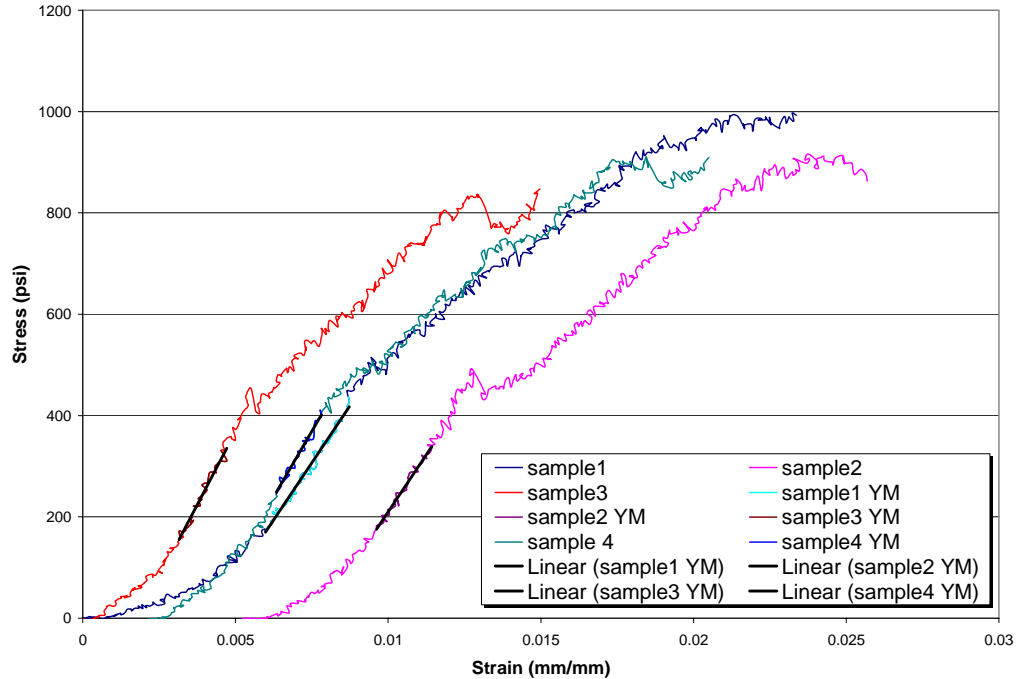


Figure 2—Young's modulus testing of Composition 5
(Type I latex without fibers)





**Figure 3—Young’s modulus testing of Composition 6
(Type I latex with fibers)**



Tensile Strength Testing

The data presented in **Table 7** indicate that the tensile strength of Composition 4 was significantly higher than that of the other compositions tested.

Table 7—Tensile Strength Comparison

Slurry	Tensile Strength (psi)
Composition 1	394* / 213**
Composition 3	253
Composition 4	1071
Composition 5	539
Composition 6	902

* Sample was cured outside the mold.

** Sample was cured in the mold.



Hydrostatic Pressure Testing

The first hydrostatic pressure tests performed on a 10 lb/gal slurry (**Table 8**) were discussed in Report 2, and is being included in Report 3 for comparison purposes, as we present results obtained with a 12-lb/gal slurry (**Table 9**).

In both sets of tests, the initial sample was tested to failure. Subsequent cycle tests were performed with separate samples. The results are shown in Figures 4 through 9.

Table 8—Hydrostatic Cycles for 10-lb/gal Foam

Cycle No.	Hydrostatic (psi)	Young's Modulus (psi)
1 (initial)*	—	5.57E+05
2 (up)**	1000	3.38E+05
3 (down)**	100	6.71E+05
4 (up)**	1500	5.71E+05
5 (down)**	100	7.98E+05
6 (up)**	2000	6.68E+05
7 (down)**	100	8.49E+05***

* Initial sample taken to failure

** Tests performed on separate (not initial) samples

*** No deformation calculations performed for Cycle 7

Table 9—Hydrostatic Cycle for 12-lb/gal Foam

Cycle No.	Hydrostatic (psi)	Young's Modulus (psi)
1 (initial)*	—	8.24E+05
2 (up)**	600	1.30E+05

*Initial sample taken to failure

**Separate sample tested



Figure 4—Young's modulus testing of 10-lb/gal foamed cement

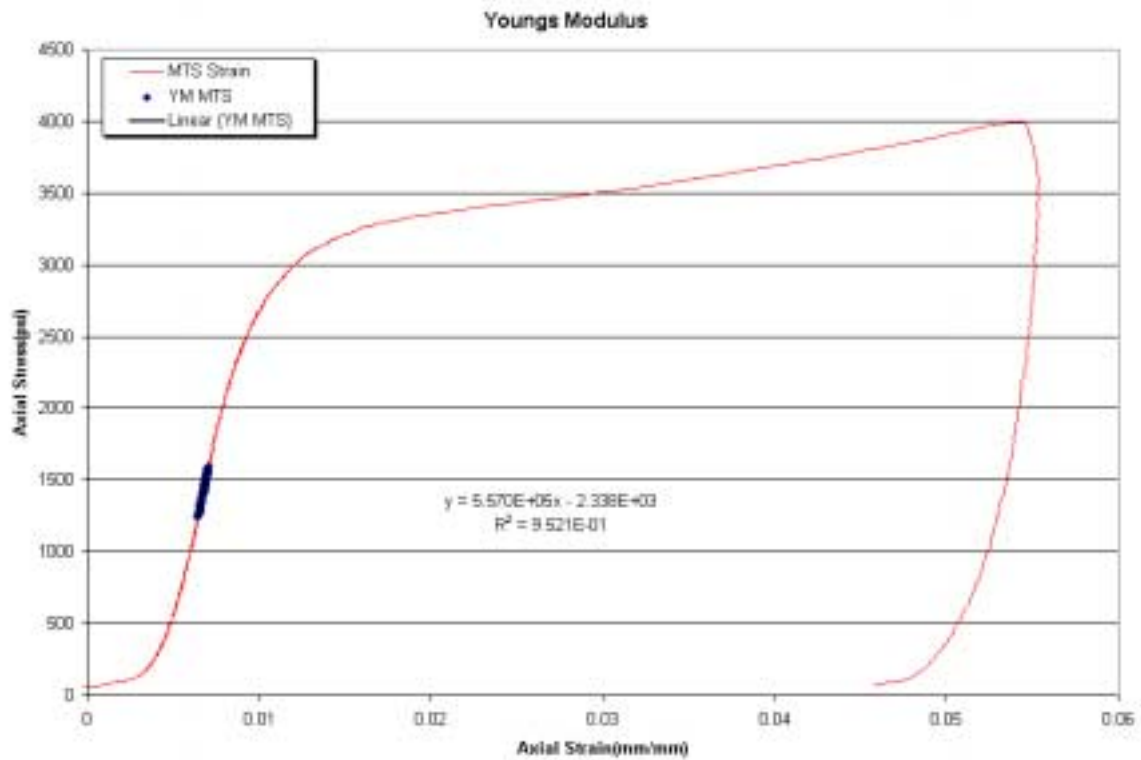




Figure 5—Young’s modulus testing of 10-lb/gal foamed cement during hydrostatic cycling

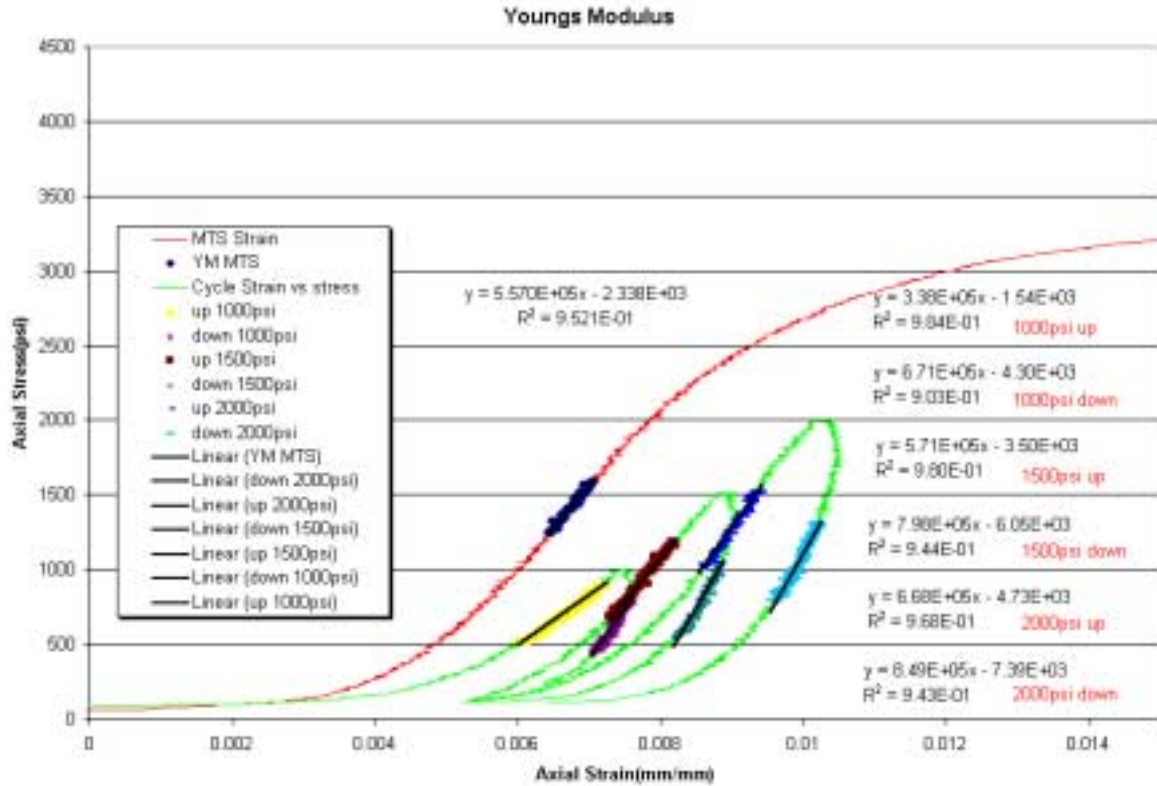




Figure 6—Deformation of 10 lb/gal foamed cement during hydrostatic cycling

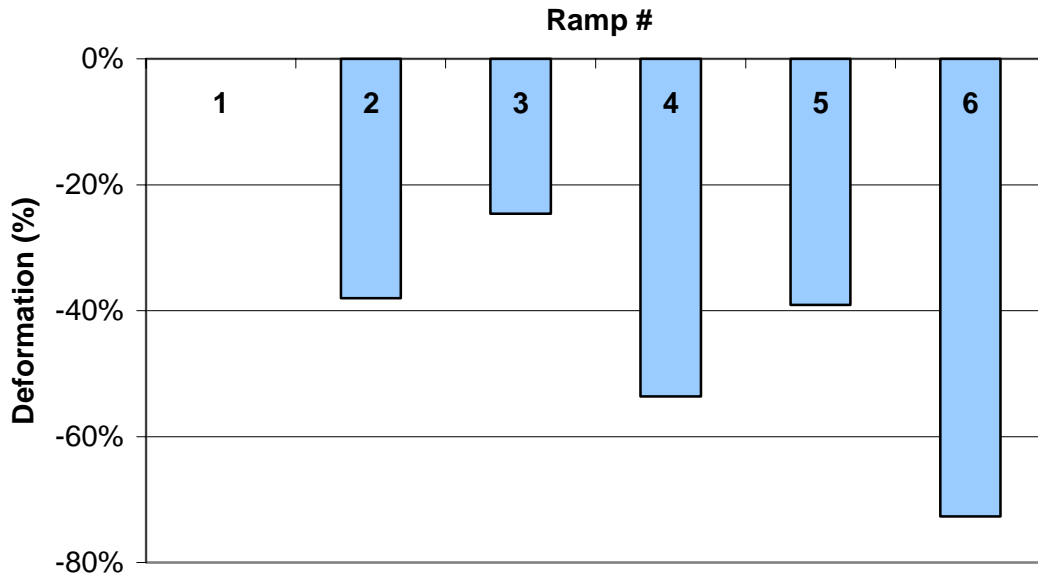
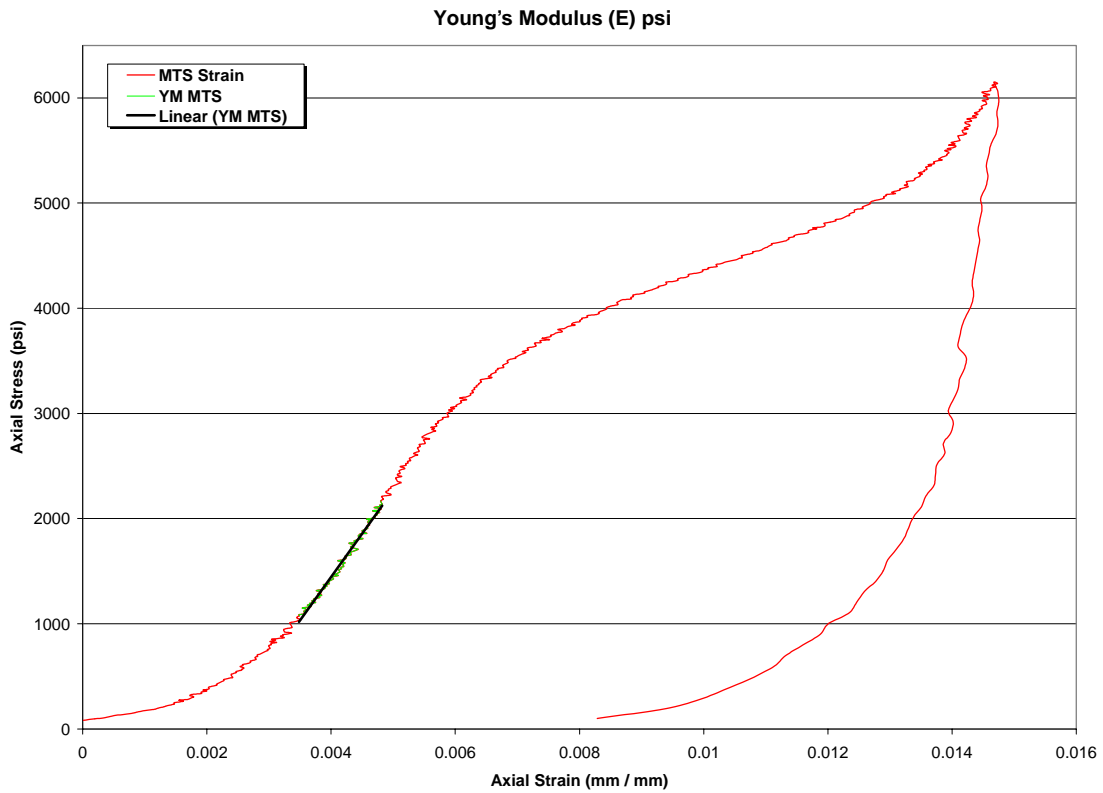
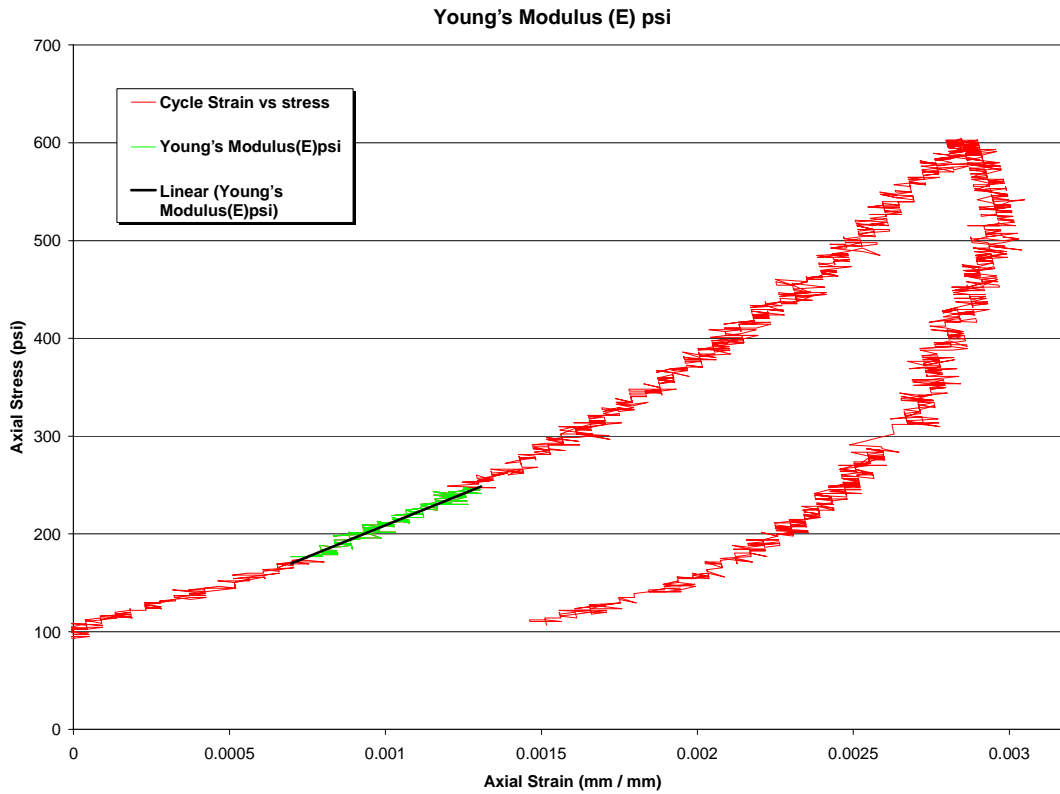


Figure 7— Young's modulus testing of 12-lb/gal foamed cement (Composition 2)



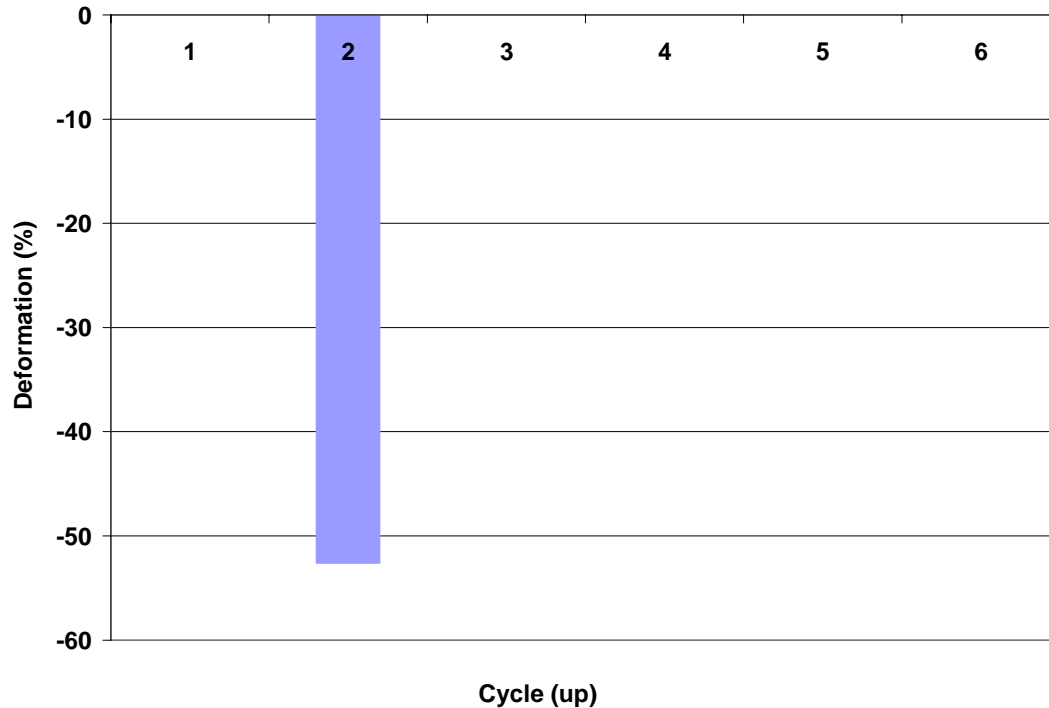


**Figure 8—Young's modulus testing of 12-lb/gal foamed cement
(Composition 2) during hydrostatic cycling**





**Figure 9—Deformation of 12-lb/gal foamed cement
(Composition 2) during hydrostatic cycling**



Chandler Engineering, Inc. Mechanical Properties Device

For comparison purposes, Chandler Engineering, Inc. and CSI have agreed to exchange data generated by two different systems – the rock mechanics system at Westport Laboratory and an acoustics-based system operated by Chandler. The same six slurries were tested in each device, and the comparative data is presented in **Tables 10 and 11**.

Initial results of Poisson’s ratio testing on these lightweight cement compositions are not interpretable. The majority of tests yielded a negative Poisson’s ratio, indicating a negative radial strain resulting from a positive axial strain. Several possible explanations for this phenomenon are under investigation. However, until the question is resolved, no Poisson’s ratio data will be reported.

The Young’s modulus values for latex cement with fibers, Class H cement, and Class H cement with fibers were not available at the time this report was prepared.

Like the UCA, Chandler’s new analyzer measures the Young’s modulus and compressive strength of a slurry as it cures at elevated temperatures and pressures, eliminating the



potentially damaging effects of depressurization and cooling involved with traditional core testing. For more information on this device, see Appendix F.

Table 10—Chandler Device

Composition	Poisson's Ratio	Compressive Young's Modulus
1	0.20	2.3 E 6
4	0.31	1.5 E 6
5	0.39	1.4 E 6
6	0.19	2.5 E 6
7	0.24	2.2 E 6
8	0.25	2.3 E 6

Table 11—Rock Mechanics Data

Composition	Poisson's Ratio	Compressive Young's Modulus
1	—	1.7 E 6
4	—	9.5 E 5
5	—	5.6 E 5
6	—	—
7	—	—
8	—	—

Unconventional Performance Testing

Shear Bond Testing

Table 12 presents results of shear bond strength tests performed with temperature and pressure cycling on Compositions 1, 3, 4, and 5. For more information on test procedures, see Appendix C.

Table 12—Shear Bond Strengths (psi)

System	Simulated Formation	Comp. 1	Comp. 3	Comp. 4	Comp. 5
Baseline	hard	1194	127/98	109/78	—
	soft	198	233	143	223
Temperature-Cycled	hard	165	299/215	191/269	—
	soft	72	7	56	149
Pressure-Cycled	hard	194/106	276/228	294/170	—
	soft	23	22*	23*	11

* Visual inspection revealed samples were cracked.



Shrinkage Testing

Information on test procedures for shrinkage testing is provided in Appendix D.

Annular Seal Testing

Table 13 presents the results of annular seal tests performed on Compositions 1, 3, and 4. For information on test procedures for annular seal testing, see Appendix E.

Table 13—Annular Seal Tests

Condition Tested	Formation Simulated	Composition 1	Composition 3	Composition 4
Initial Flow	Hard	0 Flow	0 Flow	0 Flow
	Soft	0 Flow	0.5K (md)	0 Flow
Temperature-Cycled	Hard	0 Flow	0 Flow	0 Flow
	Soft	0 Flow	123K md / (2200 md)	43K (md)*
Pressure-Cycled	Hard	0 Flow	0 Flow	0 Flow
	Soft	27K (md)	0.19K (md)*	3K (md)

* Visual inspection revealed samples were cracked.

Pipe-in-Pipe Testing

A pipe-in-pipe test was designed to simulate the shrinkage of cement that can lead to fluid leakage when no external fluid is present outside the cement. Four models were tested:

- 6-in. flange
- 6-in. flange with 200-psi pressure
- 5-ft flange with vacuum
- 5-ft flange with 200-psi pressure

In all cases, no leaks were observed. The cement provided a tight seal to gas flow.

Mathematical Modeling

The graphs in this section represent an average of test results obtained in testing the performance of a neat cement (baseline), latex cement, and foamed cement. The compressive and tensile strengths and shear bond strength of the cements are shown in **Table 14**.

The abbreviations “PIP” and “PIS” are used in the following graphs to differentiate between test conditions that simulate hard formations (pipe-in-pipe) and those that simulate soft formations (pipe-in-soft).



Table 14—Compressive Strength

Cement	Compressive Strength After 10 Days (psi)	Tensile Strength (psi)	Shear Bond	
			PIP	PIS
Composition 3	3436	578	321	147
Composition 5	3630	504	432	237
Composition 1	4035	673	519.6	203

Compressive Failure

Figures 10 and 11 show the results of tests used to predict the effect of casing pressure and confining pressure on the radial stress experienced by the inner pipe, the cement sheath, and a hard formation.

The model showed that annular cement retains its integrity at high casing pressures and at high confining pressures in a hard formation.

When casing pressure was varied (**Figure 10**), and no confining pressure was applied, virtually no variation in the radial stress was observed for the cement or the formation. All variation, rather, was limited to the internal casing.

When confining pressure was varied (**Figure 11**), and casing pressure was fixed at 5,000 psi, the greatest variation in radial stress was observed in the inner casing and outer pipe (representing the formation), with very little variation observed in the cement. This is because of the differences in the Young's modulus properties of the cement vs. the Young's modulus of the steel pipe.



Figure 10—Compressive failure, simulated hard formation (1 of 2)

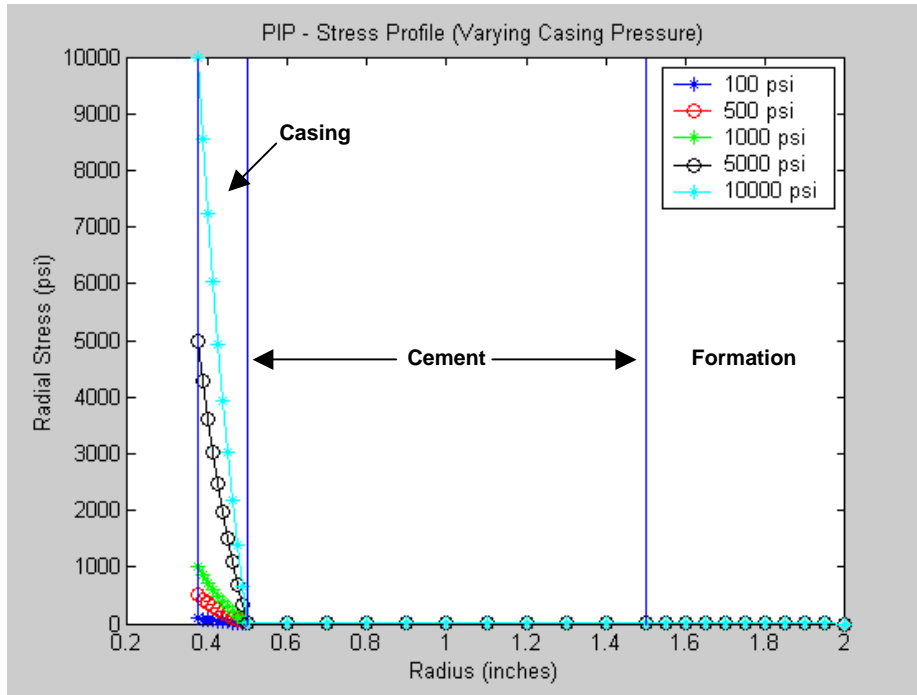
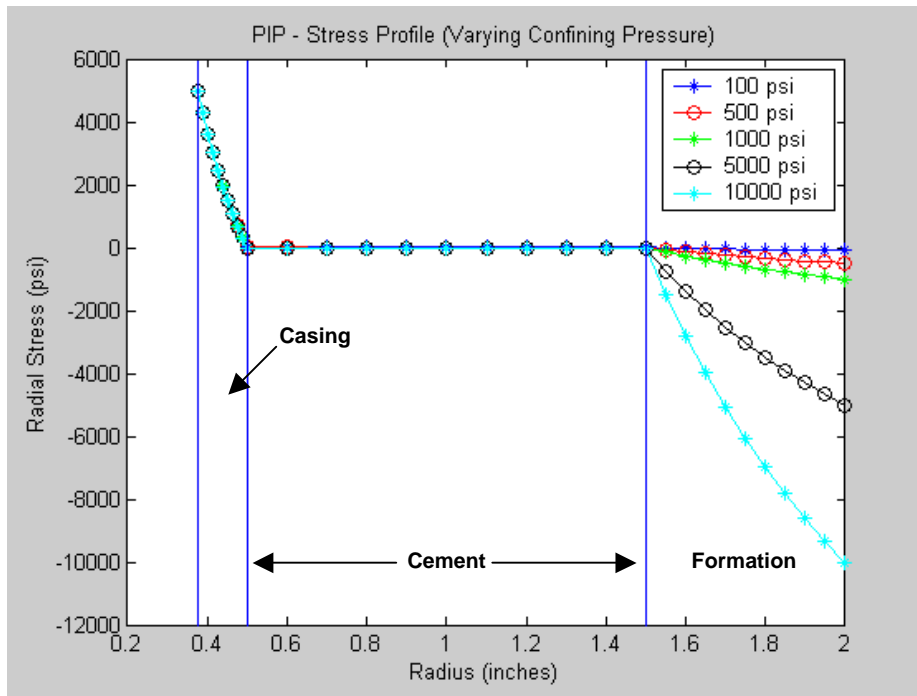


Figure 11—Compressive failure, simulated hard formation (2 of 2)





Cements were then tested to determine the effects of varying casing pressure and confining pressure in a soft formation scenario. Without confining pressure (**Fig. 12**), the cement and the formation experience no variation in radial stress as casing pressure increases. As in the test with the hard formation, the variation is limited to the inner casing.

However, when the casing pressure is fixed at 500 psi, and the confining pressure is increased from 100 psi to 10,000 psi (**Fig. 13**), the radial stress in the cement layer increases accordingly, to a point beyond which the sheath can withstand. At pressures of 5,000 psi and above, the cement sheath will almost certainly fail.

The positive and negative values shown in Figure 13 are used to differentiate radial stress (positive values) from the opposite of radial stress (negative values).

Figure 12—Compressive failure, simulated soft formation (1 of 2)

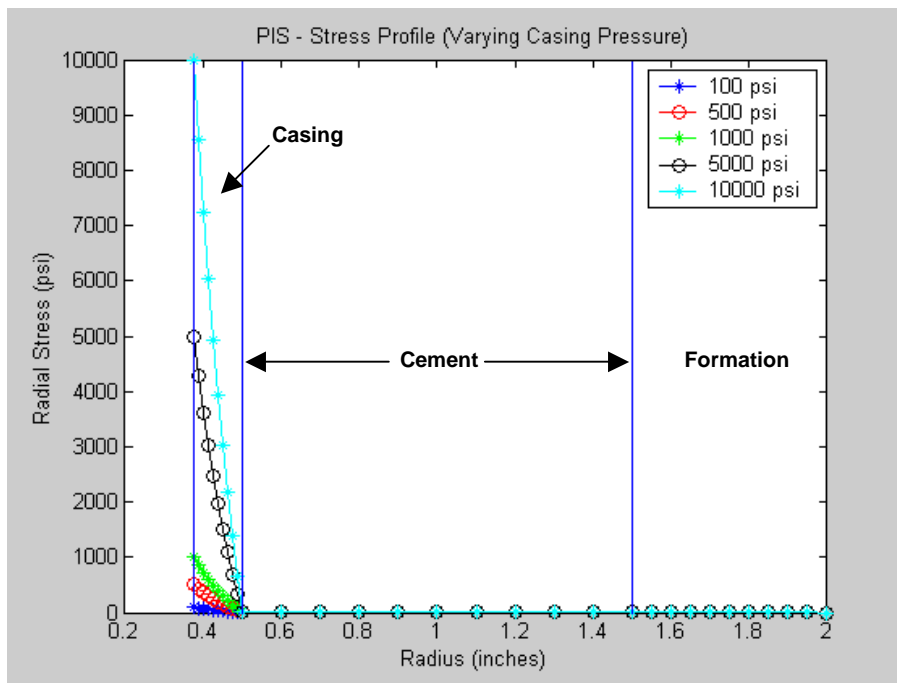
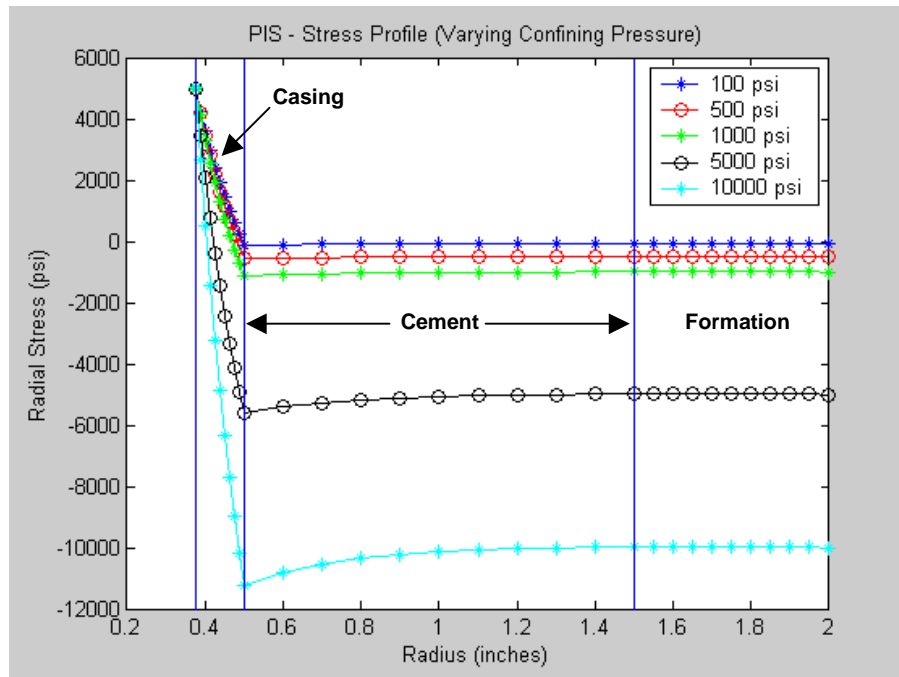




Figure 13— Compressive failure, simulated soft formation (2 of 2)



Shear Failure (Hoop Stress)

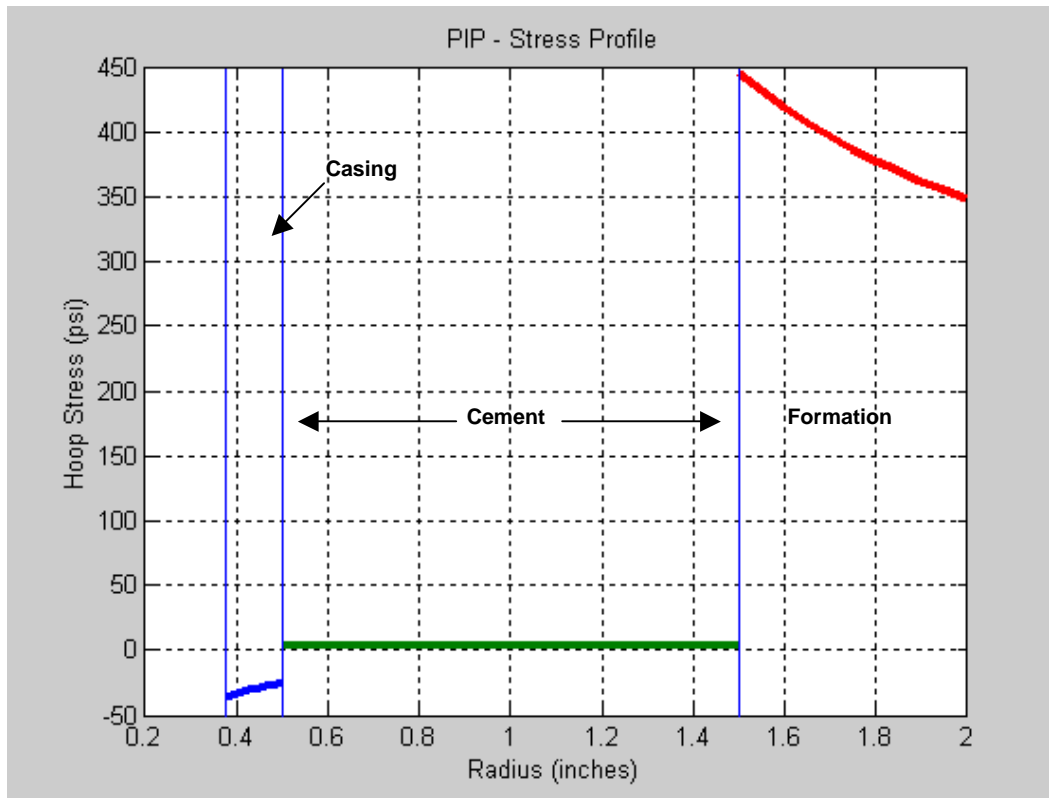
In a simulated hard formation (**Figure 14**), the variation in hoop stress at the pipe-cement interface is significantly less than that at the cement-formation interface. No significant variation in hoop stress is observed in the cement layer. Therefore, if failure occurs, it will most likely occur at the cement-formation interface.

In a simulated soft formation (**Figure 15**), there is almost no variation in the formation hoop stress, and there is slightly more variation in the hoop stress of the cement sheath. While the magnitude of variation between the pipe-cement interface and the cement-formation interface is significant, it is not as great as in the simulated hard formation shown in Figure 14. That is because the soft formation is more flexible and does not create the high stress contrast during displacement.

If failure occurs, it will most likely be at the pipe-cement interface.



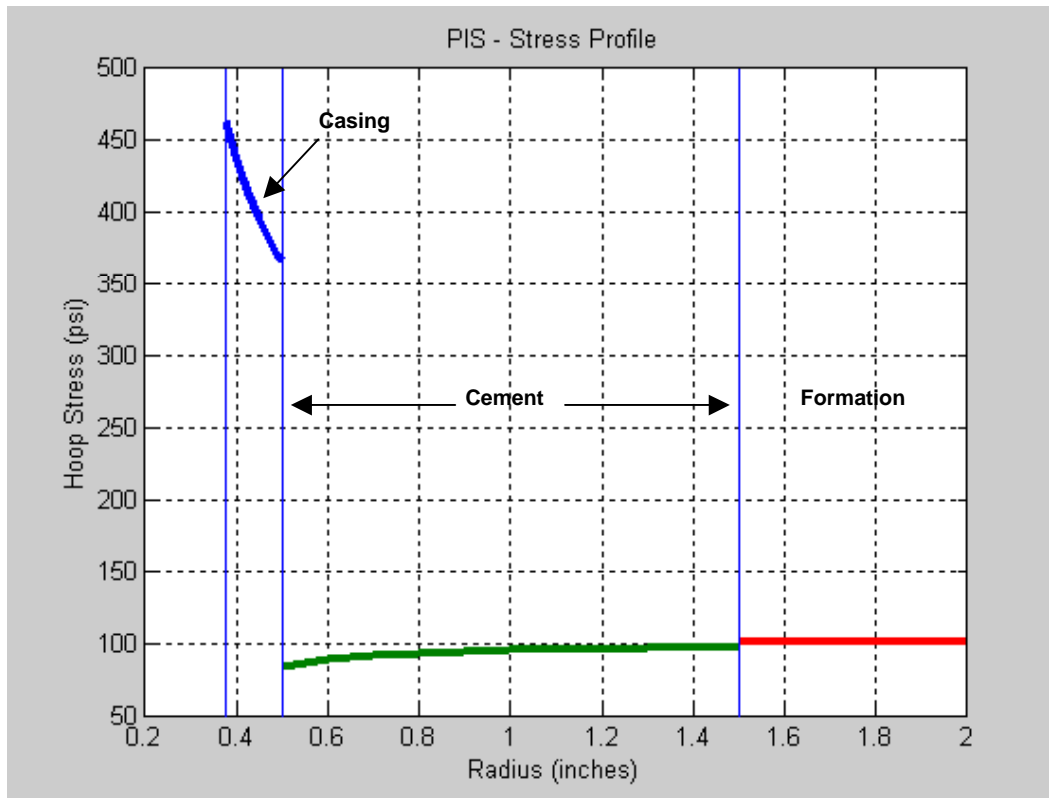
Figure 14—Shear failure, simulated hard formation (1 of 2)



Casing Pressure	15 psi
Confining Pressure	100 psi
Hoop Stress Contrast	~ 450 psi



Figure 15—Shear failure, simulated soft formation (2 of 2)



Casing Pressure	15 psi
Confining Pressure	100 psi
Hoop Stress Contrast	~ 300 psi

Heat of Hydration

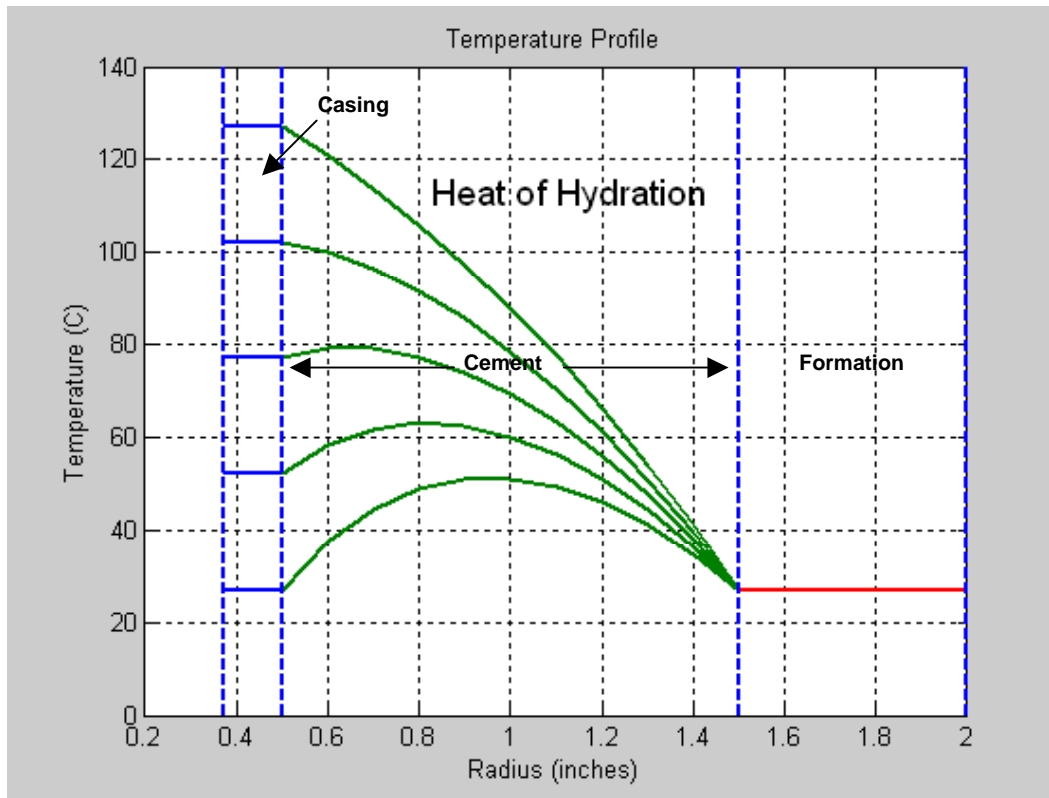
Cements were tested for the effect of heat of hydration on the cement integrity. First, the borehole temperature was increased from 300K to 400K, and the heat of hydration rate was held constant (Figure 16). As the temperature increased, the peak temperature moves closer to the pipe-cement interface. Because the steel pipes conduct heat very well, little if any variation is seen in the inner casing or outer pipe.

With a fixed borehole temperature (Figure 17), increasing the heat of hydration rate causes an increase in the temperature of the cement sheath. At the peak heat of hydration rate, the temperature is increased by nearly 30C, which can cause considerable stress on the cement system.



When viewed as a radial stress profile (Figure 18), the highest heat of hydration rate creates a radial stress of 600 psi on the cement sheath, but little variation of radial stress is observed within the cement.

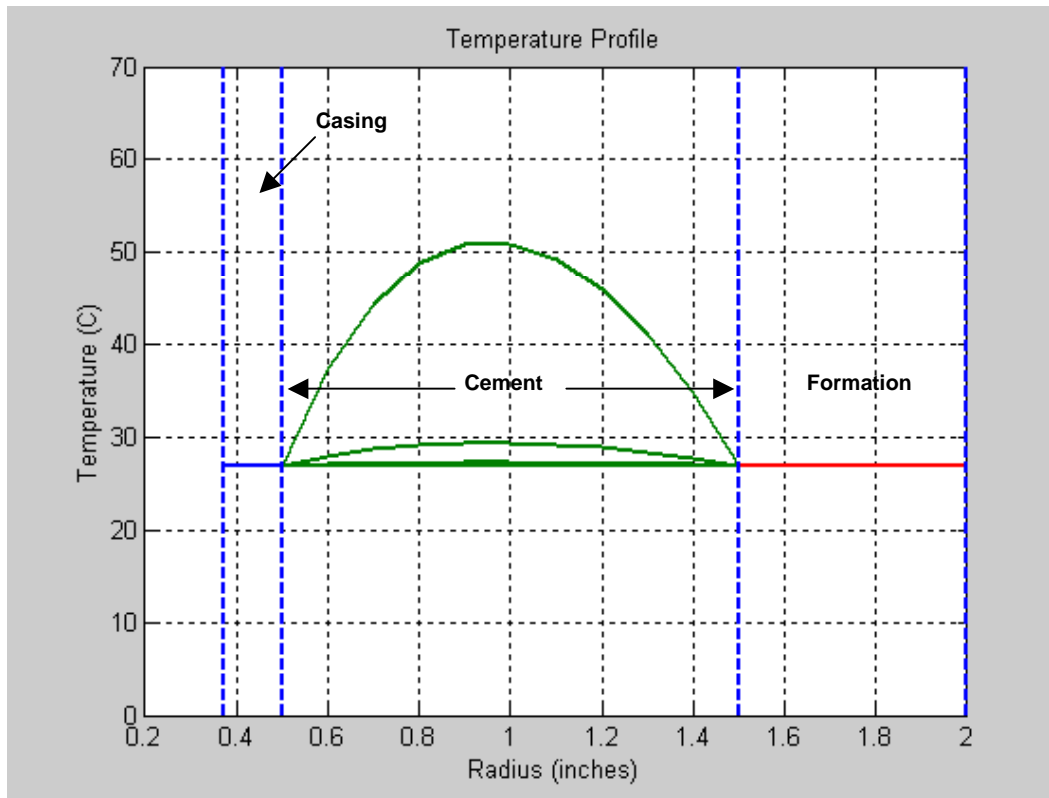
Figure 16—Heat of hydration, temperature profile (1 of 2)



Borehole Temperature	300 K to 400 K
Heat of Hydration Rate	3.5 KJ/Kg.sec



Figure 17—Heat of hydration, temperature profile (2 of 2)



Borehole Temperature

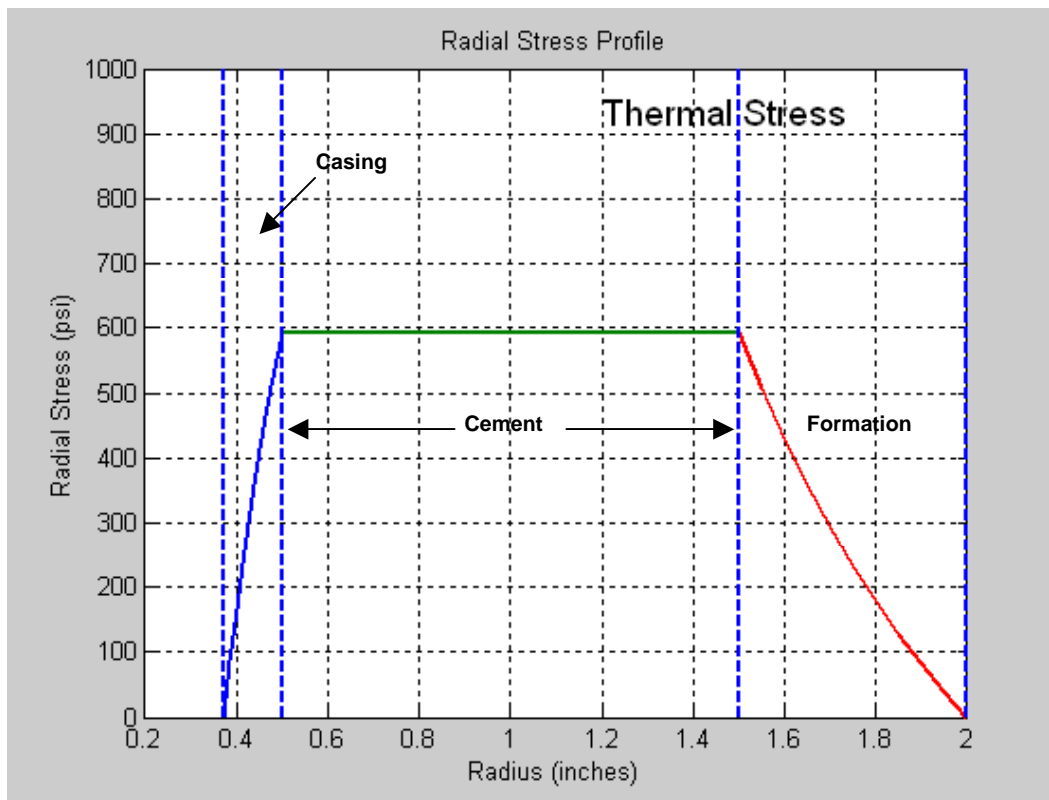
300 K

Heat of Hydration Rate

3.5 KJ/Kg.sec - 3.5 KJ/Kg.sec



Figure 18—Heat of hydration, radial stress profile



Borehole Temperature 300 K

Reservoir Temperature 300 K

Linear Superposition with Elastic Stress

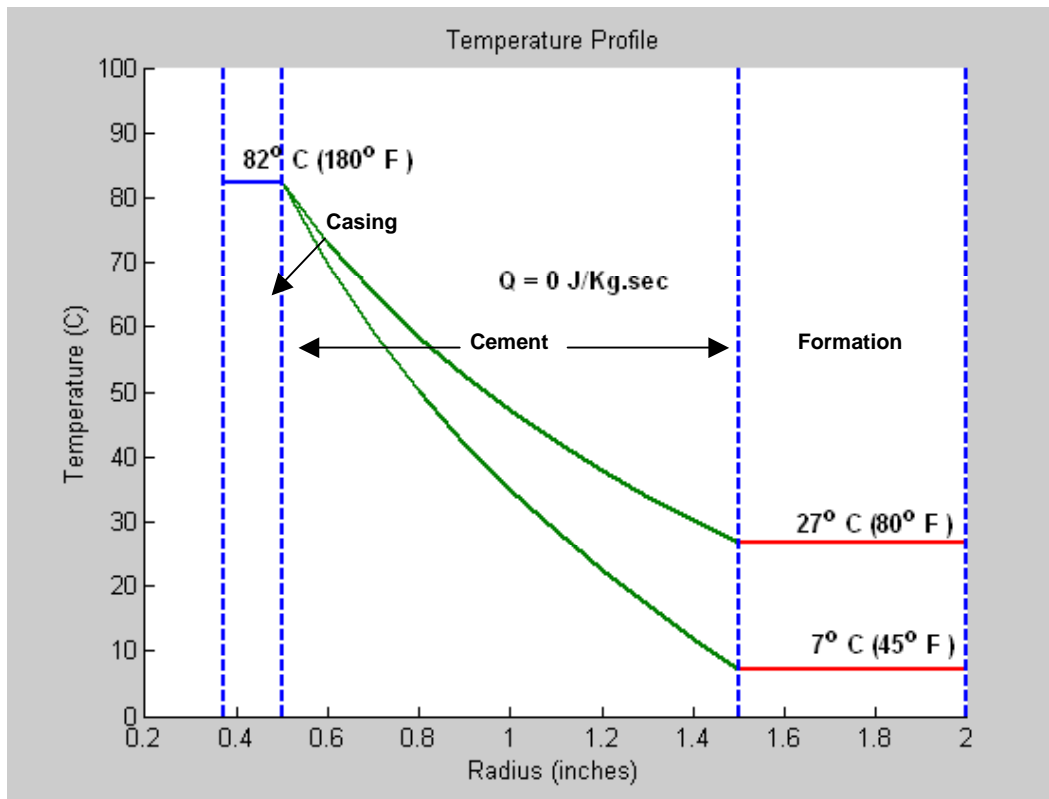


Thermal Stress

Thermal stress tests were performed to evaluate the effect of thermal stress on the cement. **Figure 19** plots the differences between the borehole temperature and two different reservoir temperatures.

The large temperature contrast between the inner casing and formation can cause significant radial stress (as much as 700 psi in **Figure 20**), which can affect the integrity of cement. However, the radial stress does not vary greatly within the cement.

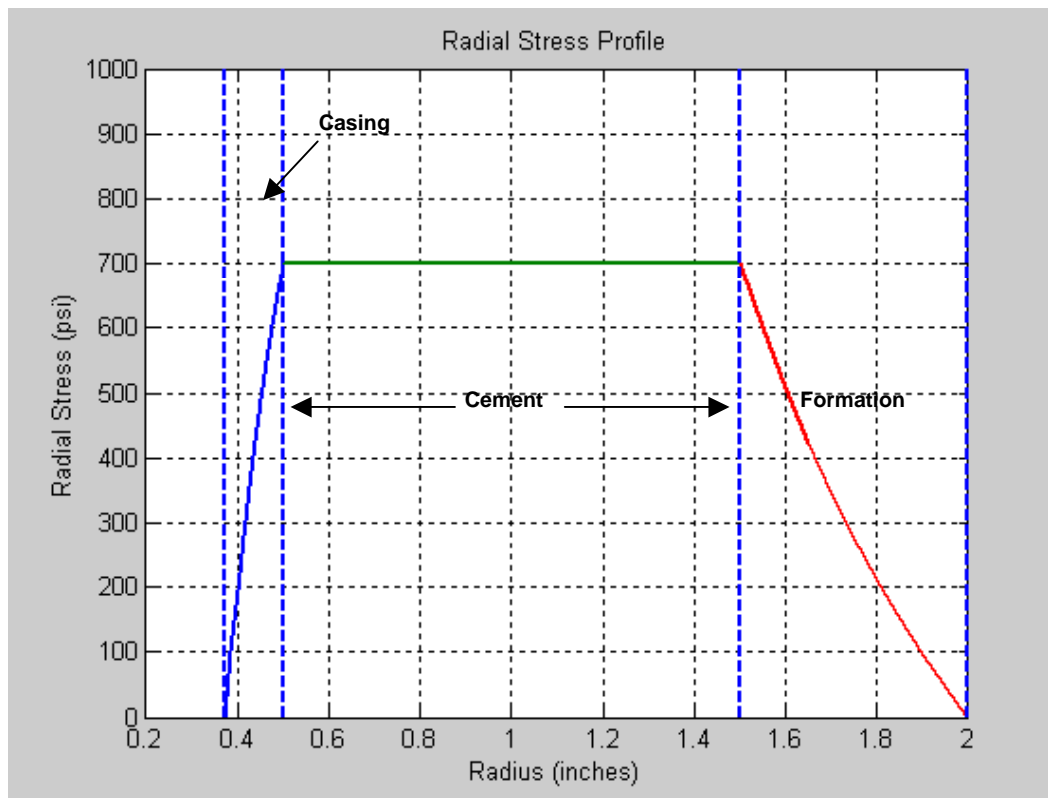
Figure 19—Thermal stress, temperature profile



Borehole Temperature	180°F
Reservoir Temperature	45°F, 80°F
Heat of Hydration Rate	0 J/Kg.sec



Figure 20—Thermal stress, radial stress profile



Borehole Temperature	180°F
Reservoir Temperature	45°F, 80°F
Heat of Hydration Rate	0 J/Kg.sec

- Higher thermal stress
- No significant variation within cement

Hoop Stress (Tensile) without Confining Pressure

Cements were tested to determine how hoop stress would affect the cement, given a specific casing pressure. No hoop stress variation was observed in either the cement or the outer pipe in simulated hard formations (**Figure 21**) and soft formations (**Figure 22**). The only contrast in hoop stress was apparent at the pipe-cement interface. This can be attributed to the difference in the elastic Young's modulus properties of the pipe and the cement.



Figure 21—Hoop stress (tensile), simulated hard formation, 0-psi confining pressure

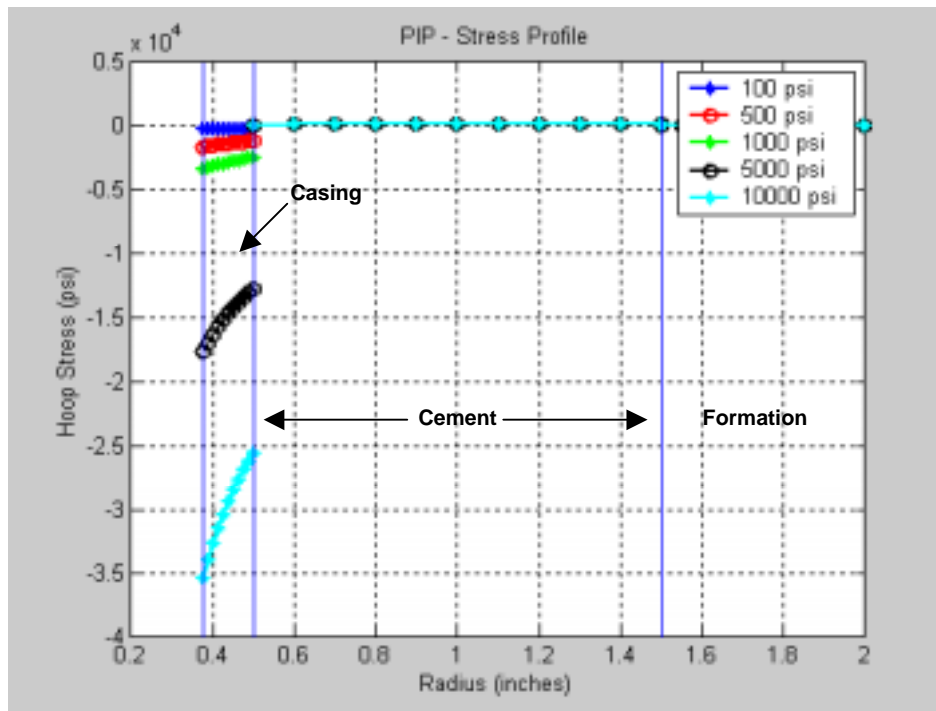
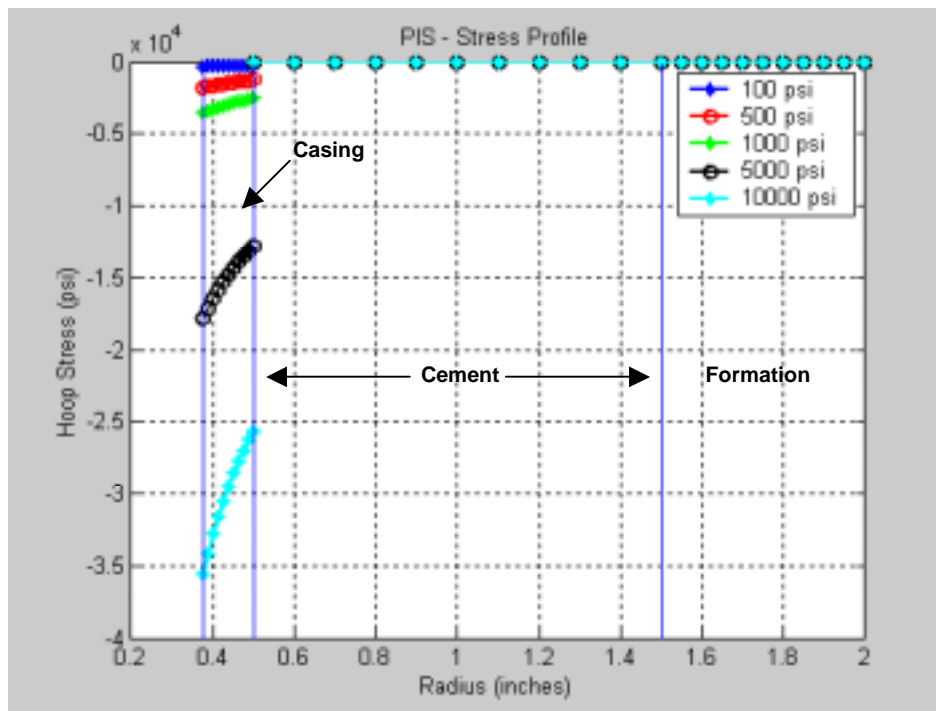


Figure 22—Hoop stress (tensile), simulated soft formation, 0-psi confining pressure





Displacement (No Confining Pressure)

The next set of simulations was conducted to determine the effect of varying casing pressures on displacement, in both hard and soft formations with no confining pressure. In hard formation tests, a larger displacement, and incidentally, a larger variation in displacement, was observed within the cement (**Figure 23**). The displacement of the cement is significantly large to absorb the load.

In simulated soft formations (**Figure 24**), a large displacement (and variation in displacement) was observed for both the cement and the formation.

Figure 23—Displacement profile, simulated hard formation, 0-psi confining pressure

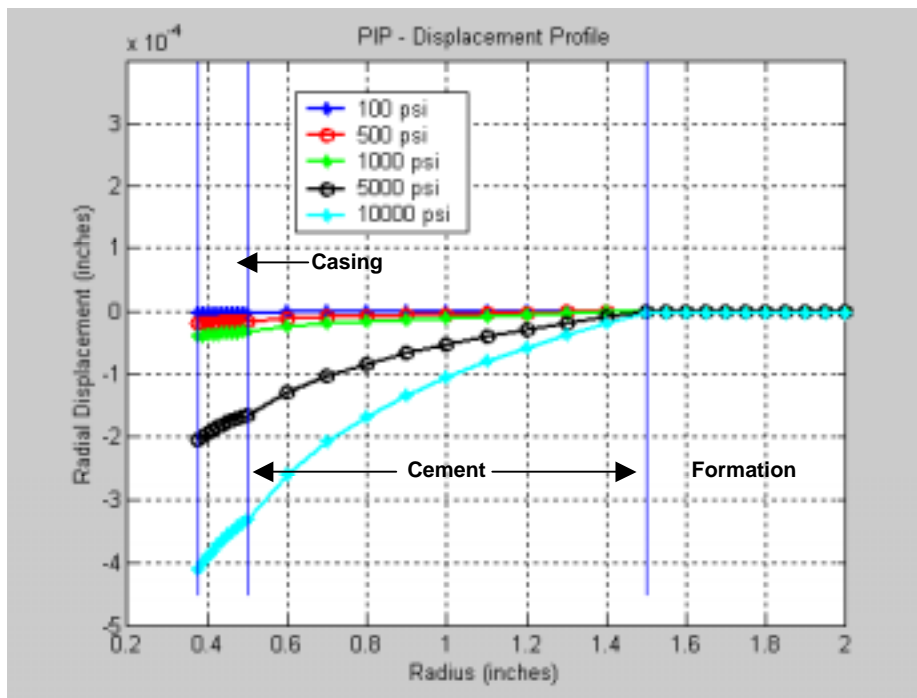
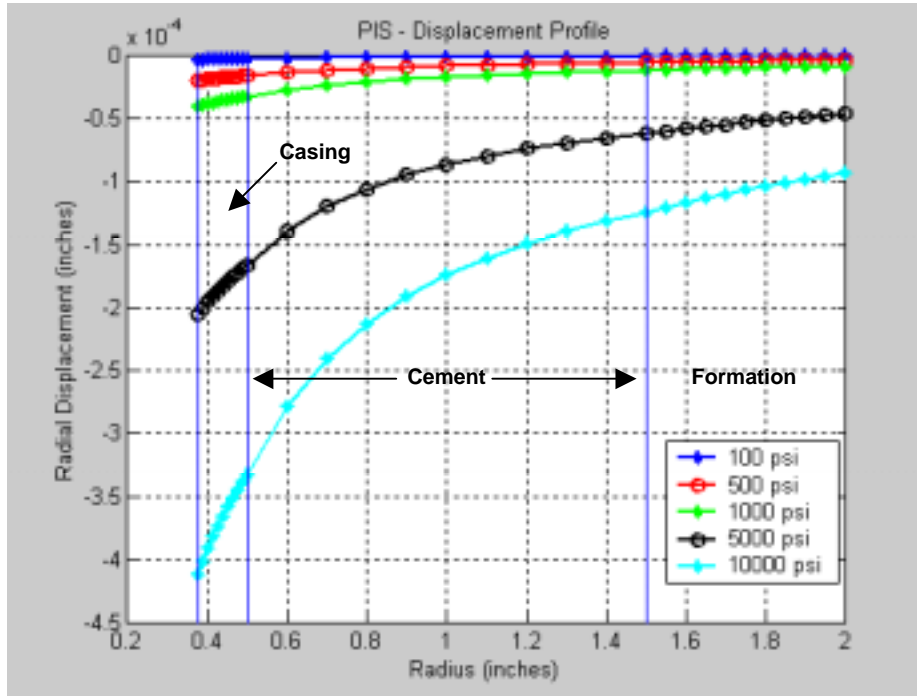




Figure 24—Displacement profile, simulated soft formation, 0-psi confining pressure





Hoop Stress (Tensile) with Confining Pressure

Tests were also performed to determine the effect of varying casing pressures on hoop stress with 500-psi confining pressure.

When applied to a simulated hard formation configuration (**Figure 25**), the test indicated that increasing casing pressures result in an increase in hoop stress at the cement-outer pipe interface; yet, the cement itself does not experience much hoop stress.

Increasing casing pressures in the simulated soft formation test (**Figure 26**) revealed a slightly higher hoop stress in the cement and the formation, but no significant contrast in hoop stress at the cement-formation interface.

Figure 25—Hoop stress (tensile), simulated hard formation, 500-psi confining pressure

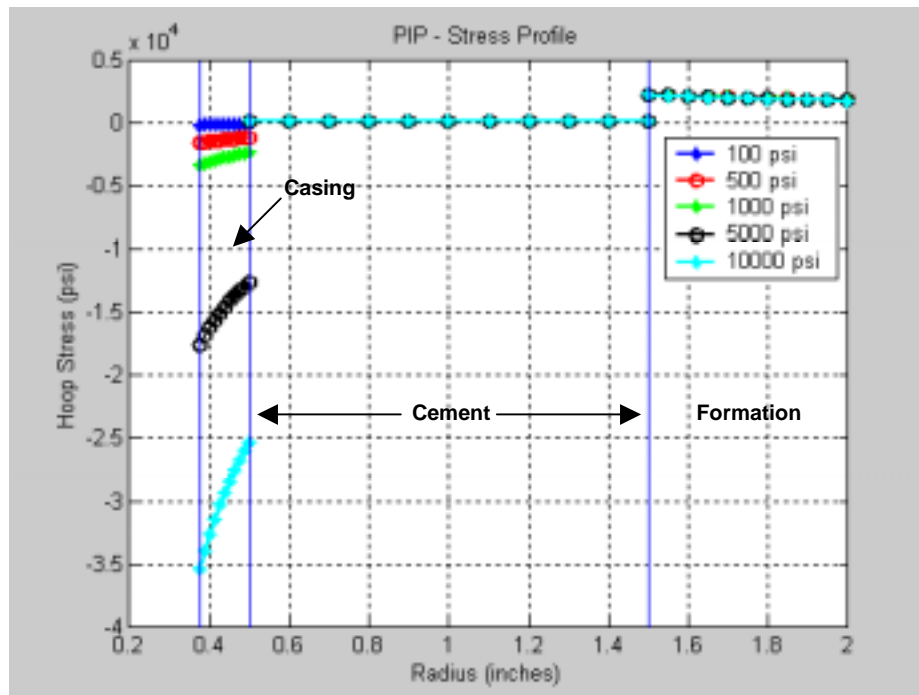
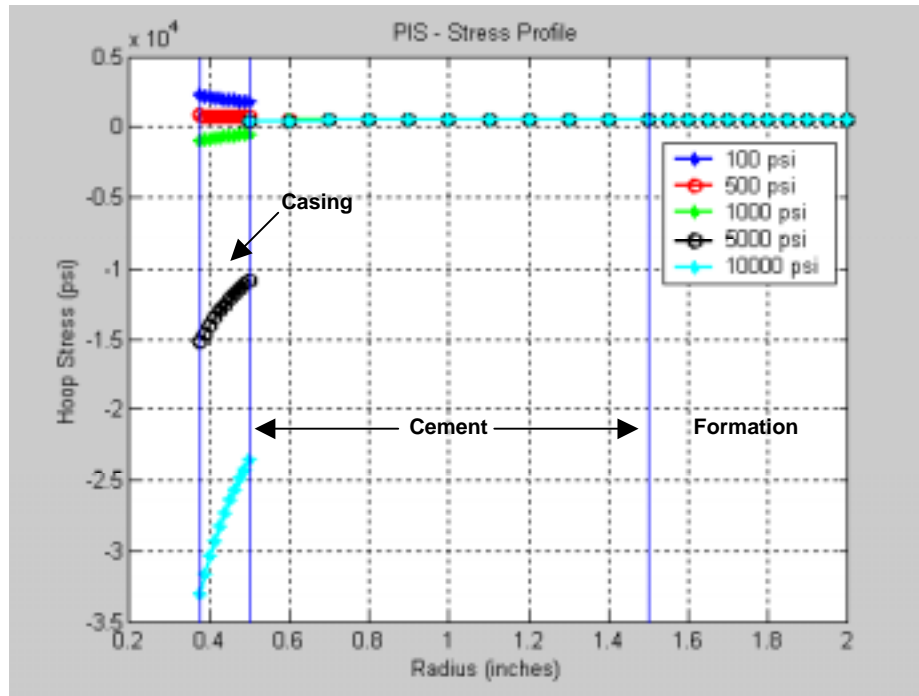




Figure 26—Hoop stress (tensile), simulated soft formation, 500-psi confining pressure



Displacement with Confining Pressure

As casing pressures vary and confining pressure is held constant in a hard formation, hoop stress increases in the formation, and stays constant in the cement. Displacement, rather, varies within the cement, and is almost constant in the formation (**Figure 27**).

As casing pressures are varied and confining pressure is held constant in a soft formation, hoop stress is slightly greater than that of the hard formation, and remains constant through the cement-formation interface. Displacement varies significantly in both the cement and the formation (**Figure 28**). This variation helps explain why no significant difference in hoop stress values is seen at the cement-formation interface in Figure 26.



Figure 27—Displacement profile, simulated hard formation, 500-psi confining pressure

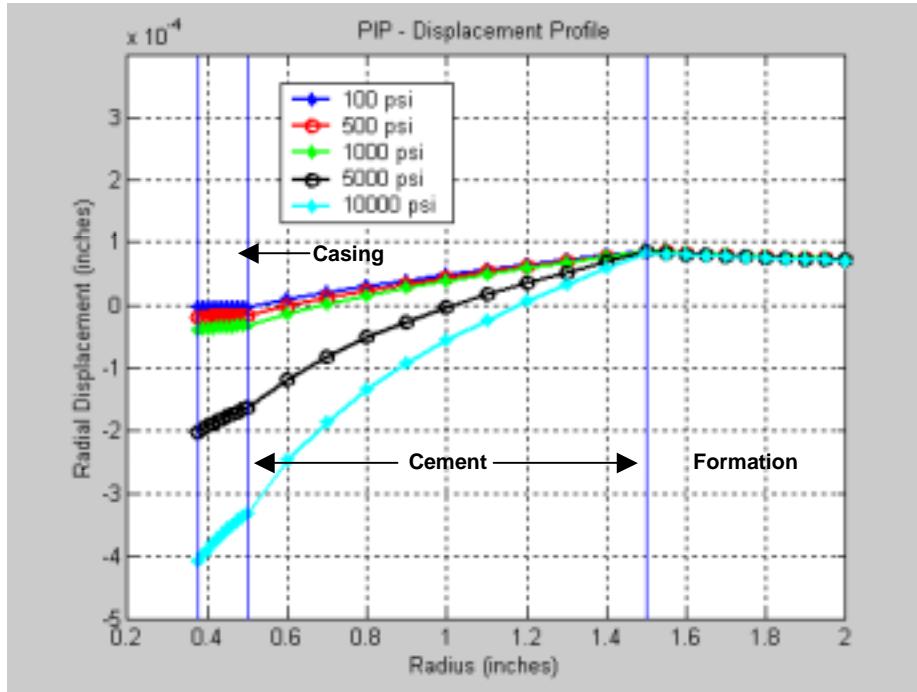
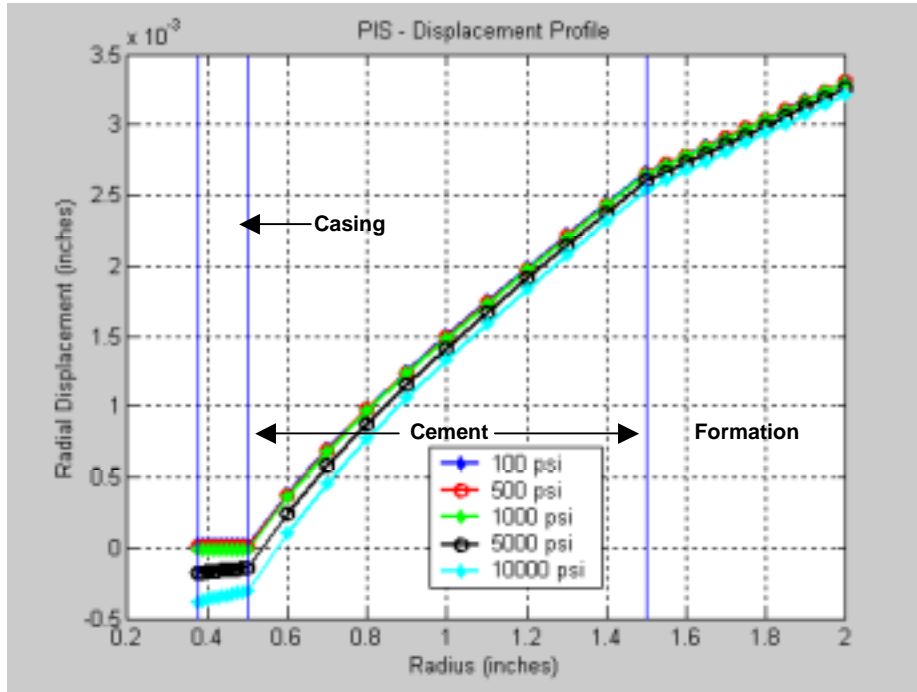




Figure 28— Displacement profile, simulated soft formation, 500-psi confining pressure





Appendix A—Young’s Modulus Testing

Traditional Young’s modulus testing was performed using ASTM C469¹, Standard Test Method for Static Modulus of Elasticity (Young’s Modulus) and Poisson’s Ratio of Concrete in Compression.

The following procedure is used for the Young’s modulus testing.

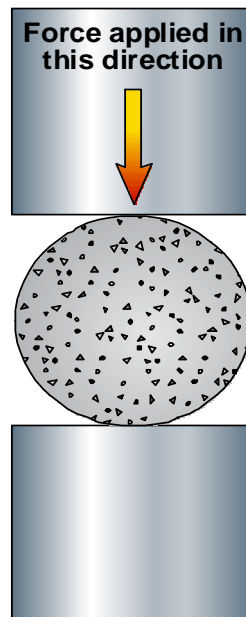
1. Each sample is inspected for cracks and defects.
2. The sample is cut to a length of 3.0 in.
3. The sample’s end surfaces are then ground to get a flat, polished surface with perpendicular ends.
4. The sample’s physical dimensions (length, diameter, weight) are measured.
5. The sample is placed in a Viton jacket.
6. The sample is mounted in the Young’s modulus testing apparatus.
7. The sample is brought to 100-psi confining pressure and axial pressure. The sample is allowed to stand for 15 to 30 min until stress and strain are at equilibrium. (In case of an unconfined test, only axial load is applied.)
8. The axial and confining stress are then increased at a rate of 25 to 50 psi/min to bring the sample to the desired confining stress condition. The sample is allowed to stand until stress and strain reach equilibrium.
9. The sample is subjected to a constant strain rate of 2.5 mm/hr.
10. During the test, the pore-lines on the end-cups of the piston are open to atmosphere to prevent pore-pressure buildup.
11. After the sample fails, the system is brought back to the atmospheric stress condition. The sample is removed from the cell and stored.



Appendix B—Tensile Strength Testing

Tensile strength was tested using ASTM C496² (Standard Test Method for Splitting Tensile Strength of Cylindrical Concrete Specimens). For this testing, the specimen dimensions were 1.5 in. diameter by 1 in. long. **Figure B1** shows a general schematic of how each specimen is oriented on its side when tested. The force was applied by constant displacement of the bottom plate at a rate of 1 mm every 10 minutes. Change in the specimen diameter can be calculated from the test plate displacement. The (compressive) strength of the specimen during the test can be graphed along with the diametric strain (change in diameter/original diameter) to generate the tensile Young's modulus.

Figure B1—Sample Orientation for ASTM C496-90 Testing





Appendix C—Shear Bond Strength Testing

Shear bond strength tests are used for investigating the effect that restraining force has on shear bond. Samples are cured in a pipe-in-pipe configuration (**Figure C1**) and in a pipe-in-soft configuration (**Figure C2**). The pipe-in-pipe configuration consists of a sandblasted internal pipe with an outer diameter (OD) of $1\frac{1}{16}$ in. and a sandblasted external pipe with an internal diameter (ID) of 3 in. and lengths of 6 in. A contoured base and top are used to center the internal pipe within the external pipe. The base extends into the annulus 1 in. and cement fills the annulus to a length of 4 in. The top 1 in. of annulus contains water.

For the pipe-in-soft shear bonds, plastisol is used to allow the cement to cure in a less-rigid, lower-restraint environment. Plastisol is a mixture of a resin and a plasticizer that creates a soft, flexible substance. This particular plastisol blend (PolyOne's Denflex PX-10510-A) creates a substance with a hardness of 40 duro.

The pipe-in-soft configuration contains a sandblasted external pipe with an ID of 4 in. A molded plastisol sleeve with an ID of 3.0 in. and uniform thickness of 0.5 in. fits inside this external pipe. With the aid of a contoured base and top, a sandblasted internal pipe with an OD of $1\frac{1}{16}$ in. is then centered within the plastisol sleeve. The pipes and sleeve are 6 in. long. The base extends into the annulus 1 in. and cement fills the annulus to a length of 4 in. between the plastisol sleeve and the inner $1\frac{1}{16}$ -in. pipe. The top inch of annulus is filled with water.

Figure C1—Cross-Section of Pipe-in-Pipe Configuration for Shear Bond Tests

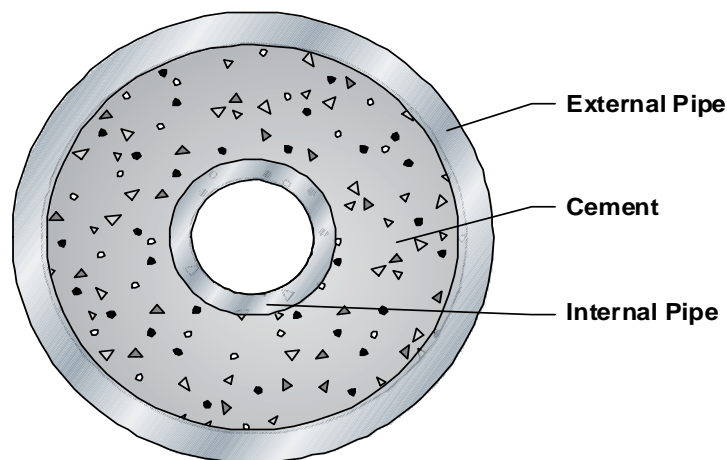
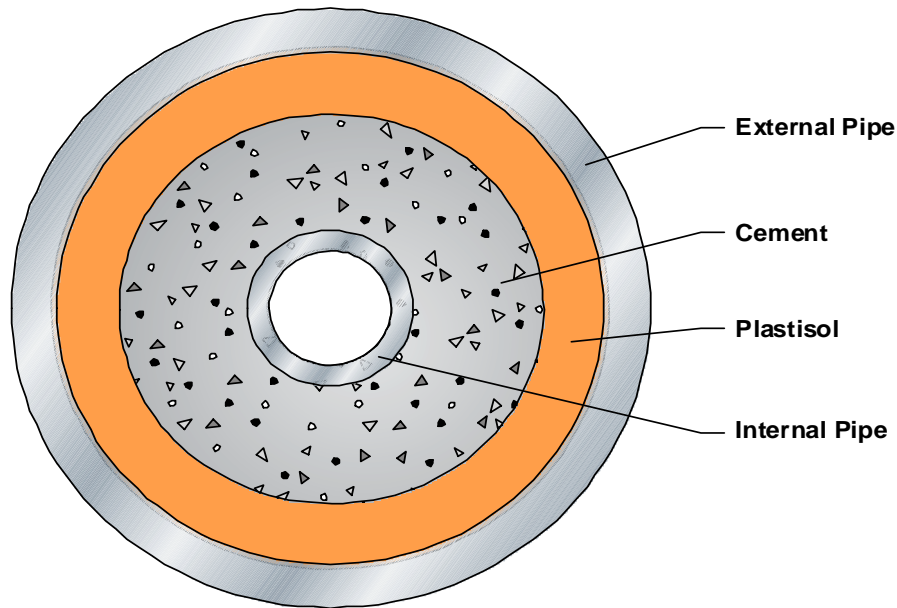
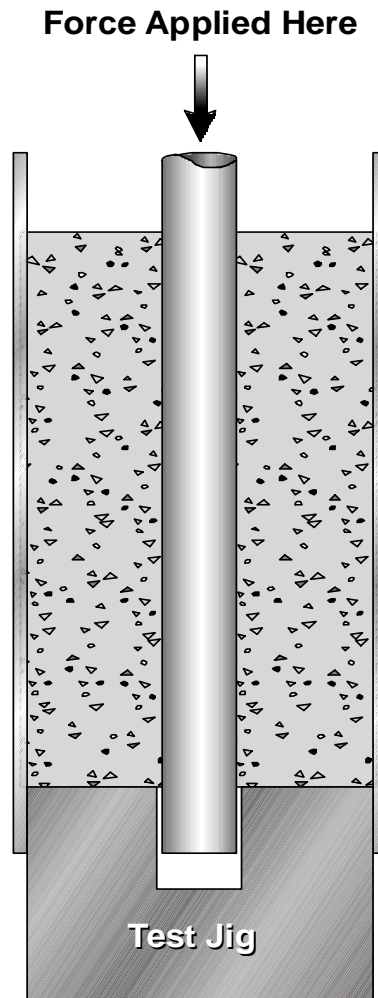


Figure C2— Cross-Section of Pipe-in-Soft Configuration for Shear Bond Tests



The shear bond measures the stress necessary to break the bond between the cement and the internal pipe. This was measured with the aid of a test jig that provides a platform for the base of the cement to rest against as force is applied to the internal pipe to press it through. **(Figure C3)** The shear bond force is the force required to move the internal pipe. The pipe is pressed only to the point that the bond is broken; the pipe is not pushed out of the cement. The shear bond strength is the force required to break the bond (move the pipe) divided by the surface area between the internal pipe and the cement.

Figure C3—Configuration for Testing Shear Bond Strength



Temperature Cycling

The effect that temperature cycling has on shear bond is tested as follows.

The temperature cycling procedure is designed to simulate temperature conditions that might be encountered during production of a well. The samples are first cured for 14 days in a 45°F water bath at atmospheric pressure. They are then subjected to five days of temperature cycling. During each of these five days of temperature cycling, the cured samples are cycled as follows.

1. Samples are removed from 45°F water bath and placed in 96°F water bath for one hour.
2. Samples are placed in 180°F water bath for four hours.
3. Samples are placed in 96°F water bath for one hour.



4. Samples are placed back in 45°F water bath.

Pressure Cycling

The effect that pressure cycling has on shear bond is tested as follows.

The pressure cycling procedure is designed to simulate pressure conditions that might be encountered during production of a well. Because these samples will be dealing with high pressures, the interior pipe of each sample was made from 1-in. diameter, 40/41 coiled tubing pipe that can withstand 10,000 psi. Each end of the pipe is threaded. One end will have a pressure-tight cap on it during pressure cycling and the other end of the pipe will be connected to the pressure source.

The samples are first cured for 14 days in a 45°F water bath at atmospheric pressure. They are then subjected to five periods of pressure cycling in which the interior pipe is pressured to 5,000 psi for 10 minutes and then allowed to rest at 0 psi for 10 minutes.



Appendix D—Shrinkage Testing

Using a modified Chandler Model 7150 Fluid Migration Analyzer, tests are performed to determine shrinkage of the neat Type I cement. The following procedures are used for performing the shrinkage testing.

1. Fill the test cell with 180 cm³ of the cement slurry.
2. Place 40 mL of water on top of cement slurry.
3. Place the hollow hydraulic piston into the test cell and on top of the water.
4. Close off the test cell and attach the pressure lines and piston displacement analyzer.
5. Close all valves except valve on top of test cell cap. Purge air out of system.
6. Apply 1,000-psi hydrostatic piston pressure to the test cell and begin recording data (time, piston displacement, and pressure).
7. Run test and gather data for desired amount of time.



Appendix E—Annular Seal Testing

The following procedures are for the use of the Pipe-in-Soft annular seal apparatus (for simulating soft formations) and the Pipe-in-Pipe annular seal apparatus (for simulating hard formations). The Pipe-in-Soft apparatus is to be used with cores that were formed using a soft gel mold surrounding the cement slurry to form a core that was cured to set by using a semi-restricting force on the outside of the core. The Pipe-in-Pipe apparatus is to be used with cores that were made inside steel pipes, giving the cement slurry a restricting force outside of the core.

Simulated Soft Formation Test Procedure

- 1.) After the core is cured, place the core inside the gel mold sleeve.
- 2.) Place the core and sleeve inside the Pipe-in-Soft steel cell.
- 3.) Once inside, both ends of the core are supported with o-rings.
- 4.) The o-rings are then tightened to close off air-leaks that might be present.
- 5.) Using water, pressurize the exterior circumference of the sleeve to 25 psi. Once the pressurized water is applied to the cell, check for leaks on the ends of the cell.
- 6.) Using the cell's end caps, cap off both ends of the steel cell. One end cap has a fitting that allows for N₂ gas to be applied into the cell, and the other end cap allows for the gas to exit the cell.
- 7.) Attach the pressure in-line to one end and then attach the pressure out-line to the other end.
- 8.) Apply pressure to the in-line. (Do not exceed 20 psig.) Measure the output of the out-line with flowmeters.

Simulated Hard Formation Test Procedure

- 1.) After the core is cured inside the steel pipe, using steel end caps, cap off each end of the pipe. Each end cap has a fitting that allows for gas to be applied into the pipe on one end, and also allows for the gas to exit the pipe on the other end.
- 2.) Attach the pressure in-line to one end, and then attach the pressure out-line to the other end.
- 3.) Apply pressure to the in-line. (Do not exceed 20 psig.) Measure the pressure output of the out-line with flowmeters.



Cementing Solutions, Inc.

Appendix F—Chandler Engineering Mechanical Properties Analyzer

See the attached brochure for a detailed description of the Chandler Engineering Mechanical Properties Analyzer, its applications, and its benefits.

MECHANICAL PROPERTIES ANALYZER

In recent years the oil/gas industry has begun to understand the implication of cement sheath mechanical properties on the ability of the cement to perform its zonal isolation function long term. With computer modeling capabilities, the mechanical compliance of the cement sheath relative to the deformation of the contacting rock and casing can be optimized to improve wellbore sealing. Cement formulations are being developed to address the need for flexure of the cement, rather than say the need for high compressive strength. However, the measurement of cement mechanical properties at elevated pressure and temperature has limited the implementation of cement mechanical properties as a design protocol.

With a technological breakthrough (patent applied), Chandler Engineering has developed the first high-pressure, high-temperature instrument designed specifically to measure the mechanical properties (elastic moduli and compressive strength) of oil/gas-well cements. Like the Ultrasonic Cement Analyzer (UCA), testing with the new Mechanical Properties Analyzer (Model 6265 MPro) begins with a cement slurry, which is placed into a pressure vessel. Measurements are then taken directly from this sample as it cures at elevated temperature and pressure.

The **CHANDLER** Model 6265 MPro has several advantages over routine mechanical properties testing. First, by providing continuous measurements, a single test with the MPro can provide more information about the cement properties than one would get from a series of routine tests. Second, samples for routine testing are typically cured in one vessel returned to room conditions, and then cored and/or cut, before testing begins in a different pressure vessel. With the MPro the sample conditions and integrity are maintained for the duration of the test (which may be days, weeks, or even months). Thus,



MODEL 6265 MPro

the MPro samples are neither subjected to damage from preparation, and handling, nor from unrealistic cooling and depressurization.

The **CHANDLER** Model 6265 MPro is optionally configured to perform UCA (compressive strength) Analyses in addition to the elastic mechanical properties measurements - thus providing a suite of information from a single sample and single test, and optimizing laboratory efficiency.

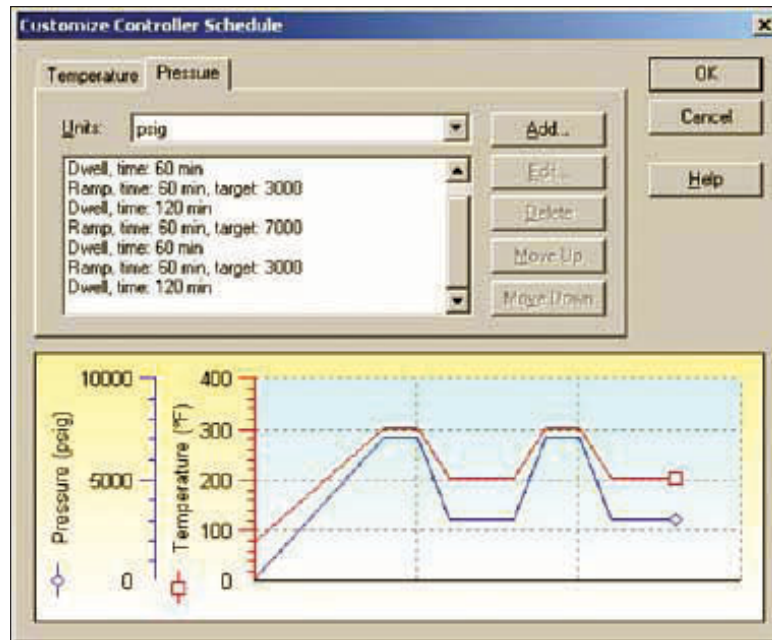
The new Model 6265 MPro includes programmable temperature control which provides the capability to investigate the impact of temperature variations on the cement mechanical properties. With the Chandler Model 6265P programmable pressure control module, the user can simulate realistic pressure conditions to evaluate the impact on the mechanical properties of the cement sample.

Combining the programmable pressure control module with programmable temperature control, will allow the investigator to replicate realistic pressure and temperature conditions.

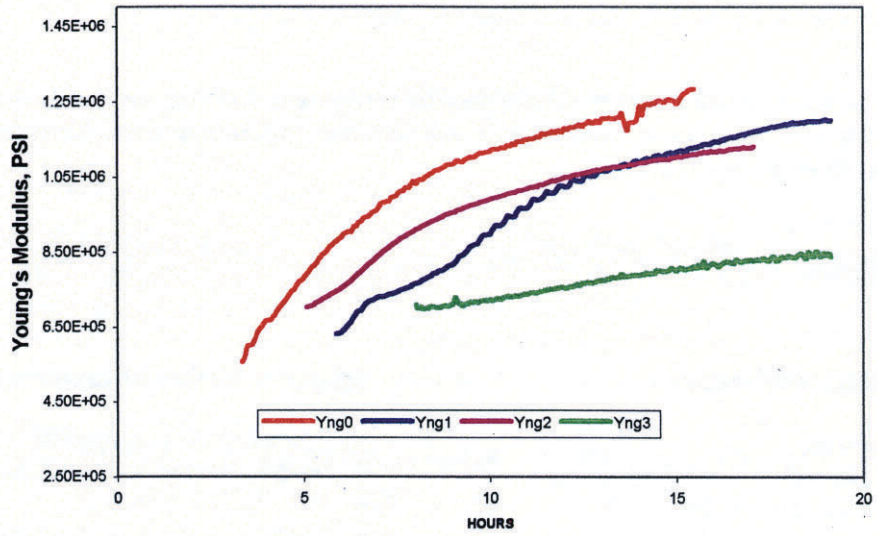
Using Chandler Engineering's state-of-the-art 5270 Automation System, complex-testing protocols can be easily set up and run using a standard PC. The 5270 System can be optionally configured to control and collect/display/analyze data from several Model 6265 MPro's.



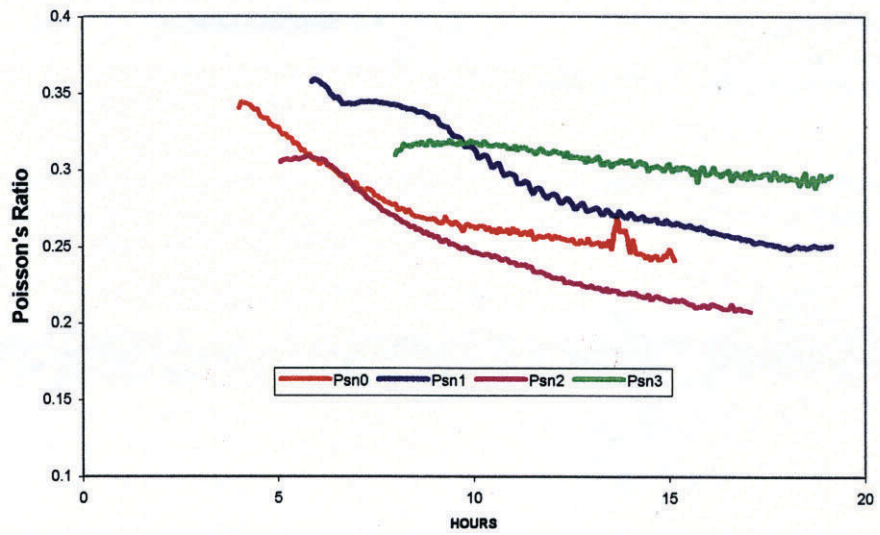
MODEL 6265P
PROGRAMMABLE PRESSURE
CONTROL MODULE



Cement Mechanical Properties Testing
Chandler Engineering Model 6265 Data
Young's Modulus vs Time



Cement Mechanical Properties Testing
Chandler Engineering Model 6265 Data
Poisson's Ratio vs Time



All Chandler Engineering products are covered by a full one-year warranty against defects in materials and workmanship. Sales terms, conditions and warranty statements are included with each quotation or confirmation of order.

More than 50 years ago, Chandler Engineering pioneered High Pressure and High Temperature Equipment. Today, Chandler Engineering is the leading manufacturer of a broad range of innovative and extremely reliable Measurement Instruments for the Energy Industry.

Chandler Engineering specializes in outfitting laboratories designed for testing cement, drilling muds and stimulation fluids. Through Research & Development, experienced manufacturing and worldwide logistic operations, Chandler Engineering provides for your complete laboratory requirements.

DRILLING AND COMPLETION INSTRUMENTS

- Cement Consistometers
- Cement Curing Chambers
- Cement Gas Migration Instruments
- Compressive Strength Testers
- Computer Automated Core-flow Instruments
- Constant Speed Mixers
- Corrosion Test Apparatus
- Data Acquisition System
- Liquid/Slurry HPHT Rheometers
- Portable Mud/Cement Laboratories
- Static Gel Strength Analyzer (SGSA)
- Stirred Fluid Loss Cells
- Ultrasonic Cement Analyzer (UCA)
- Viscometers (Atmospheric and Pressurized)

PIPELINE AND INDUSTRIAL INSTRUMENTS

- Carle Gas Chromatographs
- Hydraulic Pressure Testers and Gauges
- Liquid Densitometers
- Natural Gas Heating Value Analyzers
- Natural Gas Moisture Analyzers
- Ranarex Gas Gravimeters

RUSKA FLUID TECHNOLOGY INSTRUMENTS

- PVT Systems
- Digital Gasometers
- Digital High Pressure Pumps
- Phase Detection Systems
- Sample Cylinders

Plus a full range of replacement parts and accessories for all our instruments.

Contact us for our latest catalog of Cement Testing Laboratory Equipment, and other instruments for testing Oil Well Cements, Drilling Fluids, and Precision Physical Property Measurement Instrumentation for the Natural Gas Industry.

Copyright 2002 Chandler Engineering Company L.L.C.



CSI Technologies

Appendix IV

Report 4

MMS Project
Long-Term Integrity of Deepwater Cement
Systems Under Stress/Compaction Conditions

Report 4

Issued April 10, 2003



CEMENTING SOLUTIONS, INC.



Table of Contents

Objectives	1
Observations and Recommendations for Future Work	1
Testing Program and Procedures	2
<i>Cement Design Performance Testing.....</i>	<i>3</i>
<i>Mechanical Properties Testing.....</i>	<i>3</i>
<i>Mechanical Integrity Testing</i>	<i>4</i>
<i>Numerical Simulation.....</i>	<i>4</i>
<i>New Testing Methods</i>	<i>4</i>
Shear Bond and Annular Seal Test Modifications.....	4
Cement Column Seal Tests	5
Hydrostatic Testing to Anelastic Strain and Fatigue	5
Test Results	5
<i>Tensile Strength.....</i>	<i>5</i>
<i>Young’s Modulus with Various Confining Forces.....</i>	<i>6</i>
<i>Poission’s Ratio Testing.....</i>	<i>6</i>
<i>Strain Tests.....</i>	<i>7</i>
<i>Rock Properties Testing.....</i>	<i>7</i>
<i>Shear Bond Tests</i>	<i>10</i>
<i>Annular Seal Tests</i>	<i>10</i>
Appendix A—Test Procedures.....	11
<i>Modified Blending Procedures</i>	<i>11</i>
<i>Free-Fluid Testing.....</i>	<i>11</i>
<i>Compressive Strength Testing.....</i>	<i>12</i>
Sample Curing.....	12
<i>Young’s Modulus and Poisson’s Ratio Testing.....</i>	<i>12</i>
<i>Anelastic Strain and Cycling</i>	<i>13</i>
<i>Tensile Strength and Tensile Young’s Modulus.....</i>	<i>13</i>



<i>Annular Seal Testing Procedure</i>	14
Simulated Soft-Formation Test.....	14
Simulated Hard-Formation Test	15
Simulated Moderate-Strength Formation Test	15
Temperature and Pressure Cycling.....	15
<i>Shear Bond Strength Testing</i>	16
Pressure Cycling Schedule	17
Temperature Cycling Schedule	17
<i>Cement Column Seal Tests</i>	18
Appendix B—Test Data	20
Appendix C—Numerical Modeling	35
<i>Introduction</i>	35
<i>Mathematical Model</i>	36
Assumptions	38
Stress Conditions	38
Parametric Studies	39



Objectives

The overall objective of this project is to determine the properties that affect cement's capability to produce a fluid-tight seal in an annulus. The project primarily focuses on deepwater applications, but general applications will also be examined. The research conducted thus far is focused on the measurement of cement's mechanical properties and correlation of these properties to the cement's performance. Also, research was conducted to determine which laboratory methods should be used to establish the cement's key properties.

Results obtained during this reporting period focused on

- continued measurement of mechanical properties of tensile strength and Young's modulus under various confining loads
- mechanical bond integrity testing to include shear bond and annular seal testing on specimens cured under various cyclic curing schedules
- mathematical simulation of stresses induced in a cemented annulus

These results are tabulated in the Results section below. All rock properties test results developed during this project, including available graphical data, are presented in Appendix B.

Observations and Recommendations for Future Work

Results of testing during this reporting period indicate:

1. Significant variation in Poisson's ratio with varying stress rate. Loading samples at a faster rate resulted in higher Poisson's ratio values. Inclusion of a CT scan for mechanical properties samples revealed another variable: air entrainment. The presence of entrained air appeared to lower Poisson's ratio values.
2. Questions regarding comparability of data for different compositions normalized with respect to each composition's hydrostatic yield strength. A modification of the test procedure is suggested to standardize the confining stress at 500-psi and cycle samples repeatedly to 25%, 50%, and 75% of each composition's compressive strength under that confining stress. Measurement of anelastic strain with cycling should provide a more comparable value of each composition's performance.
3. Several compositions tested in the annular seal apparatus did not fail with repeated cycling. Therefore, the addition of more aggressive test conditions is required to induce seal failure. The addition of an intermediate formation strength is also proposed for further quantifying the performance of various compositions.

Future work includes:

- implementation of a modified test procedure with future testing
- quantification of anelastic strain magnitudes and analysis of consequences in the well environment



- completion of numerical analyses after annular seal testing is complete

Testing Program and Procedures

This section does not flow as well as it could. I assume that the Task 1 is completed; are these tasks performed sequentially or concurrently?

The following cement slurries will be examined: Type 1 cement, foamed cement, bead cement, Class H cement, and latex cement. The effects of fibers and expansion additives on the performance of various cements are also examined. The cements are tested primarily for deepwater applications, but their performance under all application conditions is also examined.

Tasks in the project are listed below:

- Task 1 – Problem Analysis
- Task 2 – Property Determination
- Task 3 – Mathematical Analysis
- Task 4 – Testing Baseline
- Task 5 – Refine Procedures
- Task 6 – Composition Matrix
- Task 7 – Conduct Tests
- Task 8 – Analysis of Results
- Task 9 – Decision Matrix

Compositions tested in this project are outlined in Table 1 below. The compositions chosen represent those that are traditionally used in deepwater applications as well as newly developed compositions and compositions designed to improve performance.



Table 1—Cement Compositions for Testing

Description	Cement	Additives	Water Requirement (gal/sk)	Density (lb/gal)	Yield (ft ³ /sk)
Neat Type I slurry	Type 1	—	5.23	15.6	1.18
Type I slurry with fibers	Type 1	3.5% carbon fibers-milled	5.2	15.6	1.16
Latex slurry	Type 1	1.0 gal/sk LT-D500	4.2	15.63	1.17
Latex slurry with fibers	Type 1	1.0 gal/sk LT-D500 3.5% carbon fibers-milled 0.50% Melkcrete	4.09	15.63	1.20
Foam slurry (12-lb/gal)	Type 1	0.03 gal/sk Witcolate 0.01 gal/sk Aromox C-12 1% CaCl	5.2	12.0	1.19
Bead slurry	Type 1	13.19% K-46 beads	6.69	12.0	1.81
Neat Class H slurry	Class H	—	4.3	16.4	1.08
Class H slurry with fibers	Class H	—	4.3	16.4	1.08
Sodium metasilicate slurry	Type 1	—	14.22	12.0	2.40

Testing and analysis of the cements is divided into four categories:

1. cement design performance testing
2. mechanical properties testing
3. mechanical integrity testing
4. numerical simulation

Cement Design Performance Testing

Standard cement design performance testing, including rheology, thickening time, free fluid, set time, compressive strength, etc. are performed according to procedures outlined in API Spec. 10.

Mechanical Properties Testing

Mechanical properties tested include: tensile strength/tensile Young’s modulus (T), compressive Young’s modulus, Poisson’s ratio, and hydrostatic pressure cycling.

Tensile strengths are determined with the Brazilian Test Method. From this test, the tensile Young’s modulus (T) will be computed, as well as the maximum yield of the slurry.

The compressive Young’s modulus are determined through compression tests with confining loads (defined by 0-psi break) with a baseline of a 14-day cure. Chandler’s new



mechanical properties device will also obtain acoustic data on the slurry used in these tests. The Poisson's ratio will also be determined from these tests, and it is variable with respect to the stress rate, slurry type, presence of air entrainment, and perhaps other variables.

Mechanical Integrity Testing

The mechanical integrity issues of the cement slurries include the flow of fluids around the cement, through the matrix of the cement, and stresses in the cement. To predict the flow of fluid around the cement, various cement slurries will be tested for bonding capability, microannuli formation, and deformation. The flow of fluids through the matrix of the cement will be examined through tests of the cement slurries' resistance to cracking and permeability changes. The stress applied to the cement slurries will be determined as a function of pressure, temperature, pipe buckling, and formation compaction. The stresses will also be determined under cyclic conditions.

Shear bond and annular seal measurements are taken under cyclical conditions for both soft and hard formations. The cement specimens to be tested for shear bond are cured at 45°F for 14 days and then temperature-cycled once per day from 45°F to 180°F and back to 45°F during the cycling period.

The temperature cycling procedure is as follows:

1. Samples are placed in a 96°F water bath for 1 hour.
2. Samples are placed in a 180°F water bath for 4 hours.
3. Samples are placed in a 96°F water bath for 1 hour.
4. Samples are placed back into a 45°F water bath.

Numerical Simulation

Deepwater cement systems will be numerically modeled to aid in the understanding of how various stress conditions affect the long-term integrity of cement. This process is discussed in detail in Appendix C of this report.

New Testing Methods

Shear Bond and Annular Seal Test Modifications

Results from testing thus far with hard formation and soft formation simulation indicate the need for a simulated formation of intermediate strength. The altered shear and annular seal testing will include a simulated medium-strength formation with Schedule 40 PVC pipe as the outside mold for the cement sheath.

Additional stresses will be imposed on all test specimens by increasing the maximum pressure to which the inner pipe is stressed. Additionally, shear bond tests will be run only after a composition has been tested for annular seal. The shear bond test specimens



will be subjected to the same pressure cycling and temperature cycling that produced annular seal failure. This will provide a comparison between shear bond and annular seal behavior.

Cement Column Seal Tests

A series of cement column seal tests was initiated to illustrate the sealing effectiveness of several cements that are subjects of the project. These tests are designed to test a cement’s ability to isolate gas pressure across an enclosed column. Ten-foot lengths of 2-in. pipe are filled with cement slurry, pressurized to 1000 psi, and then cured for eight days. After curing, low-pressure gas (100 or 200 psi) is periodically applied to one end of each test pipe and the gas flow rate through the cement column is measured. This testing will continue for the duration of the project.

Hydrostatic Testing to Anelastic Strain and Fatigue

Hydrostatic test results were reviewed, and questions were raised regarding comparability of data for different compositions normalized with respect to each composition’s hydrostatic yield strength. The group decided to modify the test procedure to standardize confining stress at 500 psi and cycle samples repeatedly to 25%, 50%, and 75% of each composition’s compressive strength under that confining stress. Measurement of anelastic strain with cycling should provide a more comparable value of each composition’s performance.

Test Results

This section contains results from testing conducted throughout this project period, as well as results from previous test periods. All mechanical property test results and performance test results obtained throughout the project are tabulated here. Graphical data for all mechanical property tests are presented in Appendix B of this report.

Tensile Strength

The results of all tensile strength tests are presented in Tables 2 through 6. Table 2 illustrates the effects of carbon fibers on tensile strength. The two- to three-fold increase in tensile strength is significant, indicating the potential for fibers to increase the durability of cement.

Table 2—Tensile Strength and Young's Modulus

Slurry	Tensile Strength (psi)	Young’s Modulus
Foam slurry (12-lb/gal)	253	3.23 E4
Neat Type I slurry	394/213	19.15/8.16 E4
Type I slurry with fibers	1071	9.6 E4
Latex slurry	539	5.32 E4
Latex slurry with fibers	902	8.5 E4



Young's Modulus with Various Confining Forces

The effects of confining stress on compressive strength and Young's modulus are presented in Tables 3 through 6. These results indicate a significant increase in compressive strength with increasing confining stress in lower-strength compositions such as foam cement and latex cement.

Table 3—Type I, Compressive Young's Modulus

Confining Pressure (psi)	Effective Strength (psi)	Young's Modulus (psi)
0	8645	16.7 E5
1500	8160	11.1 E5
5000	8900	9.1 E5

Table 4—12-lb/gal Foam, Compressive Young's Modulus

Confining Pressure (psi)	Effective Strength (psi)	Young's Modulus (psi)
0	2885	5.8 E5
500	3950	6.8 E5
1000	4510	6.1 E5

Table 5—12-lb/gal Bead, Compressive Young's Modulus

Confining Pressure (psi)	Effective Strength (psi)	Young's Modulus (psi)
0	5150	9.5 E5
500	6000	8.1 E5
1000	6150	1 E6

Table 6—Latex, Compressive Young's Modulus

Confining Pressure (psi)	Effective Strength (psi)	Young's Modulus (psi)
0	3500	5.6 E5
250	5250	8.9 E5
500	6000	9.4 E5

Poisson's Ratio Testing

Initial results of Poisson's ratio testing on these lightweight cement compositions were unexpectedly low. Continued Poisson's ratio testing during this test period to determine reasons for these low values confirmed the accuracy of these early results. The low Poisson's ratio values for these compositions are theorized to be related to the porosity of the specimens. Several published technical reports have documented this tendency for Poisson's ratio to be effectively lowered as porosity increases.

Another potential variable in Poisson's ratio testing is load rate. An investigation into the



effect of load rate on Poisson’s ratio indicated that load rate does affect Poisson’s ratio measurement (Table 7). Table 8 presents data generated with a load rate of 250 psi/min. While these values are lower than what has traditionally been considered acceptable, the data are generally positive.

CT scans performed on Poisson’s ratio test specimens indicated a link between large voids or pore spaces and variable Poisson’s ratio. This procedure will be included in future testing and samples with large voids will be discarded. CT scans are included in Appendix B.

Table 7—Effect of Load Rate on Poisson's Ratio

Load Rate	Poisson's Ratio
100 psi/min	0.1
250 psi/min	0.08
500 psi/min	-0.01

**Table 8—Poisson's Ratio
(50-psi confining pressure, 250 psi/min load rate)**

Slurry	Failure (psi)	v Radial (ft ³ /sk)
Foam slurry (12-lb/gal)	3100	0.00
Bead slurry	4100	-0.01
Neat Class H slurry	6450	0.0012
SMS slurry	920	0.005
Type I slurry	6500	0.1

Strain Tests

The following data indicate that foam cement underwent the most anelastic strain during cycling. These results will be expanded upon in future anelastic strain testing.

Table 9—Strain Amounts/Cycling

Slurry	1000 psi	2000 psi	3000 psi	4700 psi
Foam slurry (12-lb/gal)	0.00261	0.00167	—	—
Bead slurry	0.00191	0.00158	0.00115	—
Class H slurry	0.00161	0.0015	0.00102	—
Type I slurry	0.00108	0.0008	0.00069	—

Rock Properties Testing

Results obtained with the Chandler Engineering device are generally in line with expected values. However, Poisson’s ratio values are very high compared to results from this study and Young’s modulus data are somewhat elevated compared to values measured with traditional methods.



Table 10—Data Obtained with Chandler Device

Slurry	Poisson's Ratio	Compressive Young's Modulus
Type I slurry	0.20	2.3 E6
Bead slurry	0.31	1.5 E6
Latex slurry	0.39	1.4 E6
Latex slurry with fibers	0.19	2.5 E6
Class H	0.24	2.2 E6
Class H slurry with fibers	0.25	2.3 E6

Table 11—Data Obtained with

Slurry	Poisson's Ratio	Compressive Young's Modulus
Type I slurry	0.1	1.7 E6
Bead slurry	0.0	9.5 E5
Latex slurry	—	5.6 E5
Latex slurry with fibers	—	—
Class H slurry	0.0	1.0 E6
Class H slurry with fibers	—	—

The data in Table 12 were gathered to illustrate the variations between radial measurement techniques. Note that wide variations exist between Poisson's ratios measured with point measurement devices, even among measurements taken from the same sample.



Table 12—Effects of Variable Confinement and Load Rates on Rock Properties

Slurry	Length (in.)	Diameter (in.)	Saturated Wt (g)	Test Type	Confining Stress	Failure (psi)	Young's Modulus x(E6)	ν Circumferential	ν Radial Point Meas. 1	ν Radial Point Meas. 2	Test Rate (psi/min)
Foam	2.98	1.4	126.39	confine fail	50 psi	3,100	0.432	-5.00E-05	1.6	1.7	250
Bead	3.03	1.4	113.75	confine fail	50 psi	4,100	0.616	-0.01	-4.6	0.26	250
Class H	2.89	1.4	156.82	confine fail	50 psi	6,450	1	0.0012	3.75	-0.79	250
SMS	3.01	1.4	111.08	confine fail	50 psi	921	0.086	0.005	1.92	-0.95	250
Type I	3.08	1.4	152.1	confine fail	50psi	6,500	1	0.1	-1.8	-0.05	250



Shear Bond Tests

Results of shear bond testing (Table 13) indicated that the bond was degraded extensively both by pressure cycling and temperature cycling. This degradation seemed to be aggravated by the soft formation. Modifications are being made to the shear bond test method so that the results of future tests will be more comparable with the results from annular seal tests.

Table 13—Shear Bond Strengths (psi)

System	Simulated Formation	Type I Slurry	Foam Slurry	Bead Slurry	Latex Slurry
Baseline	hard	1194	127/98	109/78	—
	soft	198	233	143	223
Temperature-Cycled	hard	165	299/215	191/269	—
	soft	72	7	56	149
Pressure-Cycled	hard	194/106	276/228	294/170	—
	soft	23	22*	23*	11

* Visual inspection revealed samples were cracked.

Annular Seal Tests

Results presented in Table 14 indicate that in cyclic testing, all specimens tested in a soft formation simulation failed whereas all specimens tested in a hard-formation simulation maintained a seal. A simulated formation with intermediate strength is needed to further differentiate seal effectiveness. To determine the failure point in the simulated hard-formation tests, additional stresses must be imposed by heating or pressure application.

Table 14—Annular Seal Tests

Condition Tested	Formation Simulated	Type I Slurry	Foamed Slurry	Bead Slurry
Initial Flow	Hard	0 Flow	0 Flow	0 Flow
	Soft	0 Flow	0.5 (md)	0 Flow
Temperature-Cycled	Hard	0 Flow	0 Flow	0 Flow
	Soft	0 Flow	123 md	43 md*
Pressure-Cycled	Hard	0 Flow	0 Flow	0 Flow
	Soft	27 md	0.19 md*	3 md

* Visual inspection revealed samples were cracked.



Appendix A—Test Procedures

Following the procedures set forth in API Spec. 10¹, thickening-time tests were performed on all cement systems. The test conditions started at 80°F and 600 psi, and were ramped to 65°F and 5,300 psi within 48 minutes.

Modified Blending Procedures

Some preparation and testing methods were modified to adapt to the lightweight bead and foamed slurries.

The following blending procedure was used for the bead slurry. It was modified to minimize bead breakage due to the high shear of API blending procedures.

1. Weigh out the appropriate amounts of the cement, water, and beads into separate containers.
2. Mix the cement slurry (without beads) according to Section 5.3.5 of API Spec. 10¹.
3. Pour the slurry into a metal mixing bowl and slowly add beads while continuously mixing by hand with a spatula. Mix thoroughly.
4. Pour the slurry back into the Waring blender and mix at 4,000 rev/min for 35 seconds to evenly distribute the contents.

Testing methods for the foamed slurries were also modified. For example, thickening time is performed on unfoamed slurries only. Because the air in the foam does not affect the hydration rate, the slurry is prepared as usual per API Spec. 10¹ and then the foaming surfactants are mixed into the slurry by hand without foaming the slurry.

Free-Fluid Testing

The free-fluid testing that was performed on the Type I cement, foamed cement and bead slurries came from API Spec. 10¹ (Table A1). The free-fluid procedure, also referred to as operating free water, is used with a graduated cylinder that is oriented vertically.

Table A1—Free Fluid Test Results

Slurry System	Thickening Time to 100 Bc (hr:min)	Percentage of Free Fluid
Neat	4:38	0.8
Foamed	3:42	0.0
Bead	5:04	0.8



Compressive Strength Testing

The compressive strengths were derived using the 2-in. cube crush method specified in API Spec. 10¹. The samples were cured in an atmospheric water bath at 45°F. The reported values were taken from the average of three samples.

Sample Curing

Test specimens for rock properties testing are mixed in a Waring blender and poured into cylinder molds. The samples are then cured for seven days in an atmospheric water bath set at 45°F.

Performance test-fixture molds are filled with cement mixed in the same manner. These fixtures are also cured in a 45°F water bath for seven days prior to testing.

Young's Modulus and Poisson's Ratio Testing

Traditional Young's modulus testing is to be performed using ASTM C469², Standard Test Method for Static Modulus of Elasticity (Young's Modulus) and Poisson's Ratio of Concrete in Compression with a modified load rate.

The following procedure is used:

1. Inspect each sample for cracks and defects. Evaluate a CT scan of each sample for excessively large pores. Discard any defective samples.
2. Cut each sample to a length of 3.0 in.
3. Ground the sample's end surfaces to create a flat, polished surface with perpendicular ends.
4. Measure the sample's physical dimensions (length, diameter, weight).
5. Place the sample in a Viton jacket.
6. Mount the sample in the Young's modulus testing apparatus.
7. Verify that the pore lines on the end caps of the piston are open to atmosphere to prevent pore-pressure buildup.
8. Bring the sample to 100-psi confining pressure and axial pressure, and allow the sample to stand for 15 to 30 minutes until stress and strain are at equilibrium. (In case of an unconfined test, apply only axial load.)
9. Increase the axial and confining stress at a rate of 25 to 50 psi/min to bring the sample to the desired confining stress condition, and allow the sample to stand until stress and strain reach equilibrium.
10. Subject the sample to a constant stress rate of 250 psi/min.
11. Measure the radial strain with a circumferential band instrumented with a strain gauge rather than multiple point deflections.
12. After the sample fails, bring the system back to the atmospheric stress condition.
13. Remove the sample from the cell and store it.



Specimens from each composition under investigation will first be tested in an unconfined (50-psi radial stress) condition to determine unrestrained yield and mechanical properties. A minimum of three samples will be tested for each test condition.

Anelastic Strain and Cycling

Anelastic strain testing is a variation of hydrostatic testing and is designed to allow a more accurate evaluation of permanent strain resulting from stressing different test compositions. This procedure standardizes confining stress at 500 psi and calls for samples to be cycled to 25%, 50%, and 75% of each composition's compressive strength under that confining stress. Measurement of anelastic strain with cycling provides a more comparable value of each composition's performance.

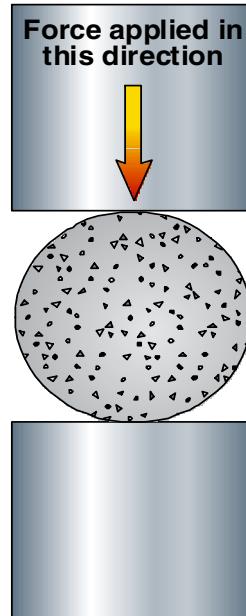
The exact procedure involves compression-testing a sample to failure in the load cell with 500-psi confining stress. Once this value is determined (from a Young's modulus test), additional samples will be tested by applying an axial load equal to 25%, 50%, and 75% of the failure load and cycling until the samples fail. A cyclic loading rate will be maintained at 250 psi/min and confining force will be maintained at 500 psi. Plastic deformation will be measured at the end of each cycle. Results will include cycles to failure and anelastic strain per cycle. CT scans will be performed on each sample prior to testing to rule out the possibility of large voids in the sample.

Tensile Strength and Tensile Young's Modulus

Tensile strength is to be tested using ASTM C496³ (Standard Test Method for Splitting Tensile Strength of Cylindrical Concrete Specimens). For this testing, the specimen dimensions were 1.5 in. in diameter by 1 in. long. **Figure A1** shows a general schematic of how a specimen is oriented on its side when tested. Force is applied by constant displacement of the bottom plate at a rate of 1 mm every 10 minutes. Change in the specimen diameter can be calculated from the test plate displacement. The (tensile) strength of the specimen during the test can be graphed along with the diametric strain (change in diameter/original diameter) to generate the tensile Young's modulus. A minimum of three samples per composition will be tested. CT scans of samples will be examined for defects prior to testing.



Figure A1—Sample Orientation for ASTM C496-90 Testing



Annular Seal Testing Procedure

Cements are mixed and poured into specified molds and cured for 7 days in an 80°F water bath. After curing, three specimens from each test composition and condition are tested.

Three separate molds simulating soft, intermediate, and hard formations are used to prepare samples:

- The soft formation mold is a soft gel mold that surrounds the cement slurry and provides a semi-restricting force on the outside of the core while it cures.
- The intermediate specimen is designed with a 3-in. diameter Schedule 40 PVC pipe as the outer containment.
- The hard formation mold features a 3-in. diameter Schedule 40 steel pipe as the outer containment, giving the cement slurry a restricting force outside of the core.

The following annular seal test procedures are all designed for use with the annular seal apparatus. The samples produced from the three mold types are each tested with a different procedure. In all annular seal testing, stress was applied to the specimens by applying hydraulic pressure to the inner pipe or heating the inner pipe.

Simulated Soft-Formation Test

1. After the core is cured, place the core inside the gel mold sleeve.
2. Place the core and sleeve inside the Pipe-in-Soft steel cell.
3. With the core inside the cell, make sure that both ends of the core are supported with O-rings.



4. Attach the end plates to tighten the O-rings and close off leaks that might be present.
5. Using water, pressurize the exterior circumference of the sleeve to 25 psi. Once the pressurized water is applied to the cell, check for leaks on the ends of the cell.
6. Using the cell's end caps, cap off both ends of the steel cell. One end cap has a fitting that allows for N₂ gas to be applied to the cell; the other end cap allows for the gas to exit the cell.
7. Attach the pressure inlet line to the bottom of the steel cell, and attach the pressure outlet line to the top of the cell.
8. Apply pressure to the inlet line. (Do not exceed 20 psig.)
9. Measure the flow out of the outlet line with flowmeters.

Simulated Hard-Formation Test

1. After the core is cured inside the steel pipe, cap off each end of the pipe with a steel end cap. Each end cap has a fitting that allows for gas to enter or exit the pipe.
2. Attach the pressure inlet line to the bottom of the steel cell, and attach the pressure outlet line to the top of the cell.
3. Apply pressure to the inlet line. (Do not exceed 20 psig.)
4. Measure the pressure out of the outlet line with flowmeters.

Simulated Moderate-Strength Formation Test

The hard formation test procedure can be used for this test by replacing the outer pipe with Schedule 40 PVC.

Temperature and Pressure Cycling

Thermal cycling was simulated by inserting heaters into the inner pipe and heating the inner pipe from 80°F to 180°F, then allowing the pipe to cool to 80°F. Three specimens were tested for each composition. The temperature schedule in Table A2 was used in the testing.

**Table A2—Temperature Schedule
for Thermal Cycling**

Hours	Temperature (°F)
1	94
2	108
3	121
4	135
5	149
6	163
7	176
8	190



For thermal testing, a thicker-walled inner pipe must be used to provide more steel volume for expansion. This change is necessary to accommodate increased stress application to induce failure in all samples. The new inside pipe will be 1.5-in. Schedule 80 pipe and the outer containment diameter will be increased to 5 in.

For pressure cycling, hydraulic pressure was applied to the inner pipe. For the initial cycle, pressure was increased from 0 to 500 psi. Pressure was then released to 0 and flow measurements were made. Additional cycles were run by increasing the upper pressure limit by 500 psi (0 to 1,000 psi, 0 to 1,500 psi, 0 to 2,000 psi, etc.) up to a maximum of 10,000 psi, and flow measurements were made at the end (0) point of each cycle. If the sample did not fail at or below 10,000 psi of pressure, the sample was cycled at 10,000 psi a minimum of 5 times. Three specimens will be tested for each composition.

Shear Bond Strength Testing

Shear bond strength tests are used for investigating the effect of restraining force on shear bond. Samples are cured in a hard formation configuration (**Figure A2**) and in a soft formation configuration (**Figure A3**). The hard configuration consists of a sandblasted internal pipe with an outer diameter (OD) of 1 1/16 in. and a sandblasted external pipe with an internal diameter (ID) of 3 in. and lengths of 6 in. A contoured base and top are used to center the internal pipe within the external pipe. The base extends into the annulus 1 in. and cement fills the annulus to a length of 4 in. The top 1 in. of annulus contains water.

Figure A2—Cross-Section of Pipe-in-Pipe Configuration for Shear Bond Tests

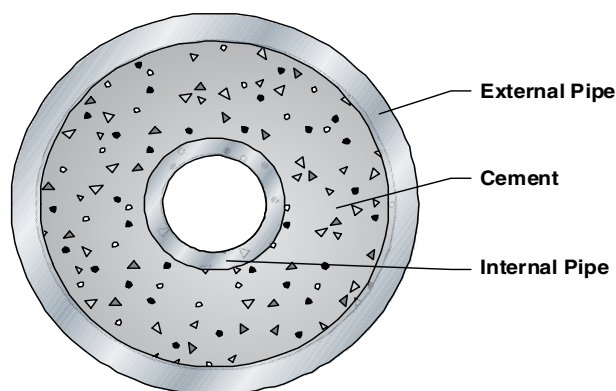
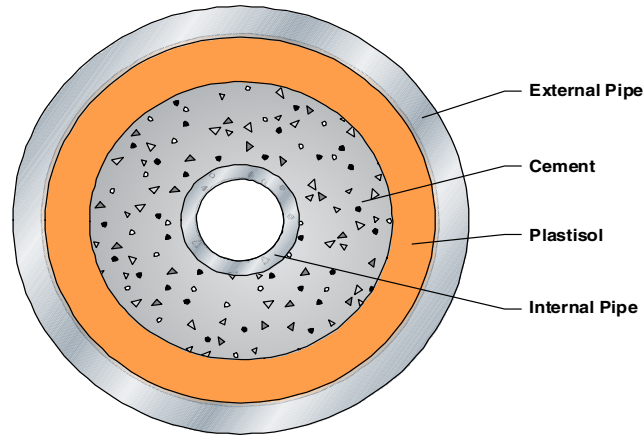




Figure A3— Cross-Section of Pipe-in-Soft Configuration for Shear Bond Tests



In the soft formation shear bond tests, Plastisol allows the cement to cure in a less-rigid, lower-restraint environment. Plastisol is a mixture of a resin and a plasticizer that creates a soft, flexible substance. This particular Plastisol blend (PolyOne's Denflex PX-10510-A) creates a substance with a hardness of 40 duro.

The soft formation configuration contains a sandblasted external pipe with a 4-in. ID. A molded Plastisol sleeve with a 3-in. ID and uniform thickness of 0.5 in. fits inside this external pipe. A sandblasted internal pipe with an OD of 1 1/16 in. is then centered within the Plastisol sleeve. The pipes and sleeve are 6 in. long. The base of the exterior pipe extends into the annulus 1 in. and cement fills the annulus to a height of 4 in. between the Plastisol sleeve and the inner 1 1/16 -in. pipe. The top inch of annulus is filled with water.

The intermediate formation test specimen will be configured just as the hard formation except the outer pipe is made of PVC.

Cycling tests for the shear bond specimens were performed according to the following test schedules:

Pressure Cycling Schedule

1. Cure specimens for 14 days at 45°F.
2. Apply 5000 psi hydraulic pressure to the inner pipe and maintain for 10 minutes.
3. Release the pressure and wait 10 minutes.
4. Repeat the cycle four more times.
5. Perform the shear bond test.

Temperature Cycling Schedule

1. Cure specimens for 14 days in a 45°F water bath.

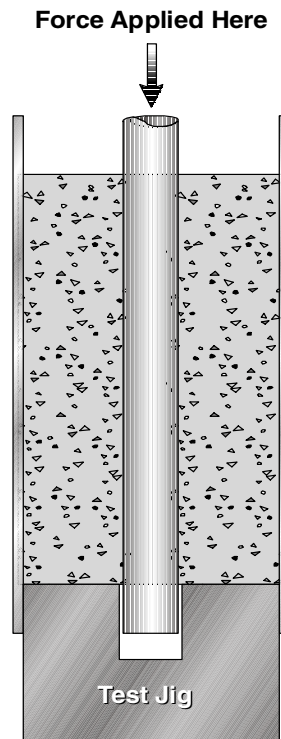


2. Move specimens from a 45°F water bath to a 96°F water bath for 1 hour.
3. Place specimens in a 180°F water bath for 4 hours.
4. Place specimens in a 96°F water bath for 1 hour.
5. Return specimens to a 45°F bath.
6. Repeat the cycle four more times.
7. Perform the shear bond test.

A new test procedure for future shear bond testing will allow the comparison of results with annular seal test results. After failure is noted in the annular seal test, the exact pressure or temperature cycle sequence will be repeated for the shear bond specimens. Shear bond will be measured after the cycling to determine the level of bond remaining.

The shear bond measures the stress necessary to break the bond between the cement and the internal pipe. This was measured with the aid of a test jig that provides a platform for the base of the cement to rest against as force is applied to the internal pipe to press it through (**Figure A4**). The shear bond force is the force required to move the internal pipe. The pipe is pressed only to the point that the bond is broken; the pipe is not pushed out of the cement. The shear bond strength is the force required to break the bond (move the pipe) divided by the surface area between the internal pipe and the cement.

Figure A4—Configuration for Testing Shear Bond Strength



Cement Column Seal Tests

Eight-foot lengths of 2-in. Schedule 40 pipe are mounted vertically and fitted with caps at



the top and bottom equipped with pressure input and outlet ports. The bottom of each pipe is filled with 6 in. of 20- to 40-mesh sand to provide an open base for gas injection. Two fixtures are filled with one of four different cement slurries (bead, Type 1, latex, and SMS). Samples are capped with water and cured for seven days under 1000 psi of pressure. After the samples are cured, 100 psi of pressure is applied to the bottom of each fixture and any flow through the column is monitored.



Appendix B—Test Data

Graphical data for all mechanical properties tests performed in this investigation are presented in this appendix.



Table B1—Hydrostatic Cycle Test

Slurry	Length (in.)	Diameter (in.)	Saturated Wt (g)	Young's Modulus x(E6)	Axial Strain at 1000 psi (ramp up)	Axial Strain at 1000 psi (ramp down)	Net Axial Strain at 1000 psi	Axial Strain at 2000 psi (ramp up)	Axial Strain at 2000 psi (ramp down)	Net Axial Strain at 2000 psi	Test Rate (psi/min)
Foam-2	3	1.4	125.2	0.65	0.00375	0.00636	0.00261	0.00542	0.00709	0.00167	250
Bead-1	3.1	1.4	114	2	0.0079	0.00981	0.00191	0.00846	0.01004	0.00158	250
Class H-1	3.1	1.4	159.1	2	0.00139	0.003	0.00161	0.00189	0.00339	0.0015	250
Neat A-1	3.1	1.4	153.9	3	0.00116	0.00224	0.00108	0.00147	0.00227	0.0008	100

Slurry	Length (in.)	Diameter (in.)	Saturated Wt (g)	Young's Modulus x(E6)	Axial Strain at 3000 psi (ramp up)	Axial Strain at 3000 psi (ramp down)	Net Axial Strain at 3000 psi	Axial Strain at 4700 psi (ramp up)	Axial Strain at 4700 psi (ramp down)	Net Axial Strain at 4700 psi	Test Rate (psi/min)
Foam-2	2.99	1.4	125.2	0.65	0.00708	0.00708	—	—	—	—	250
Bead-1	3.06	1.4	114.02	2	0.00891	0.01006	0.00115	0.01002	0.01002	—	250
Class H-1	3.1	1.4	159.06	2	0.00233	0.00335	0.00102	0.00318	0.00318	—	250
Neat A-1	3.1	1.4	153.85	3	0.00159	0.00228	0.00069	0.00177	0.00177	—	100



Figure B1—Plot of tensile strength and Young’s modulus results for latex slurry with fibers (sample 1), Type 1 slurry with fibers (sample 2), and latex slurry (sample 3).

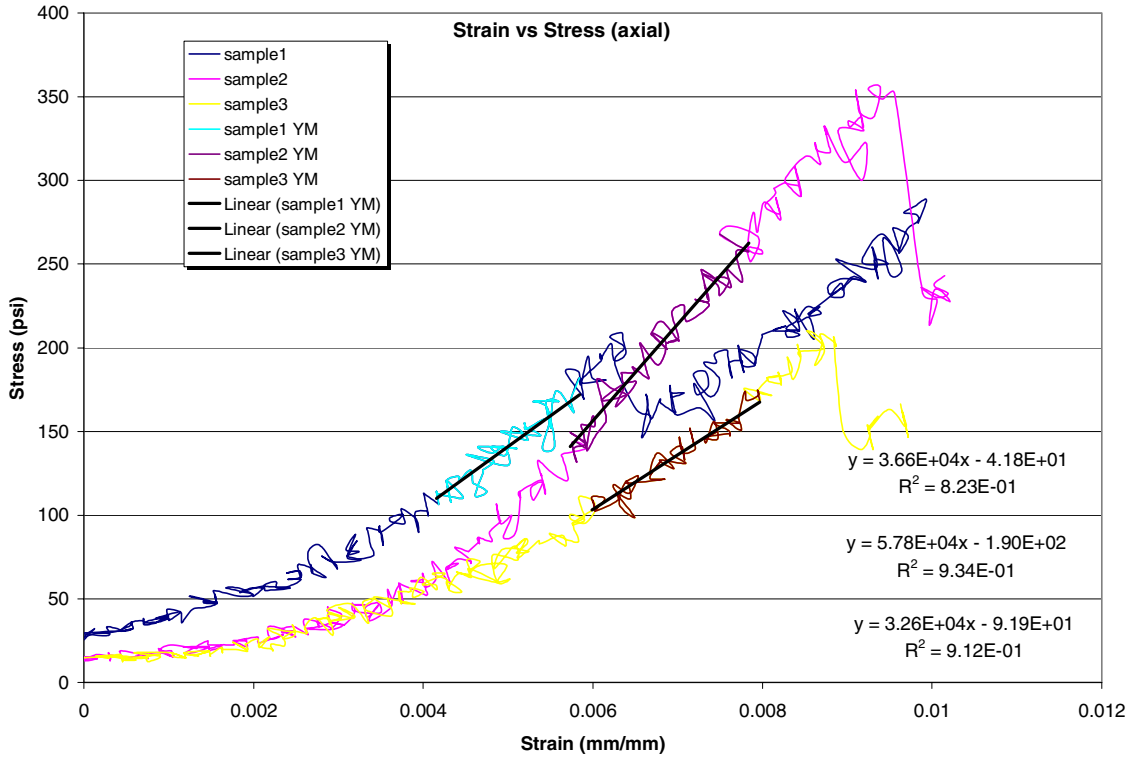




Figure B2—Plot of tensile strength and Young’s modulus results for neat Type 1 slurry cured in a confined state.

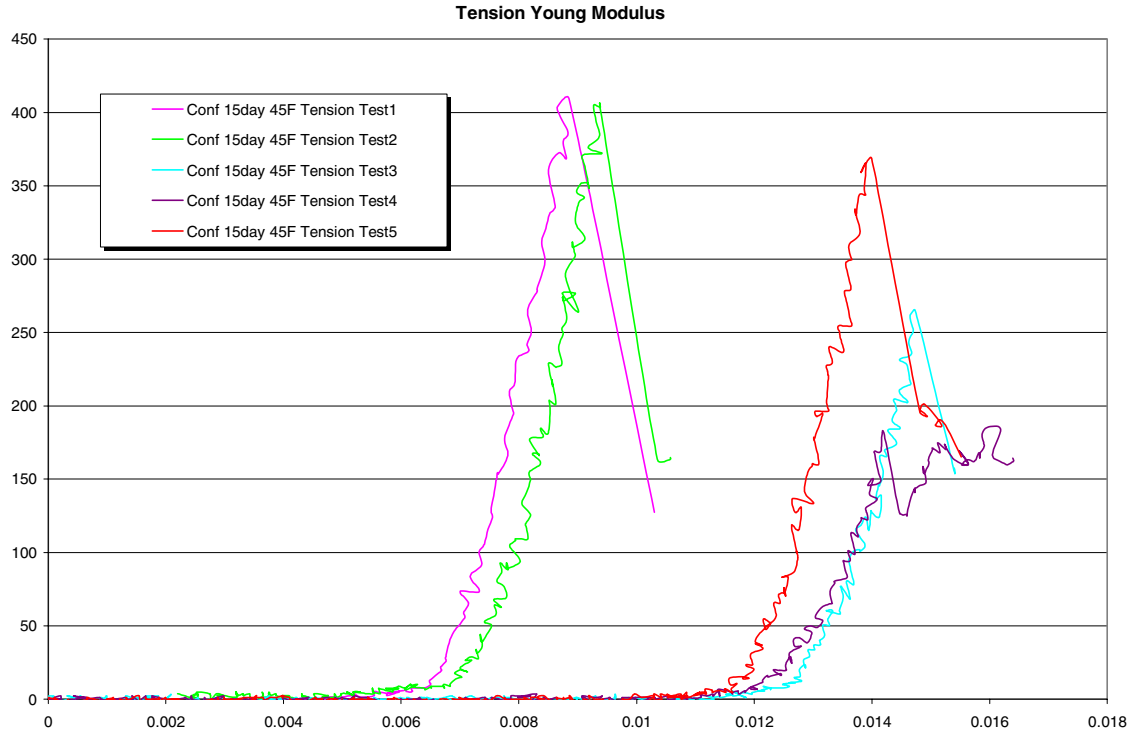




Figure B3—Plot of tensile strength and Young’s Modulus results for 12-lb/gal foam slurry.

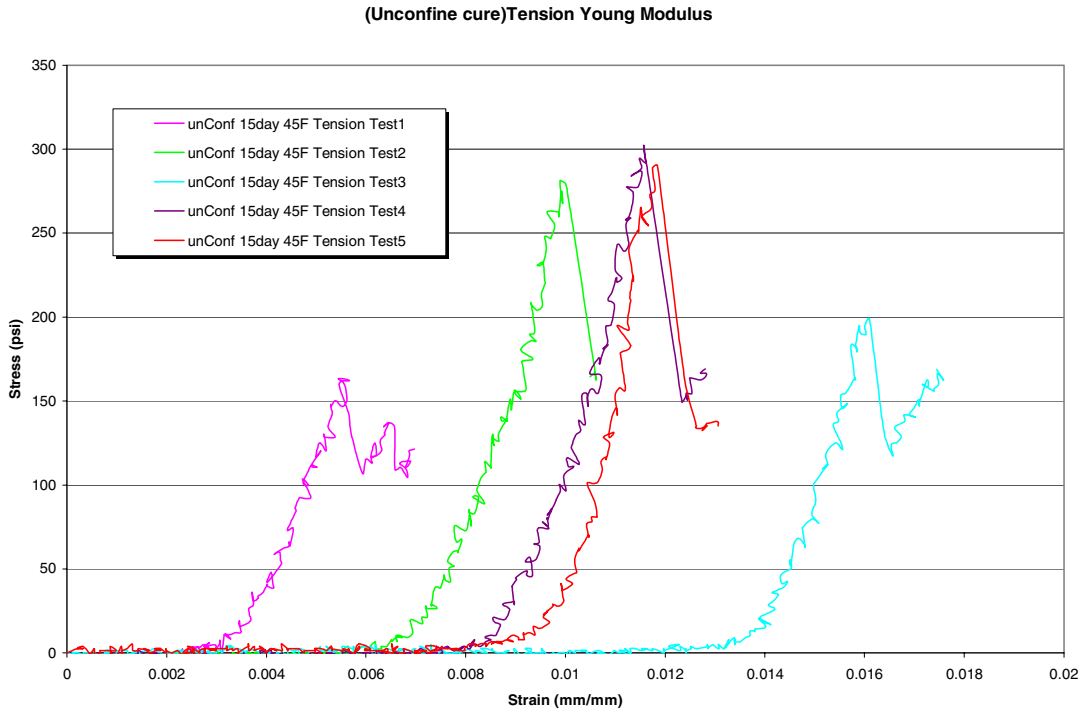


Figure B4—Plot of compressive Young’s modulus for Type 1 slurry at 0-psi confining pressure.

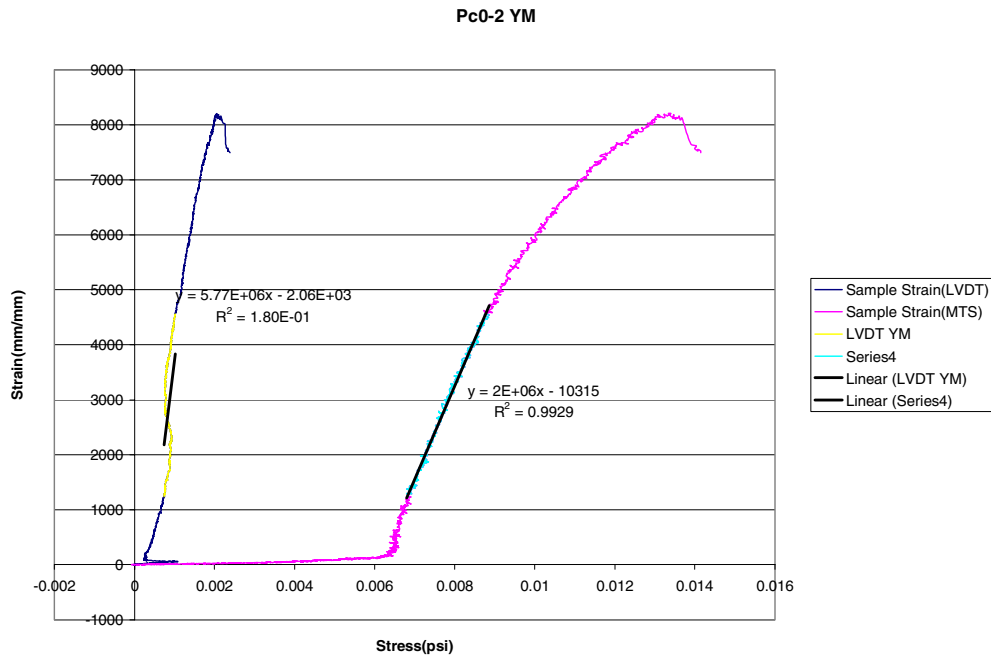




Figure B5—Plot of compressive Young’s modulus for Type 1 slurry at 1500-psi confining pressure.

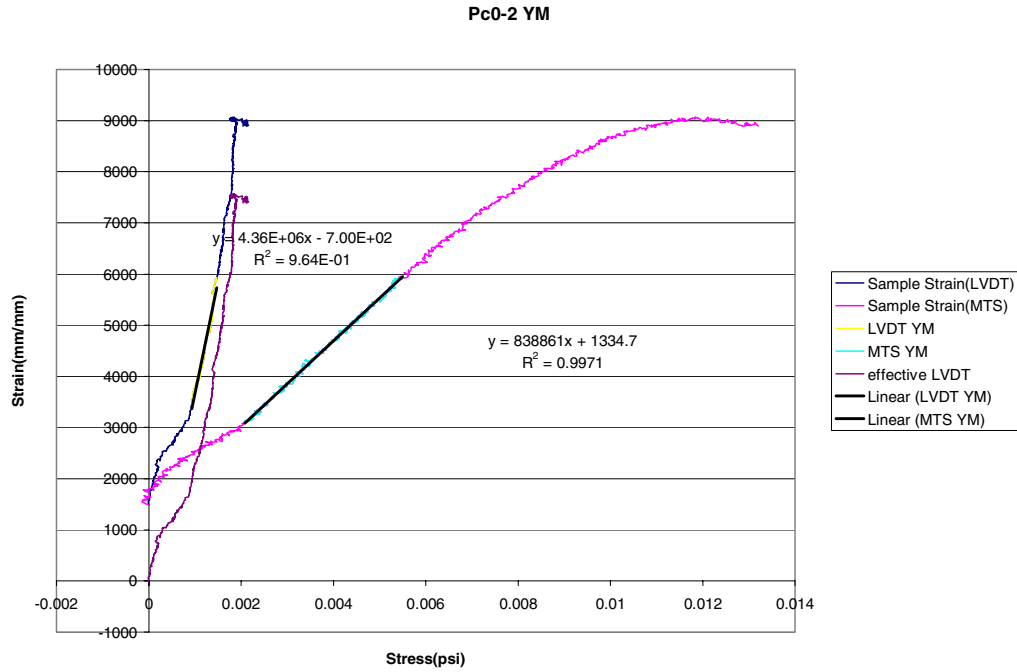


Figure B6— Plot of compressive Young’s modulus for Type 1 slurry at 5000-psi confining pressure.

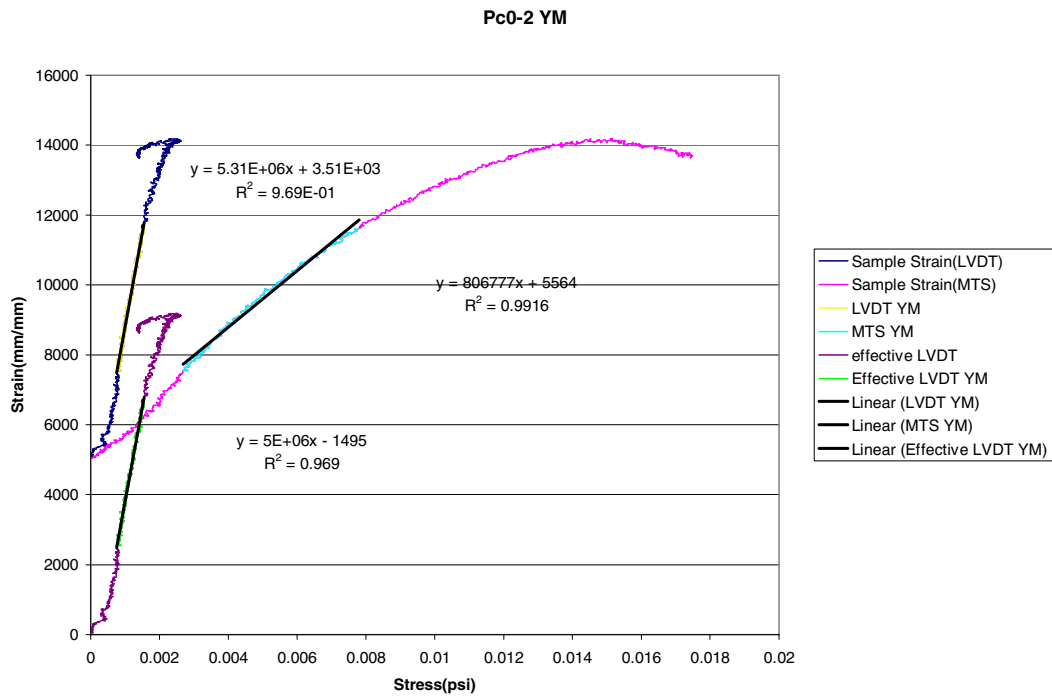




Figure B7— Plot of compressive Young’s modulus for 12-lb/gal foam slurry at 0-psi confining pressure.

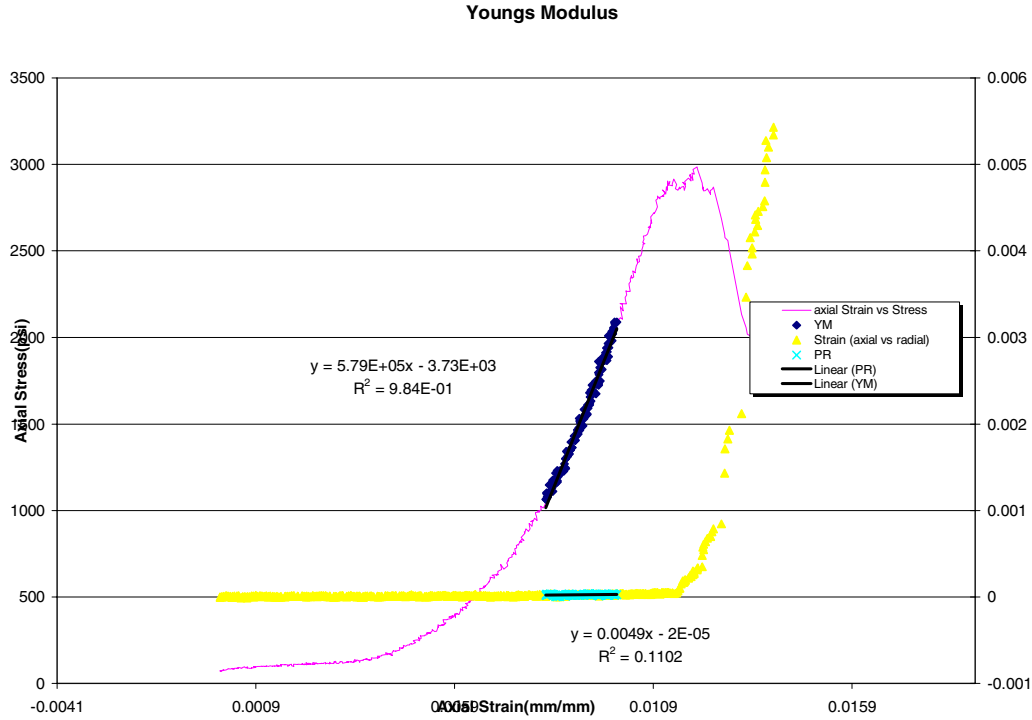


Figure B8— Plot of compressive Young’s modulus for 12-lb/gal foam slurry at 500-psi confining pressure.

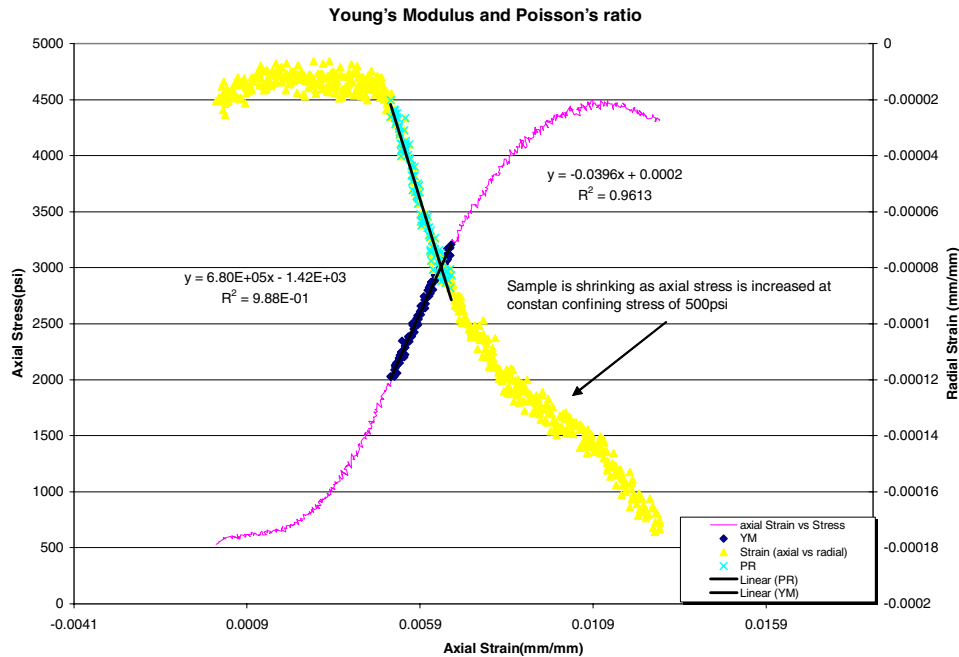




Figure B9— Plot of compressive Young’s modulus for 12-lb/gal foam slurry at 1000-psi confining pressure.

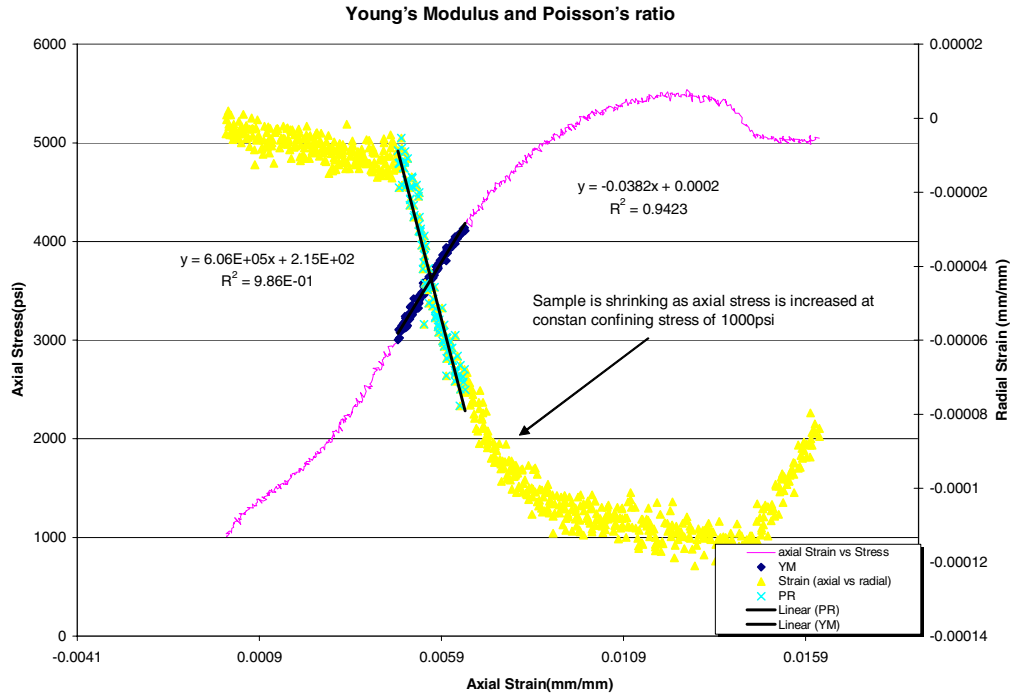


Figure B10— Plot of compressive Young’s modulus for bead slurry at 0-psi confining pressure.

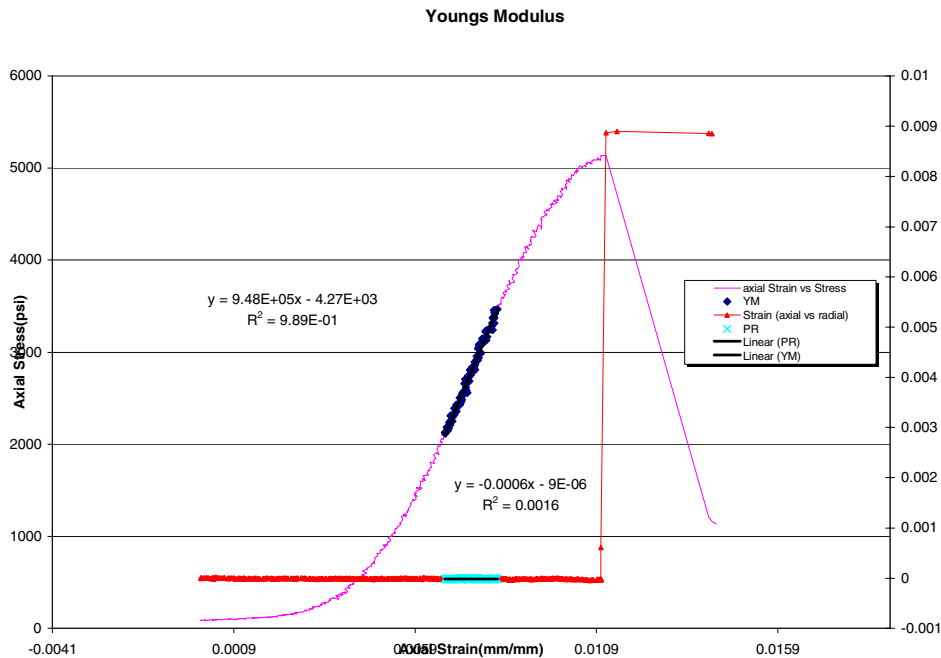




Figure B11— Plot of compressive Young’s modulus for bead slurry at 500-psi confining pressure.

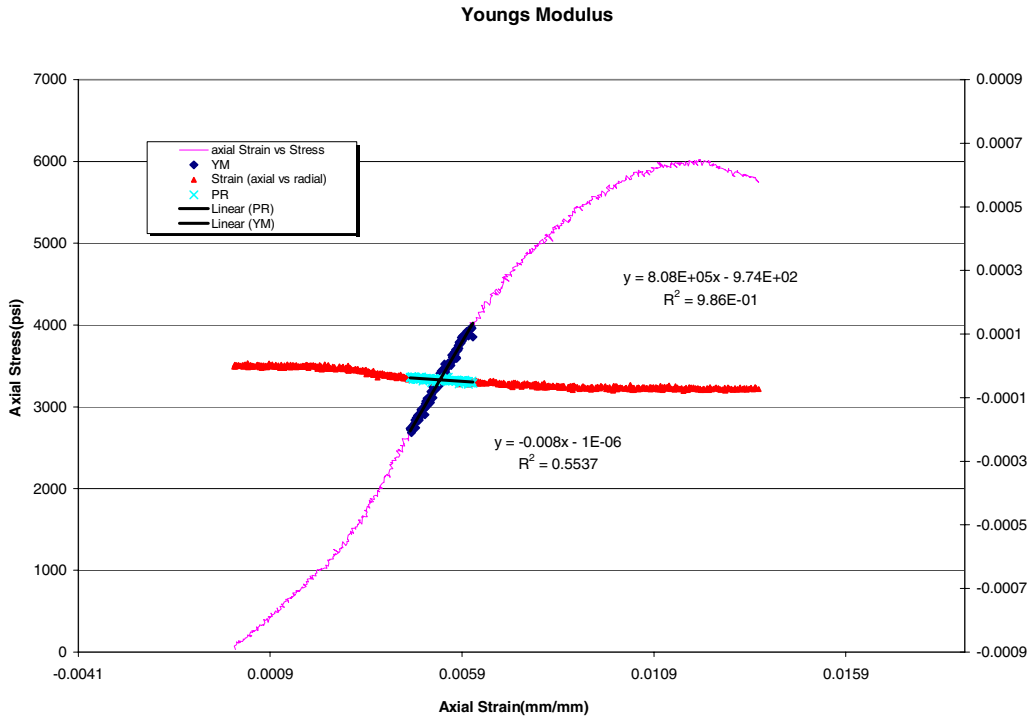


Figure B12— Plot of compressive Young’s modulus for bead slurry at 1000-psi confining pressure.

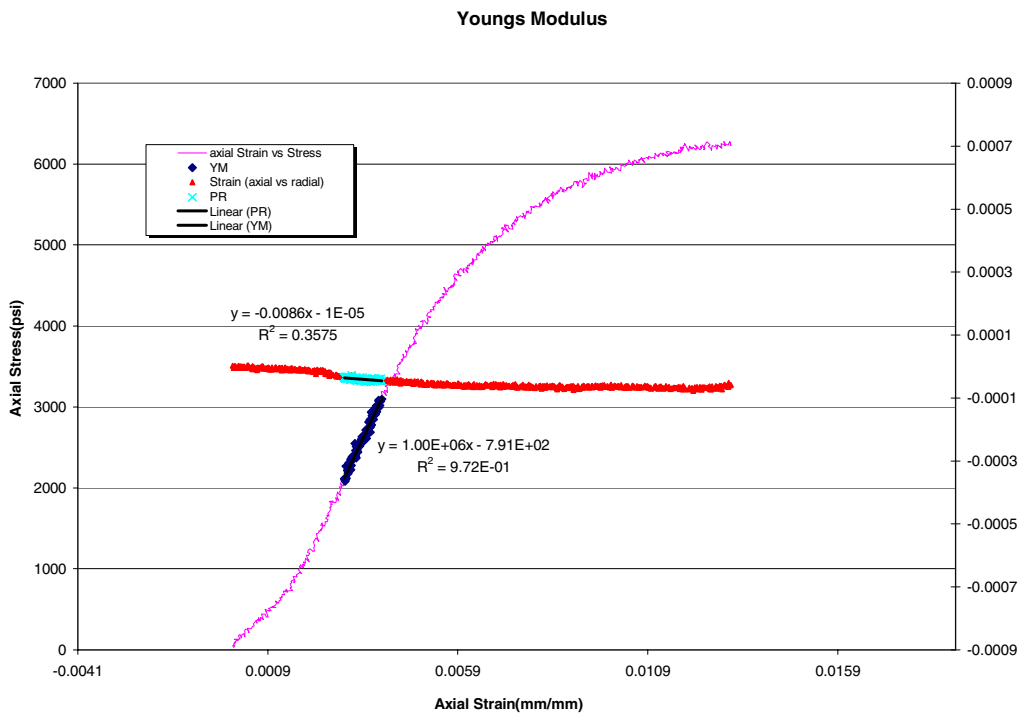




Figure B13— Plot of compressive Young’s modulus for latex slurry at 0-psi confining pressure.

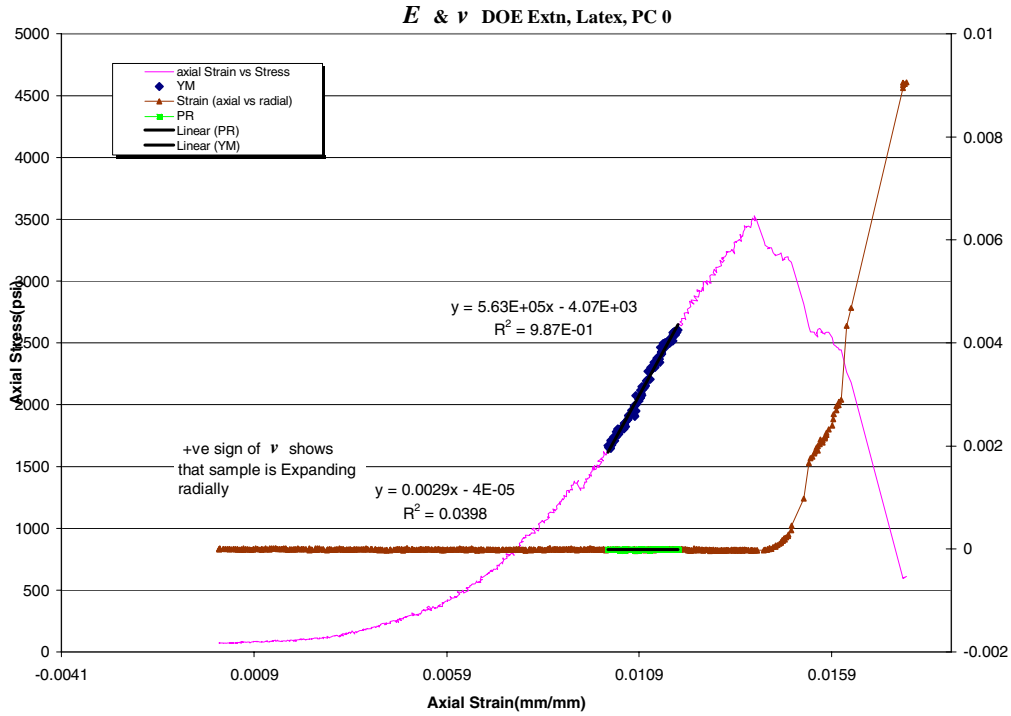


Figure B14— Plot of compressive Young’s modulus for latex slurry at 250-psi confining pressure.

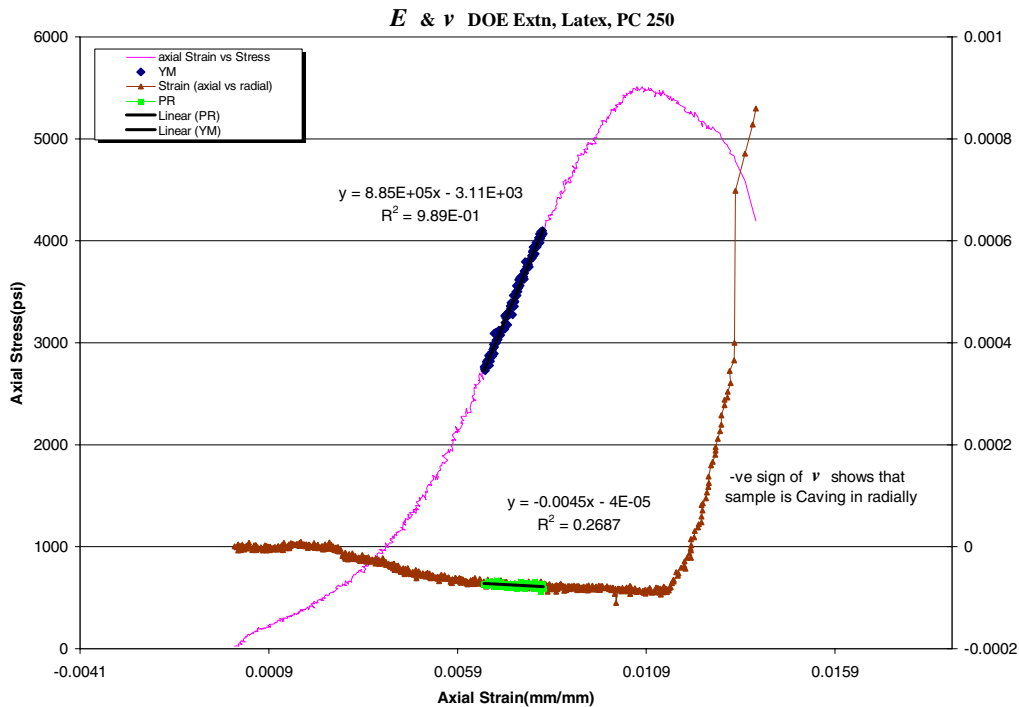




Figure B15— Plot of compressive Young’s modulus for latex slurry at 500-psi confining pressure.

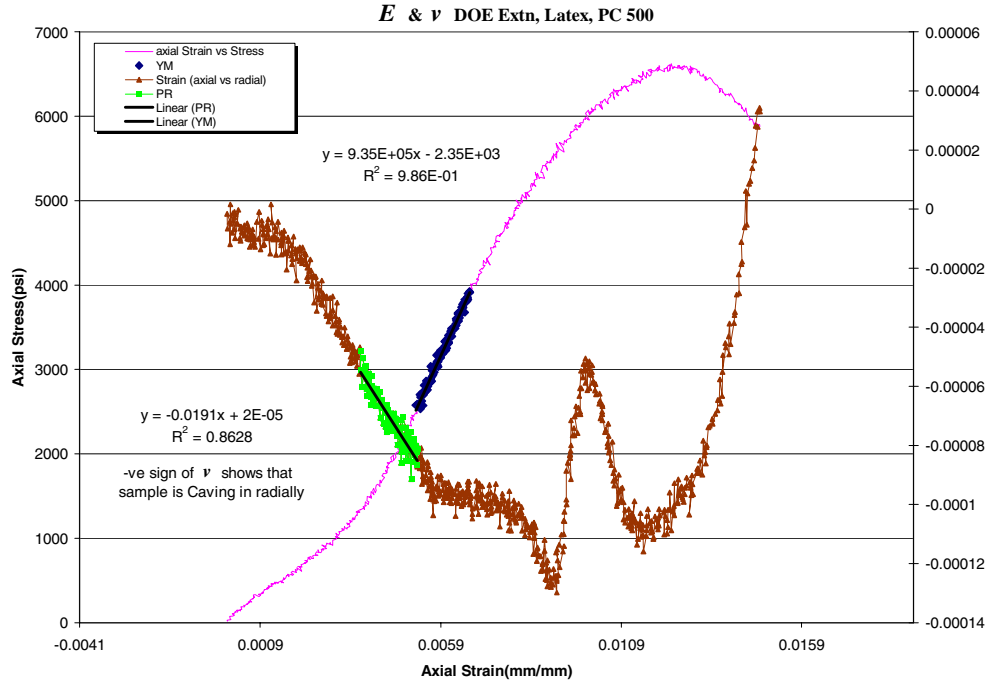


Figure B16—Young’s modulus measurements for Type I slurry at 500-psi confining stress and a 100-psi/min load rate.

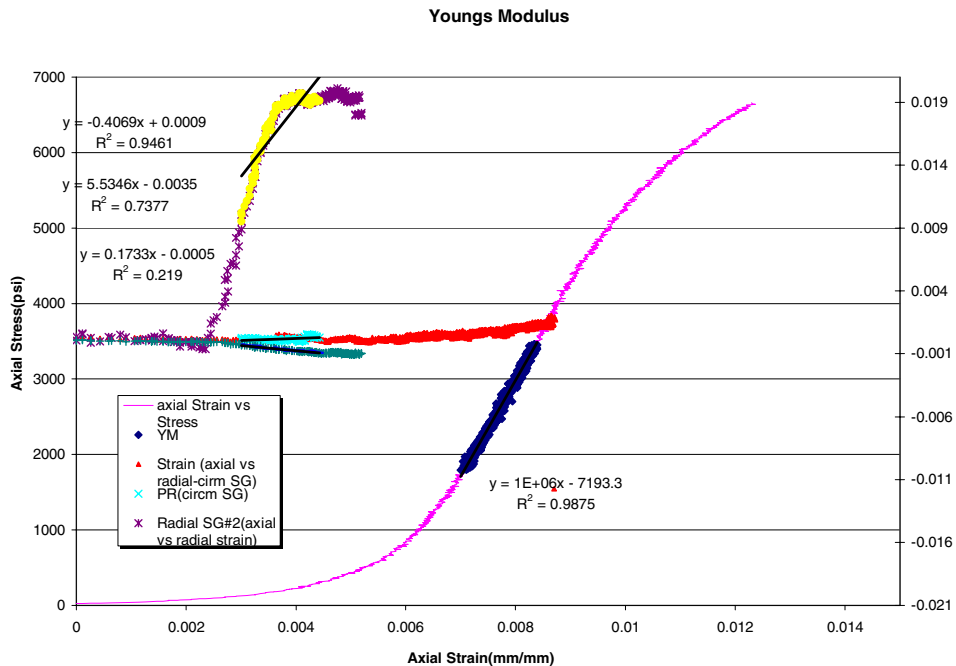




Figure B17—Young’s modulus measurements for Type I slurry at 500-psi confining stress and a 250-psi/min load rate.

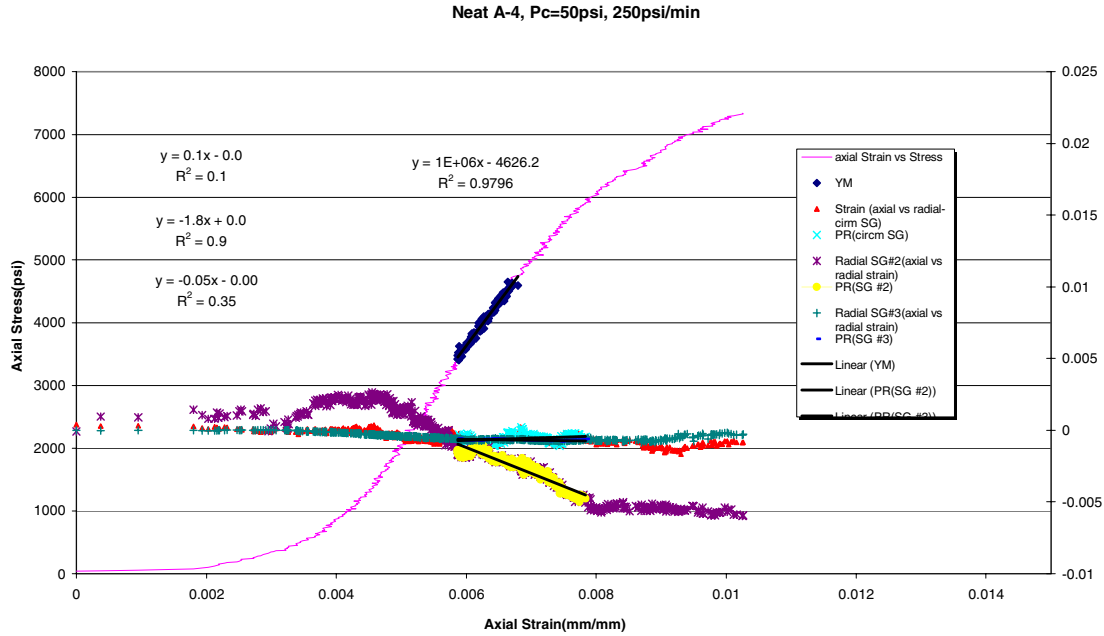


Figure B18—Young’s modulus measurements for Type I slurry at 500-psi confining stress and a 500-psi/min load rate.

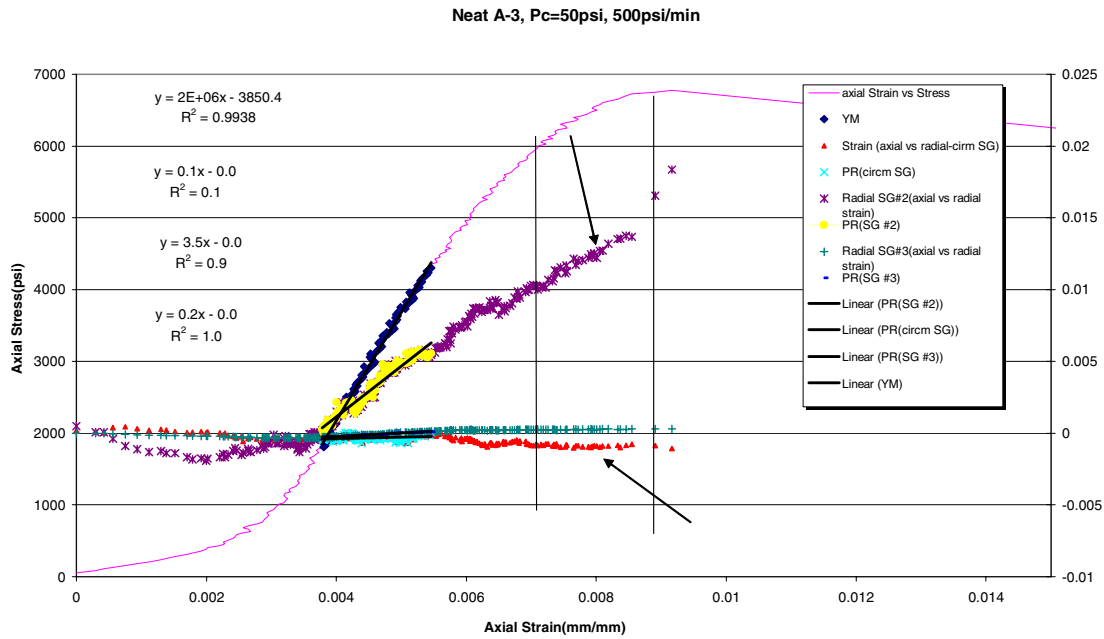




Figure B19—Hydrostatic cycling data for bead slurry showing anelastic strain.

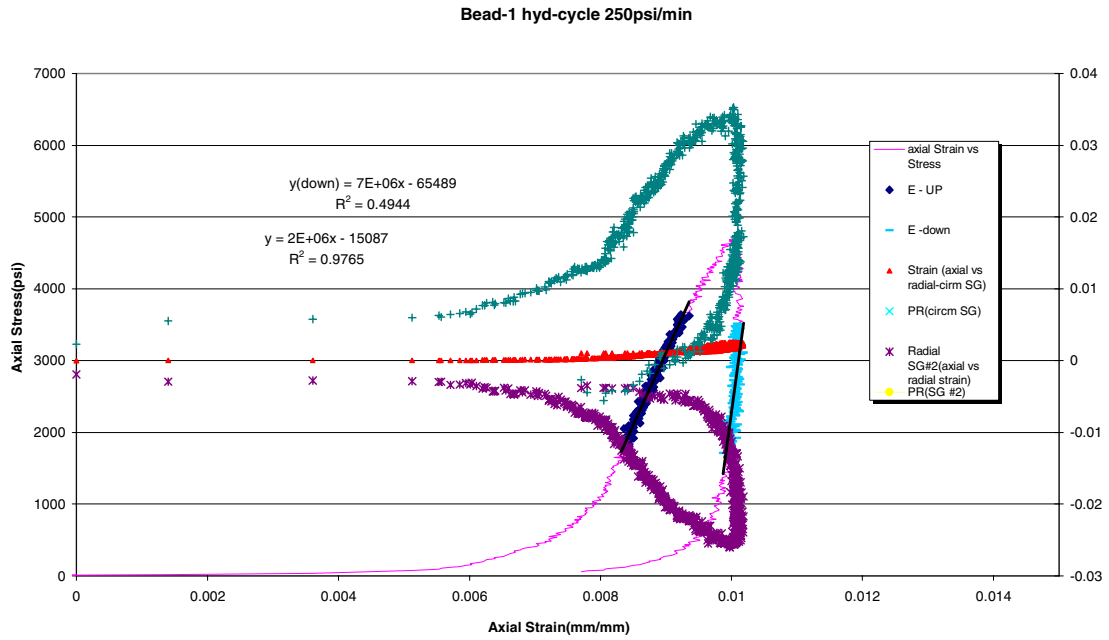


Figure B20— Hydrostatic cycling data for Class H slurry showing anelastic strain.

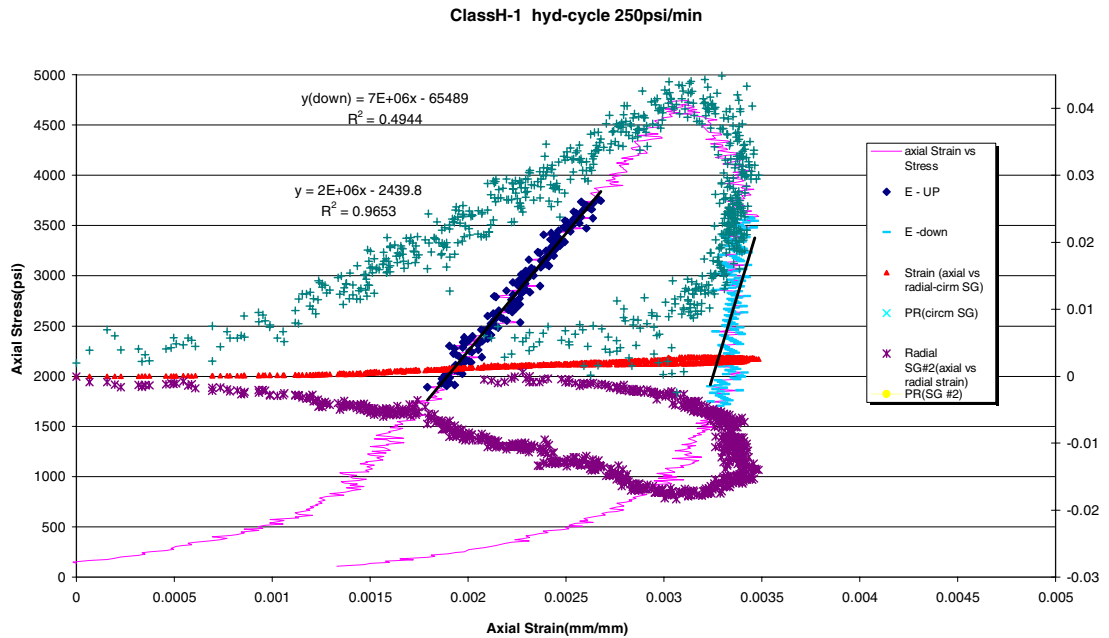




Figure B21— Hydrostatic cycling data for 12-lb/gal foam slurry showing anelastic strain.

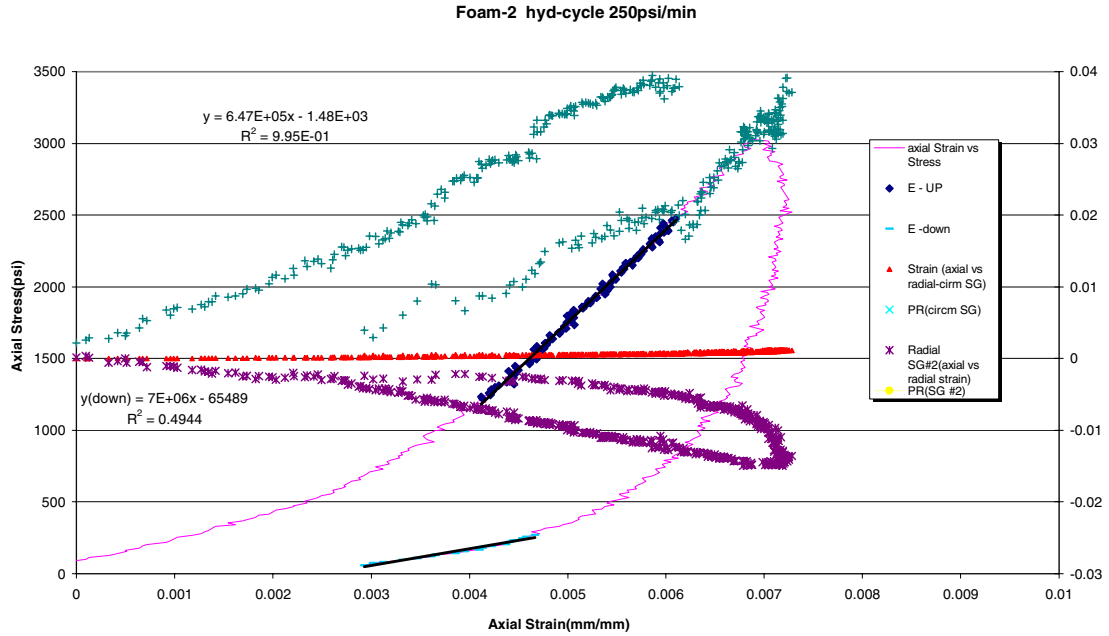


Figure B22— Hydrostatic cycling data for Type I slurry showing anelastic strain.

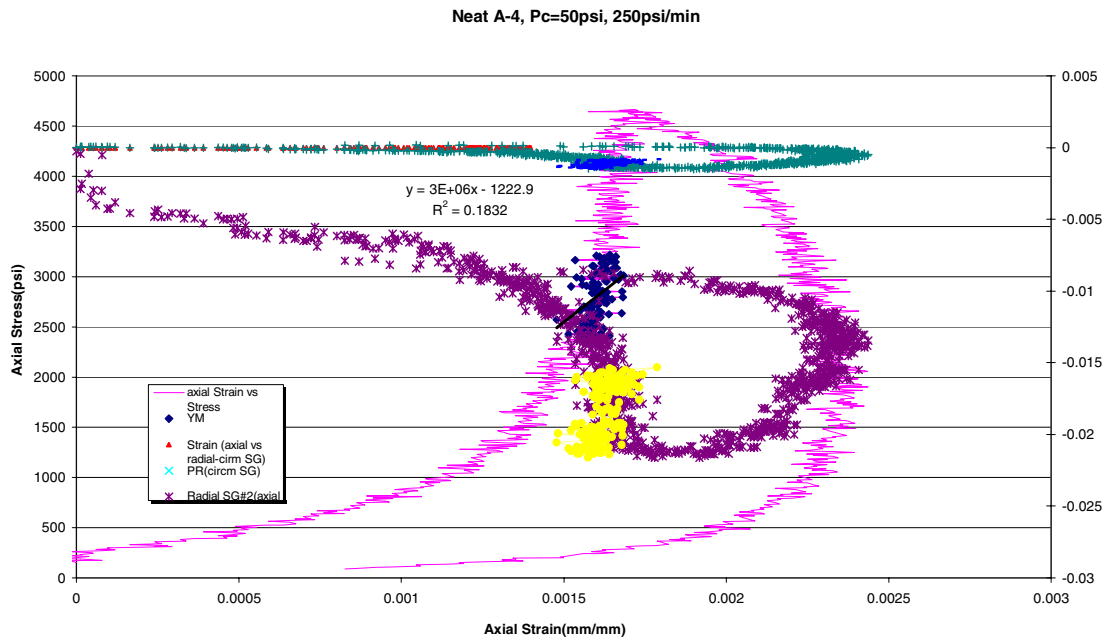
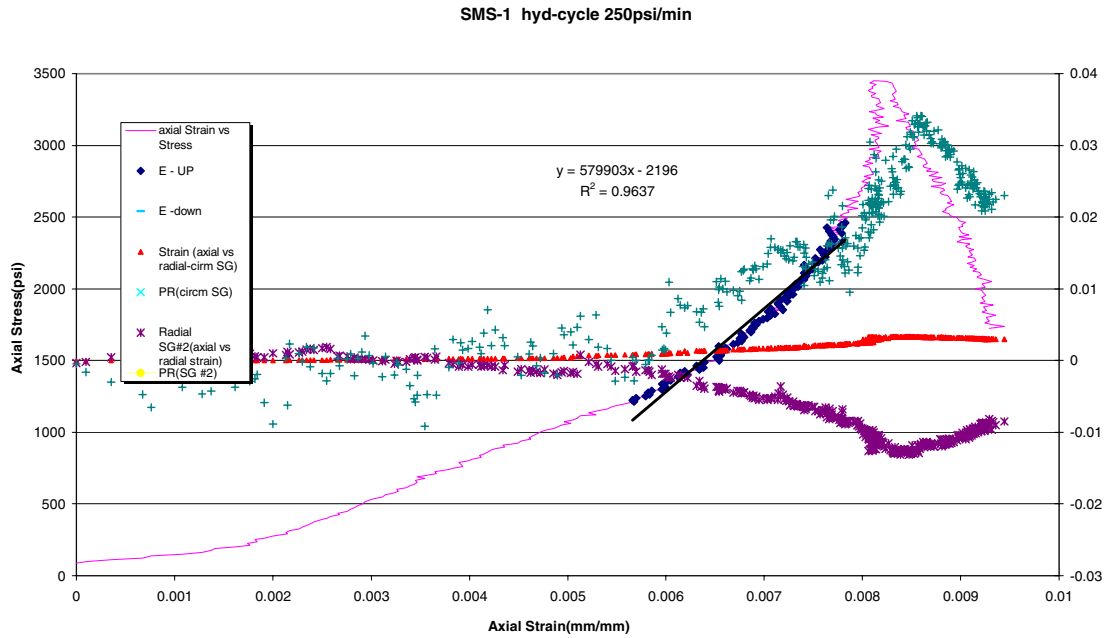




Figure B23— Hydrostatic cycling data for sodium metasilicate (SMS) slurry showing anelastic strain.





Appendix C—Numerical Modeling

The University of Houston has been contracted to perform finite element analysis (FEA) of the laboratory models used in the project (temperature and pressure cycling models).

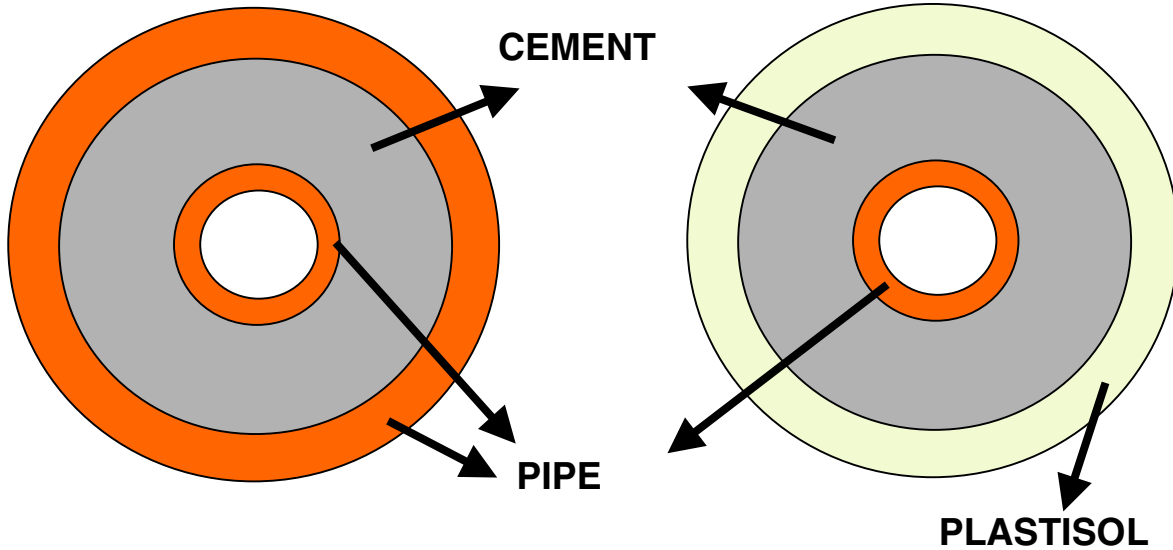
Introduction

In understanding the long-term integrity of cement in deepwater systems and determining the properties that affect the ability of cement to seal fluids, a principal step is to mathematically model the system to study different stress-causing phenomena. Besides allowing a theoretical prediction of the effect of various stress conditions such as temperature cycling, pressure cycling etc., the models will also provide a means of justification to test the designs and steer the direction of laboratory testing. The results of these models will be analyzed to determine if the stresses associated with the stress-causing conditions will result in loss of annular seal of cement.

Further, in the presence of asymmetrical far-field stresses, internally pressurized and cemented wells can experience both tensile and compressive stresses. If the internal pressure is sufficiently high, fracture initiation can result. The cement's tensile strength and the tensile stresses induced within the cement sheath make some portions of the cement sheath particularly vulnerable to fracture initiation. The stress distribution in a casing-cement-rock system needs to be estimated as a single continuous problem over disjointed domains. It is presumed that a fundamental study of such systems will provide valuable clues that will aid in the selection of well completion techniques and appropriate cement properties.

Two main configurations have been considered for modeling purposes: hard formation and soft formation (**Figure C1**). The focus will be on establishing a mathematical framework for analyzing different loading conditions, temperature gradients, and material properties and their effect on the induced stress distribution. Long-term effects such as subsidence and compaction may also necessitate changes in loading conditions. A parametric variation of a cement's material properties and thickness has been studied to determine the role of each variable in determining the overall stress and strain distributions.

Figure C1—Hard formation and soft formation configurations



The following sections describe briefly the mathematical model and discuss the main results of the analysis.

Mathematical Model

In practice, the magnitude and orientation of the *in situ* stress field is altered locally by the drilling of a well. In addition, when internal wellbore pressure and temperature gradients are present, the pre-existing stress fields are distorted significantly, giving rise to new induced stresses. The following equation summarizes the regular elasticity problem, with internal wellbore pressure and far-field boundary conditions:

$$\begin{aligned}
 \nabla \cdot \sigma &= 0 && \text{on } B \\
 \epsilon &= \frac{1}{2}(\nabla u + \nabla u^T) \\
 \sigma &= L\epsilon \\
 e_i \cdot (\sigma \cdot n) &= \hat{\sigma}_i && \text{on } \partial B_{li}
 \end{aligned}
 \tag{1}$$

where σ is the stress tensor
 ϵ is the strain tensor
 u is the displacement vector
 L is the elasticity tensor

The last equation represents the traction boundary condition specified on the internal and external boundaries.



In deepwater conditions, the subsea temperature will be lower ($< 5^{\circ}\text{C}$) than the surface temperature. However, after prolonged production, the pipelines can reach much higher temperatures (approximately 100°C). As a result, a temperature gradient is created across the annular cylinders (casing and cement sheath).

When the temperature rise in a homogeneous body is not uniform, different elements of the body tend to expand at different rates, and the requirement that the body remain continuous conflicts with the requirement that each element expand by an amount proportional to the local temperature rise. Thus, the various elements exert a restraining action upon each other that results in continuous unique displacements at every point. The system of strains produced by this restraining action cancels out all, or part of, the free thermal expansions at every point, ensuring continuity of displacement. This system of strains must be accompanied by a corresponding system of self-equilibrating stresses known as thermal stresses. A similar system of stresses may be induced in a structure made of dissimilar materials, even when the temperature change throughout the structure is uniform. Also, if the temperature change in a homogeneous body is uniform and external restraints limit the amount of expansion or contraction, the stresses produced in the body are termed thermal stresses.

In a completed wellbore system, all three conditions— nonuniform temperature distribution, dissimilar materials (casing, cement etc.), and external restraints— are present and contribute towards thermal stresses.

The desired energy equation for an isotropic, elastic solid is:

$$k\nabla^2 T = C_{e=0} \frac{\partial T}{\partial t} + \beta T_0 \frac{\partial e'}{\partial t} \quad (2)$$

where k is the thermal conductivity

T is the temperature rise from the initial uniform temperature T_0 , of the stress-free state

$\beta = E\alpha/(1-2\nu)$, $C_{e=0}$ is the heat capacity per unit volume at zero strain

e' is the dilatation

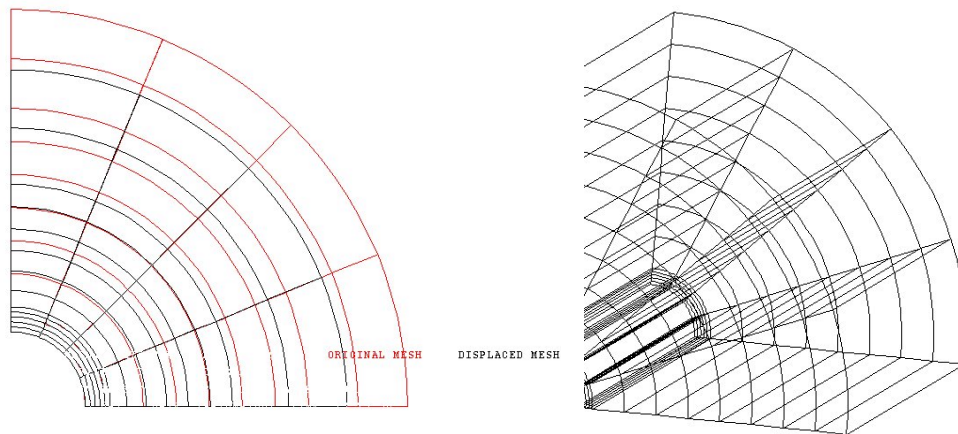
This equation, based on the Fourier law of heat condition and the linear thermoelastic stress-strain relations, shows that the temperature distribution in a body depends upon the dilatations throughout the body. Thus, the temperature and strain (stress) distributions are coupled and an exact analysis requires the simultaneous determination of the stress and temperature profiles.

For numerical modeling purposes, the casing-cement-rock system is considered to be concentric cylindrical structures in continuous contact with each other. The hard formation configuration represents a hard formation, while the soft formation configuration represents a soft formation. A generic, 3D finite element model is



developed for this composite system with Abaqus 5.7 and Matlab 6.0 (**Figure C2**). Pure elastic stress-strain analysis is performed with customized Matlab programs, while thermal stress analysis is performed with Abaqus. For laboratory tests involving homogeneous casing and confining pressures, the system is axi-symmetric and hence, only a quadrant of the annular structure is studied.

Figure C2—3D finite element model grid



Assumptions

The following assumptions are made in modeling a cement system:

- The system can be modeled on the basis of linear elastic theory.
- The composite system retains continuity at the interfaces.
- The system is axi-symmetric because of the boundary conditions.
- All materials are homogeneous and continuous.
- Plastisol has the same material properties as rubber.
- Plane stress condition is valid.

Stress Conditions

The following stress-causing conditions have been considered for mathematical modeling purposes:

- Normal production operation
- Pressure cycling (casing pressure)
- Subsidence, compaction (confining pressure)
- Temperature cycling (thermal stress)

The normal production operation includes an operating casing pressure and an external confining pressure (*in situ* stresses), along with a steady thermal gradient. All elastic and thermoelastic simulations represent steady-state conditions. A fully rigorous, coupled



thermoelastic equation is considered for numerical modeling purposes. However, the effect of dilatation is negligible when the system is allowed to evolve up to steady-state conditions.

Parametric Studies

The following parameters and cement properties have been varied to study their influence on stress distribution in the cement:

- Casing pressure (100 to 10,000 psi)
- Confining pressure (100 to 1000 psi)
- Temperature gradient (80 to 180°F)
- Young's modulus (1000 to 7000 psi)
- Poisson's ratio (0.15 to 0.45)
- Cement thickness (1 to 7 in.)

All numerical simulations are representative of laboratory testing conditions, with the parameter ranges provided by CSI from experimental results. All parametric studies are conducted with respect to the following reference case:

Parameter	Value
Casing pressure	500 psi
Confining pressure	500 psi
Young's modulus	5000 psi
Poisson's ratio	0.35
Cement thickness	1 in.
No thermal gradient	

Stress, displacement, and temperature profiles for both the soft and hard formation configurations are computed using a 3D finite element model with quadratic elements. **Figure C3** shows the first principal stress and horizontal displacement profiles for a representative case (hard formation) with an internal casing pressure of 500 psi and no confining pressure or thermal gradient. A Young's modulus of 5000 psi and a Poisson's ratio of 0.35 were used for the cement sheath. When the cement has a relatively high Young's modulus (3.05×10^7 psi), most of the stress variation is arrested within the inner pipe (made of steel). As a result, very little stress is transferred across to the cement sheath. The outer pipe experiences hardly any load in the absence of a direct confining pressure, as is evident from the negligible stresses and displacements.



Cement	Compressive Strength* (psi) *After 10 days	Tensile Strength (psi)	Shear Bond (psi)	
			PIP	PIS
Foam	3436	578	321	147
Latex	3630	504	432	237
Baseline	4035	673	519.6	203

Casing pressure. The casing pressure is varied from 100 to 10,000 psi for the hard formation configuration in the absence of confining pressure or a thermal gradient. The first principal stress and horizontal displacement along the x-axis is plotted in **Figure C4**. Clearly, the inner steel pipe limits the transfer of any load to the cement sheath because of its high Young’s modulus. A sharp stress contrast is observed at the casing-cement interface, while the continuity requirement of displacement at the interface manifests itself as differing gradients in the two materials and reaches zero at the external boundary. Since the inner steel pipe is the dominant material in determining load distribution, the cement sheath is hardly affected.

The same result, though more pronounced, is observed for the stress distribution in the soft formation configuration (**Figure C5**) in the absence of confining pressure. However, larger displacements are observed in comparison to the hard formation case, suggesting that the cement sheath can move further from its set position and can potentially lose its annular seal in a soft formation.

Confining pressure. In addition to base casing pressure of 500 psi, a confining pressure is applied on the outside of the casing, ranging from 100 to 1000 psi. All other conditions are held constant as before. The stress profile (**Figure C6**) is similar to that of casing pressure only, since both the inner and outer pipes are assumed to be of the same material (steel). The cement sheath has a reduced and almost uniform stress distribution, while the steel pipes arrest most of the variation.

For the soft formation configuration, a confining pressure results in relatively large deformations in both the cement and the Plastisol layer. However, increasing the confining pressure from 100 to 1000 psi has little effect on the magnitude of displacement in all three materials (**Figure C7**).

Young’s modulus and Poisson’s ratio. The cement material properties (Young’s modulus and Poisson’s ratio) are varied to study their effect on stress distribution in the hard formation configuration. The Young’s modulus is varied between 1000 and 7000 psi, and the Poisson’s ratio is varied from 0.15 to 0.45. Because the steel pipe transfers



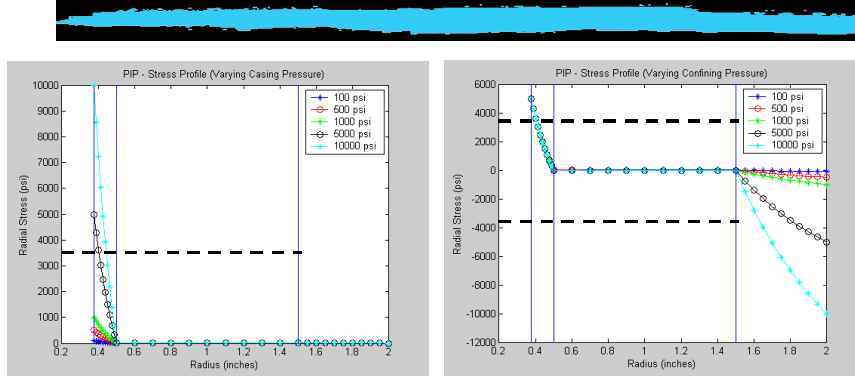
very little stress to the cement sheath, there is a negligible influence on the stress and strain distribution in the cement sheath (**Figures C8 and C9**).

Cement thickness. The thickness of the cement layer is varied from 1 to 7 in. for the hard formation configuration. As the thickness increases, a larger portion of the cement is under compression, which increases horizontal displacement for the same casing and confining pressure, as shown in **Figure C10**. The same amount of net displacement is experienced by the inner and outer steel pipes, as compared with the more flexible cement sheath.

Temperature gradient. In addition to a casing pressure of 500 psi and a confining pressure of 500 psi, a thermal gradient is applied across the concentric cylinders for the hard formation configuration. The external temperature on the outer pipe is held constant at 68°F, and the temperature at the inner surface of the inner pipe is varied between 80°F and 180°F. The temperature profile is symmetric, and varies only along the radial direction (**Figure C11**). While the elastic stress acts in compression, the thermal stress arising due to nonuniform and dissimilar expansion of the composite system can lead to tensile stresses. As a result, the net stress experienced by the system is controlled by the dominant stress source. The displacement profile (**Figure C12**) indicates that the thermal stresses tend to expand the concentric cylinders. At high temperatures and low external loads, the thermal stress can control the net displacement, and vice-versa at low temperatures and high external loads.

Figure C3—

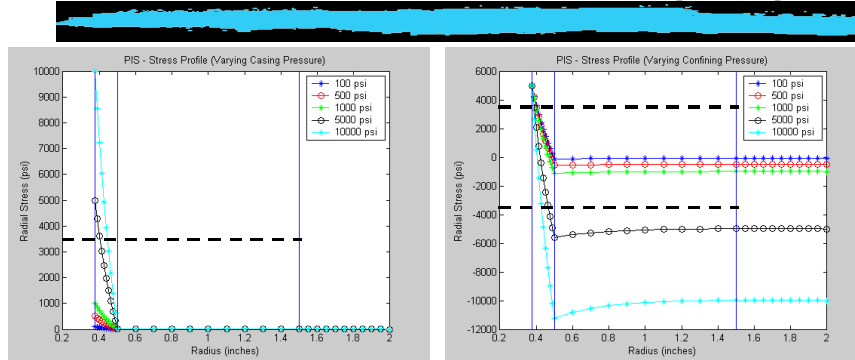
COMPRESSIVE FAILURE (PIP)



- Annular cement in PIP retains its integrity at high casing and confining pressures

Figure C4—

COMPRESSIVE FAILURE (PIS)

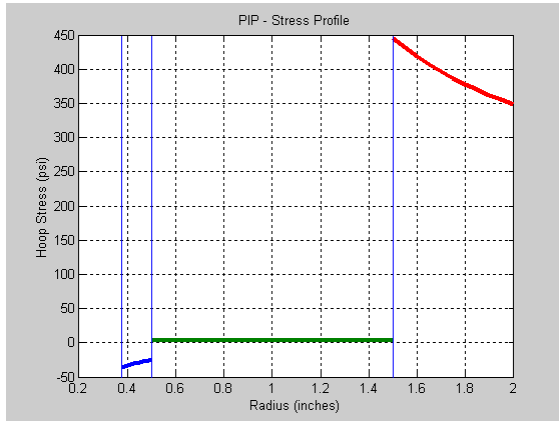


- Annular cement in PIS fails in compression at high confining pressures



Figure C5—

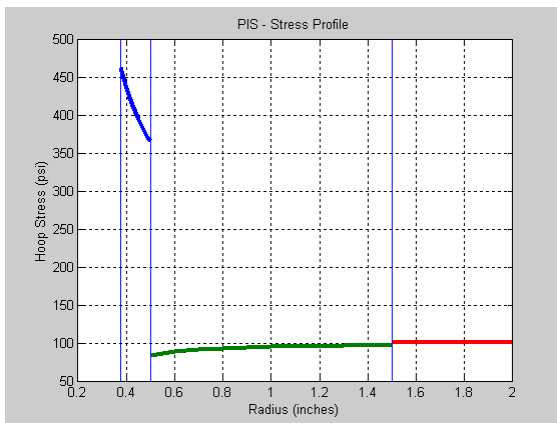
SHEAR FAILURE (PIP)



Casing Pressure 15 psi
Confining Pressure 100 psi
Hoop Stress Contrast ~ 450 psi

Figure C3—

SHEAR FAILURE (PIS)

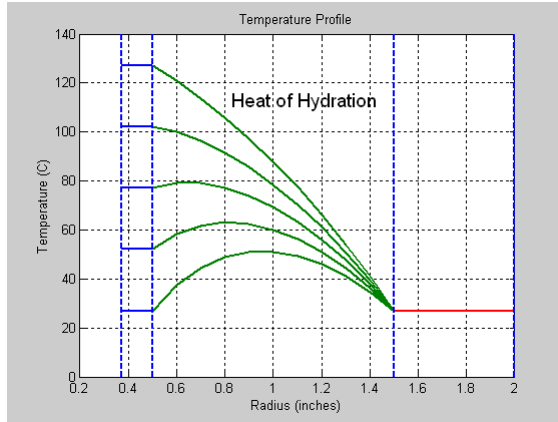


Casing Pressure 15 psi
Confining Pressure 100 psi
Hoop Stress Contrast ~ 300 psi



Figure C7—

HEAT OF HYDRATION

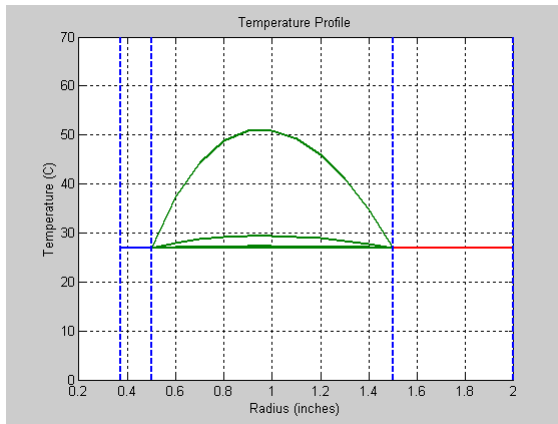


Borehole Temperature
300 K – 400 K

Heat of Hydration Rate
3.5 KJ/Kg.sec

Figure C8—

HEAT OF HYDRATION



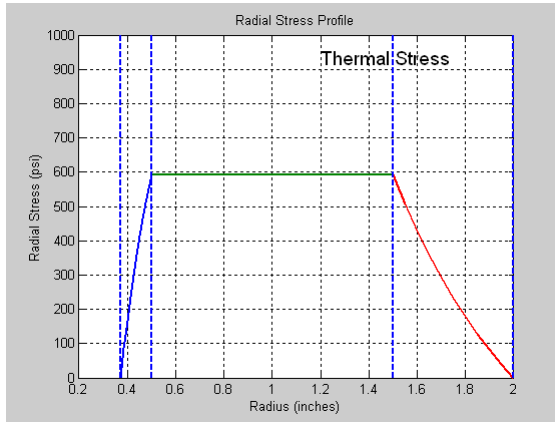
Borehole Temperature
300 K

Heat of Hydration Rate
3.5 J/Kg.sec - 3.5 KJ/Kg.sec



Figure C9—

HEAT OF HYDRATION



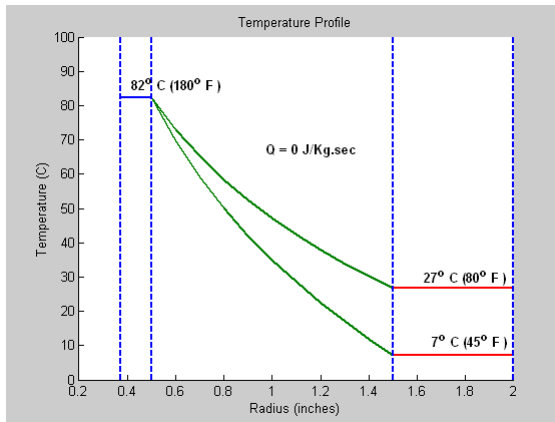
Borehole Temperature
300 K

Reservoir Temperature
300 K

Linear Superposition with
Elastic Stress

Figure C10—

THERMAL STRESS



Borehole Temperature
180° F

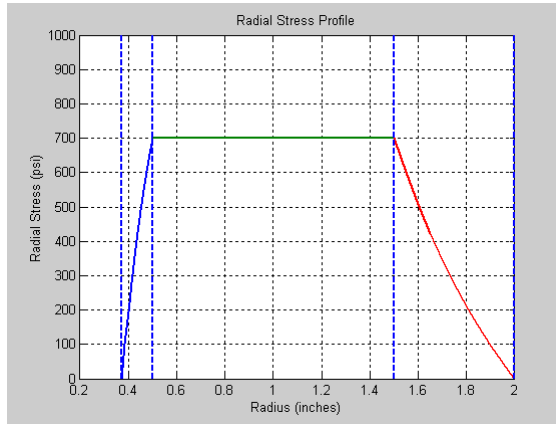
Reservoir Temperature
45° F, 80° F

Heat of Hydration Rate
0 J/Kg.sec



Figure C11—

THERMAL STRESS



Borehole Temperature
180° F

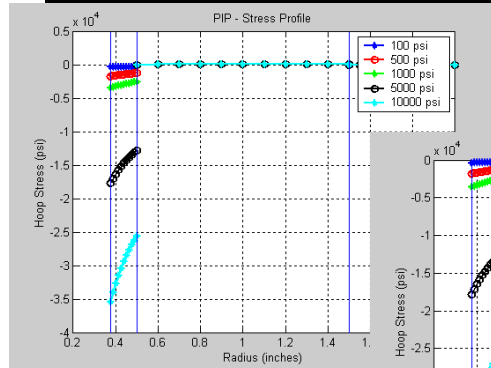
Reservoir Temperature
45° F, 80° F

Heat of Hydration Rate
0 J/Kg.sec

- Higher Thermal Stress
- No significant variation within Cement

Figure C12—

HOOP STRESS (TENSILE)



Confining Pressure
0 psi

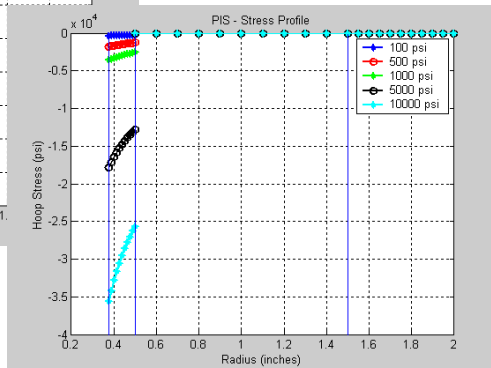




Figure C13—

DISPLACEMENT PROFILE

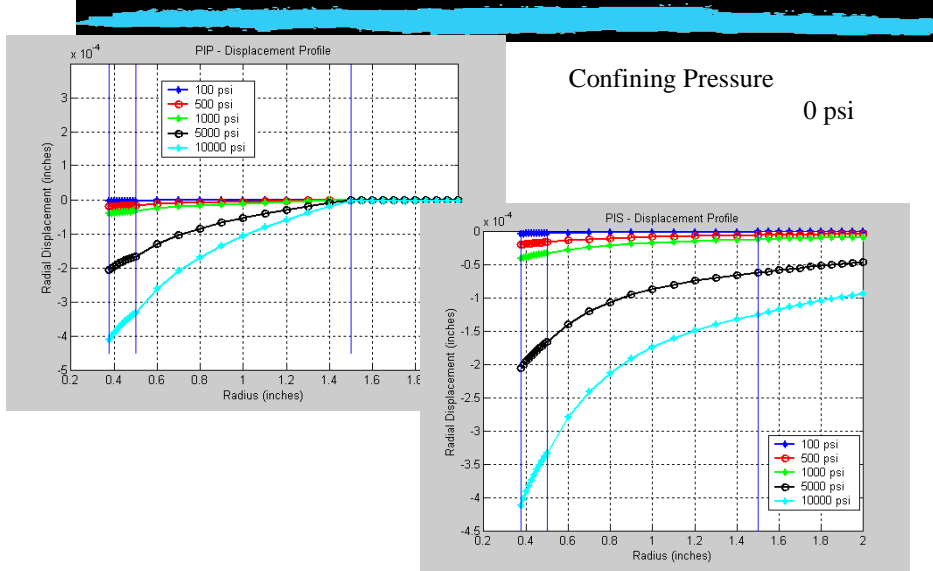


Figure C14—

HOOP STRESS (TENSILE)

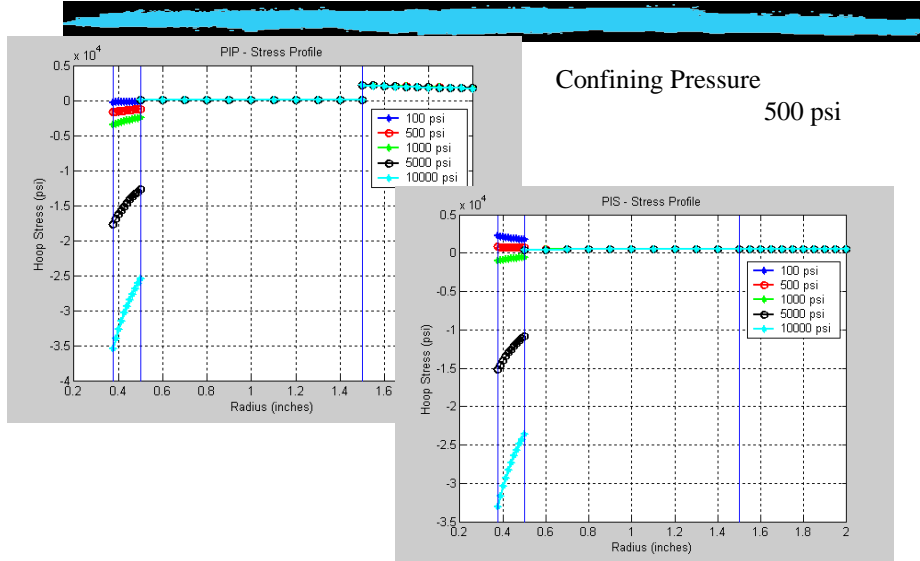
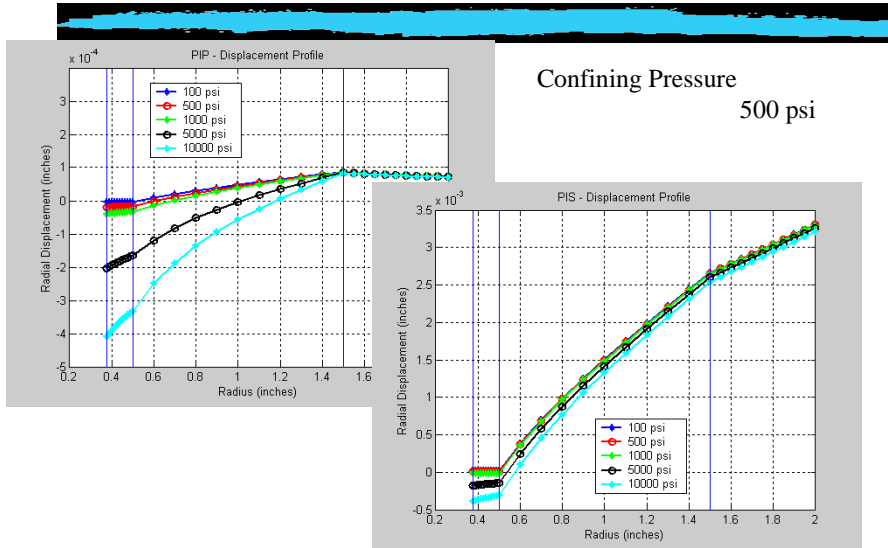




Figure C15—

DISPLACEMENT PROFILE



¹ API Spec. 10, 22nd Edition, American Petroleum Institute, Washington, D.C., December 1997.

² Standard Test Method for Static Modulus of Elasticity (Young's Modulus) and Poisson's Ratio of Concrete in Compression, ASTM C469-02, ASTM International, March 1, 2002.

³ "Standard Test Method for Splitting Tensile Strength of Cylindrical Concrete Specimens," ASTM C496-96, ASTM International, March 1, 1996.



CSI Technologies

Appendix V

Report 5

MMS Project
Long-Term Integrity of Deepwater Cement
Systems Under Stress/Compaction Conditions

Report 5

Issued September 13, 2003



CEMENTING SOLUTIONS, INC.



Table of Contents

Objectives	1
Observations and Recommendations for Future Work	1
Testing Program and Procedures.....	2
<i>Cement Design Performance</i>	<i>3</i>
<i>Mechanical Properties</i>	<i>3</i>
<i>Mechanical Integrity.....</i>	<i>4</i>
Test Results.....	4
<i>Tensile Strength</i>	<i>5</i>
<i>Young’s Modulus with Various Confining Forces.....</i>	<i>5</i>
<i>Poisson’s Ratio.....</i>	<i>5</i>
<i>Anelastic Strain.....</i>	<i>6</i>
<i>Shear Bond.....</i>	<i>7</i>
<i>Annular Seal.....</i>	<i>7</i>
<i>Cement Column Seal.....</i>	<i>8</i>
Appendix A—Test Procedures.....	9
<i>Sample Preparation.....</i>	<i>9</i>
<i>Sample Curing.....</i>	<i>9</i>
<i>Thickening Time Test</i>	<i>9</i>
<i>Free-Fluid Test</i>	<i>9</i>
<i>Compressive Strength</i>	<i>10</i>
<i>Young’s Modulus and Poisson’s Ratio Testing.....</i>	<i>10</i>
<i>Hydrostatic Cycling and Anelastic Strain</i>	<i>10</i>
<i>Tensile Strength and Tensile Young’s Modulus.....</i>	<i>11</i>
<i>Annular Seal Testing Procedure.....</i>	<i>12</i>
Soft-Formation Simulation:.....	12
Hard-Formation Simulation:	13
Intermediate Formation Simulation:	13



Shear Bond Strength Testing 14

 Pressure Cycling 14

 Temperature Cycling 14

Cement Column Seal Tests..... 16

Appendix B—Test Data..... 17



Objectives

The overall objective of this project is to determine the properties that affect cement's capability to produce a fluid-tight seal in an annulus. The project primarily focuses on deepwater applications, but general applications will also be examined. The research conducted thus far is focused on the measurement and correlation of cement's mechanical properties to the cement's performance. Also, research was conducted to determine which laboratory methods should be used to establish the cement's key properties.

Results obtained during this reporting period focused on continued measurement of and correlation of cement mechanical properties and mechanical bond integrity of a cemented annulus. Mechanical property testing included measurement of tensile strength and Young's modulus/Poisson's ratio under various confining loads. A new test procedure, anelastic strain/failure testing was begun on several compositions during this project period, and is described in Appendix A. Mechanical integrity testing included shear bond and annular seal testing on specimens cured under various cyclic curing schedules including introduction of intermediate restraint specimens. The results of these tests are tabulated in the Results section below. Additionally, all rock properties test results developed during this project, including graphical data, are presented in Appendix B.

Observations and Recommendations for Future Work

Results of testing during this reporting period indicate:

- Poisson's ratio data are at least consistent with data from other ongoing testing projects. API is currently examining measurement of Poisson's ratio with similar results.
- Measurement of anelastic strain with cycling will allow a more thorough assessment of each composition's performance.
- Intermediate formation strength simulated by PVC pipe is acceptable for mechanical integrity testing to further quantify the performance of the compositions.

Future work includes:

- implementation of test procedure for annular seal and bond strength modifications
- quantification of anelastic strain magnitudes and analysis of consequences in the well environment.
- complete analysis of column sealing tests
- completion of a decision matrix for optimizing cement composition (the final deliverable of this project)

The matrix will be similar in operation to one commissioned by 3M to select optimum lightweight cement for various conditions. This decision matrix will accept well conditions as inputs and will contain performance properties for the various cements



tested in the project. A semi-quantitative analysis of the inputs vs. cement performance will allow the user to determine the optimum cement composition for maintaining annular seal under the well conditions.

Plans are to conduct a workshop of steering committee participants in December to complete the decision matrix.

Testing Program and Procedures

The following cement slurries will be examined: Type 1, foamed cement, bead cement, Class H cement, latex cement. The effect of adding fibers or expansion additives to a slurry will also be examined. The cements are tested primarily for deepwater applications, but their performance under all application conditions is also examined.

Tasks in the project are listed below:

- Task 1 – Problem Analysis
- Task 2 – Property Determination
- Task 3 – Mathematical Analysis
- Task 4 – Testing Baseline
- Task 5 – Refine Procedures
- Task 6 – Composition Matrix
- Task 7 – Conduct Tests
- Task 8 – Analyze Results
- Task 9 – Decision Matrix

Compositions tested in this project are outlined in **Table 1** below. The range of compositions chosen covers the compositions traditionally used in deep water applications as well as newly utilized compositions and compositions designed to produce improved performance.



Table 1—Cement Compositions for Testing

Description	Cement	Additives	Water Requirement (gal/sk)	Density (lb/gal)	Yield (ft ³ /sk)
Neat Type I slurry	Type 1	—	5.23	15.6	1.18
Type I slurry with fibers	Type 1	3.5% carbon fibers-milled	5.2	15.6	1.16
Latex slurry	Type 1	1.0 gal/sk LT-D500	4.2	15.63	1.17
Latex slurry with fibers	Type 1	1.0 gal/sk LT-D500 3.5% carbon fibers-milled 0.50% Melkcrete	4.09	15.63	1.20
Foam slurry (12-lb/gal)	Type 1	0.03 gal/sk Witcolate 0.01 gal/sk Aromox C-12 1% CaCl	5.2	12.0	1.19
Bead slurry	Type 1	13.19% K-46 beads	6.69	12.0	1.81
Neat Class H slurry	Class H	—	4.3	16.4	1.08
Class H slurry with fibers	Class H	—	4.3	16.4	1.08
Sodium metasilicate slurry	Type 1	—	14.22	12.0	2.40

Four major categories of tests are used to analyze the cements: cement design performance testing, mechanical properties testing, mechanical integrity testing, and numerical simulation. Results of mechanical properties testing and mechanical integrity testing are provided in the “Test Results” section of this report, beginning on Page 4.

Cement Design Performance

Standard cement design performance testing, including rheology, thickening time, free fluid, set time, compressive strength, etc. are performed according to procedures outlined in API Spec. 10.

Mechanical Properties

Mechanical properties tested include: tensile strength/tensile Young’s modulus (T), compressive Young’s modulus, Poisson’s ratio, and anelastic strain-fatigue testing.

The tensile strengths are determined with the Brazilian Test Method. From this test, the tensile Young’s modulus is computed, as well as the maximum yield of the slurry.

The compressive Young’s modulus will be determined through compression tests with confining loads (defined by 0 psi break) with a baseline of a 14-day cure. Poisson’s ratio will also be determined from these tests, Poisson’s ratio values will vary with respect to the stress rate, slurry type, air entrainment, and perhaps other variables.



Anelastic strain and fatigue testing is a modification of hydrostatic testing. The modified procedure involves cycling samples repeatedly to 25%, 50%, and 75% of each composition's compressive strength under 500-psi confining stress. Measurement of anelastic strain with cycling should provide a more comparable measure of each composition's performance.

Mechanical Integrity

The mechanical integrity issues of the cement slurries include stresses in the cement, and the flow of fluids around the cement and through the matrix of the cement. To predict the flow of fluid around the cement, the cement slurries will be tested for bonding capacity, presence of microannuli, and deformation. The flow of fluids through the matrix of the cement will be examined through tests for detecting cracks and permeability changes. The stress undertaken by the cement slurries will be determined as a function of pressure, temperature, pipe buckling, and formation compaction. Stresses under cyclic conditions will also be determined.

Shear bond and annular seal measurements are taken under cyclical conditions for both soft and hard formations. Results from testing with simulations of hard and soft formations indicate the need for a simulated formation of intermediate strength. The altered shear and annular seal testing will include a simulated medium-strength formation with Schedule 40 PVC pipe as the outside mold for the cement sheath.

Additional stresses will be imposed on all test specimens by increasing the maximum pressure to which the inner pipe is stressed. Additionally, shear bond tests will be run only after a composition has been tested for annular seal. The shear bond test samples will be subjected to the same pressure and temperature cycling that produced annular seal failure before shear bond is evaluated. This procedure will provide a comparison between shear bond and annular seal behavior.

Cement column seal tests illustrate the sealing effectiveness of several cements that are subjects of the project. These tests are designed to test a cement's capacity to isolate gas pressure across an enclosed column. Ten-foot lengths of 2-in. pipe are filled with cement slurry, pressurized to 1000 psi, and then cured for 8 days. After the test samples have cured, low-pressure gas (100 to 200 psi) is periodically applied to one end of each test pipe and the gas flow rate through the cement column is measured. As time increases with no flow, increased pressure is applied to the pipe to eventually induce failure and flow.

Test Results—Mechanical Properties

This section contains results from testing conducted throughout this project period, as well as additional mechanical property test results selected from previous test periods. Graphical data for all mechanical property tests are presented in Appendix B of this report.



Tensile Strength

Table 2 shows the effects of carbon fibers on tensile strength. The two-fold to three-fold increase in tensile strength is significant, indicating the potential for fibers to enhance the durability of cement.

Table 2—Tensile Strength and Young's Modulus

Slurry	Tensile Strength (psi)	Young's Modulus
Foam slurry (12-lb/gal)	253	3.23 E4
Neat Type I slurry	394/213 ^a	19.15/8.16 E4 ^a
Type I slurry with fibers	1071	9.6 E4
Latex slurry	539	5.32 E4
Latex slurry with fibers	902	8.5 E4

^aData taken from two different specimens.

Young's Modulus with Various Confining Forces

The effects of confining stress on compressive strength and Young's modulus are presented in Table 3. A significant increase in compressive strength is observed among lower-strength compositions such as foam cement and latex cement, as confining stress is increased.

Table 3—Young's Modulus at Various Confining Stresses

Slurry Composition	Confining Pressure (psi)	Young's Modulus (psi)
Type I slurry	0	16.7 E 5
	1500	11.1 E 5
	5000	9.1 E 5
Foam slurry (12 lb/gal)	0	5.8 E 5
	500	6.8 E 5
	1000	6.1 E 5
Bead slurry (12 lb/gal)	0	9.5 E 5
	500	8.1 E 5
	1000	1 E 6
Latex slurry	0	5.6 E 5
	250	8.9 E 5
	500	9.4 E 5

Poisson's Ratio

Initial results of Poisson's ratio testing on these lightweight cement compositions were unexpectedly low. Continued Poisson's ratio testing during this test period to determine reasons for these low values confirmed the accuracy of these early results. The low Poisson's ratio values for these compositions are theorized to be related to the porosity of



the specimens. Several published technical reports have documented this tendency for Poisson’s ratio to be effectively lowered as porosity increases.

Another potential variable in Poisson’s ratio testing is load rate. An investigation into the effect of load rate on Poisson’s ratio indicated that load rate does affect Poisson’s ratio measurement (Table 4). Table 5 presents data generated with a load rate of 250 psi/min. While these values are lower than what has traditionally been considered acceptable, the data are generally positive.

CT scans performed on Poisson’s ratio test specimens indicated a link between large voids or pore spaces and variable Poisson’s ratio. This procedure will be included in future testing and samples with large voids will be discarded. CT scans are included in Appendix B.

Table 4—Effect of Load Rate on Poisson's Ratio

Load Rate	Poisson's Ratio
100 psi/min	0.1
250 psi/min	0.08
500 psi/min	-0.01

**Table 5—Poisson's Ratio
(50-psi confining pressure, 250 psi/min load rate)**

Slurry	Failure (psi)	Poisson's Ratio
Foam slurry (12-lb/gal)	3100	0.00
Bead slurry	4100	-0.01
Neat Class H slurry	6450	0.0012
SMS slurry	920	0.005
Type I slurry	6500	0.1

Anelastic Strain

Anelastic strain testing is a variation of hydrostatic testing and is designed to allow a more accurate evaluation of permanent strain resulting from stressing different test compositions. This procedure standardizes confining stress at 500 psi and calls for samples to be cycled to 25%, 50%, and 75% of each composition’s compressive strength under that confining stress. Measurement of anelastic strain with cycling provides a more comparable value of each composition’s performance.

Results of initial anelastic strain testing are presented in Table 6. Strain data are reported as final strain minus initial strain measurements, with final being at the end of three cycles. A point on the stress axis indicating minimum linear strain was picked for comparison of strains at the beginning and end of cycling. This comparison point is listed also. Data generation will continue and will include a round of samples tested to a common stress maximum to provide two alternate methods of comparison.



Table 6—Results of Anelastic Strain Testing

Composition	Failure (psi)	Comparison Stress (psi)	Strain (mm/mm)	
			25%	50%
Type I slurry	6000	600	0.0006	0.0007
Foam slurry	2000	300	0.001	—
Bead slurry	3300	400	0.0007	—
Class H slurry	6000	600	0.0007	0.0009

Test Results—Mechanical Integrity

This section contains results from testing conducted throughout this project period, as well as additional mechanical integrity test results selected from previous test periods.

Shear Bond

Results of shear bond testing (Table 7) indicated that bond was degraded extensively both by pressure and temperature cycling. This degradation seemed to be aggravated by the simulated soft formation. In future tests, a modified shear bond method will be used to help ensure that the results are more comparable to annular seal tests. Shear bond testing simulating intermediate formation strength with PVC pipe was initiated, and a successful beta test has been completed. It is anticipated that intermediate formation strength will be completed during the next test period.

Table 7—Shear Bond Strengths (psi)

System	Simulated Formation	Type I Slurry	Foam Slurry	Bead Slurry	Latex Slurry
Baseline	hard	1194	127/98	109/78	—
	soft	198	233	143	223
Temperature-Cycled	hard	165	299/215	191/269	—
	soft	72	7	56	149
Pressure-Cycled	hard	194/106	276/228	294/170	—
	soft	23	22*	23*	11

* Visual inspection revealed samples were cracked.

Annular Seal

Results presented in Table 8 indicate that all cyclic testing specimens failed in the soft formation simulation while all specimens in the hard-formation tests maintained seal. These results indicate the need for a simulated formation with intermediate strength to further differentiate seal effectiveness. Additional stresses for the hard-formation simulation must be imposed through application of heat or pressure. .

A series of annular seal tests was performed with the intermediate strength formation simulated by PVC pipe. Results with Type 1 cement indicated failure after the third



temperature cycle. Unfortunately, problems with flow meter calibration caused the quantitative data to be worthless. This testing will be repeated for all cement compositions.

Table 8—Annular Seal Tests

Condition Tested	Formation Simulated	Type I Slurry	Foamed Slurry	Bead Slurry
Initial Flow	Hard	0 Flow	0 Flow	0 Flow
	Soft	0 Flow	0.5 (md)	0 Flow
Temperature-Cycled	Hard	0 Flow	0 Flow	0 Flow
	Soft	0 Flow	123 md	43 md*
Pressure-Cycled	Hard	0 Flow	0 Flow	0 Flow
	Soft	27 md	0.19 md*	3 md

* Visual inspection revealed samples were cracked.

Cement Column Seal

Four duplicate sets of models were filled with cement compositions listed in Table 9.

Table 9—Compositions Tested for 8-ft Permeability Models

Composition	Density (lb/gal)	Yield (ft ³ /sk)	Water (gal/sk)	Columns
Type I slurry	15.6	1.18	5.23	1 and 2
SMS slurry	12	2.38	14.05	3 and 4
Bead slurry	12	1.81	6.69	5 and 6
Latex slurry	15.63	1.17	4.20	7 and 8

These cements were allowed to cure for 7 days, and were then tested with differential pressure as described in the procedure section. Results, summarized in Table 10, are for days tested after the initial curing period. Actual results are shown in Appendix B, Table B1, page 34.

Table 10—Failure of 8-ft Permeability Models

Column	Days Tested at Initial Flow	Differential (psi)	Flow Rate (cc/min)
1	107	500	0.09
2	51	200	0.1
3	1	100	33
4	1	100	26
5	78	400	0.03
6	84	400	0.02
7	84	400	0.02
8	99	500	3.1

These results indicate that the sodium metasilicate (SMS) cement failed very quickly on the first day of testing. Other compositions including the neat Type 1 cement required up to 500 psi over the 8-ft column to induce failure. Further analysis of the complete data will be performed to determine bulk permeability with time.



Appendix A—Test Procedures

Sample Preparation

Some preparation and testing methods were modified to adapt for the lightweight bead and foamed slurries. The mixing procedures for the bead slurry were also modified to minimize bead breakage due to high shear from API blending procedures. The following blending procedure was used for the bead slurry.

1. Weigh out the appropriate amounts of the cement, water, and beads into separate containers.
2. Mix the cement slurry (without beads) according to Section 5.3.5 of API RP 10B.
3. Pour the slurry into a metal mixing bowl and slowly add beads while continuously mixing by hand with a spatula. Mix thoroughly.
4. Pour this slurry back into the Waring blender and mix at 4,000 rev/min for 35 seconds to mix and evenly distribute the contents.

Testing methods for the foamed slurries were also modified. For example, thickening time is performed on unfoamed slurries only. Because the air in the foam does not affect the hydration rate, the slurry is prepared as usual per API RP 10B and then the foaming surfactants are mixed into the slurry by hand without foaming the slurry.

Sample Curing

Test specimens for rock properties testing are mixed in a Waring blender and poured into cylinder molds. Samples are cured for 7 days in a 45°F atmospheric water bath.

Performance test fixture molds are filled with cement mixed in the same manner. These fixtures are also cured in a 45°F water bath for 7 days prior to testing.

Thickening Time Test

Following the procedures set forth in API RP 10B¹, thickening-time tests were performed on the three cement systems. The test conditions started at 80°F and 600 psi, and were ramped to 65°F and 5,300 psi in 48 minutes.

Free-Fluid Test

The free-fluid testing that was performed on the Type 1, foamed cement and bead cement came from API RP 10B. The free-fluid procedure, also referred to as operating free water procedure, uses a graduated cylinder that is oriented vertically. The slurry is maintained at 65°F, and the free fluid that accumulates at the top of the slurry is measured. See Table A1 for test results.



Table A1—Free Fluid Test Results

Slurry System	Thickening Time to 100 Bc (hr:min)	Percentage of Free Fluid
Neat	4:38	0.8
Foamed	3:42	0.0
Bead	5:04	0.8

Compressive Strength

The compressive strengths were derived using the 2-in. cube crush method specified in API RP 10B. The samples were cured in an atmospheric water bath at 45°F. The reported values were taken from the average of three samples.

Young's Modulus and Poisson's Ratio Testing

Traditional Young's modulus testing was performed using ASTM C469², Standard Test Method for Static Modulus of Elasticity (Young's Modulus) and Poisson's Ratio of Concrete in Compression.

The following procedure is used for the Young's modulus testing.

1. Each sample is inspected for cracks and defects.
2. The sample is cut to a length of 3.0 in.
3. The sample's end surfaces are then ground to get a flat, polished surface with perpendicular ends.
4. The sample's physical dimensions (length, diameter, weight) are measured.
5. The sample is placed in a Viton jacket.
6. The sample is mounted in the Young's modulus testing apparatus.
7. The sample is brought to 100-psi confining pressure and axial pressure. The sample is allowed to stand for 15 to 30 min until stress and strain are at equilibrium. (In case of an unconfined test, only axial load is applied.)
8. The axial and confining stress are then increased at a rate of 25 to 50 psi/min to bring the sample to the desired confining stress condition. The sample is allowed to stand until stress and strain reach equilibrium.
9. The sample is subjected to a constant strain rate of 2.5 mm/hr.
10. During the test, the pore-lines on the end-cups of the piston are open to atmosphere to prevent pore-pressure buildup.

After the sample fails, the system is brought back to the atmospheric stress condition. The sample is removed from the cell and stored.

Following a review of this procedure during the February meeting, the decision was made to conduct additional load tests in the constant stress mode rather than the constant strain mode.

Hydrostatic Cycling and Anelastic Strain

Hydrostatic cycling testing was then performed on cement specimens in the same load configuration as for Young's modulus and Poisson's ratio. This testing was conducted



with axial loading and radial loading being maintained equally throughout the load ramping process. For such testing, the hydrostatic pressure is cycled through the following ramping procedures.

1. Ramp up to 1,000 psi.
2. Ramp down to 100 psi.
3. Ramp up to 1,500 psi.
4. Ramp down to 100 psi.
5. Ramp up to 2,000 psi.
6. Ramp down to 100 psi.
7. Continue to failure.

Each ramp was conducted at 16.7 psi/min and the sample was held at the destination hydrostatic pressures (i.e., 100; 1,000; 1,500; and 2,000 psi) for no longer than two minutes before proceeding to the next ramp step.

Hydrostatic cycling was studied further to investigate the deformation that occurs during each of the ramps. The value (size) of the sample at 250 psi during the first ramp to 1,000 psi is the reference value for determining the percentile of deformation. This reference value (sample size) is then compared to the sample size at 250 psi during each subsequent ramp step.

Concern over the ability to compare results of this testing among different compositions led to the development of a test for determining strain and cyclic loading effects under similar conditions with respect to each composition's ultimate strength. This test is referred to as anelastic strain testing.

Anelastic strain testing, a variation of hydrostatic testing, is designed to allow a more accurate evaluation of permanent strain resulting from stressing different test compositions. Samples are cycled to 25%, 50%, and 75% of each composition's compressive strength under 500-psi confining stress. Measurement of anelastic strain with cycling provides a more comparable value of each composition's performance. The first step in the procedure involves compression testing a sample to failure in the load cell with 500-psi confining stress. Once this failure load value is determined, additional samples will be tested by applying axial loads equal to 25%, 50%, and 75% of the failure load, and cycling until samples fail. The cyclic loading rate will be maintained at 250 psi/min and the confining force will be maintained at 500 psi. Plastic deformation will be measured at the end of each cycle. Results will include cycles to failure and anelastic strain per cycle. CT scans will be performed on each sample prior to testing to rule out the presence of any large voids.

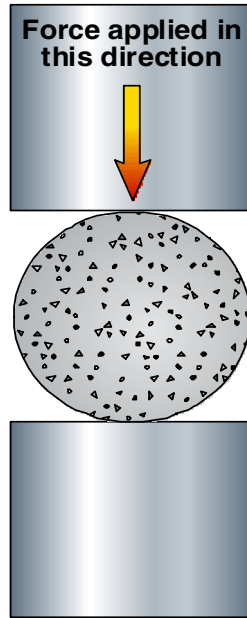
Tensile Strength and Tensile Young's Modulus

Tensile strength was tested using ASTM C496³ (Standard Test Method for Splitting Tensile Strength of Cylindrical Concrete Specimens). For this testing, the specimen dimensions were 1.5 in. diameter by 1 in. long. **Figure A1** shows a general schematic of how each specimen is oriented on its side during testing. The force was applied by



constant displacement of the bottom plate at a rate of 1 mm every 10 minutes. Change in the specimen diameter can be calculated from the test plate displacement. The (compressive) strength of the specimen during the test can be graphed along with the diametric strain (change in diameter/original diameter) to generate the tensile Young's modulus.

Figure A1—Sample Orientation for ASTM C496-90 Testing



Annular Seal Testing Procedure

Samples for annular seal testing are prepared by mixing cement compositions, pouring them into specified molds, and curing them for 7 days in 45°F water baths. After curing, three specimens for each test composition and condition are tested.

These procedures are for use with the annular seal apparatus. Specific procedures are applied as necessary for each formation simulation: soft, intermediate, and hard. The soft apparatus test procedure is to be used with cores cured to set in a soft gel mold, which provides a semi-restricting force on the outside of the core. The intermediate specimen mold uses a 3-in. diameter Schedule 40 PVC pipe as the outer containment. The hard apparatus uses a 3-in. Schedule 40 steel pipe as the outside containment, giving the cement slurry a restricting force outside of the core.

Soft-Formation Simulation

1. After the core is cured, place the core inside the gel mold sleeve.
2. Place the core and sleeve inside the pipe-in-soft steel cell.
3. Once inside, both ends of the core are supported with O-rings.



4. The O-rings are then tightened by interior end plates to close off leaks that might be present.
5. Using water, pressurize the exterior circumference of the sleeve to 25 psi and check for leaks on the ends of the cell.
6. Cap off both ends of the steel cell with the cell end caps. One end cap has a fitting that allows for N₂ gas to be applied into the cell, and the other end cap allows gas to exit the cell.
7. Attach the pressure inlet line to the bottom of the cell and attach the pressure outlet line to the top of the cell.
8. Apply pressure to the inlet line (do not exceed 20 psig) and measure the flow out using flow meters.

Hard-Formation Simulation

1. After the core is cured inside the steel pipe, cap off each end of the pipe with steel end caps. Each end cap has a fitting that allows for gas to be applied into the pipe or to exit the pipe.
2. Attach the pressure inlet line to the bottom of the pipe, and attach the pressure outlet line to the top of the pipe.
3. Apply pressure to the inlet line (do not exceed 20 psig) and measure the pressure out of the outlet line using flow meters.

Intermediate Formation Simulation

The test fixture for performing tests with a simulated intermediate formation is very similar to that used for tests with simulated hard formations, except the outer pipe is made of Schedule 40 PVC. Stress is applied to the specimens by applying hydraulic pressure or heat to the inner pipe.

Thermal cycling resulted from the insertion of heaters into the inner pipe and the heating of the inner pipe from 80° to 180°F then allowing the pipe to cool to 80°F. Flow through the model was measured at each endpoint on the cycle, and cycles were repeated a minimum of five times per sample. Three specimens of each composition were tested.

To ensure that sufficient stress could be applied to induce failure in all samples, the thermal cycling test procedure was modified to allow use of a thicker-walled inner pipe that provides more steel volume for expansion. The modified test fixture now features an inside pipe with a 1.68-in. outside diameter and a 1.25-in. inside diameter, giving a wall thickness of 0.190 in. Additionally, the outer containment diameter will be increased to 3 in.

Pressure cycling resulted from the application of hydraulic pressure to the inner pipe. For the initial cycle, pressure was increased from 0 to 500 psi. Pressure was then released and allowed to return to 0, and flow measurements were made. Additional cycles were made by increasing the upper pressure limit by 500 psi (0 to 1,000 to 0 psi, 0 to 1,500 to 0 psi, etc.) and measuring flow at the endpoint (0) of each cycle. If specimens were cycled to 10,000 psi without failure, the 0 to 10,000 to 0 psi pressure cycle was repeated a



minimum of five times. The original test procedure was modified to establish a maximum pressure of 10,000 psi during pressure cycles.

Shear Bond Strength Testing

Shear bond strength tests are used for investigating the effect that restraining force has on shear bond. Samples are cured in a hard-formation configuration (**Figure A2**) and in a soft-formation configuration (**Figure A3**). The hard-formation configuration consists of a sandblasted internal pipe with an outer diameter (OD) of 1 ¹/₁₆ in. and a sandblasted external pipe with an internal diameter (ID) of 3 in. Both pipes are 6 in. long. A contoured base and top are used to center the internal pipe within the external pipe. The base extends into the annulus 1 in. and cement fills the annulus to a height of 4 in. The top inch of annulus contains water.

For the soft-formation shear bond tests, plastisol is used to allow the cement to cure in a less-rigid, lower-restraint environment. Plastisol is a mixture of a resin and a plasticizer that creates a soft, flexible substance. This particular plastisol blend (PolyOne's Denflex PX-10510-A) creates a substance with a hardness of 40 duro.

The soft formation configuration contains a sandblasted external pipe with an ID of 4 in. A molded plastisol sleeve with an ID of 3.0 in. and uniform thickness of 0.5 in. fits inside the external pipe. With the aid of a contoured base and top, a sandblasted internal pipe with an OD of 1 ¹/₁₆ in. is then centered within the plastisol sleeve. The pipes and sleeve are 6 in. long. The base extends into the annulus 1 in. and cement fills the annulus to a height of 4 in. between the plastisol sleeve and the inner 1 ¹/₁₆ -in. pipe. The top inch of annulus is filled with water.

The intermediate formation test fixture will feature the same configuration as the hard formation fixture except the outer pipe is made of PVC.

Cycling tests for the shear bond specimens were performed according to the following test schedules:

Pressure Cycling

1. Cure specimens for 14 days at 45°F.
2. Apply 5000 psi hydraulic pressure to inner pipe and maintain for 10 minutes.
3. Release and maintain for 10 minutes.
4. Repeat the cycle four more times.
5. Test shear bond.

Temperature Cycling

1. Cure specimens for 14 days at 45°F.
2. Move specimens from 45°F water bath to 96°F for 1 hour.
3. Place specimens in 180°F water bath for 4 hours.
4. Place specimens in 96°F water bath for 1 hour.



5. Return specimens to 45°F bath
6. Repeat the cycle four more times.
7. Test shear bond.

If additional shear bond testing is required, a new test procedure will be used that is designed to allow correlation with annular seal test results. After failure is noted in the annular seal test, the exact pressure or temperature cycle sequence is repeated for the shear bond specimens. Shear bond will be measured after the cycling to determine the level of bond remaining.

Figure A2—Cross-section of pipe-in-pipe test fixture configuration for shear bond test.

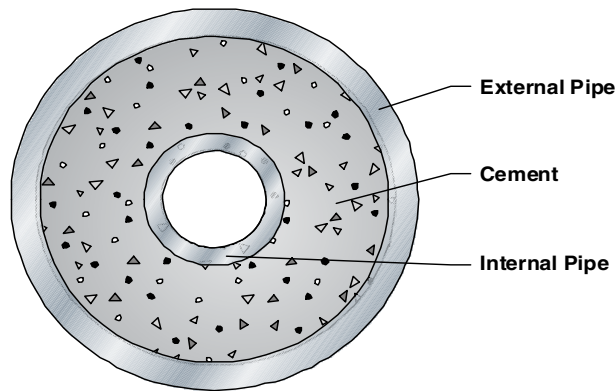
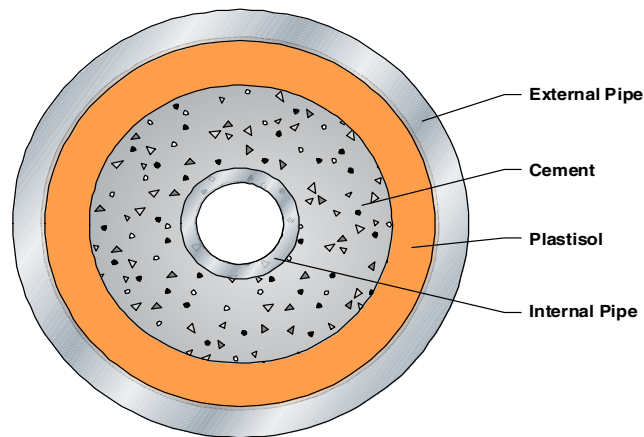


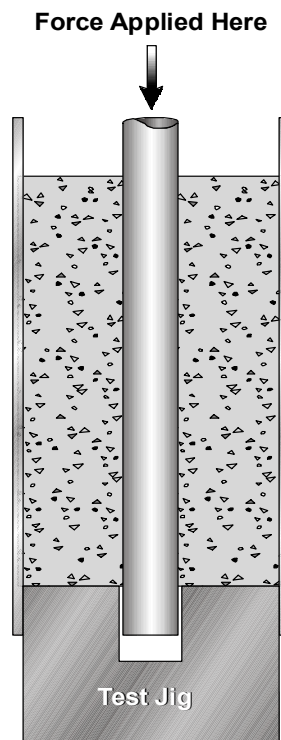
Figure A3—Cross-section of pipe-in-soft test fixture configuration for shear bond test.





The shear bond measures the stress necessary to break the bond between the cement and the internal pipe. This was measured with the aid of a test jig that provides a platform for the base of the cement to rest against as force is applied to the internal pipe to press it through. (Figure A4) The shear bond force is the force required to move the internal pipe. The pipe is pressed only to the point that the bond is broken; the pipe is not pushed out of the cement. The shear bond strength is the force required to break the bond (move the pipe) divided by the surface area between the internal pipe and the cement.

Figure A4—Test jig for testing shear bond strength



Cement Column Seal Tests

Eight-foot lengths of 2-in. Schedule 40 pipe are mounted vertically and fitted at the top and bottom with end caps equipped with pressure inlet and outlet ports. The bottom of each pipe is filled with 6 in. of 20-40 sand to provide an open base for gas injection. Sets of two fixtures are each filled with one of four different cement slurries: bead, Type 1, latex, and sodium metasilicate. Samples are covered with water and cured for 7 days under 1000-psi pressure. After the samples are cured, 100 psi of pressure is applied to the bottom of each fixture and any flow through the column is monitored.



Appendix B—Test Data

Graphical data for all mechanical properties tests performed in this investigation are presented in this appendix.

Figure B1—Plot of tensile strength and Young’s modulus results for latex slurry with fibers (sample 1), Type 1 slurry with fibers (sample 2), and latex slurry (sample 3).

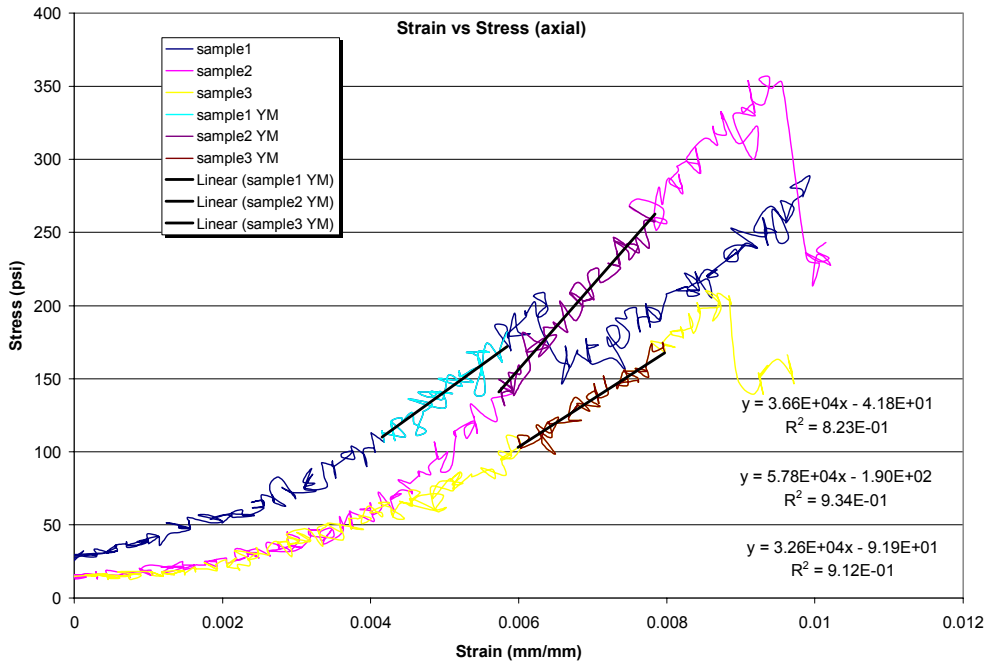




Figure B2—Plot of tensile strength and Young’s modulus results for neat Type 1 slurry cured in a confined state.

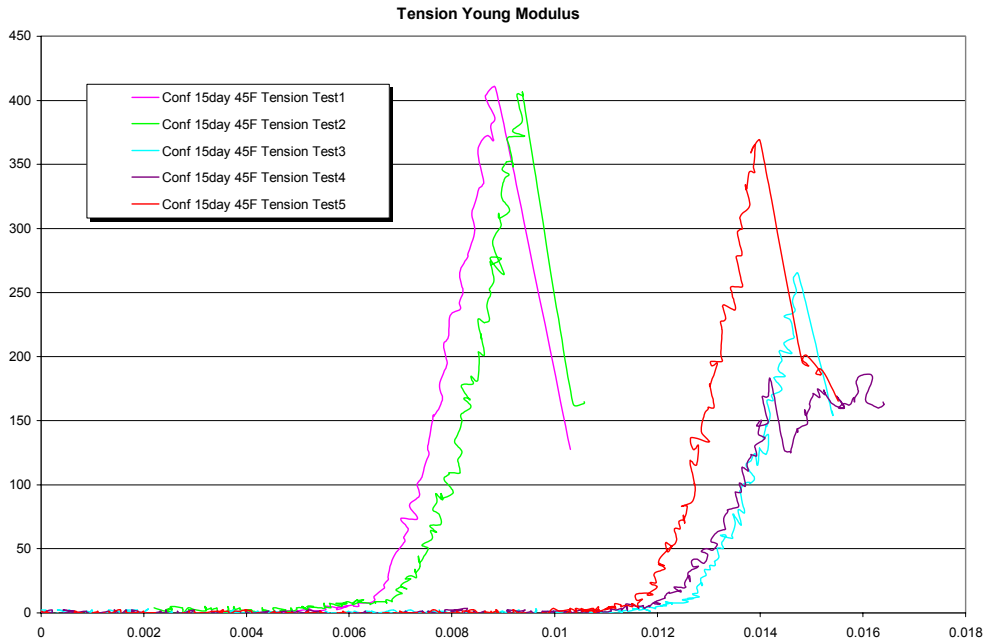


Figure B3—Plot of tensile strength and Young’s Modulus results for 12-lb/gal foam slurry.

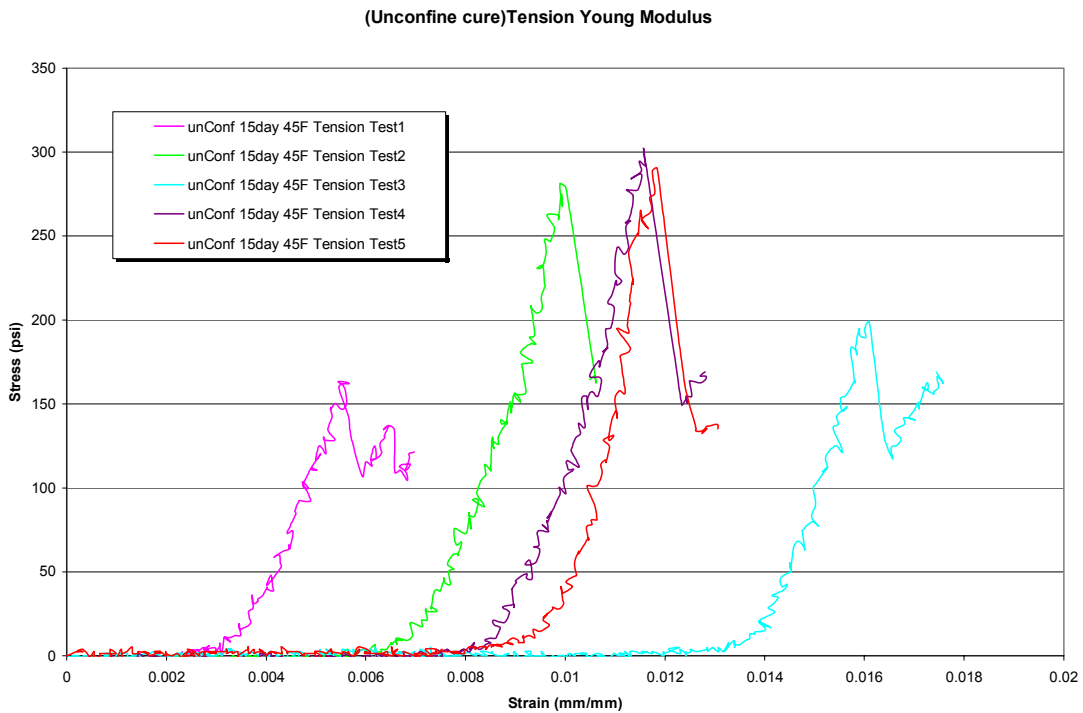




Figure B4—Plot of compressive Young’s modulus for Type 1 slurry at 0-psi confining pressure.

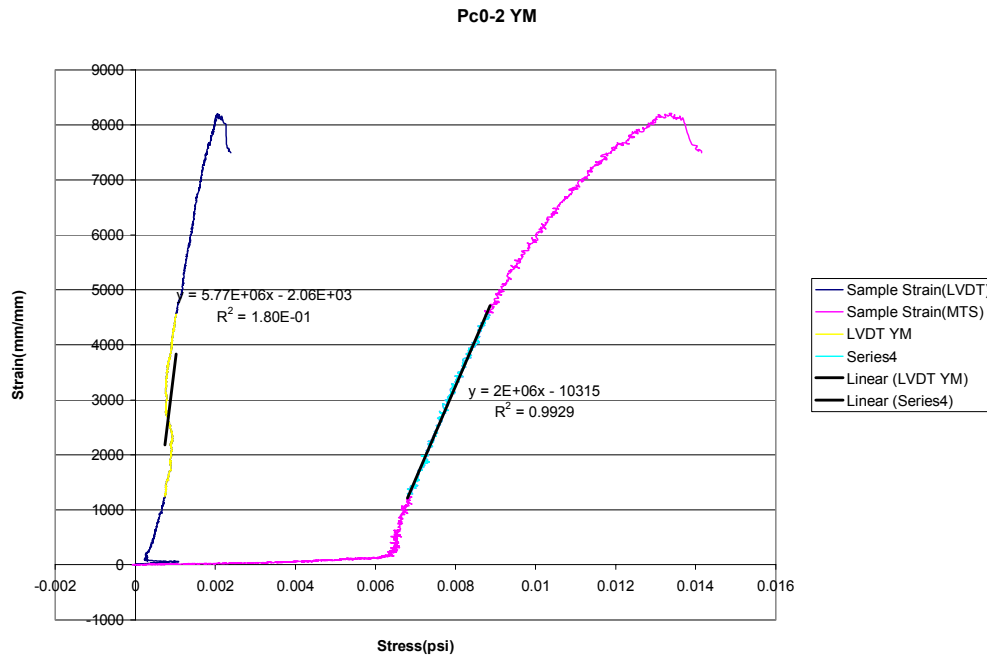


Figure B5—Plot of compressive Young’s modulus for Type 1 slurry at 1500-psi confining pressure.

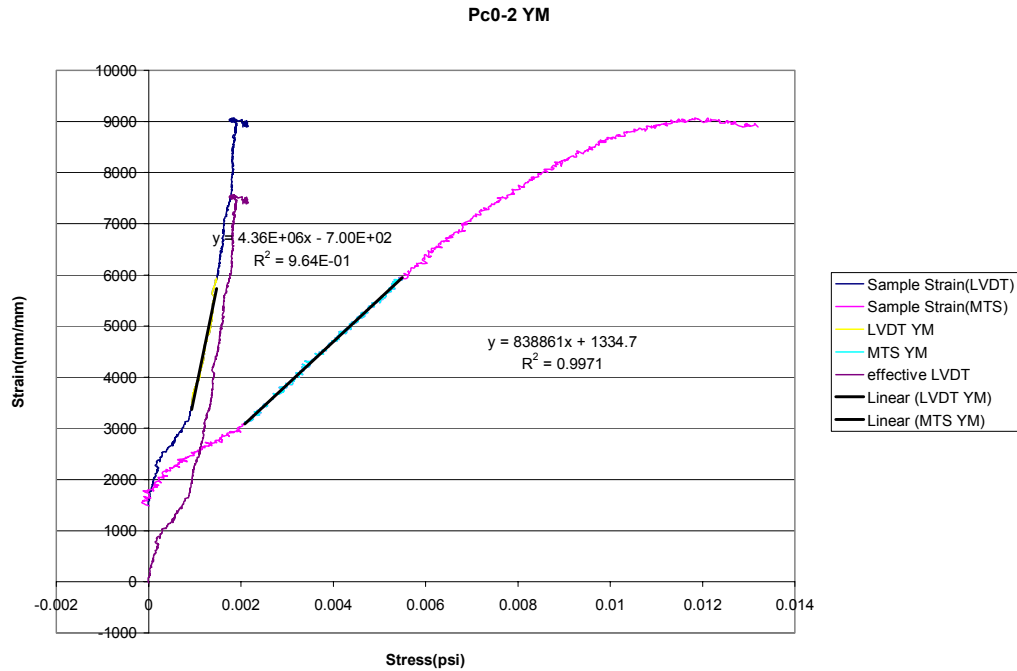




Figure B6— Plot of compressive Young’s modulus for Type 1 slurry at 5000-psi confining pressure.

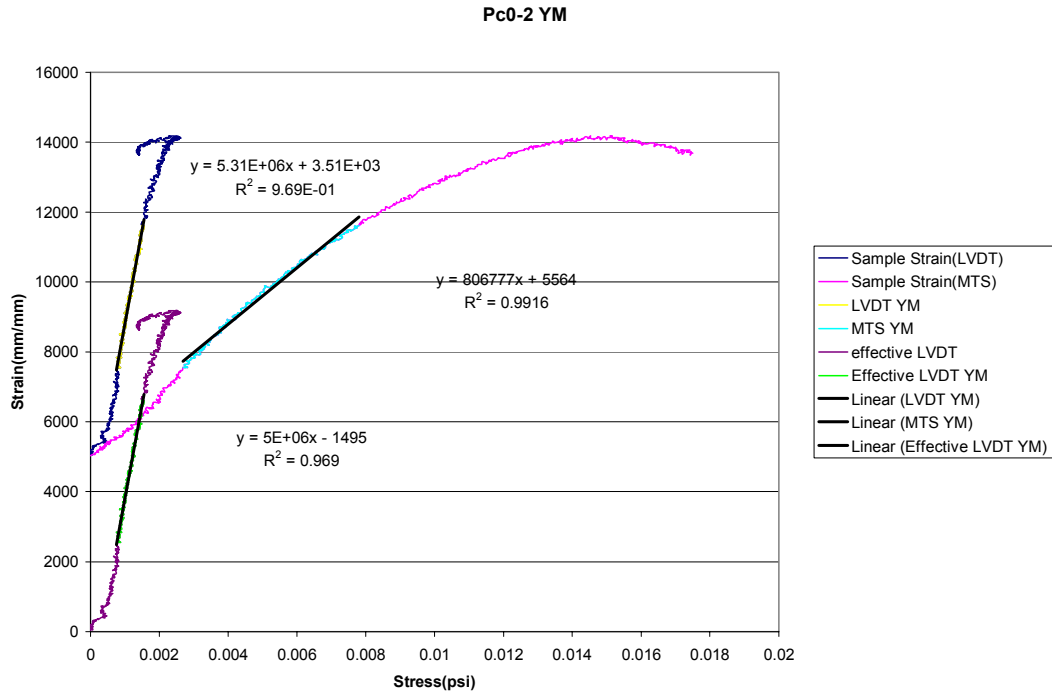


Figure B7— Plot of compressive Young’s modulus for 12-lb/gal foam slurry at 0-psi confining pressure.

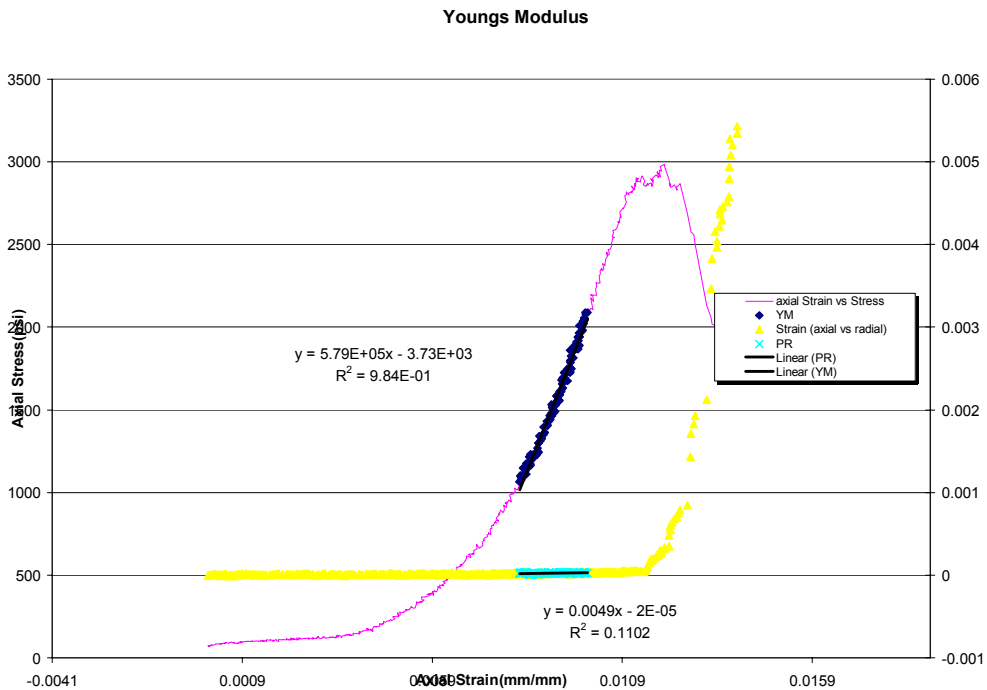




Figure B8— Plot of compressive Young's modulus for 12-lb/gal foam slurry at 500-psi confining pressure.

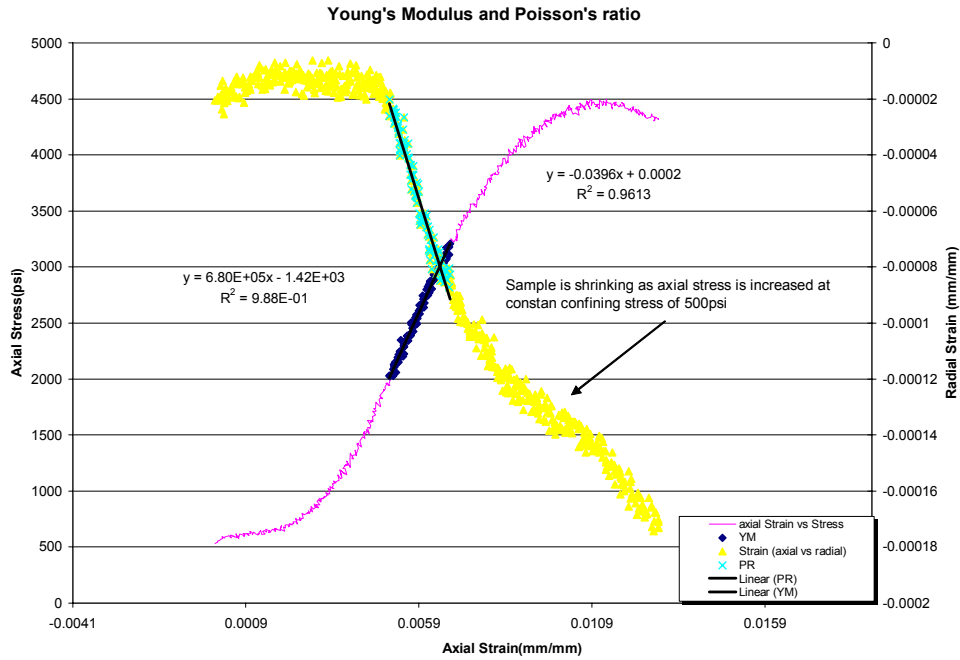


Figure B9— Plot of compressive Young's modulus for 12-lb/gal foam slurry at 1000-psi confining pressure.

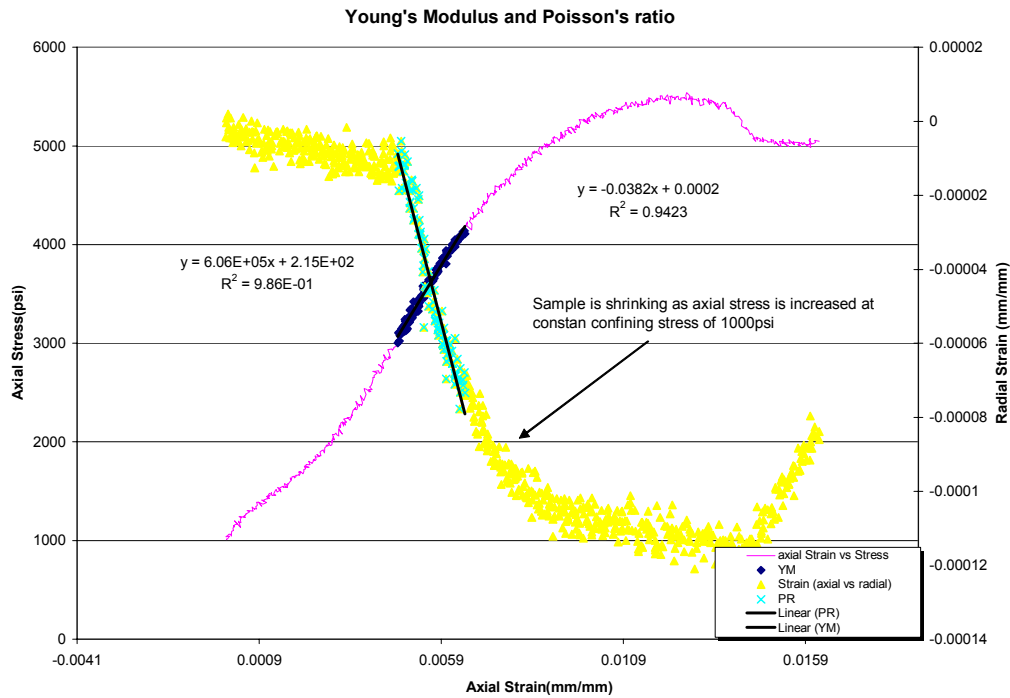




Figure B10— Plot of compressive Young’s modulus for bead slurry at 0-psi confining pressure.

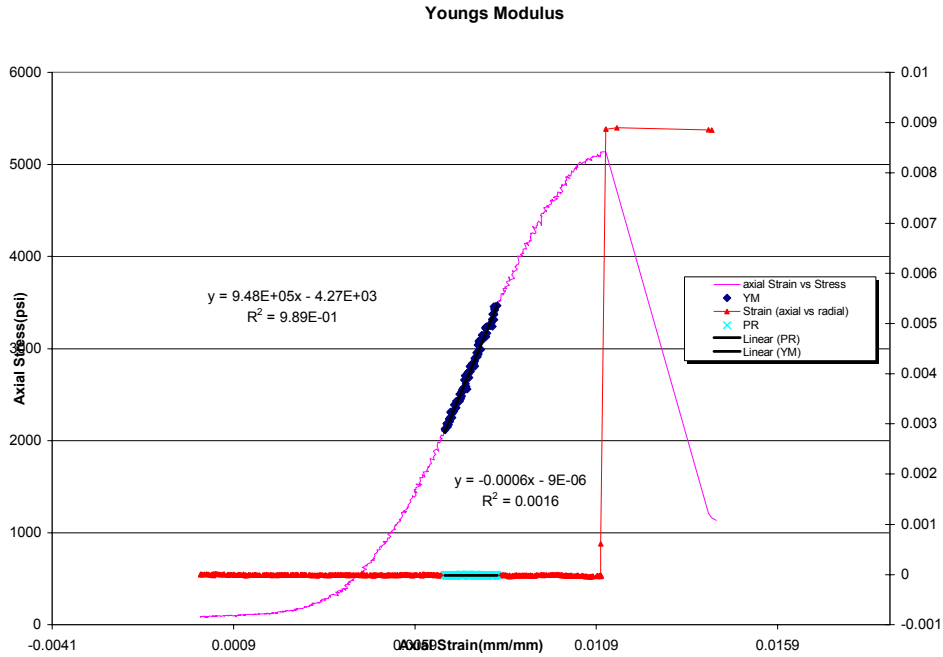


Figure B11— Plot of compressive Young’s modulus for bead slurry at 500-psi confining pressure.

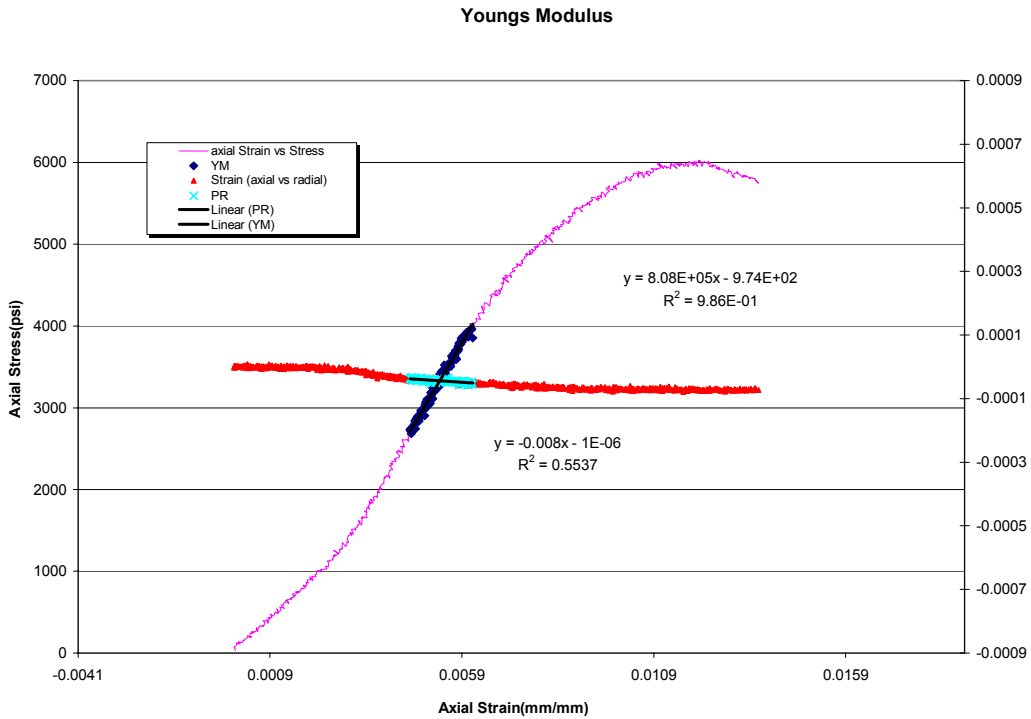




Figure B12— Plot of compressive Young’s modulus for bead slurry at 1000-psi confining pressure.

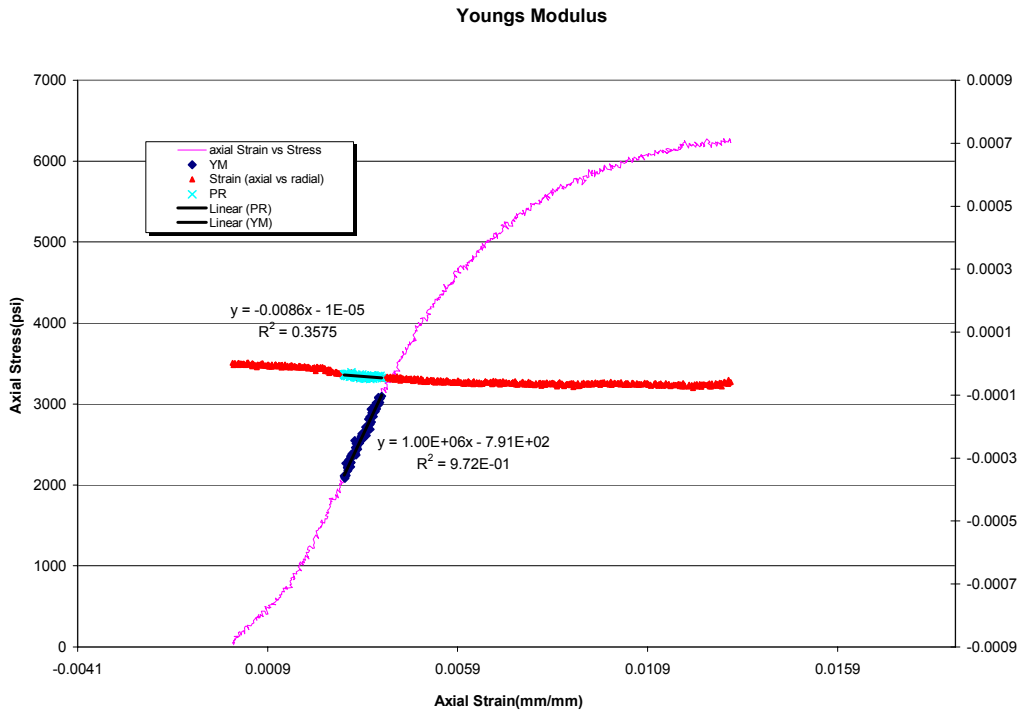


Figure B13— Plot of compressive Young’s modulus for latex slurry at 0-psi confining pressure.

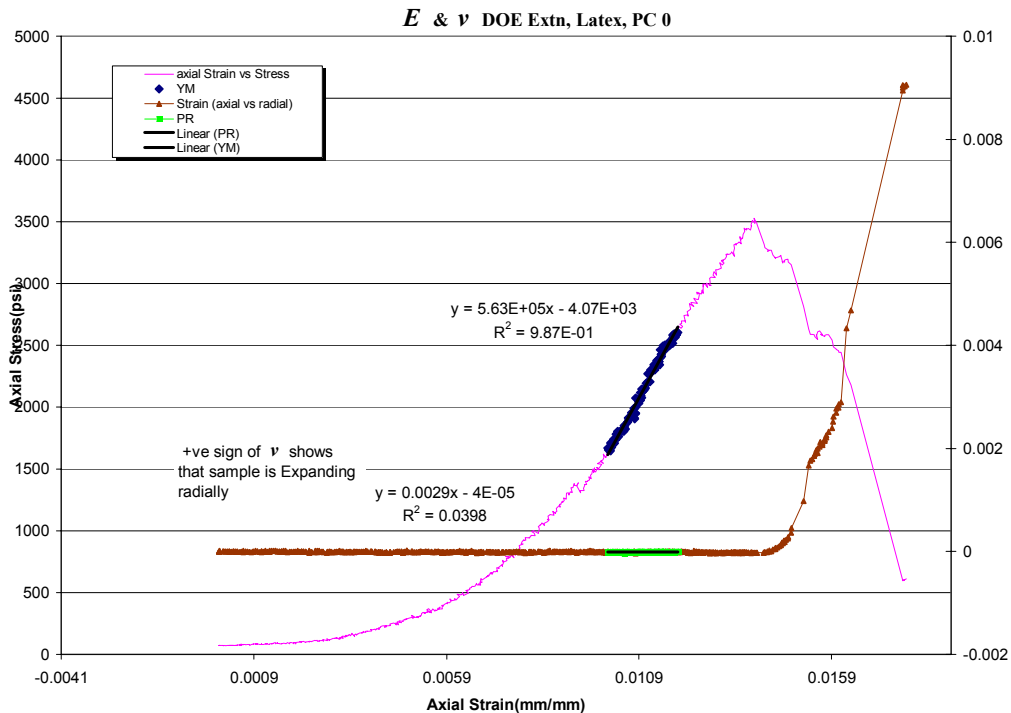




Figure B14— Plot of compressive Young’s modulus for latex slurry at 250-psi confining pressure.

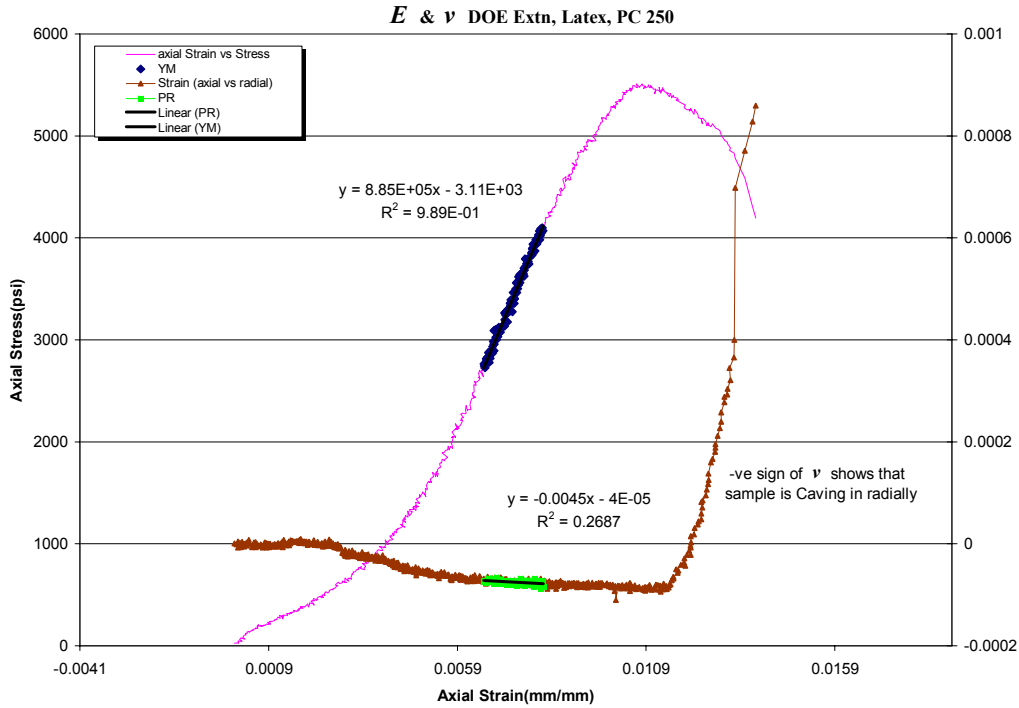


Figure B15— Plot of compressive Young’s modulus for latex slurry at 500-psi confining pressure.

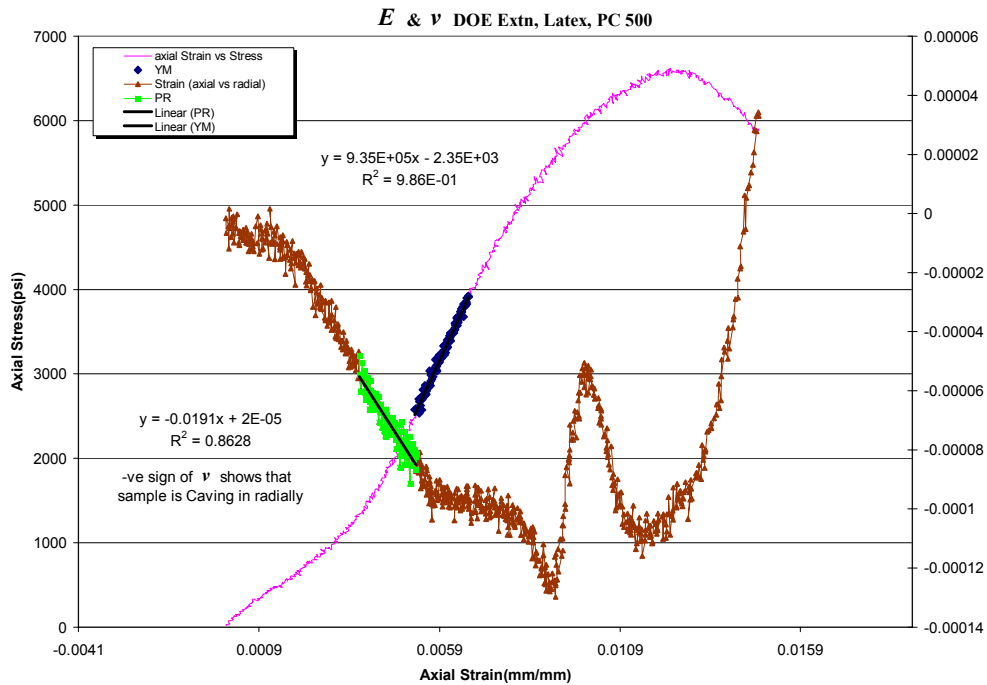




Figure B16—Young’s modulus measurements for Type 1 slurry at 500-psi confining stress and a 100-psi/min load rate.

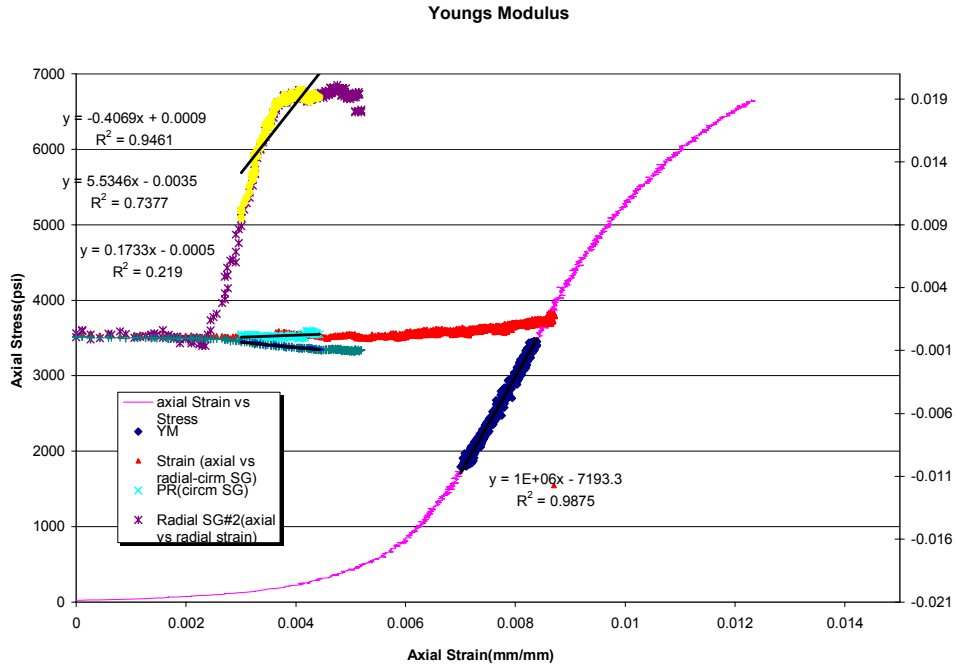


Figure B17—Young’s modulus measurements for Type 1 slurry at 500-psi confining stress and a 250-psi/min load rate.

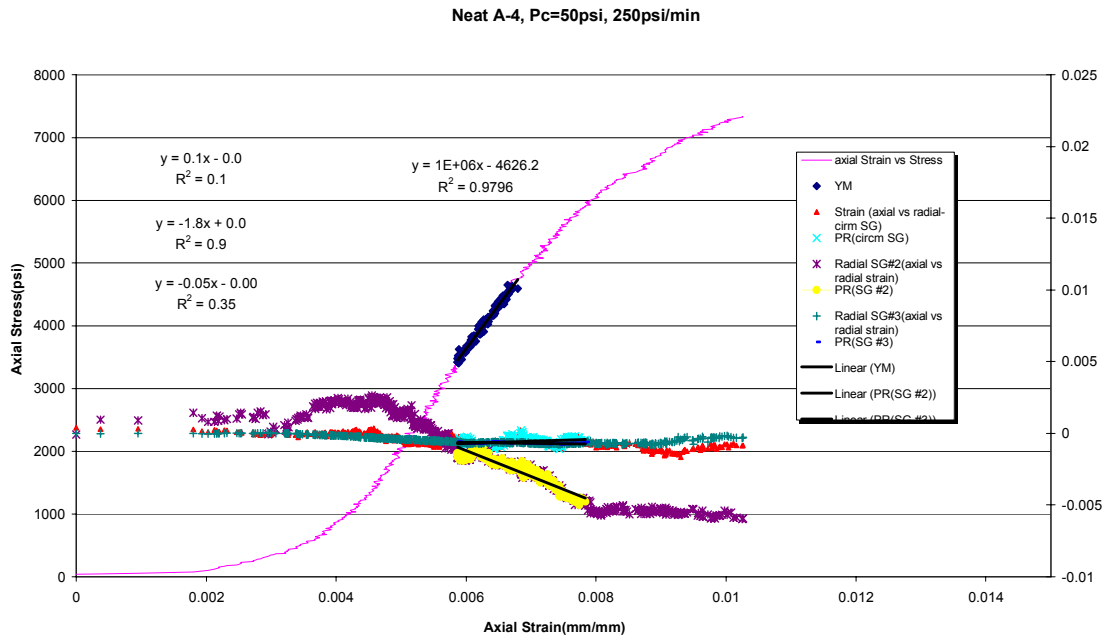




Figure B18—Young’s modulus measurements for Type 1 slurry at 500-psi confining stress and a 500-psi/min load rate.

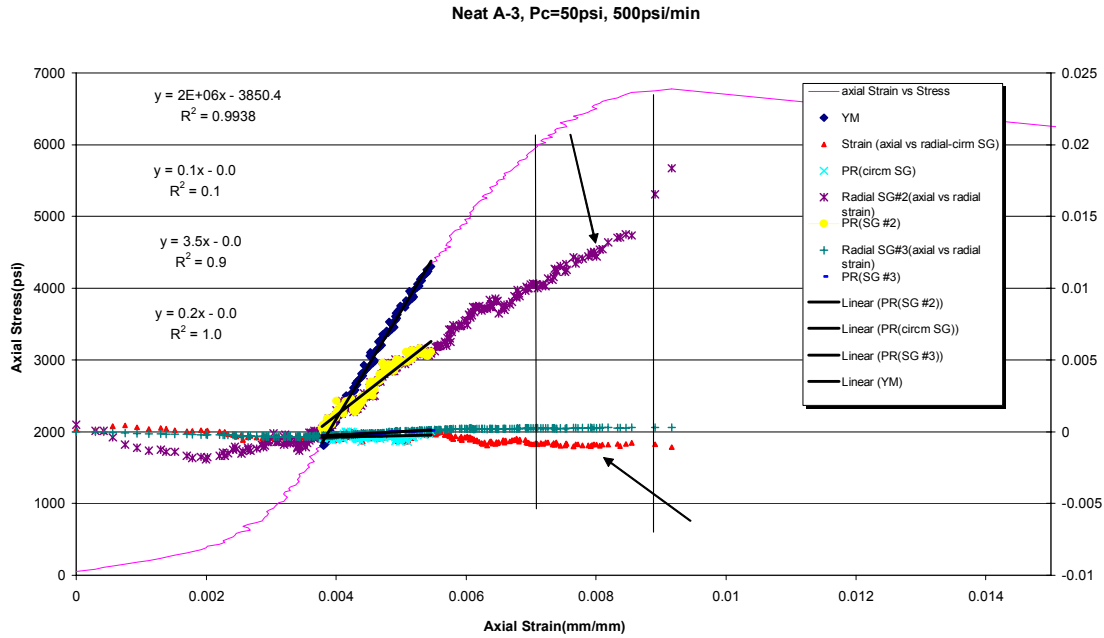


Figure B19—Hydrostatic cycling data for bead slurry showing anelastic strain.

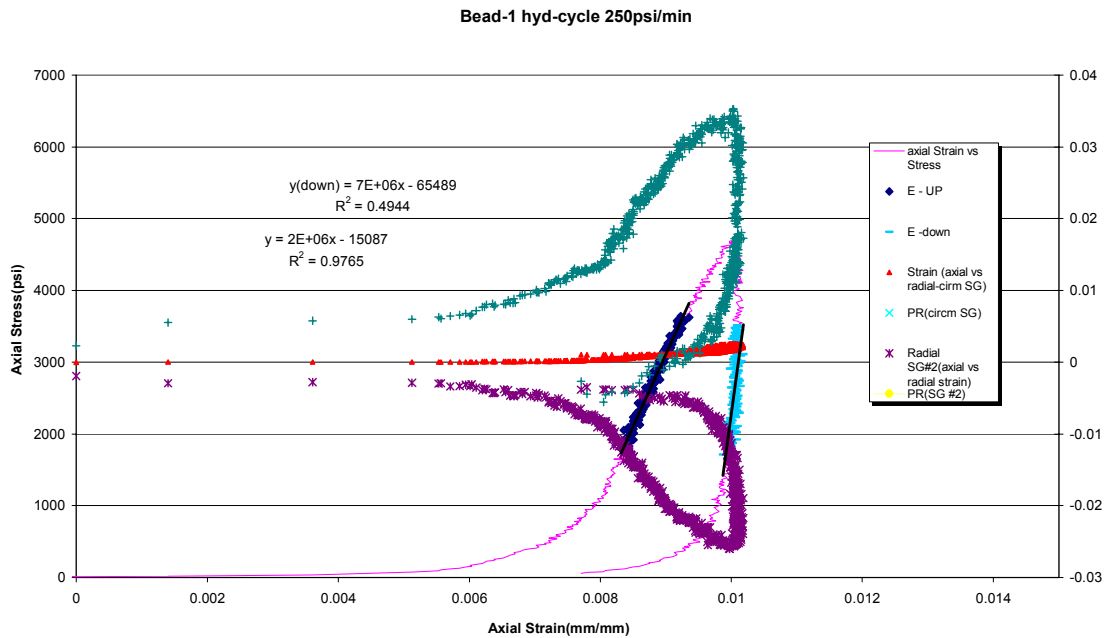




Figure B20— Hydrostatic cycling data for Class H slurry showing anelastic strain.

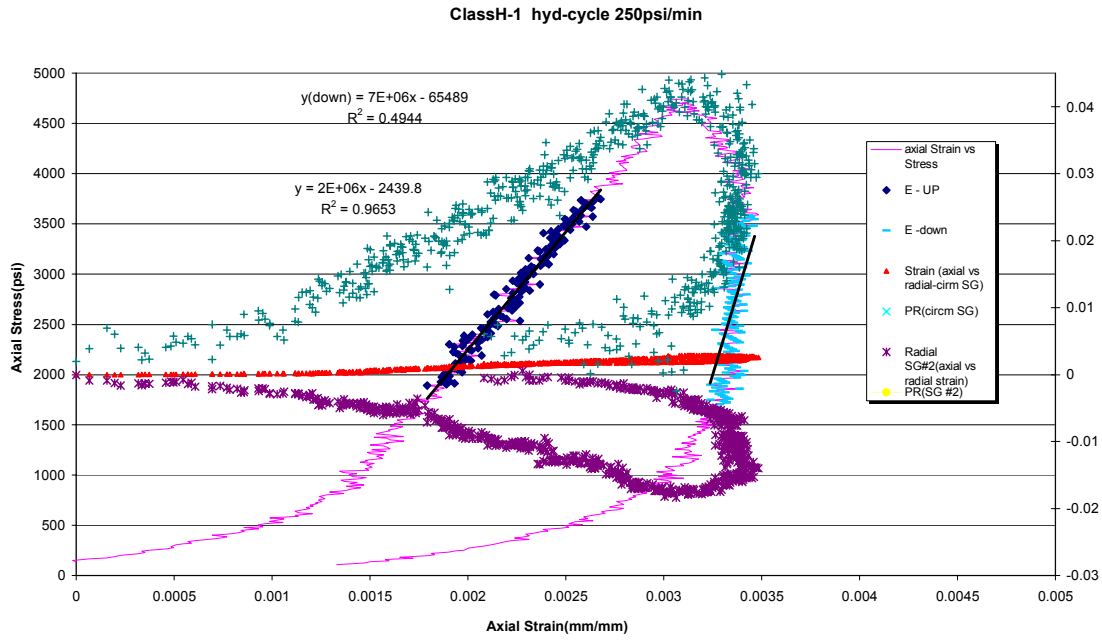


Figure B21— Hydrostatic cycling data for 12-lb/gal foam slurry showing anelastic strain.

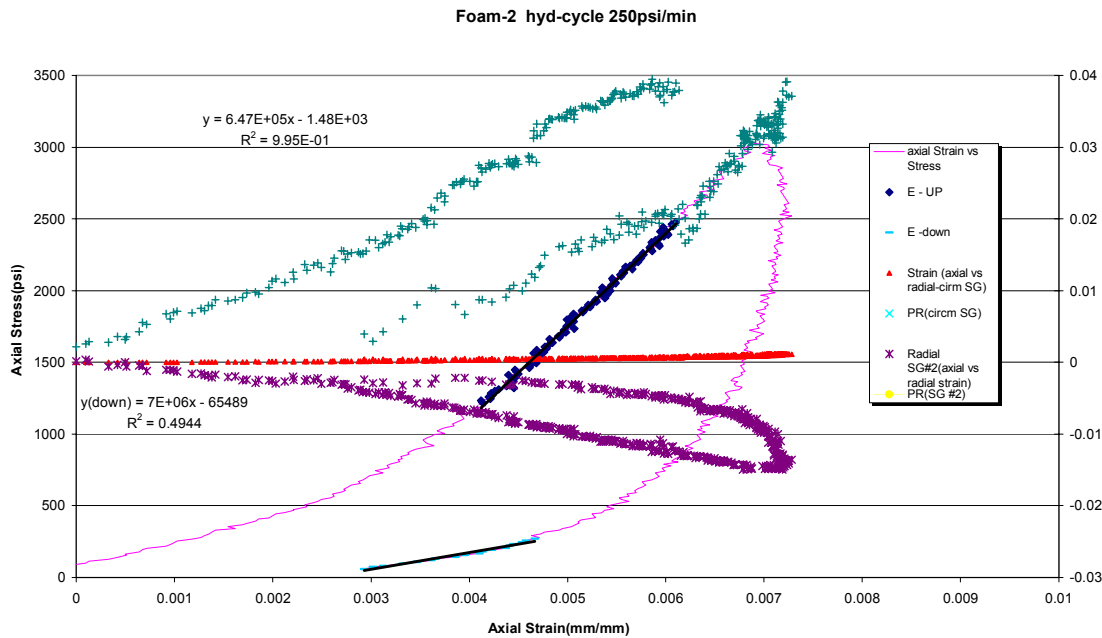




Figure B22— Hydrostatic cycling data for Type 1 slurry showing anelastic strain.

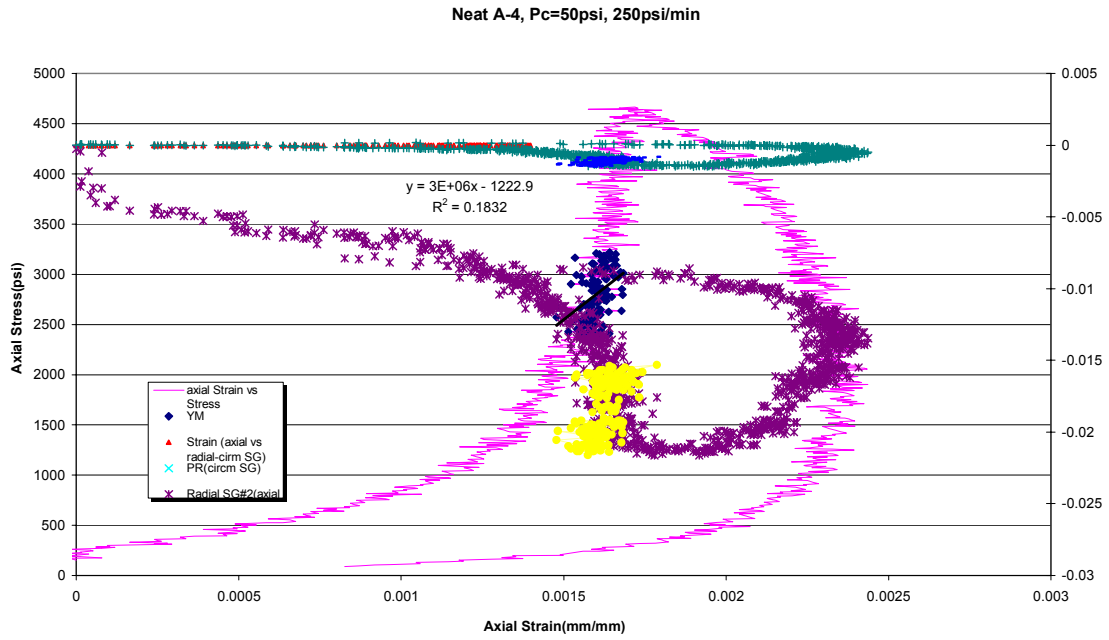


Figure B23— Hydrostatic cycling data for sodium metasilicate (SMS) slurry showing anelastic strain.

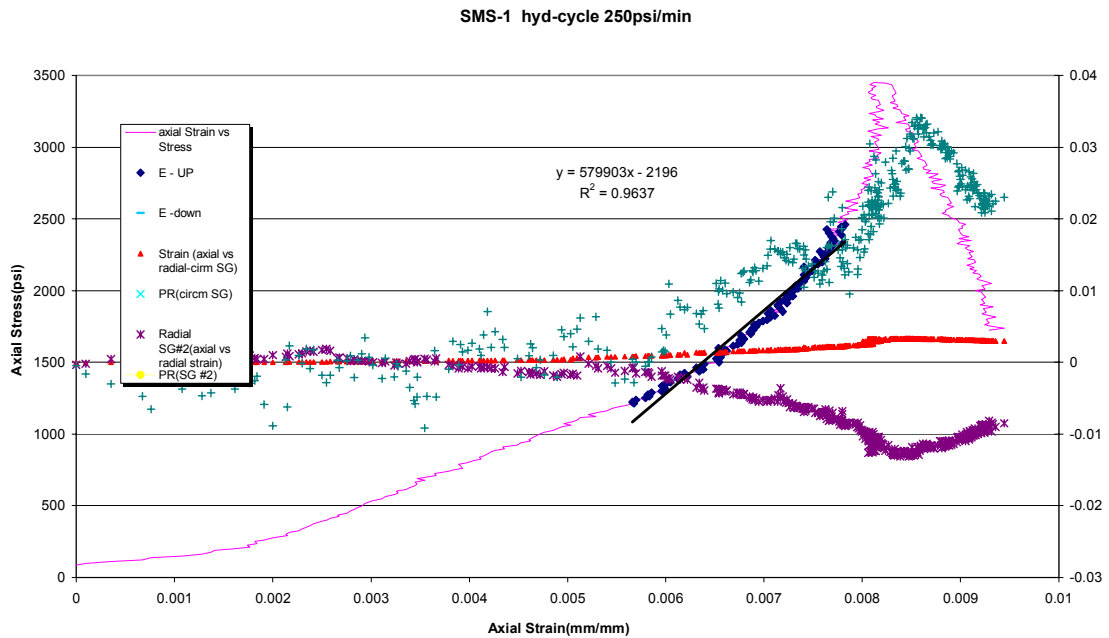




Figure B24— Anelastic strain failure load for neat Type 1 slurry at a load rate of 250 psi/min and confining pressure of 500 psi.

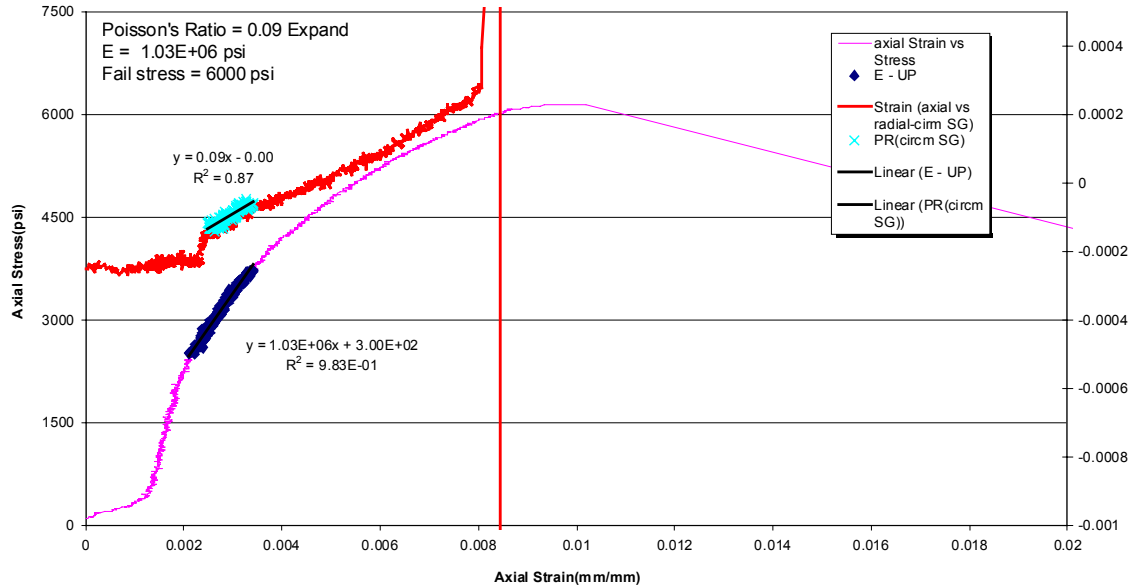


Figure B25— Anelastic strain failure load for foam slurry at a load rate of 250 psi/min and confining pressure of 500 psi.

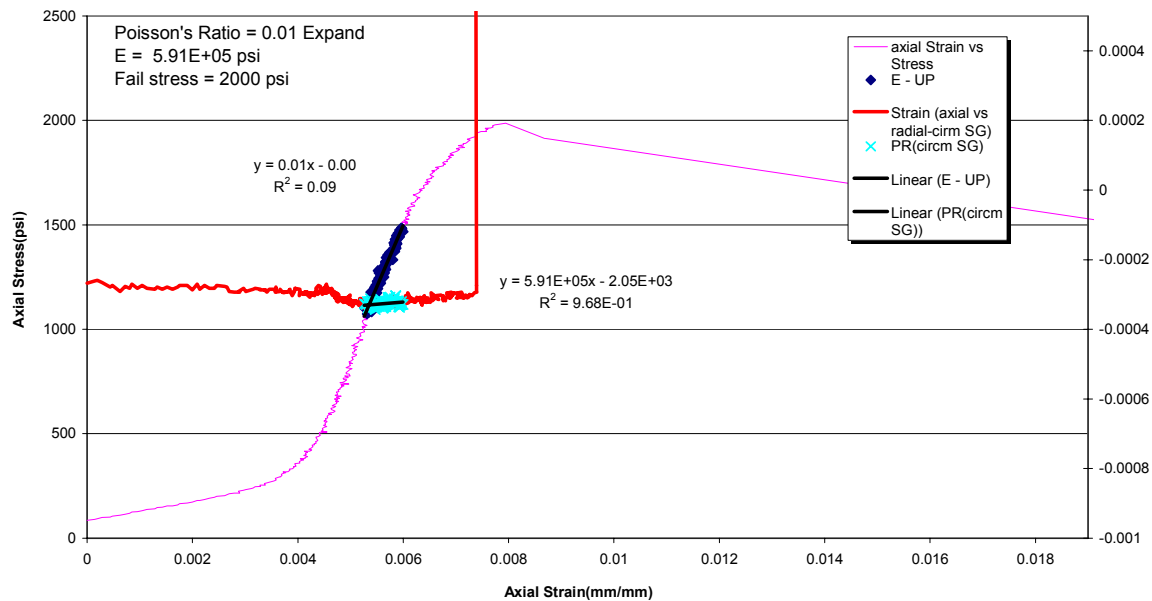




Figure B26—Anelastic strain failure load for bead slurry at a load rate of 250 psi/min and confining pressure of 500 psi.

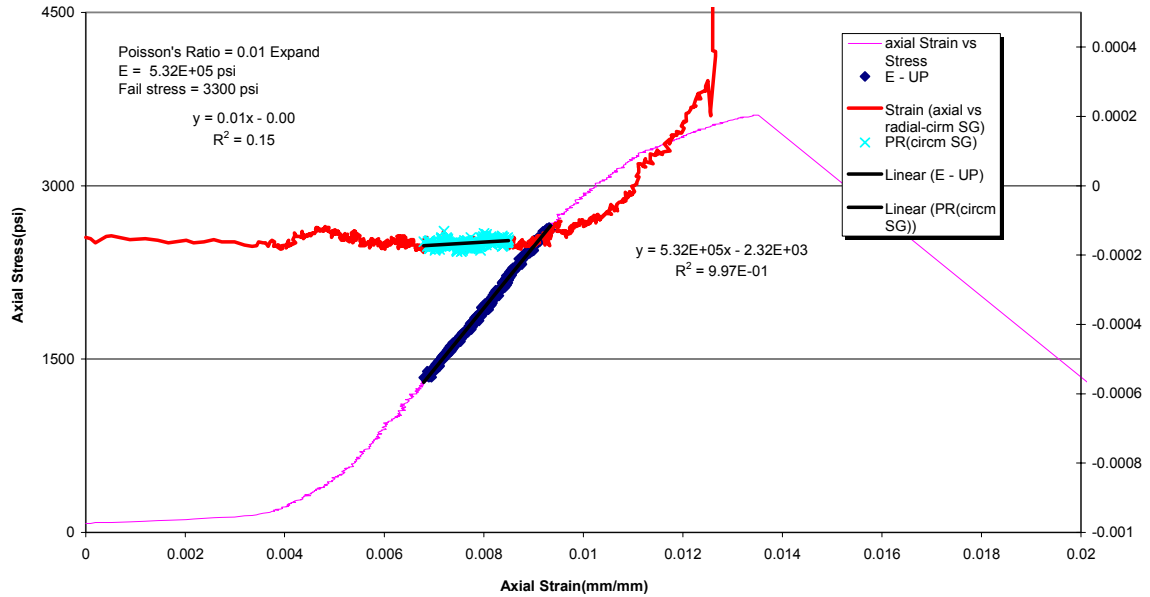


Figure B27—Anelastic strain failure load for latex slurry at a load rate of 250 psi/min and confining pressure of 500 psi.

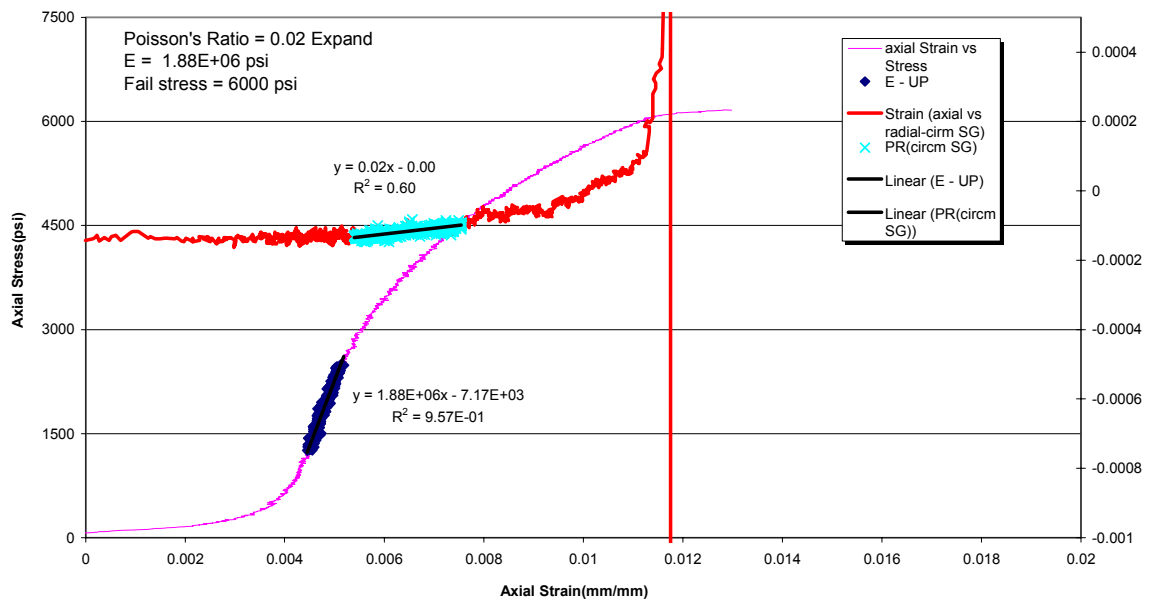




Figure B28—Anelastic strain, cycled to 25% of failure load, for Type 1 slurry at a load rate of 250 psi/min and confining pressure of 500 psi.

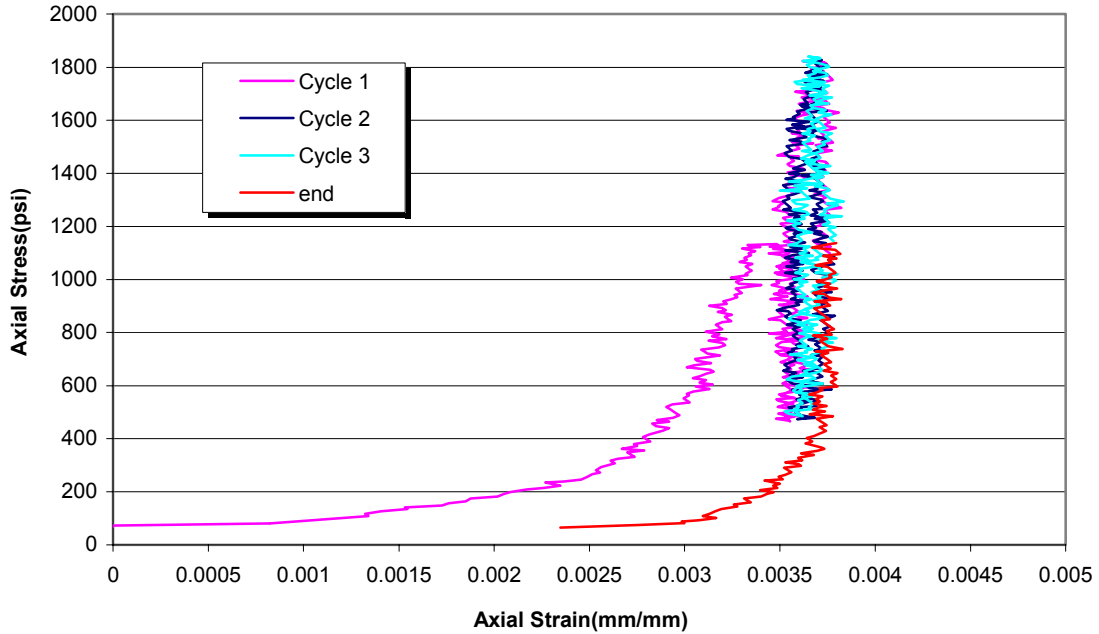


Figure B29—Anelastic strain, cycled to 25% of failure load, for foam slurry at a load rate of 250 psi/min and confining pressure of 500 psi.

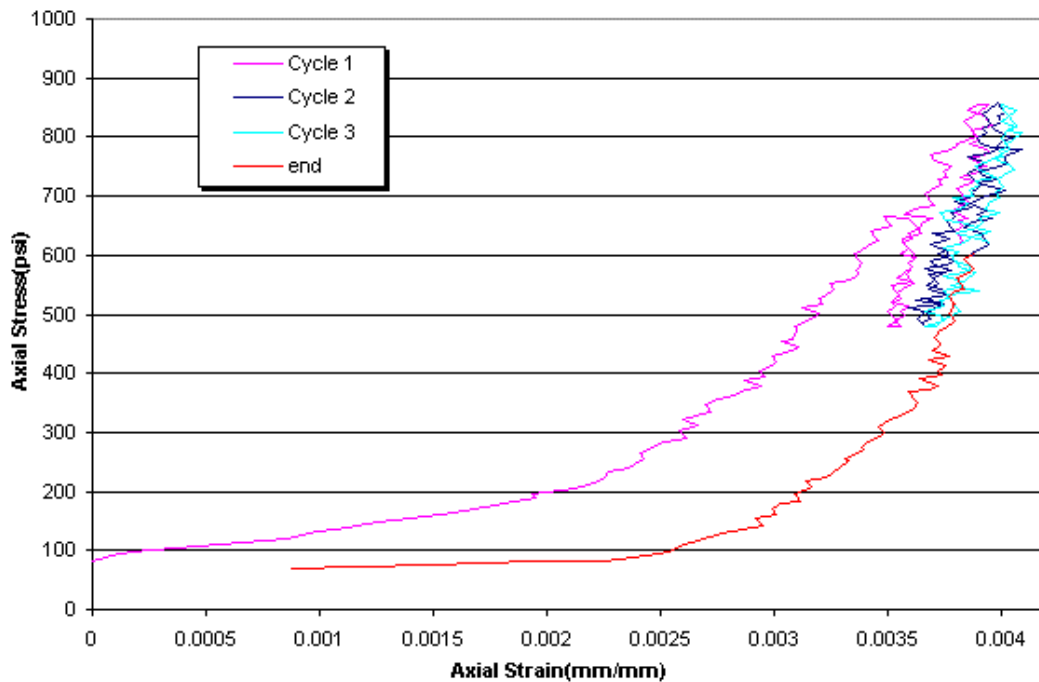




Figure B30—Anelastic strain, cycled to 25% of failure load, for bead slurry at a load rate of 250 psi/min and confining pressure of 500 psi.

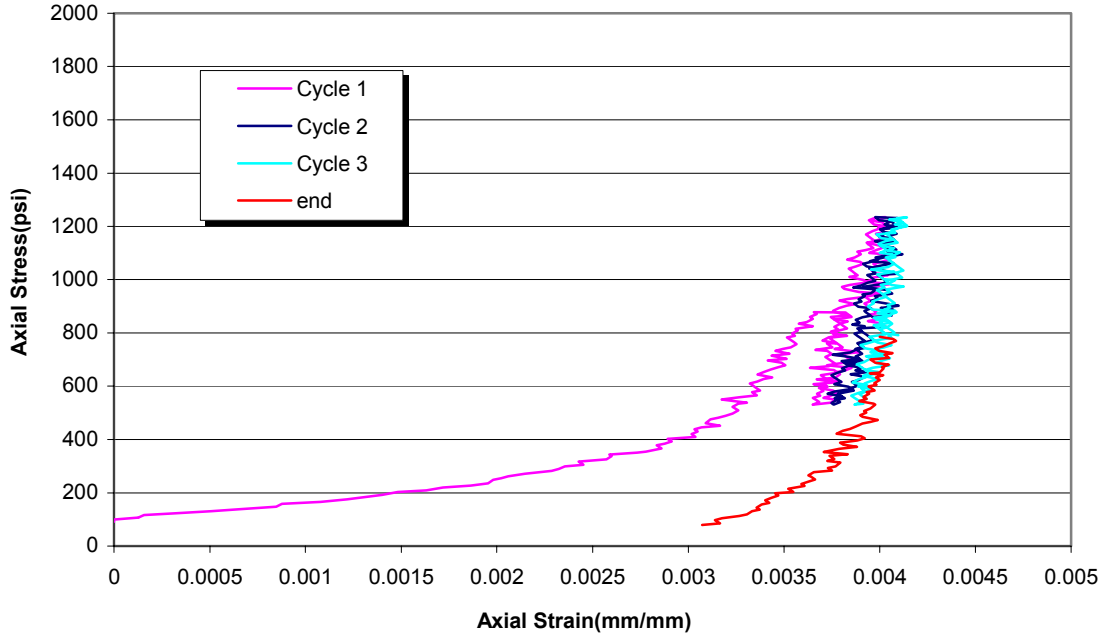


Figure B31—Anelastic strain, cycled to 25% of failure load, for latex slurry at a load rate of 250 psi/min and confining pressure of 500 psi.

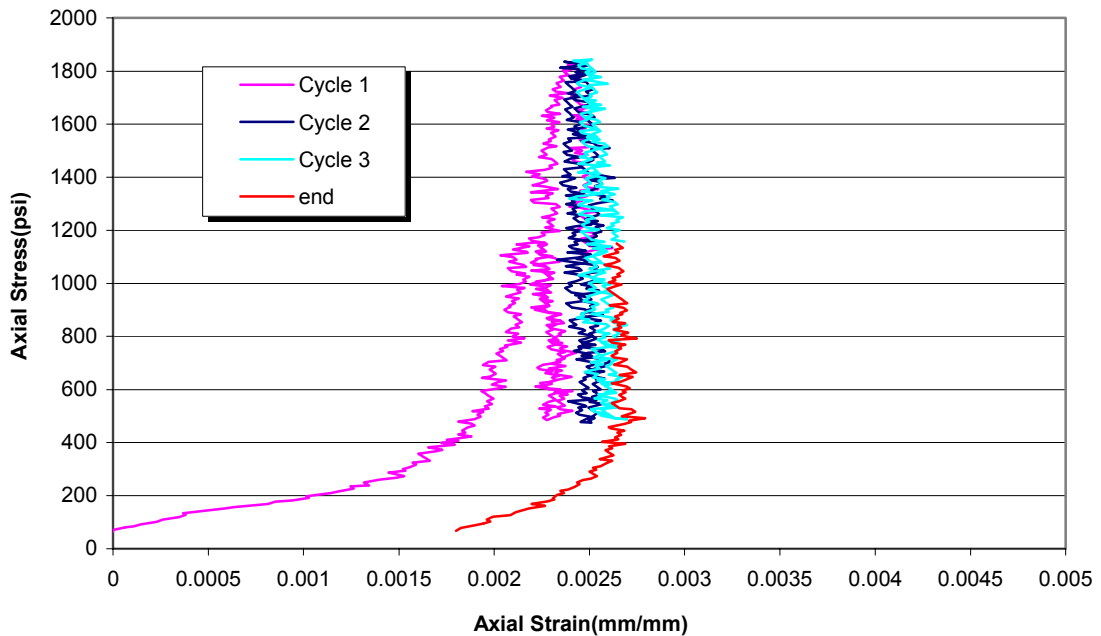




Figure B32—Anelastic strain, cycled to 50% of failure load, for Type 1 slurry at a load rate of 250 psi/min and confining pressure of 500 psi.

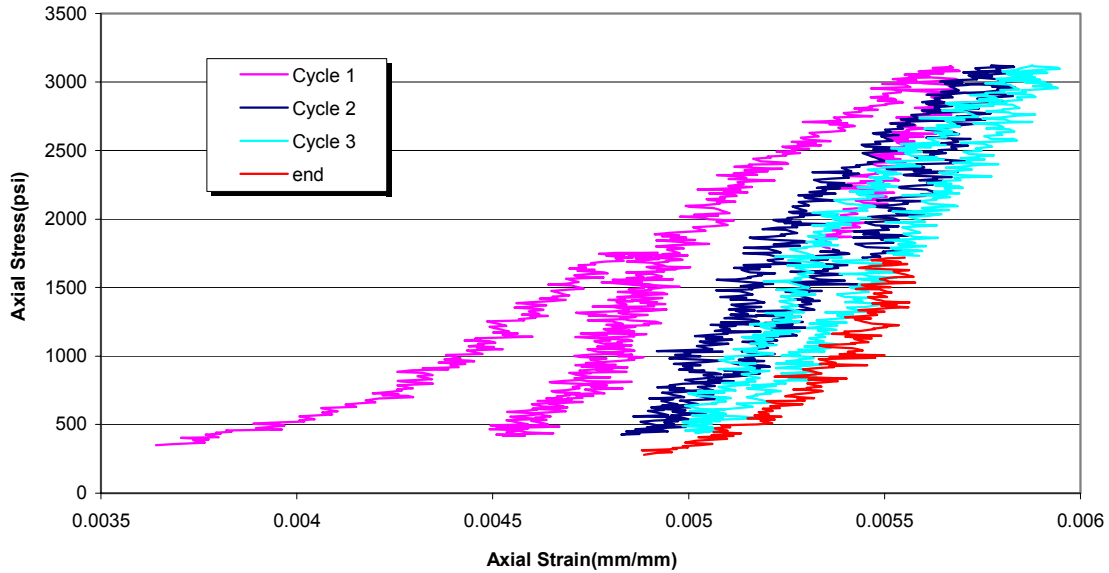


Figure B33—Anelastic strain, cycled to 50% of failure load, for latex slurry at a load rate of 250 psi/min and confining pressure of 500 psi.

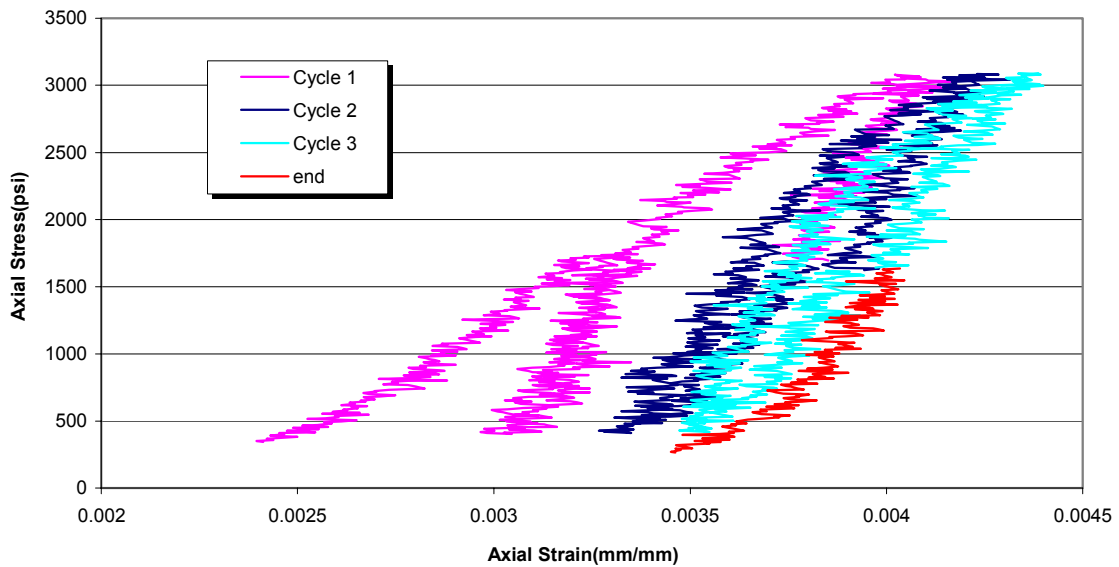




Table B1—Chronicle of 8-ft Permeability Model Testing (cc/min)

Days Tested											
Slurry	1	7	14	23	37	44	51	60	63	65	66
Type 1	0	0	0	0	0	0	0	0	0	0	0
	0	0	0	0	0	0	0.107	0.12	0.116	0.05	0.05
SMS	33	71	72	70	71	71	*	*	*	*	*
	26	57	60	42	30	30	*	*	*	*	*
Bead	0	0	0	0	0	0	0	0	0	0	0
	0	0	0	0	0	0	0	0	0	0	0
Latex	0	0	0	0	0	0	0	0	0	0	0
	0	0	0	0	0	0	0	0	0	0	0
Days Tested											
Slurry #	67	71	73	78	79	80	84	85	86	87	88
Type 1	0	0	0	0	0	0	0	0	0	0	0
	0.05	0	0.05	0.03	0.03	0.02	0	0	0	0	0
SMS	*	*	*	*	*	*	*	*	*	*	*
	*	*	*	*	*	*	*	*	*	*	*
Bead	0	0	0	0.03	0.03	0.03	0.02	0.02	0.02	0.02	0.02
	0	0	0	0	0	0	0.02	0.02	0.02	0.02	0.02
Latex	0	0	0	0	0	0	0.02	0.02	0.02	0.02	0.02
	0	0	0	0	0	0	0	0	0	0	0
Days Tested											
Slurry #	99	100	101	105	106	107	108	113			
Type 1	0	0	0	0	0	0.09	0.08	0.11			
	0	0	0	0.23	0.217	1.3	1.24	1.71			
SMS	*	*	*	*	*	*	*	*			
	*	*	*	*	*	*	*	*			
Bead	0	0	0	0	0	0	0	0			
	0.02	0.02	0.02	0	0	0.01	0	0			
Latex	0.6	0.8	0.8	0.74	0.87	2.75	*	*			
	3.1	3.51	3.51	3.51	*	*	*	*			
Day 1 Thru 44 - 100 PSI		Day 51 - 200 PSI			Day 60 Thru 73 - 300 PSI			Day 78 Thru 88 - 400 PSI			
Day 88 Thru 113 - 500 PSI											

¹ API Recommended Practice 10B: “Recommended Practice for Testing Well Cements,” 22nd Edition, American Petroleum Institute, Washington, D.C., December 1997.

² ASTM C469, Standard Test Method for Static Modulus of Elasticity (Young’s Modulus) and Poisson’s Ratio of Concrete in Compression.

³ “Standard Test Method for Splitting Tensile Strength of Cylindrical Concrete Specimens,” ASTM C496-96, West Conshohocken, PA, 1996.



CSI Technologies

Appendix VI

Report 6

MMS Project
Long-Term Integrity of Deepwater Cement
Systems Under Stress/Compaction Conditions

Report 6

Issued June 17, 2004

Fred Sabins
f.sabins@cementingsolutions.com

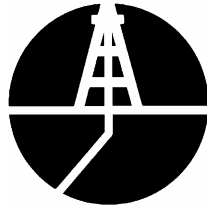




Table of Contents

Objectives	1
Observations and Recommendations for Future Work.....	1
Testing Program and Procedures	1
<i>Cement Design Performance.....</i>	<i>3</i>
<i>Mechanical Properties.....</i>	<i>3</i>
<i>Mechanical Integrity.....</i>	<i>3</i>
Test Results—Mechanical Properties	4
<i>Tensile Strength</i>	<i>4</i>
<i>Young’s Modulus with Various Confining Forces.....</i>	<i>5</i>
<i>Poisson’s Ratio</i>	<i>5</i>
<i>Anelastic Strain.....</i>	<i>6</i>
Test Results—Mechanical Integrity	13
<i>Shear Bond</i>	<i>13</i>
<i>Annular Seal.....</i>	<i>14</i>
<i>Cement Column Seal.....</i>	<i>24</i>
Appendix A—Test Procedures	30
<i>Sample Preparation</i>	<i>30</i>
<i>Sample Curing.....</i>	<i>30</i>
<i>Thickening Time Test</i>	<i>30</i>
<i>Free-Fluid Test</i>	<i>30</i>
<i>Compressive Strength</i>	<i>31</i>
<i>Young’s Modulus and Poisson’s Ratio Testing</i>	<i>31</i>
<i>Hydrostatic Cycling and Anelastic Strain.....</i>	<i>31</i>
<i>Tensile Strength and Tensile Young’s Modulus.....</i>	<i>32</i>
<i>Annular Seal Testing Procedure.....</i>	<i>33</i>
Soft-Formation Simulation	34
Hard-Formation Simulation	34
Intermediate Formation Simulation.....	34



CSI Technologies

<i>Shear Bond Strength Testing</i>	35
<i>Cement Column Seal Tests</i>	37
Appendix B—Test Data	38



Objectives

The overall objective of this project is to determine the properties that affect cement's capability to produce a fluid-tight seal in an annulus. The project primarily focuses on deepwater applications, but general applications will also be examined. The research conducted thus far is focused on the measurement and correlation of cement's mechanical properties to the cement's performance. Also, research was conducted to determine which laboratory methods should be used to establish the cement's key properties.

Results obtained during this reporting period focused on continued measurement of and correlation of cement mechanical properties and mechanical bond integrity of a cemented annulus. Anelastic strain/failure testing results are presented in the Results section below. Mechanical integrity testing included shear bond and annular seal testing on specimens cured under various cyclic curing schedules. The results of these tests are tabulated in the Results section below. Additionally, all test results developed during this project, including graphical data, are presented in Appendix B.

Observations and Recommendations for Future Work

Results of testing during this reporting period indicate:

- Modified Annular Seal and Shear Bond testing performed with the intermediate strength formation was successful and was duplicated for hard and soft formations.
- Analysis of Annular Seal data via Total Energy calculations produced an acceptable method of quantifying the test results.
- Thermal cycling appears to negatively affect foam cement's sealing ability to a greater degree than pressure cycling.
- TXI LightWeight cement performed well in the 8-foot model testing.

Future work includes:

- complete analysis of column sealing tests
- completion of a decision support system (DSS) for optimizing cement composition (the final deliverable of this project)

The DSS will be similar in operation to one commissioned by 3M to select optimum lightweight cement for various conditions. This DSS will accept well conditions as inputs and will contain performance properties for the various cements tested in the project. A semi-quantitative analysis of the inputs vs. cement performance will allow the user to determine the optimum cement composition for maintaining annular seal under the well conditions.

Testing Program and Procedures

The following cement slurries are examined: Type 1, foamed cement, bead cement, Class



H cement, and latex cement. Latex cement designation refers to cements designed with the gas migration control additive D500 which is a microgel type additive. The effects of adding fibers and/or expansion additives to a slurry are also examined. The cements are tested primarily for deepwater applications, but their performance under all application conditions is considered.

Tasks in the project are listed below:

- Task 1 – Problem Analysis
- Task 2 – Property Determination
- Task 3 – Mathematical Analysis
- Task 4 – Testing Baseline
- Task 5 – Refine Procedures
- Task 6 – Composition Matrix
- Task 7 – Conduct Tests
- Task 8 – Analyze Results
- Task 9 – Decision Matrix

Compositions tested in this project are outlined in **Table 1** below. The range of compositions chosen covers the compositions traditionally used in deep water applications as well as newly utilized compositions and compositions designed to produce improved performance.

Table 1—Cement Compositions for Testing

Description	Cement	Additives	Water Requirement (gal/sk)	Density (lb/gal)	Yield (ft ³ /sk)
Neat Type I slurry	Type 1	—	5.23	15.6	1.18
Type I slurry with fibers	Type 1	3.5% carbon fibers-milled	5.2	15.6	1.16
Latex slurry	Type 1	1.0 gal/sk LT-D500	4.2	15.63	1.17
Latex slurry with fibers	Type 1	1.0 gal/sk LT-D500 3.5% carbon fibers-milled 0.50% Melkrete	4.09	15.63	1.20
Foam slurry (12-lb/gal)	Type 1	0.03 gal/sk Witcolate 0.01 gal/sk Aromox C-12 1% CaCl	5.2	12.0	1.19
Bead slurry	Type 1	13.19% K-46 beads	6.69	12.0	1.81
Neat Class H slurry	Class H	—	4.3	16.4	1.08
Class H slurry with fibers	Class H	—	4.3	16.4	1.08
Sodium metasilicate slurry	Type 1	—	14.22	12.0	2.40



Four major categories of tests are used to analyze the cements: cement design performance testing, mechanical properties testing, mechanical integrity testing, and numerical simulation. Results of mechanical properties testing and mechanical integrity testing are provided in the “Test Results” section of this report, beginning on Page 4.

Cement Design Performance

Standard cement design performance testing, including rheology, thickening time, free fluid, set time, compressive strength, etc. are performed according to procedures outlined in API RP 10B.

Mechanical Properties

Mechanical properties tested include: tensile strength/tensile Young’s modulus (T), compressive Young’s modulus, Poisson’s ratio, and anelastic strain-fatigue testing.

The tensile strengths are determined with the Brazilian Test Method. From this test, the tensile Young’s Modulus is computed, as well as the maximum yield of the sample. By definition, Young’s Modulus is stress applied to the test specimen divided by elastic strain resulting from the stress. Strain is measured in the same direction as applied stress. Tensile Young’s modulus as calculated from these Brazilian Tensile tests is actually a hybrid value since strain is measured in the same direction as applied compressive stress. However, this is orthogonal to resulting tensile stress direction. This accounts for the relatively constantly lower Young’s Modulus determined by this method. The two values are actually related by Poisson’s Ratio.

The compressive Young’s Modulus will be determined through compression tests with confining loads with a baseline of a 14-day cure. Confining loads applied to each composition are varied from 0 psi up to the magnitude of the composition’s compressive failure to determine the affects of confinement on rock properties. Poisson’s ratio will also be determined from these tests. Poisson’s Ratio values will vary with respect to the stress rate, slurry type, air entrainment, and perhaps other variables.

Anelastic strain and fatigue testing is a modification of hydrostatic testing. The modified procedure involves cycling samples repeatedly to 25% or 50% of each composition’s compressive strength under 500-psi confining stress. Measurement of anelastic strain with cycling provides a comparable measure of each composition’s performance.

Mechanical Integrity

The mechanical integrity issues of the cement slurries include stresses in the cement, and the flow of fluids around the cement and through the matrix of the cement. To predict the flow of fluid around the cement, the cement slurries are tested for bonding capacity, presence of microannuli, and deformation. The flow of fluids through the matrix of the cement is examined through tests for detecting cracks and permeability changes. The stress undertaken by the cement slurries is determined as a function of pressure, temperature, and confining formation strength.



Shear bond and annular seal measurements are taken under cyclical conditions for soft, intermediate strength, and hard formations. Intermediate-strength formation is simulated with Schedule 40 PVC pipe as the outside mold for the cement sheath.

Stresses are imposed on all test specimens by increasing the maximum pressure to which the inner pipe is stressed or by heating the inner pipe. Seal integrity is monitored while stressing the specimens. Additionally, shear bond tests are run only after a composition has been tested for annular seal. The shear bond test samples are subjected to the same pressure and temperature cycling that produced annular seal failure before shear bond is evaluated. This procedure provides a comparison between shear bond and annular seal behavior.

Additional analysis was performed on the complete suite of annular seal data. The analytical method involved measuring sample failure as a function of total work done on the sample by heating or pressure cycling. This analysis revealed a strong relationship between quantity of work applied to a test fixture and failure of the seal.

Cement column seal tests illustrate the sealing effectiveness of several additional cements. These tests are designed to test a cement's capacity to isolate gas pressure across an enclosed column. Eight-foot lengths of 2-in. pipe are filled with cement slurry, pressurized to 1000 psi, and then cured for 8 days. After the test samples have cured, low-pressure gas (100 to 200 psi) is periodically applied to one end of each test pipe and the gas flow rate through the cement column is measured. As time increases with no flow, increased pressure is applied to the pipe to eventually induce failure and flow.

Test Results—Mechanical Properties

This section contains results from testing conducted throughout this project period, as well as additional mechanical property test results selected from previous test periods. Graphical data for all mechanical property tests are presented in Appendix B of this report.

Tensile Strength

Table 2 shows the effects of carbon fibers on tensile strength. The two-fold to three-fold increase in tensile strength is significant, indicating the potential for fibers to enhance the durability of cement.



Table 2—Tensile Strength and Tensile Young's Modulus

Slurry	Tensile Strength (psi)	Young's Modulus
Foam slurry (12-lb/gal)	253	3.23 E4
Neat Type I slurry	394/213 ^a	19.15/8.16 E4 ^a
Type I slurry with fibers	1071	9.6 E4
Latex slurry	539	5.32 E4
Latex slurry with fibers	902	8.5 E4

^aData taken from two different specimens.

Young's Modulus with Various Confining Forces

The effects of confining stress on compressive strength and Young's modulus are presented in Table 3. A significant increase in compressive strength is observed among lower-strength compositions such as foam cement and latex cement, as confining stress is increased.

Table 3—Young's Modulus at Various Confining Stresses

Slurry Composition	Confining Pressure (psi)	Young's Modulus (psi)
Type I slurry	0	16.7 E 5
	1500	11.1 E 5
	5000	9.1 E 5
Foam slurry (12 lb/gal)	0	5.8 E 5
	500	6.8 E 5
	1000	6.1 E 5
Bead slurry (12 lb/gal)	0	9.5 E 5
	500	8.1 E 5
	1000	1 E 6
Latex slurry	0	5.6 E 5
	250	8.9 E 5
	500	9.4 E 5

Poisson's Ratio

Initial results of Poisson's ratio testing on these lightweight cement compositions were unexpectedly low. Continued Poisson's ratio testing confirmed the accuracy of these early results. The low Poisson's ratio values for these compositions are theorized to be related to the porosity of the specimens. Several published technical reports have documented this tendency for Poisson's ratio to be effectively lowered as porosity increases.

Another potential variable in Poisson's ratio testing is load rate. An investigation into the



effect of load rate on Poisson’s ratio indicated that load rate does affect Poisson’s ratio measurement (Table 4). Testing with Type I Cement at 16.4 lb/gal indicated a decreasing Poisson’s ratio with increasing stress rate. A stress rate of 250 psi/min was settled on for remainder of this testing.

Table 4—Effect of Load Rate on Poisson's Ratio

Load Rate	Poisson's Ratio
100 psi/min	0.1
250 psi/min	0.08
500 psi/min	-0.01

Table 5 presents data generated with a load rate of 250 psi/min. While these values are lower than what has traditionally been considered acceptable, the data are generally positive. CT scans performed on Poisson’s ratio test specimens indicated a link between large voids or pore spaces and variable Poisson’s ratio. This procedure will be included in future testing and samples with large voids will be discarded.

**Table 5—Poisson's Ratio
(50-psi confining pressure, 250 psi/min load rate)**

Slurry	Failure (psi)	Poisson's Ratio
Foam slurry (12-lb/gal)	3100	0.00
Bead slurry	4100	-0.01
Neat Class H slurry	6450	0.0012
SMS slurry	920	0.005
Type I slurry	6500	0.1

Anelastic Strain

Anelastic strain testing is a variation of hydrostatic testing and is designed to allow a more accurate evaluation of permanent strain resulting from stressing different test compositions. This procedure standardizes confining stress at 500 psi and calls for samples to be cycled to 25% and 50% of each composition’s compressive strength or failure load under that confining stress. Measurement of anelastic strain with cycling provides a more comparable value of each composition’s performance. See Figures 5 and 6.

Results of anelastic strain testing are presented in Table 6. Strain data are reported as final strain minus initial strain measurements, with final being at the end of three cycle s. In order to analyze data for different compositions uniformly, a stress point was chosen on the stress-strain plot at a point that the strain appeared to be linear. Strains at this stress magnitude at the beginning and end of cycling were measured and used to calculate plastic deformation. This comparison point is listed also. Data were then normalized with respect to sample length so results appear in units of mm/mm. This step eliminates



apparent variations in deformation data due to variations in sample size.

Table 6—Results of Anelastic Strain Testing

Composition	Failure (psi)	Comparison Stress (psi)	Strain (mm/mm)	
			25%	50%
Type I slurry	6000	600	0.0006	0.0007
Foam slurry	2000	400	0.0009	0.0007
Bead slurry	3300	400	0.0007	0.0005
Latex slurry	6000	600	0.0007	0.0009

Data generation also includes a round of samples tested to a common stress maximum as seen in Figures 7 through 10 to provide two alternate methods of comparison.

Figure 1— Anelastic strain failure load for neat Type 1 slurry at a load rate of 250 psi/min and confining pressure of 500 psi.

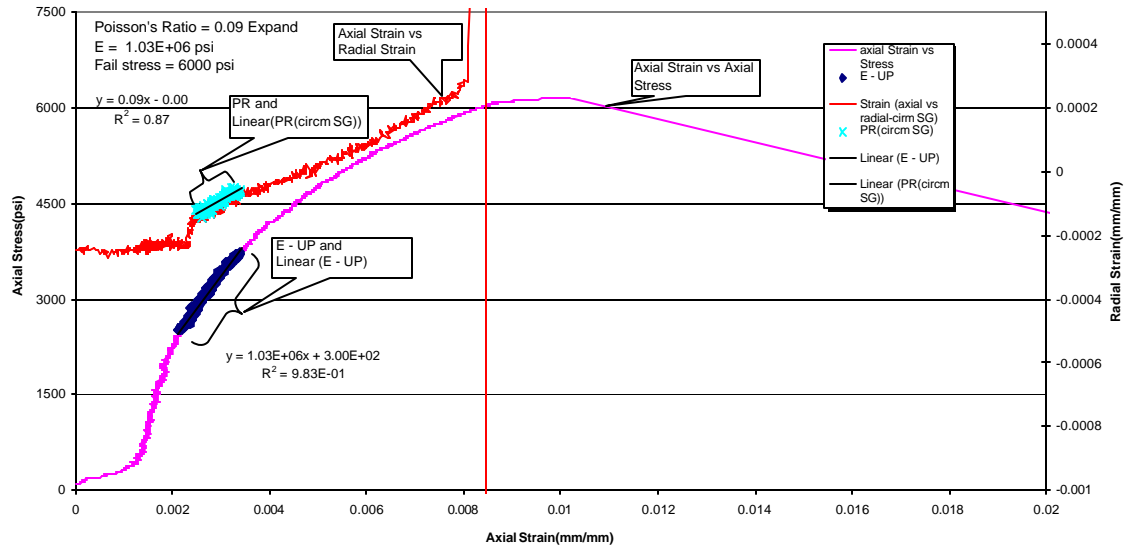




Figure 2— Anelastic strain failure load for foam slurry at a load rate of 250 psi/min and confining pressure of 500 psi.

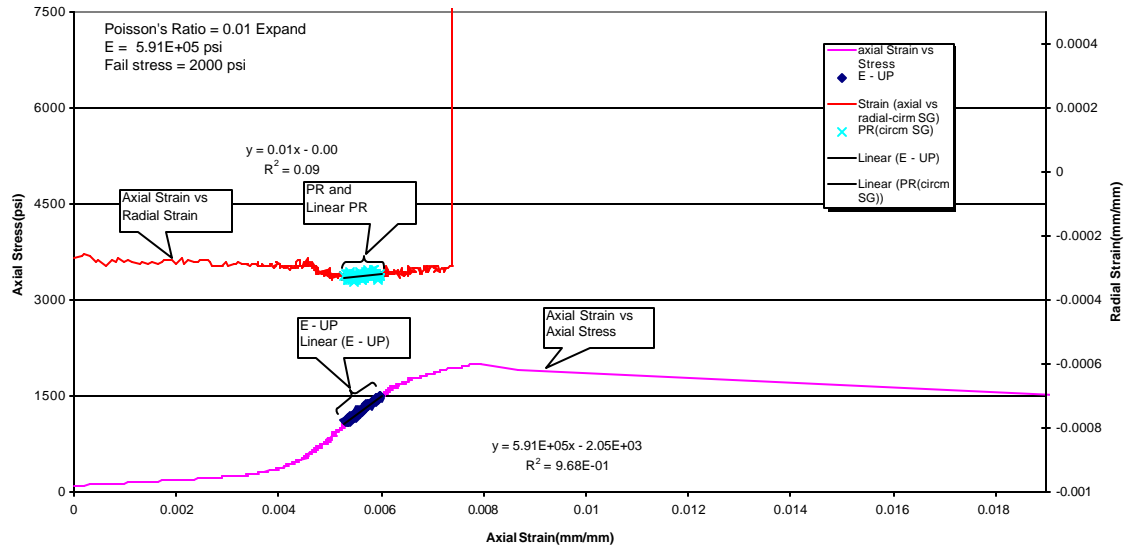


Figure 3— Anelastic strain failure load for bead slurry at a load rate of 250 psi/min and confining pressure of 500 psi.

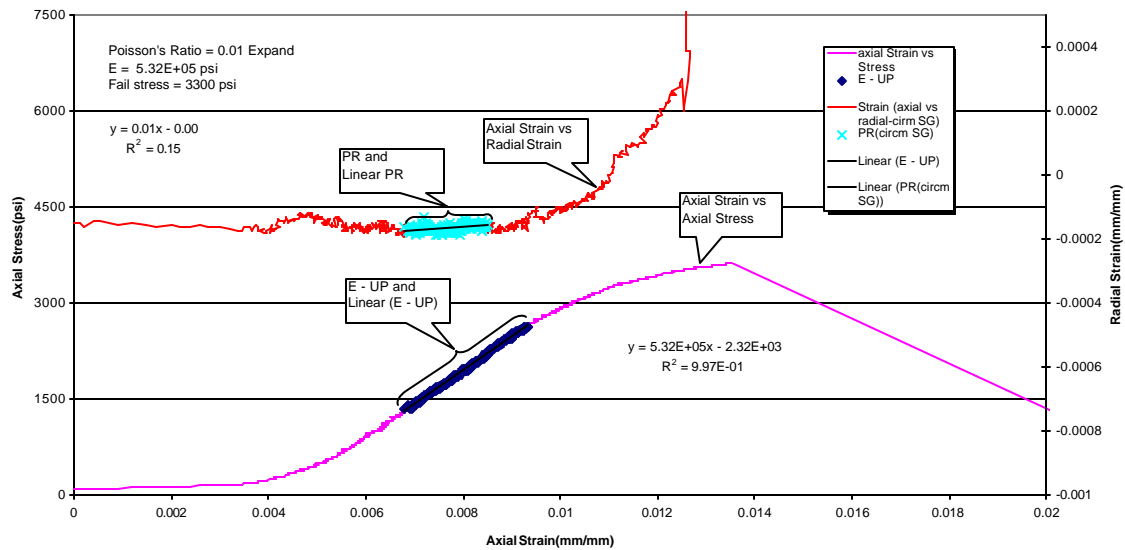
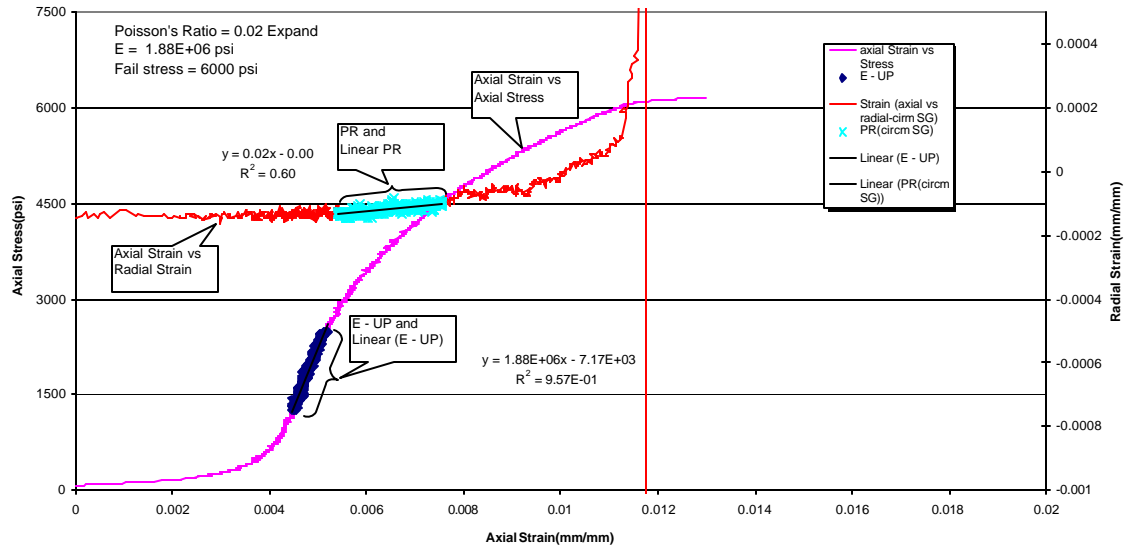




Figure 4—Anelastic strain failure load for latex slurry at a load rate of 250 psi/min and confining pressure of 500 psi.



Figures 5 and 6 present strain vs. cycle data for the four compositions at 25% and 50% of each composition's failure stress. Dashed lines represent the slope of each line. Note that all trends are increasing indicating that each specimen would undergo additional anelastic strain with increased cycles. Comparison of the data sets indicates larger strains for low density compositions than for normal density cements.



Figure 5—Anelastic strain comparison of cycles to 25% of failure load

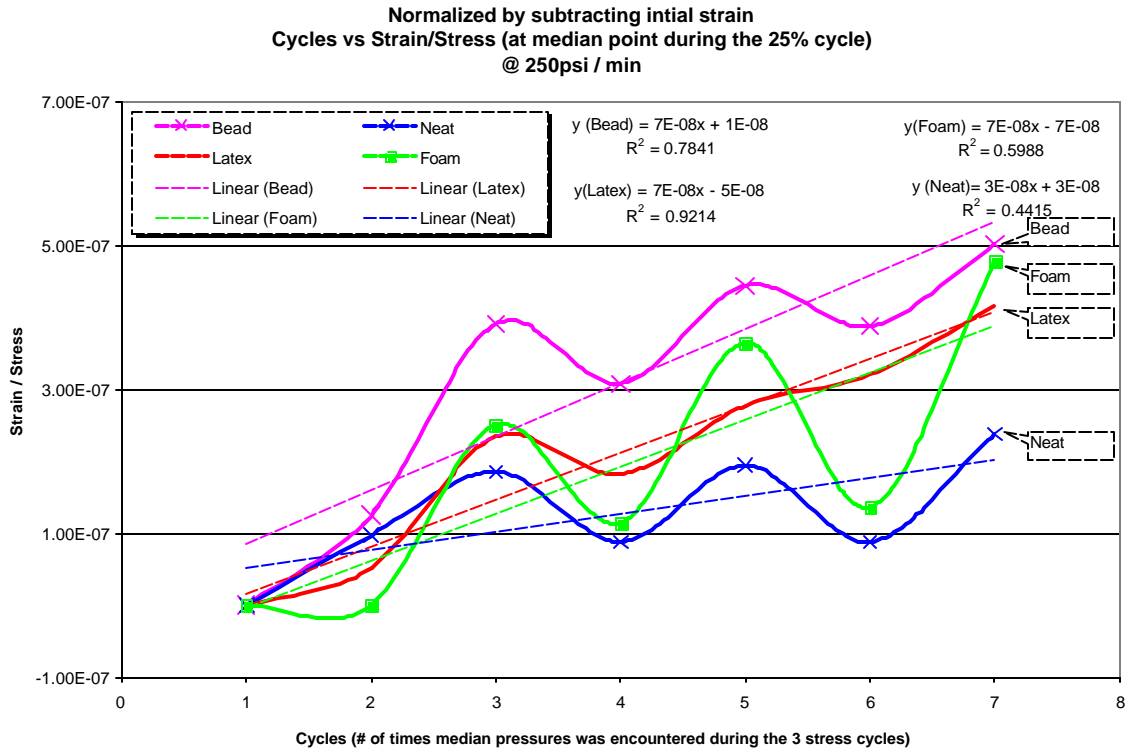
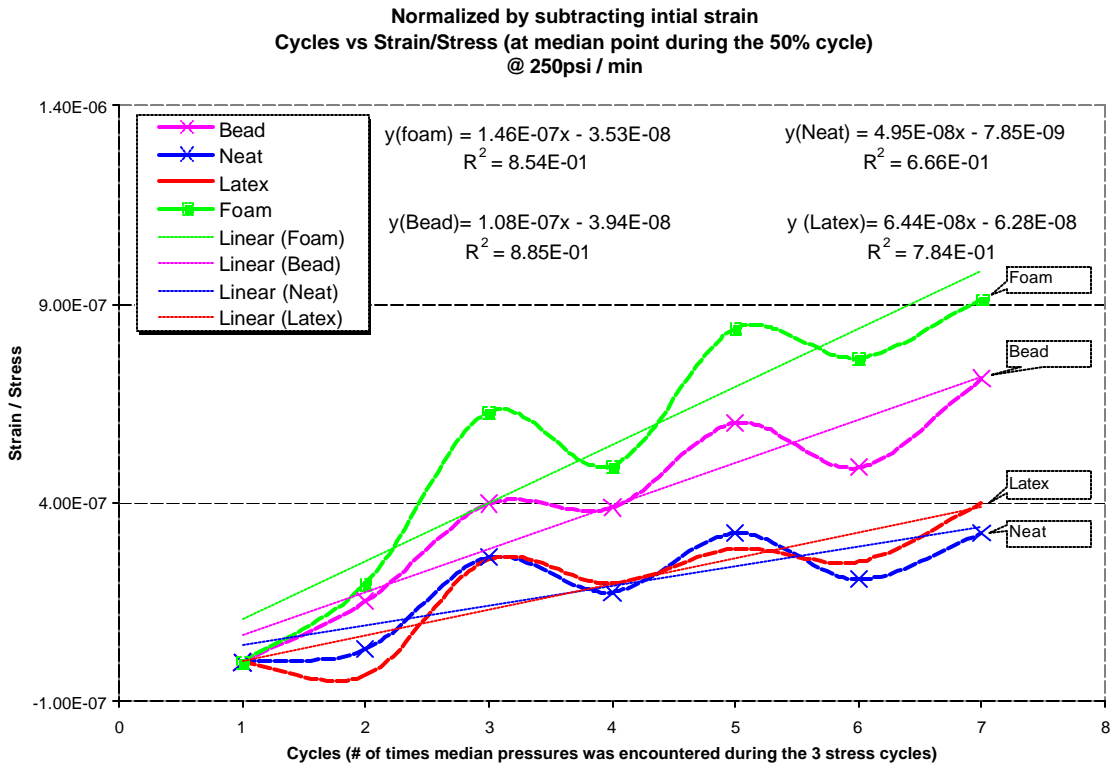


Figure 6—Anelastic strain comparison of cycles to 50% of failure load





Results of strain vs. time under stress testing are presented in Figures 7 and 8. These results indicate that both foam and bead cement exhibit increasing strain with time under stress. Foam cement's level of strain with increasing stress was slightly more than bead cement.

Figure 7—Anelastic strain vs. Time comparison of Foam and Bead

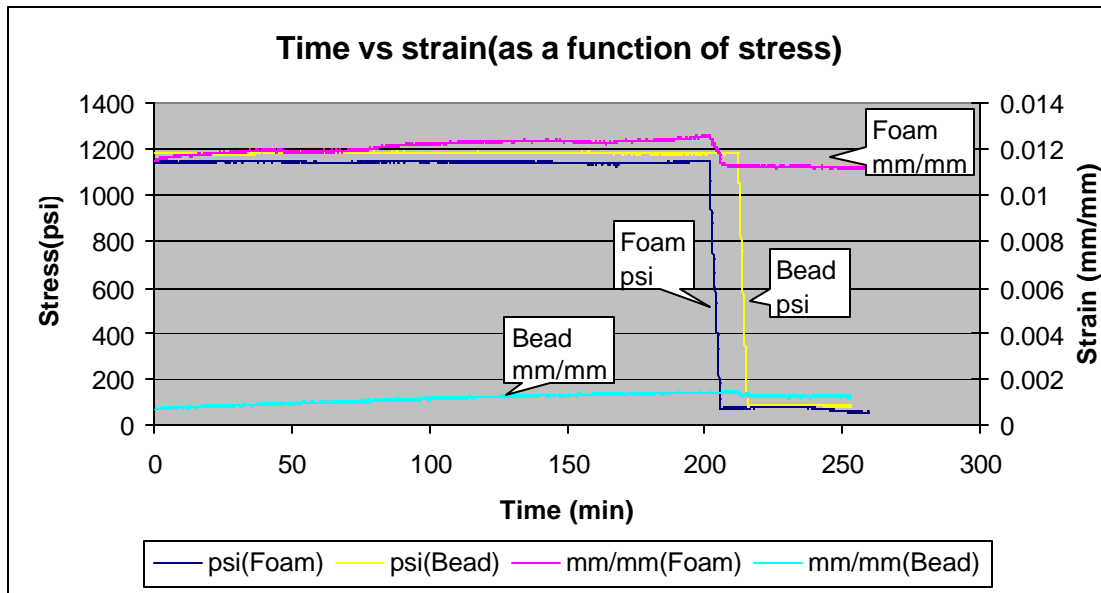
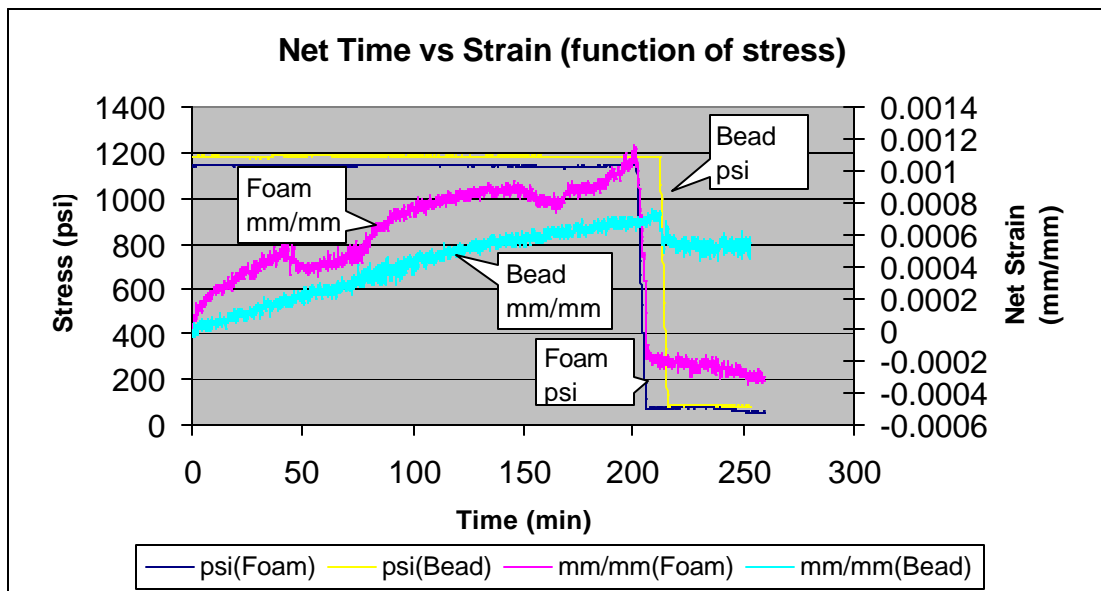


Figure 8—Anelastic strain comparison of Foam and Bead systems. Strain values from Figure 7 are normalized with respect to each sample's initial strain for comparison.





Figures 9 and 10 present results of strain measurement vs cyclic stress application. Data from Figure 9 are raw data while those in Figure 10 are normalized with respect to initial strain for each sample. These results indicate significant increase in cycling effect for foam compared to the other three compositions.

Figure 9—Cyclic Strain comparison of Bead, Foam, Neat and Latex systems

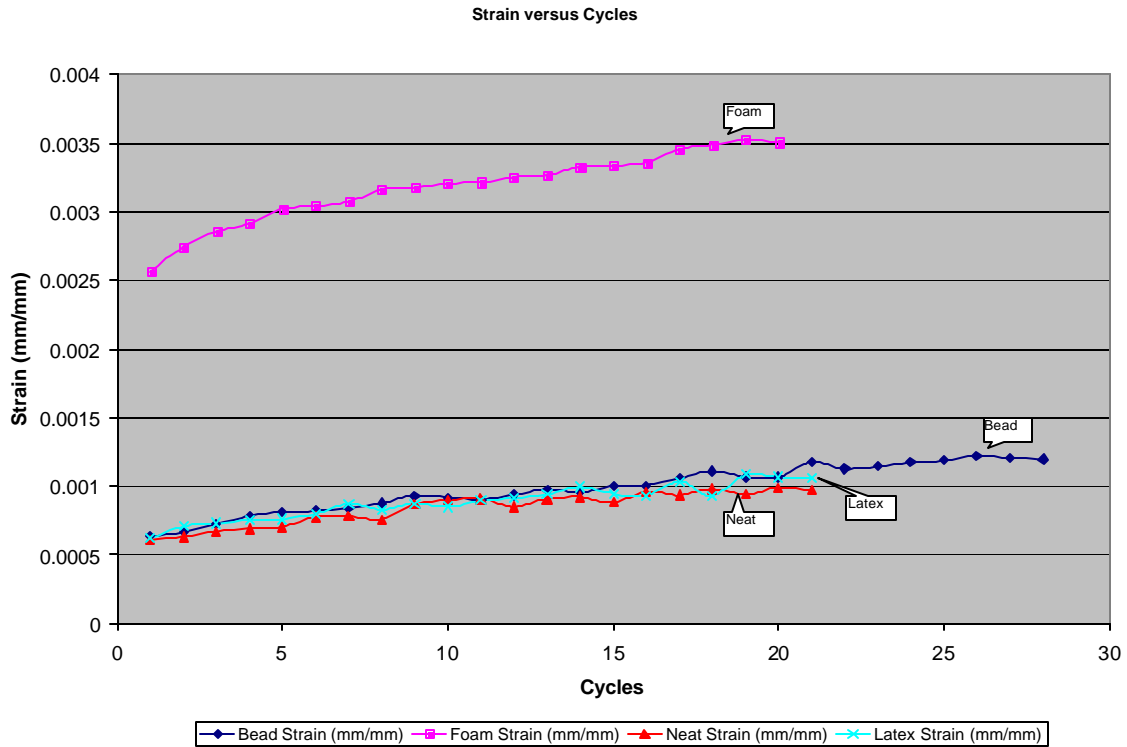
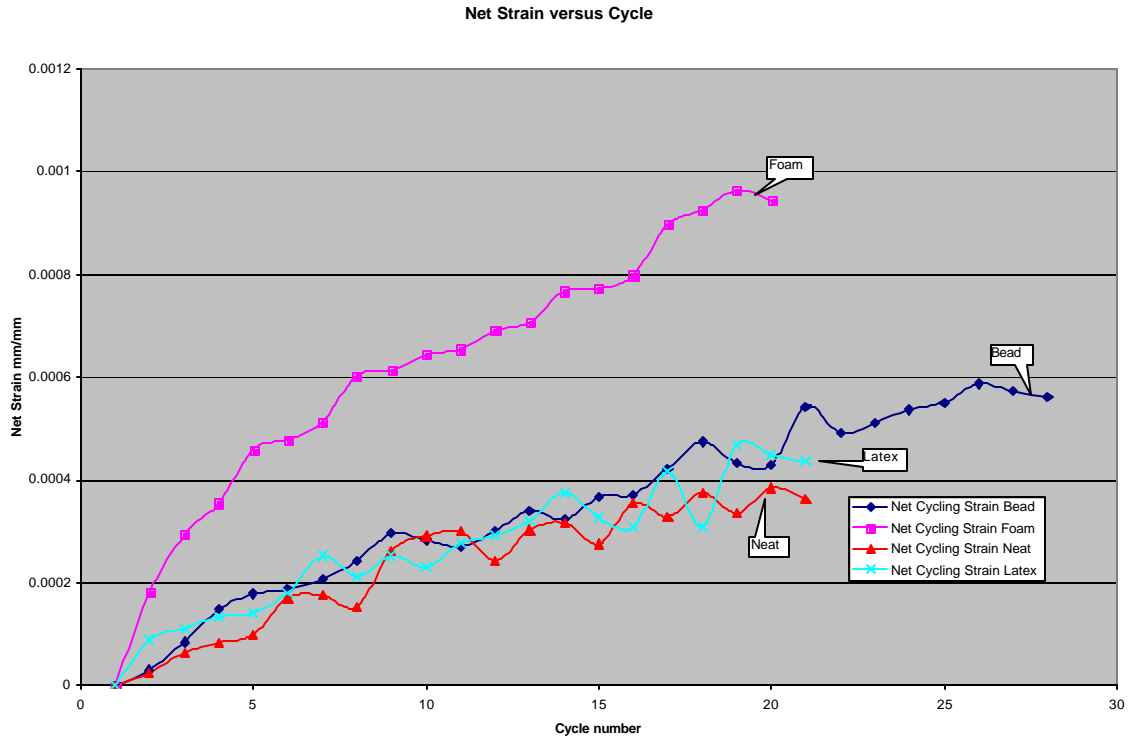




Figure 10—Net Cyclic Strain comparison of Bead, Foam, Neat and Latex systems



Test Results—Mechanical Integrity

This section contains results from testing conducted throughout this project period, as well as additional mechanical integrity test results selected from previous test periods.

Shear Bond

Results of shear bond testing (Table 7) indicate that bond is degraded extensively both by pressure and temperature cycling. This degradation seemed to be increased by the presence of simulated soft formation. A modified shear bond method was used with all simulated formations to help ensure that the results are more comparable to annular seal tests (Tables 9, 10, 11 and 13). The test method is explained in Appendix A page 33. Results with hard, intermediate, and soft formations were repeated with the new procedure and results reported in Table 7.



Table 7—Shear Bond Strengths (psi)

System	Simulated Formation	Type I Slurry	Foam Slurry	Bead Slurry	Latex Slurry
Baseline	Hard	1228	911	1061	876
	Intermediate	520	298	294	448
	Soft	198	233	143	223
Temperature-Cycled	Hard	293	228	260	244
	Intermediate	209	217	246	194
	Soft	105	44	71	89
Pressure-Cycled	Hard	463	321	386	283
	Intermediate	234	193	192	278
	Soft	141	110	105	84

Annular Seal

Results presented in Table 8 indicate that all cyclic testing specimens failed in the soft formation simulation while all specimens in the hard-formation tests maintained seal. These results indicate the need for a simulated formation with intermediate strength to further differentiate seal effectiveness. Additional stresses for the hard-formation simulation must be imposed through application of heat or pressure.

Table 8—Annular Seal Tests

Condition Tested	Formation Simulated	Type I Slurry	Foamed Slurry	Bead Slurry
Initial Flow	Hard	0 Flow	0 Flow	0 Flow
	Soft	0 Flow	0.5 (md)	0 Flow
Temperature-Cycled	Hard	0 Flow	0 Flow	0 Flow
	Soft	0 Flow	123 md	43 md*
Pressure-Cycled	Hard	0 Flow	0 Flow	0 Flow
	Soft	27 md	0.19 md*	3 md

* Visual inspection revealed samples were cracked.

Modified annular seal testing procedures were employed as outlined in Appendix A page 31 and all three formations including hard, intermediate, and soft were retested using this new procedure. Results for both temperature and pressure cycling are found in Tables 9 through 13. The test methods are explained in Appendix A page 32.

Failure of annular seals was achieved in all formations by increasing cycling until achieving flow. The general trend as can be seen in Tables 9 through 13 was that hard formations needed the greatest amount of cycling to achieve failure. Intermediate formations required less cycling to achieve failure and Soft formations required the least amount of cycling to achieve failure.



Annular seal testing with intermediate-strength formation and increased cyclic loading indicated all materials failed to maintain a seal. Interestingly, foam cement faired best in pressure cycling and worst in temperature cycling.

Table 14 represents a quantifiable measurement of the energy needed whether pressure or temperature induced to produce failure of annular seal. Results of these energy measurements are graphed and compared in Figures 15 and 16.

Table 9—Annular Seal Pressure-Cycled Slurry Comparison

Slurry	Form.	Cycle	Pressure (psi)											
			1000-4000	5000	6000	7000	8000	9000	10,000	10,000	10,000	10,000	10,000	
Type 1	Hard	1	0	0	0	0	0	0	0	0	0	0	0	0
		2	0	0	0	0	0	0	0	0	0	0	0	0
		3	0	0	0	0	0	0	0	0	0	0	0	0
		4	0	0	0	0	0	0	0	0	0	0.14mD	0.42mD	2.10mD
	Inter.	1	0	0	0	0	0.01 mD	1.1 mD	1.31 mD	2.04 mD	-	-	-	
Soft	1	0	0	0.39 mD	0.39 mD	1.38 mD	+6.69 mD	-	-	-	-	-		
Foam	Hard	1	0	0	0	0	0	0	0	0	0	0	0	
		2	0	0	0	0	0	0	0	0	0.14mD	0.28mD	0.42mD	1.12mD
	Inter.	1	0	0	0	0	0	0	0	0	0	0	0.79mD	
	Soft	1	0	0	0.96 mD	3.2 mD	5.88 mD	+6.4 mD	-	-	-	-	-	
Bead	Hard	1	0	0	0	0	0	0	0	0	0	0	0	
		2	0	0	0	0	0	0	0	0	0	0	0	
		3	0	0	0	0	0	0	0	0	0	0.28mD	1.68mD	2.24mD
	Inter.	1	0	0	0	0	0	0	0.66mD	0.18mD	0.80mD	0.56mD	0.80mD	
	Soft	1	0	0	0	0.13 mD	0.39 mD	5.76 mD	+6.4 mD	-	-	-	-	
Latex	Hard	1	0	0	0	0	0	0	0	0	0	0	0	
		2	0	0	0	0	0	0	0	0	0	0	0	
		3	0	0	0	0	0	0	0	0.03mD	0.14mD	0.28mD	1.4mD	2.1mD
	Inter.	1	0	0	0	0	0.80 mD	2.10 mD	-	-	-	-	-	
	Soft	1	0	1.25 mD	+6.4 mD	-	-	-	-	-	-	-	-	



Table 10—Annular Seal Pressure-Cycled Formation Comparison

Slurry	Form.	Cycle	Pressure (psi)											
			1000-4000	5000	6000	7000	8000	9000	10,000	10,000	10,000	10,000	10,000	
Hard	Type 1	1	0	0	0	0	0	0	0	0	0	0	0	0
		2	0	0	0	0	0	0	0	0	0	0	0	0
		3	0	0	0	0	0	0	0	0	0	0	0	0
		4	0	0	0	0	0	0	0	0	0	0.14mD	0.42mD	2.10mD
	Foam	1	0	0	0	0	0	0	0	0	0	0	0	0
		2	0	0	0	0	0	0	0	0	0.14mD	0.28mD	0.42mD	1.12mD
	Bead	1	0	0	0	0	0	0	0	0	0	0	0	0
		2	0	0	0	0	0	0	0	0	0	0	0	0
		3	0	0	0	0	0	0	0	0	0	0.28mD	1.68mD	2.24mD
	Latex	1	0	0	0	0	0	0	0	0	0	0	0	0
		2	0	0	0	0	0	0	0	0	0	0	0	0
		3	0	0	0	0	0	0	0	0.03mD	0.14mD	0.28mD	1.4mD	2.1mD
Interm	Type 1	1	0	0	0	0	0.01 mD	1.1 mD	1.31 mD	2.04 mD	-	-	-	
	Foam	1	0	0	0	0	0	0	0	0	0	0	0.79mD	
	Bead	1	0	0	0	0	0	0	0.66mD	0.18mD	0.80mD	0.56mD	0.80mD	
	Latex	1	0	0	0	0	0.80 mD	2.10 mD	-	-	-	-	-	
Soft	Type 1	1	0	0	0.39 mD	0.39 mD	1.38 mD	+6.69 mD	-	-	-	-	-	
	Foam	1	0	0	0.96 mD	3.2 mD	5.88 mD	+6.4 mD	-	-	-	-	-	
	Bead	1	0	0	0	0.13 mD	0.39 mD	5.76 mD	+6.4 mD	-	-	-	-	
	Latex	1	0	1.25 mD	+6.4 mD	-	-	-	-	-	-	-	-	



Table 11—Annular Seal Temperature-Cycled Slurry Comparison

Slurry	Form.	Cycles	Temperature Cycles (degrees F)									
			74	94	108	121	135	149	163	176	190	
Type 1	Hard	1	0	0	0	0	0	0	0	0	0	0
		2	0	0	0	0	0	0	0	0	0	0
		3	0	0	0	0	0	0	0	0	0	0
		4	0	0	0	0	0	0	0	0	0	0
		5	0	0	0	0	0	0	0.53mD	1.42mD	1.78mD	1.78mD
	Interm.	1	0	0	0	0	0	0	0	0	0	0
		2	0	0	0	0	0	2.89mD	3.34mD	5.78mD	-	-
	Soft	1	0	0	0	0	0	0	0	0	0	0
2		0	0	1.23mD	1.63mD	1.63mD	7.98mD	+8.16mD	-	-	-	
Foam	Hard	1	0	0	0	0	0	0	0	0	0	
		2	0	0	0	0	0.71mD	1.07mD	2.67mD	3.56mD	4.45mD	
	Interm.	1	0	0	0	0.07mD	0.22mD	1.22mD	-	-	-	
		Soft	1	0	0.49mD	0.65mD	0.98mD	1.21mD	1.31mD	1.31mD	1.31mD	+8.16mD
Bead	Hard	1	0	0	0	0	0	0	0	0	0	
		2	0	0	0	0	0	0	0	0	0	
		3	0	0	1.78mD	3.56mD	5.34mD	8.90mD	-	-	-	
	Interm.	1	0	0	0	0	0	0	0	0	0	
		2	0	0	0	0	0	0	0	0	0	
		3	0	0	0	0	0	0	0	3.11mD	3.71mD	-
	Soft	1	0	0	0	0	0	0	0	0	0	0
2		0	0	0.41mD	2.45mD	+8.16mD	-	-	-	-	-	
Latex	Hard	1	0	0	0	0	0	0	0	0	0	
		2	0	0	0	0	0	0	0	0	0	
		3	0	0	0	0	0	0	0	0	0	
		4	0	0	0	0	0	0	0.89mD	2.31mD	2.67mD	3.56mD
	Interm.	1	0	0	0	0	0	0.01mD	0.93mD	1.33mD	3.34mD	-
		Soft	1	0	0	0	0.82mD	1.01mD	1.14mD	1.24mD	1.96mD	+8.16mD

Failure of the cement sheath in a wellbore environment is due to imposed stresses that are greater than the cement can withstand. Measurement of stresses becomes difficult, even in laboratory models because of the non-homogeneous composite nature of the cement itself. Specifically, the different types of cements contribute to the difficulty, because of the very different ways in which they respond to applied pressure and temperature loads. While pressure loads can be related to gross stress relatively simply, the effect of temperature is problematic due to the complex wellbore geometry and the many and variable system constraints. To address this difficulty and quantify performance of the various test compositions in the annular seal model, failure was related to the total energy input to the wellbore / cement / formation system. Energy input is in one of two forms, pressure or temperature. Ultimately, the stresses imposed are caused by the input of energy to the system. This simplification bypasses the problem of the non-uniform distribution of these stresses in the non-homogeneous material.

The correlation of energy input to ultimate cement failure was done in order to better understand the mechanisms associated with wellbore cement integrity. The results of this correlation are presented in Tables 12 through 14 and Figures 11 through 16. Further work is required to fully understand the mechanisms by which hydraulic or thermal



energy ultimately leads to cement failure. In the current small sample, the following observations are offered:

- With only two exceptions, the amount of energy (pressure or temperature) required to induce cement sheath failure increases with the competence of the formation. The stronger the formation, the more support it lends to the cement sheath so that it can withstand the imposed loads.
 - The two exceptions involve the temperature energy applied to Bead systems. In these cases, the energy to initiate failure is slightly higher in the intermediate formation than the hard, although statistically they may be equivalent. The explanation is that in the case of temperature, the superior insulating properties of the beads reduce the importance of formation competence, within limits. This represents an important finding supporting the use of beads in cases that may traditionally have indicated foam. The stronger encapsulation of the air pocket in bead vs foam means that the bead cements will withstand heat better than foam systems.
- Bead cements performed very well in all the testing, as evidenced in the cases of weaker formations. In the case of pressure energy, foam also performed better than Type 1 and Latex slurries with weaker formation support. This may be due to better anelastic behavior, in which the cement is more ductile than the higher-strength systems.
- In all cases, the amount of temperature energy required to initiate failure is much lower than the pressure energy to failure. The reason for this is believed to be the destructive effects of matrix water expansion with temperature.
- At this point, with limited data, the results cannot be scaled up from lab to field geometries with confidence. More work is required to understand the energy absorption of the various wellbore components, so that the energy applied to the slurry itself is isolated and understood. As a qualitative example, heavier wall internal pipe will absorb more energy, thereby reducing the energy input to the slurry. More testing will allow in-depth understanding of energy distribution in the wellbore.



Table 12—Dissipated Energy to Failure

Results Summary

Dissipated Energy to failure

Pressure Results

Joules / cu in cement				Joules / lbm cement			
		Formation				Formation	
Cement	Hard	Intermed	Soft	Cement	Hard	Intermed	Soft
Bead	741	131	61	Bead	14,269	2,518	1,175
Foam	436	247	44	Foam	8,393	4,756	839
Latex	683	81	29	Latex	10,096	1,203	430
Type 1	1,017	81	44	Type 1	15,065	1,205	646

Temperature Results

Joules / cu in cement				Joules / lbm cement			
		Formation				Formation	
Cement	Hard	Intermed	Soft	Cement	Hard	Intermed	Soft
Bead	283	316	170	Bead	5,453	6,085	3,267
Foam	186	65	44	Foam	3,578	1,242	851
Latex	421	72	65	Latex	6,227	1,069	954
Type 1	535	186	170	Type 1	7,920	2,752	2,513



Figure 11—Pressure Specific Energy to Failure per unit Volume vs Cement Type

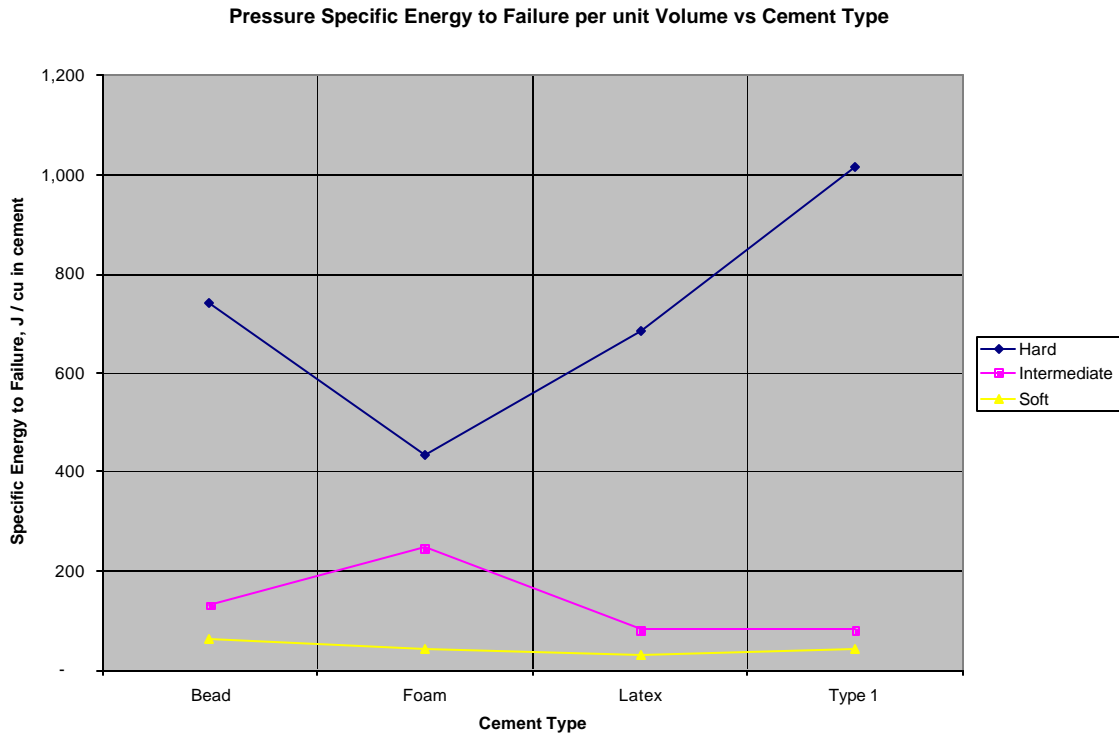


Figure 12—Pressure Specific Energy to Failure per unit Mass vs Cement Type

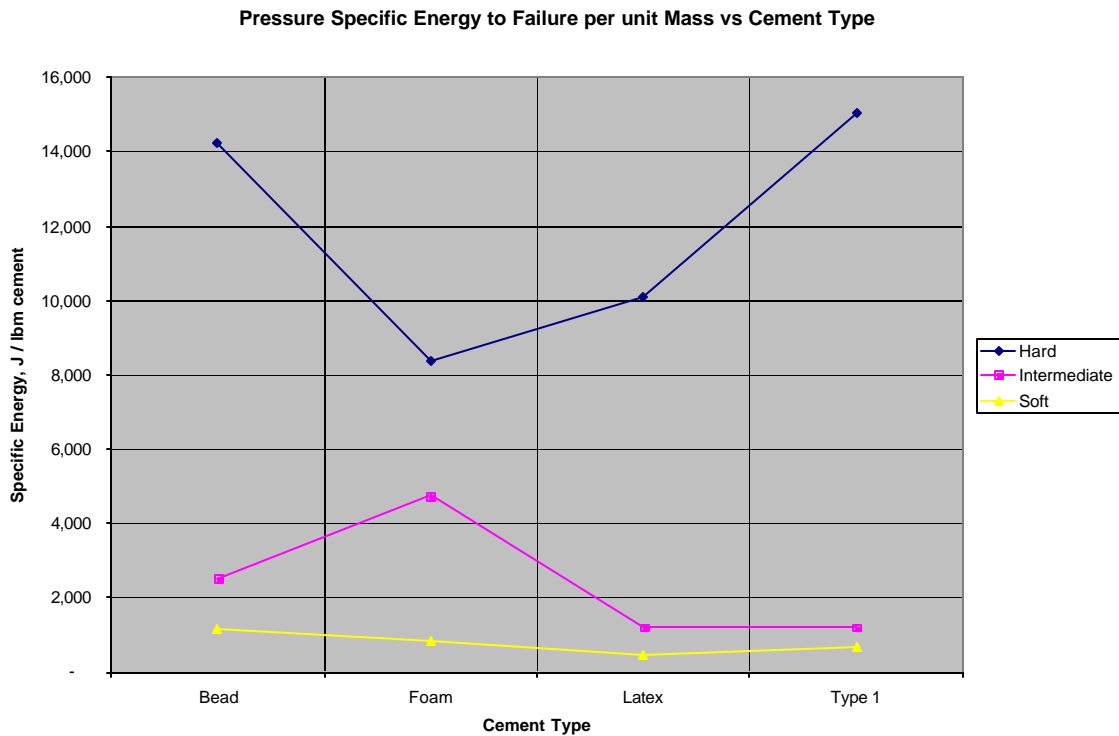




Figure 13—Temp. Specific Energy to Failure per unit Volume vs Cement Type

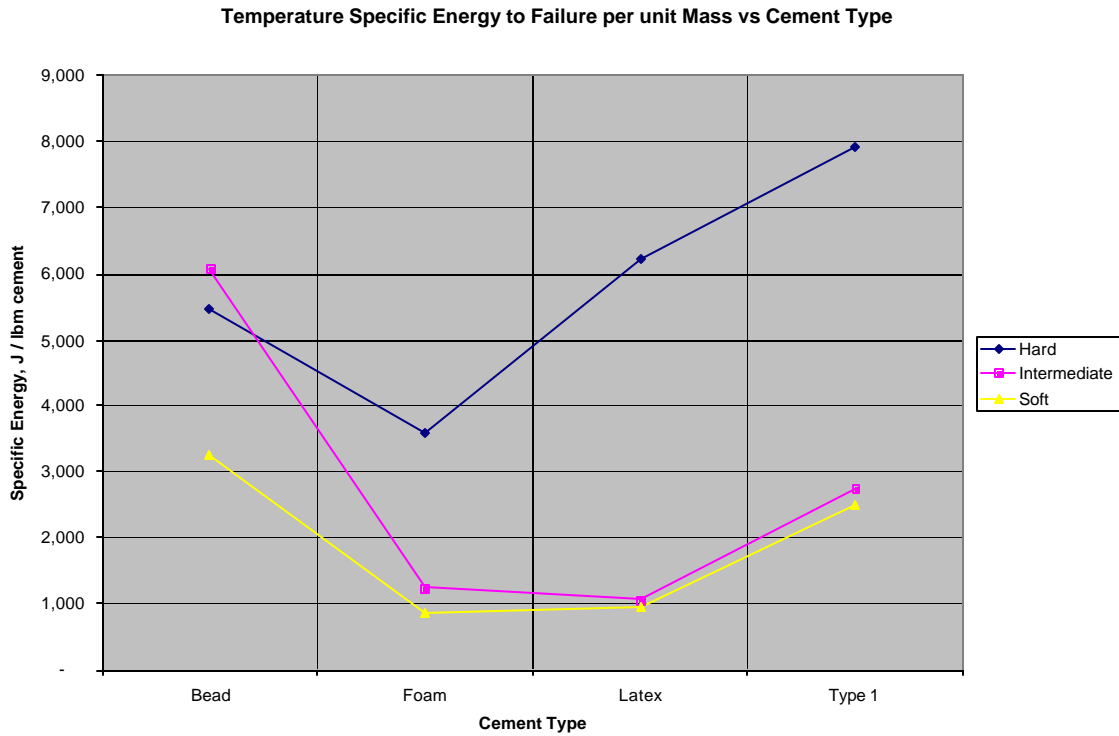


Figure 14—Temp. Specific Energy to Failure per unit Mass vs Cement Type

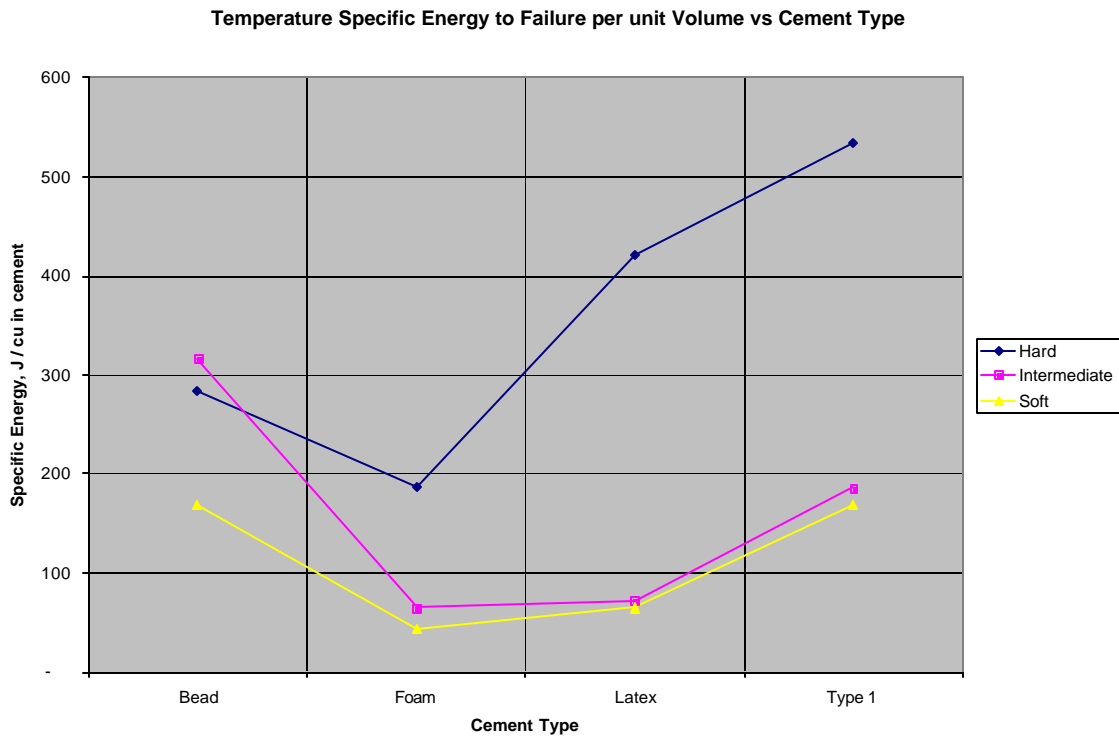




Table 13—Annular Seal Temperature-Cycled Formation Comparison

Slurry	Form.	Cycles	Temperature Cycles (degrees F)									
			74	94	108	121	135	149	163	176	190	
Hard	Type 1	1	0	0	0	0	0	0	0	0	0	0
		2	0	0	0	0	0	0	0	0	0	0
		3	0	0	0	0	0	0	0	0	0	0
		4	0	0	0	0	0	0	0	0	0	0
		5	0	0	0	0	0	0	0.53mD	1.42mD	1.78mD	1.78mD
	Foam	1	0	0	0	0	0	0	0	0	0	0
		2	0	0	0	0	0	0.71mD	1.07mD	2.67mD	3.56mD	4.45mD
	Bead	1	0	0	0	0	0	0	0	0	0	0
		2	0	0	0	0	0	0	0	0	0	0
		3	0	0	1.78mD	3.56mD	5.34mD	8.90mD	-	-	-	-
	Latex	1	0	0	0	0	0	0	0	0	0	0
		2	0	0	0	0	0	0	0	0	0	0
		3	0	0	0	0	0	0	0	0	0	0
		4	0	0	0	0	0	0	0.89mD	2.31mD	2.67mD	3.56mD
	Interm	Type 1	1	0	0	0	0	0	0	0	0	0
			2	0	0	0	0	2.89mD	3.34mD	5.78mD	-	-
Foam		1	0	0	0	0.07mD	0.22mD	1.22mD	-	-	-	
Bead		1	0	0	0	0	0	0	0	0	0	
		2	0	0	0	0	0	0	0	0	0	
		3	0	0	0	0	0	0	3.11mD	3.71mD	-	
Latex		1	0	0	0	0	0.01mD	0.93mD	1.33mD	3.34mD	-	
Soft		Type 1	1	0	0	0	0	0	0	0	0	0
	2		0	0	1.23mD	1.63mD	1.63mD	7.98mD	+8.16mD	-	-	
	Foam	1	0	0.49mD	0.65mD	0.98mD	1.21mD	1.31mD	1.31mD	1.31mD	+8.16mD	
	Bead	1	0	0	0	0	0	0	0	0	0	
		2	0	0	0.41mD	2.45mD	+8.16mD	-	-	-	-	
	Latex	1	0	0	0	0.82mD	1.01mD	1.14mD	1.24mD	1.96mD	+8.16mD	



Table 14—Annular Seal Cumulative Energy at Failure (Joules)

Formation	Type 1		Foam		Bead		Latex	
	Temp.-Cycled	Press.-Cycled	Temp.-Cycled	Press.-Cycled	Temp.-Cycled	Press.-Cycled	Temp.-Cycled	Press.-Cycled
Hard	13,226	25,157	4,596	10,782	7,004	18,329	10,418	16,891
Intermediate	4,596	2,013	1,596	6,110	7,817	3,235	1,788	2,013
Soft	4,197	1,078	1,094	1,078	4,197	1,509	1,596	719

Figure 15—Annular Seal Failure for Temperature-Cycled

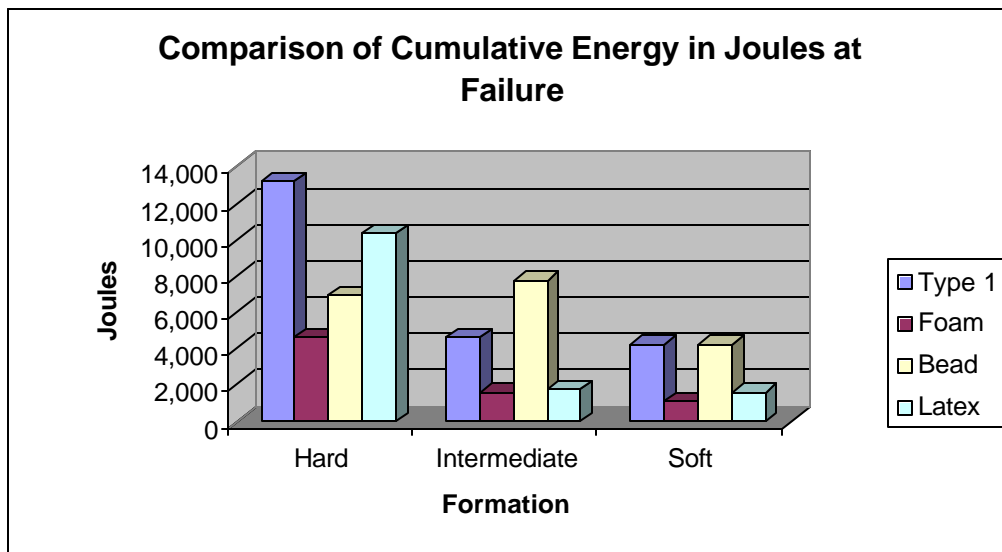
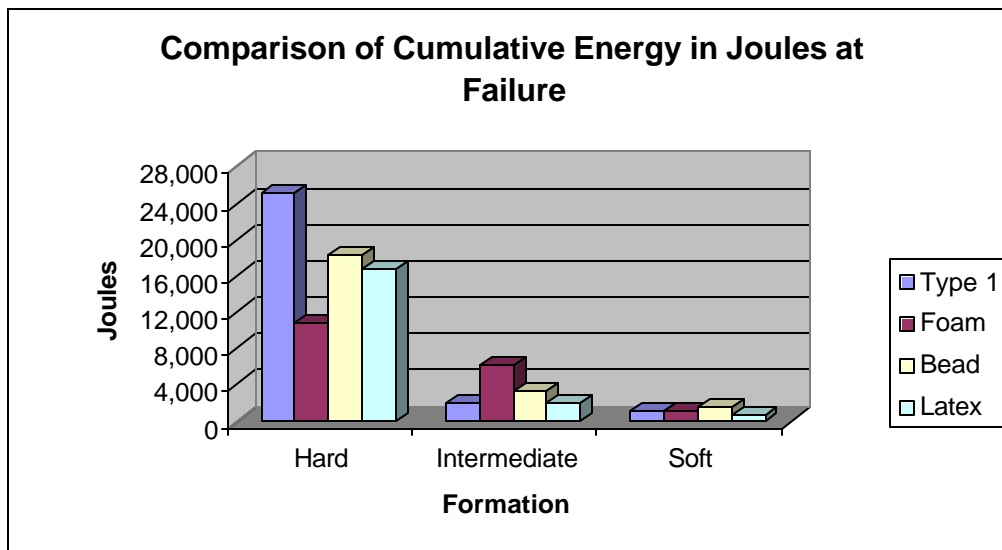


Figure 16—Annular Seal Failure for Pressure-Cycled





Cement Column Seal

Four duplicate sets of models were filled with cement compositions listed in Table 15.

Table 15—Compositions Tested for 8-ft Permeability Models

Composition	Density (lb/gal)	Yield (ft ³ /sk)	Water (gal/sk)	Columns
Type I slurry	15.6	1.18	5.23	1 and 2
SMS slurry	12	2.38	14.05	3 and 4
Bead slurry	12	1.81	6.69	5 and 6
Latex slurry	15.63	1.17	4.20	7 and 8

These cements were allowed to cure for 7 days, and were then tested with differential pressure as described in the procedure section. Results, summarized in Table 16, are for days tested after the initial curing period. Actual results are shown in Appendix B, Table B1, page 54.

Table 16—Failure of 8-ft Permeability Models

Column	Days Tested until Failure	Pressure Differential (psi)	Permeability (mD)
1	107	500	0.09
2	51	200	0.1
3	1	100	33
4	1	100	26
5	78	400	0.03
6	84	400	0.02
7	84	400	0.02
8	99	500	3.1

These results indicate that the sodium metasilicate (SMS) cement failed very quickly on the first day of testing. Other compositions including the neat Type 1 cement required up to 500 psi over the 8-ft column to induce failure.

A second set of 8ft. Permeability models were filled with cement compositions listed in Table 17. These compositions were selected to represent a range of materials that could be formulated from conventional light-weight additives. Density ranges from 12 to 13 lb/gal were tested to determine at what density each additive might produce a successfully-sealing cement.



Table 17--Compositions Tested for second set of 8-ft Permeability Models

Composition	Density (lb/gal)	Yield (ft³/sk)	Water (gal/sk)	Columns
Type I slurry with 20% Gel	12.0	2.77	16.24	1
Type I slurry with 18% Gel	12.5	2.4	13.56	2
Type I slurry with 16% Gel	13.0	2.11	11.47	3
Type I slurry with 3% SMS	12.5	2.11	12.05	4
Type I slurry with 2.5% SMS	13.0	1.88	10.32	5
65:35 Typel:Poz slurry with 16% Gel	12.0	1.79	10.11	6
65:35 Typel:Poz slurry with 12% Gel	12.5	1.38	7.12	7
65:35 Typel:Poz slurry with 10% Gel	13.0	2.4	13.71	8
TXI LW slurry with 2% SMS	12.0	2.04	11.19	9
Neat TXI LW slurry	13.0	1.79	9.4	10

These cements were allowed to cure for 3 days, and were then tested with differential pressure as described in the procedure section. Results, summarized in Table 18 are for days tested after the initial curing period. Actual results are shown in Appendix B, Table B2, page 55.

Results from Table 18 indicate that a seal was maintained for 13-lb/gal gel and sodium silicate cements. No formula with pozzolan maintained a seal while both TXI LightWeight cements maintained seals.



Table 18--Failure of second set of 8-ft Permeability Models

Column	Days Tested at 100 psi	Permeability (mD)
1	1	2.41
2	3	1.23
3	90	0
4	3	2.29
5	90	0
6	1	6.73
7	1	0.89
8	25	0.38
9	90	0
10	90	0

A third set of 8ft. Permeability models were filled with cement compositions listed in Table 19. These compositions were selected to represent an additional range of materials that could be formulated from conventional light-weight additives. Density ranges from 11 to 13.5 lb/gal were tested to determine at what density each additive might produce a successfully-sealing cement.



Table 19--Compositions Tested for third set of 8-ft Permeability Models

Composition	Density (lb/gal)	Yield (ft³/sk)	Water (gal/sk)	Columns
Type I slurry with 2% SMS	13.4	1.72	9.17	1
Type I slurry with 2% SMS	13.0	1.87	10.28	2
TXI LW slurry with 3% SMS	11.0	2.49	15.30	3
TXI LW slurry with 3% SMS	11.5	2.10	12.35	4
65:35 Typel:Poz slurry with 6% Gel	13.5	1.56	7.84	5
50:50 Typel:Poz slurry with 6% Gel	13.4	1.51	7.46	6
50:50 Typel:Poz slurry with 8% Gel	12.8	1.75	9.14	7
50:50 Typel:Poz slurry with 10% Gel	12.4	1.95	10.61	8
TXI H slurry with 12% Gel	12.0	2.60	15.30	9
TXI H slurry with 8% Gel	12.5	2.21	12.58	10

These cements were allowed to cure for 3 days, and were then tested with differential pressure as described in the procedure section. Results, summarized in Table 20 are for days tested after the initial curing period. Actual results are shown in Appendix B, Table B3, page 56.



Results from Table 20 indicate that a seal was maintained for the 65:35 TypeI:Poz slurry with 6% Gel mixed at 13.5-lb/gal. All other formulations did not maintain seals.

Table 20--Failure of third set of 8-ft Permeability Models

Column	Days Tested at 100 psi	Permeability (mD)
1	1	7.36
2	1	8.63
3	1	2.29
4	25	1.27
5	30	0
6	18	0.38
7	1	5.97
8	1	32.12
9	1	50.53
10	1	35.29



Table 21 summarizes all three sets of permeability models.

Table 21---Flows for all sets of 8-ft Permeability Models

Composition	Density (lb/gal)	Permeability (mD)	Days Tested at 100 psi	Set Number
Type I + 2% SMS	13.4	7.36	1	3
Type I + 2% SMS	13.0	8.63	1	3
Type I + 2.5% SMS	13.0	0	90	2
Type I + 3% SMS	12.5	2.29	3	2
Type I + 3% SMS	12.0	3.75	1	1
TXI LW Neat	13.0	0	90	2
TXI LW + 2% SMS	12.0	0	90	2
TXI LW + 3% SMS	11.5	1.27	25	3
TXI LW + 3% SMS	11.0	2.29	1	3
65:35 Type I:Poz + 6% Gel	13.5	0	30	3
65:35 Type I:Poz + 10% Gel	13.0	0.38	25	2
65:35 Type I:Poz + 12% Gel	12.5	0.89	1	2
65:35 Type I:Poz + 16% Gel	12.0	6.73	1	2
50:50 Type I:Poz + 6% Gel	13.4	0.38	18	3
50:50 Type I:Poz + 8% Gel	12.8	5.97	1	3
50:50 Type I:Poz + 10% Gel	12.4	32.12	1	3
H + 8% Gel	12.5	35.29	1	3
H + 12% Gel	12.0	50.53	1	3
Type I + 16% Gel	13.0	0	90	2
Type I + 18% Gel	12.5	1.23	3	2
Type I + 20% Gel	12.0	2.41	1	2
Type I Neat	15.6	0	44	1
Type I + 13.2% Beads	12.0	0	44	1
Type I + 1 gal/sk Latex	15.6	0	44	1



Appendix A—Test Procedures

Sample Preparation

Some preparation and testing methods were modified to adapt for the lightweight bead and foamed slurries. The mixing procedures for the bead slurry were also modified to minimize bead breakage due to high shear from API blending procedures. The following blending procedure was used for the bead slurry.

1. Weigh out the appropriate amounts of the cement, water, and beads into separate containers.
2. Mix the cement slurry (without beads) according to Section 5.3.5 of API RP 10B.
3. Pour the slurry into a metal mixing bowl and slowly add beads while continuously mixing by hand with a spatula. Mix thoroughly.
4. Pour this slurry back into the Waring blender and mix at 4,000 rev/min for 35 seconds to mix and evenly distribute the contents.

Testing methods for the foamed slurries were also modified. For example, thickening time is performed on unfoamed slurries only. Because the air in the foam does not affect the hydration rate, the slurry is prepared as usual per API RP 10B and then the foaming surfactants are mixed into the slurry by hand without foaming the slurry.

Sample Curing

Test specimens for rock properties testing are mixed in a Waring blender and poured into cylinder molds. Samples are cured for 7 days in a 45°F atmospheric water bath.

Performance test fixture molds are filled with cement mixed in the same manner. These fixtures are also cured in a 45°F water bath for 7 days prior to testing.

Thickening Time Test

Following the procedures set forth in API RP 10B¹, thickening-time tests were performed on the three cement systems. The test conditions started at 80°F and 600 psi, and were ramped to 65°F and 5,300 psi in 48 minutes.

Free-Fluid Test

The free-fluid testing that was performed on the Type 1, foamed cement and bead cement came from API RP 10B. The free-fluid procedure, also referred to as operating free water procedure, uses a graduated cylinder that is oriented vertically. The slurry is maintained at 65°F, and the free fluid that accumulates at the top of the slurry is measured. See Table A1 for test results.



Table A1—Free Fluid Test Results

Slurry System	Thickening Time to 100 Bc (hr:min)	Percentage of Free Fluid
Neat	4:38	0.8
Foamed	3:42	0.0
Bead	5:04	0.8

Compressive Strength

The compressive strengths were derived using the 2-in. cube crush method specified in API RP 10B. The samples were cured in an atmospheric water bath at 45°F. The reported values were taken from the average of three samples.

Young’s Modulus and Poisson’s Ratio Testing

Traditional Young’s modulus testing was performed using ASTM C469², Standard Test Method for Static Modulus of Elasticity (Young’s Modulus) and Poisson’s Ratio of Concrete in Compression.

The following procedure is used for the Young’s modulus testing.

1. Each sample is inspected for cracks and defects.
2. The sample is cut to a length of 3.0 in.
3. The sample’s end surfaces are then ground to get a flat, polished surface with perpendicular ends.
4. The sample’s physical dimensions (length, diameter, weight) are measured.
5. The sample is placed in a Viton jacket.
6. The sample is mounted in the Young’s modulus testing apparatus.
7. The sample is brought to 100-psi confining pressure and axial pressure. The sample is allowed to stand for 15 to 30 min until stress and strain are at equilibrium. (In case of an unconfined test, only axial load is applied.)
8. The axial and confining stress are then increased at a rate of 25 to 50 psi/min to bring the sample to the desired confining stress condition. The sample is allowed to stand until stress and strain reach equilibrium.
9. The sample is subjected to a constant strain rate of 2.5 mm/hr.
10. During the test, the pore-lines on the end-cups of the piston are open to atmosphere to prevent pore-pressure buildup.

After the sample fails, the system is brought back to the atmospheric stress condition. The sample is removed from the cell and stored.

Hydrostatic Cycling and Anelastic Strain

Hydrostatic cycling testing was then performed on cement specimens in the same load configuration as for Young’s modulus and Poisson’s ratio. This testing was conducted with axial loading and radial loading being maintained equally throughout the load ramping process. For such testing, the hydrostatic pressure is cycled through the



following ramping procedures.

1. Ramp up to 1,000 psi.
2. Ramp down to 100 psi.
3. Ramp up to 1,500 psi.
4. Ramp down to 100 psi.
5. Ramp up to 2,000 psi.
6. Ramp down to 100 psi.
7. Continue to failure.

Each ramp was conducted at 16.7 psi/min and the sample was held at the destination hydrostatic pressures (i.e., 100; 1,000; 1,500; and 2,000 psi) for no longer than two minutes before proceeding to the next ramp step.

Hydrostatic cycling was studied further to investigate the deformation that occurs during each of the ramps. The value (size) of the sample at 250 psi during the first ramp to 1,000 psi is the reference value for determining the percentile of deformation. This reference value (sample size) is then compared to the sample size at 250 psi during each subsequent ramp step.

Concern over the ability to compare results of this testing among different compositions led to the development of a test for determining strain and cyclic loading effects under similar conditions with respect to each composition's ultimate strength. This test is referred to as anelastic strain testing.

Anelastic strain testing, a variation of hydrostatic testing, is designed to allow a more accurate evaluation of permanent strain resulting from stressing different test compositions. Samples are cycled to 25%, 50%, and 75% of each composition's compressive strength under 500-psi confining stress. Measurement of anelastic strain with cycling provides a more comparable value of each composition's performance. The first step in the procedure involves compression testing a sample to failure in the load cell with 500-psi confining stress. Once this failure load value is determined, additional samples will be tested by applying axial loads equal to 25%, 50%, and 75% of the failure load, and cycling until samples fail. The cyclic loading rate will be maintained at 250 psi/min and the confining force will be maintained at 500 psi. Plastic deformation will be measured at the end of each cycle. Results will include cycles to failure and anelastic strain per cycle. CT scans will be performed on each sample prior to testing to rule out the presence of any large voids.

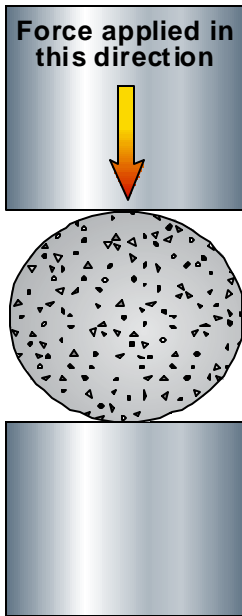
Tensile Strength and Tensile Young's Modulus

Tensile strength was tested using ASTM C496³ (Standard Test Method for Splitting Tensile Strength of Cylindrical Concrete Specimens). For this testing, the specimen dimensions were 1.5 in. diameter by 1 in. long. **Figure A1** shows a general schematic of how each specimen is oriented on its side during testing. The force was applied by constant displacement of the bottom plate at a rate of 1 mm every 10 minutes. Change in the specimen diameter can be calculated from the test plate displacement. The



(compressive) strength of the specimen during the test can be graphed along with the diametric strain (change in diameter/original diameter) to generate the tensile Young's modulus. Strain was measured by a linear displacement transducer mounted to record diameter continuously as stress was applied.

Figure A1—Sample Orientation for ASTM C496-90 Testing



Annular Seal Testing Procedure

Samples for annular seal testing are prepared by mixing cement compositions, pouring them into specified molds, and curing them for 7 days in 80°F water baths. After curing, three specimens for each test composition and condition are tested.

These procedures are for use with the annular seal apparatus. Specific procedures are applied as necessary for each formation simulation: soft, intermediate, and hard. The soft apparatus test procedure is to be used with cores cured to set in a soft gel mold, which provides a semi-restricting force on the outside of the core. The intermediate specimen mold uses a 3-in. diameter Schedule 40 PVC pipe as the outer containment. The hard apparatus uses a 3-in. Schedule 40 steel pipe as the outside containment, giving the cement slurry a restricting force outside of the core. The hard-formation configuration consists of a sandblasted internal pipe with an outer diameter (OD) of 1 ¹/₁₆ in. and a sandblasted external pipe with an internal diameter (ID) of 3 in. Both pipes are 6 in. long. A contoured base and top are used to center the internal pipe within the external pipe. The base extends into the annulus 1 in. and cement fills the annulus to a height of 4 in. The top inch of annulus contains water.

For the soft-formation annular seal tests, plastisol is used to allow the cement to cure in a



less-rigid, lower-restraint environment. Plastisol is a mixture of a resin and a plasticizer that creates a soft, flexible substance. This particular plastisol blend (PolyOne's Denflex PX-10510-A) creates a substance with a hardness of 40 duro.

The soft formation configuration contains a sandblasted external pipe with an ID of 4 in. A molded plastisol sleeve with an ID of 3.0 in. and uniform thickness of 0.5 in. fits inside the external pipe. With the aid of a contoured base and top, a sandblasted internal pipe with an OD of $1 \frac{1}{16}$ in. is then centered within the plastisol sleeve. The pipes and sleeve are 6 in. long. The base extends into the annulus 1 in. and cement fills the annulus to a height of 4 in. between the plastisol sleeve and the inner $1 \frac{1}{16}$ -in. pipe. The top inch of annulus is filled with water.

The intermediate formation test fixture features the same configuration as the hard formation fixture except the outer pipe is made of PVC.

Soft-Formation Simulation

1. After the core is cured, place the core inside the gel mold sleeve.
2. Place the core and sleeve inside the pipe-in-soft steel cell.
3. Once inside, both ends of the core are supported with O-rings.
4. The O-rings are then tightened by interior end plates to close off leaks that might be present.
5. Using water, pressurize the exterior circumference of the sleeve to 25 psi and check for leaks on the ends of the cell.
6. Cap off both ends of the steel cell with the cell end caps. One end cap has a fitting that allows for N₂ gas to be applied into the cell, and the other end cap allows gas to exit the cell.
7. Attach the pressure inlet line to the bottom of the cell and attach the pressure outlet line to the top of the cell.
8. Apply pressure to the inlet line (do not exceed 20 psig) and measure the flow out using flow meters.

Hard-Formation Simulation

1. After the core is cured inside the steel pipe, cap off each end of the pipe with steel end caps. Each end cap has a fitting that allows for gas to be applied into the pipe or to exit the pipe.
2. Attach the pressure inlet line to the bottom of the pipe, and attach the pressure outlet line to the top of the pipe.
3. Apply pressure to the inlet line (do not exceed 20 psig) and measure the pressure out of the outlet line using flow meters.

Intermediate Formation Simulation

The test fixture for performing tests with a simulated intermediate formation is very similar to that used for tests with simulated hard formations, except the outer pipe is made of Schedule 40 PVC. Stress is applied to the specimens by applying hydraulic



pressure or heat to the inner pipe.

Thermal cycling resulted from the insertion of heaters into the inner pipe and the heating of the inner pipe from 80° to 180°F over an 8 hour period then allowing the pipe to cool to 80°F. Flow through the model was measured continuously with flowmeters throughout each cycle, and cycles were repeated a minimum of five times per sample. Three specimens of each composition were tested.

To ensure that sufficient stress could be applied to induce failure in all samples, the thermal cycling test procedure was modified to allow use of a thicker-walled inner pipe that provides more steel volume for expansion. The modified test fixture now features an inside pipe with a 1.68-in. outside diameter and a 1.25-in. inside diameter, giving a wall thickness of 0.190 in. Additionally, the outer containment diameter will be increased to 3 in.

Pressure cycling resulted from the application of hydraulic pressure to the inner pipe. For the initial cycle, pressure was increased from 0 to 1000 psi. Pressure was then released and allowed to return to 0, and flow measurements were made. Additional cycles were made by increasing the upper pressure limit by 1000 psi (0 to 1,000 to 0 psi, 0 to 2,000 to 0 psi, etc.) and measuring flow at the endpoint (0) of each cycle. If specimens were cycled to 10,000 psi without failure, the 0 to 10,000 to 0 psi pressure cycle was repeated a minimum of five times. The original test procedure was modified to establish a maximum pressure of 10,000 psi during pressure cycles.

All modified testing methods performed with intermediate formations were applied to soft and hard formations also. Hard formations incorporated additional pressure cycles to 10,000 psi until achieving failure.

Shear Bond Strength Testing

Shear bond strength tests are used for investigating the effect that restraining force has on shear bond. Samples are cured in a hard-formation configuration (**Figure A2**) and in a soft-formation configuration (**Figure A3**). The hard-formation configuration consists of a sandblasted internal pipe with an outer diameter (OD) of 1 ¹/₁₆ in. and a sandblasted external pipe with an internal diameter (ID) of 3 in. Both pipes are 6 in. long. A contoured base and top are used to center the internal pipe within the external pipe. The base extends into the annulus 1 in. and cement fills the annulus to a height of 4 in. The top inch of annulus contains water.

For the soft-formation shear bond tests, plastisol is used to allow the cement to cure in a less-rigid, lower-restraint environment. Plastisol is a mixture of a resin and a plasticizer that creates a soft, flexible substance. This particular plastisol blend (PolyOne's Denflex PX-10510-A) creates a substance with a hardness of 40 duro.

The soft formation configuration contains a sandblasted external pipe with an ID of 4 in. A molded plastisol sleeve with an ID of 3.0 in. and uniform thickness of 0.5 in. fits inside



the external pipe. With the aid of a contoured base and top, a sandblasted internal pipe with an OD of $1 \frac{1}{16}$ in. is then centered within the plastisol sleeve. The pipes and sleeve are 6 in. long. The base extends into the annulus 1 in. and cement fills the annulus to a height of 4 in. between the plastisol sleeve and the inner $1 \frac{1}{16}$ -in. pipe. The top inch of annulus is filled with water.

The intermediate formation test fixture features the same configuration as the hard formation fixture except the outer pipe is made of PVC.

Cycling tests for the shear bond specimens follow all cycling procedures used for testing the annular seals. Once the annular seal cycles are performed the shear bond measurements are then taken. This allows correlation with annular seal test results. Shear bonds are measured after the cycling to determine the level of bond remaining.

Figure A2—Cross-section of pipe-in-pipe test fixture configuration for shear bond test.

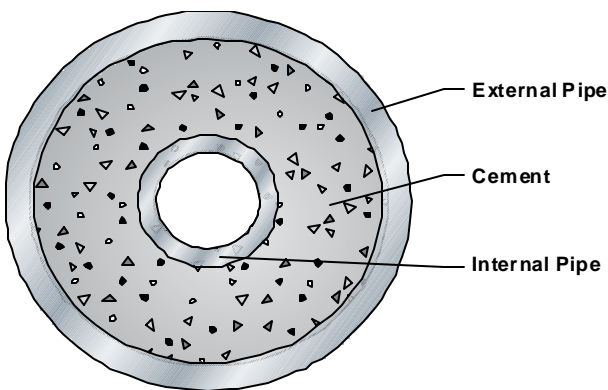
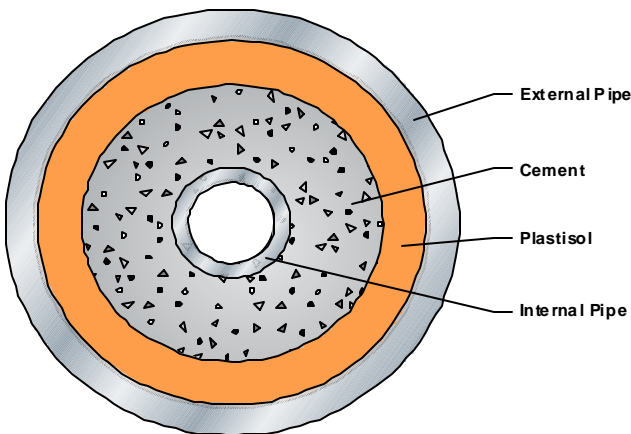


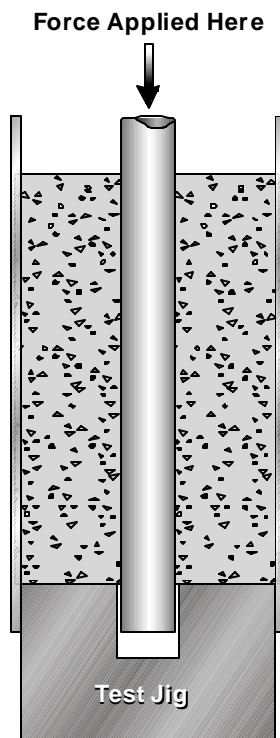
Figure A3—Cross-section of pipe-in-soft test fixture configuration for shear bond test.





The shear bond measures the stress necessary to break the bond between the cement and the internal pipe. This was measured with the aid of a test jig that provides a platform for the base of the cement to rest against as force is applied to the internal pipe to press it through. (Figure A4) The shear bond force is the force required to move the internal pipe. The pipe is pressed only to the point that the bond is broken; the pipe is not pushed out of the cement. The shear bond strength is the force required to break the bond (move the pipe) divided by the surface area between the internal pipe and the cement.

Figure A4—Test jig for testing shear bond strength



Cement Column Seal Tests

Eight-foot lengths of 2-in. Schedule 40 pipe are mounted vertically and fitted at the top and bottom with end caps equipped with pressure inlet and outlet ports. The bottom of each pipe is filled with 6 in. of 20-40 sand to provide an open base for gas injection. For the first set, sets of two fixtures are each filled with one of four different cement slurries: bead, Type 1, latex, and sodium metasilicate. Samples are covered with water and cured for 7 days under 1000-psi pressure. After the samples are cured, 100 psi of pressure is applied to the bottom of each fixture and any flow through the column is monitored. For the second and third sets, ten fixtures are each filled with ten different cement slurries. Samples are covered with water and cured for 3 days under 1000-psi pressure. After the samples are cured, 100 psi of pressure is applied to the bottom of each fixture and any flow through the column is monitored.



Appendix B—Test Data

Graphical data for all mechanical properties tests performed in this investigation are presented in this appendix.

Figure B1—Plot of tensile strength and Young’s modulus results for latex slurry with fibers (sample 1), Type 1 slurry with fibers (sample 2), and latex slurry (sample 3).

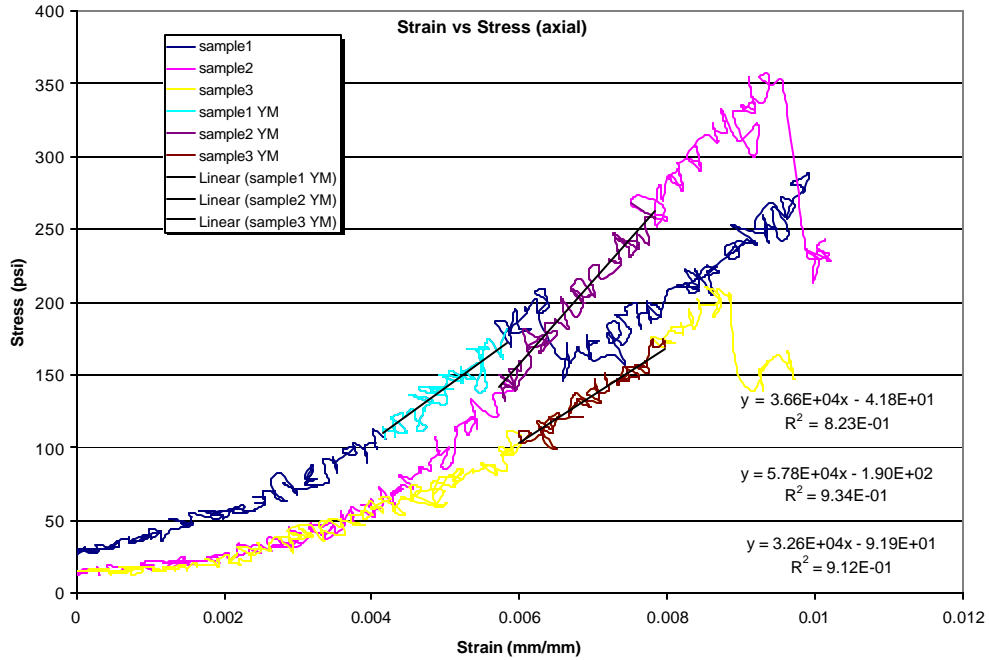




Figure B2—Plot of tensile strength and Young’s modulus results for neat Type 1 slurry cured in a confined state.

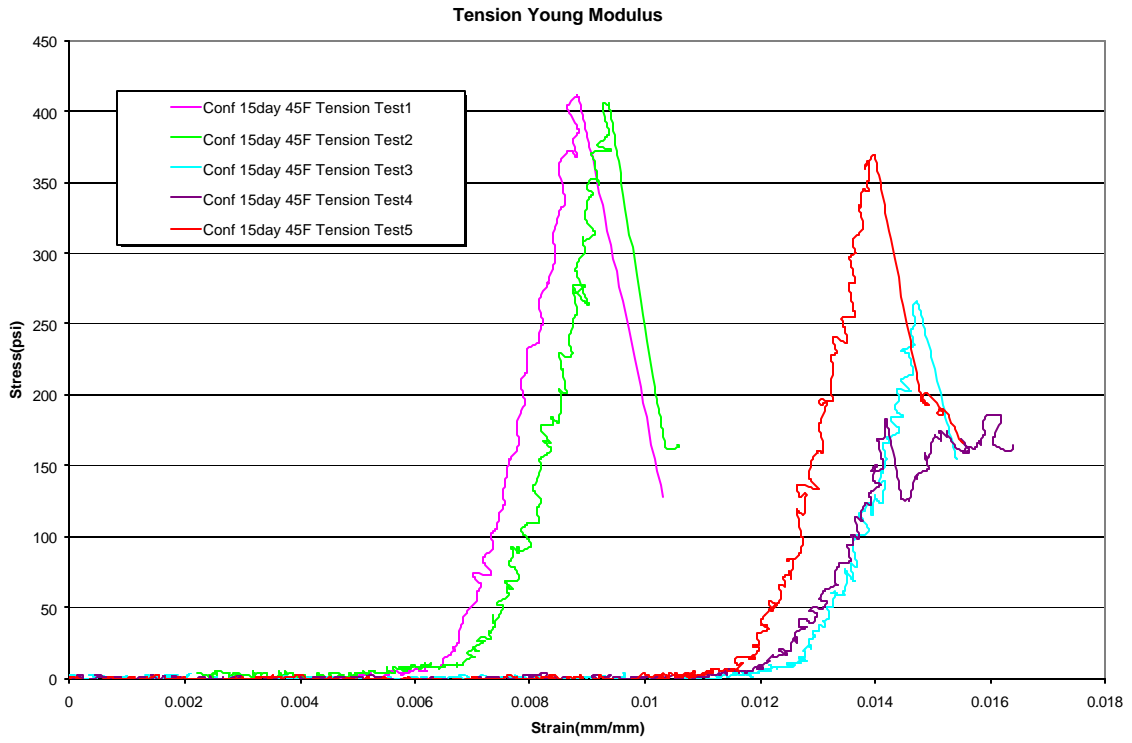




Figure B3—Plot of tensile strength and Young’s Modulus results for 12-lb/gal foam slurry.

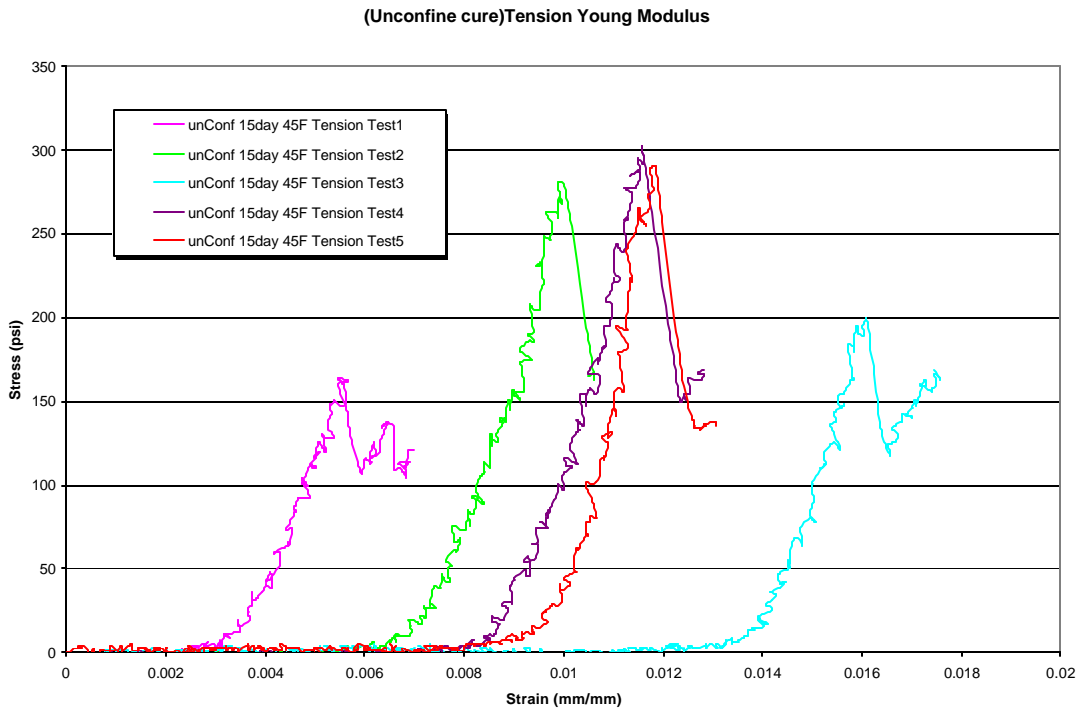




Figure B4—Plot of compressive Young’s modulus for Type 1 slurry at 0-psi confining pressure.

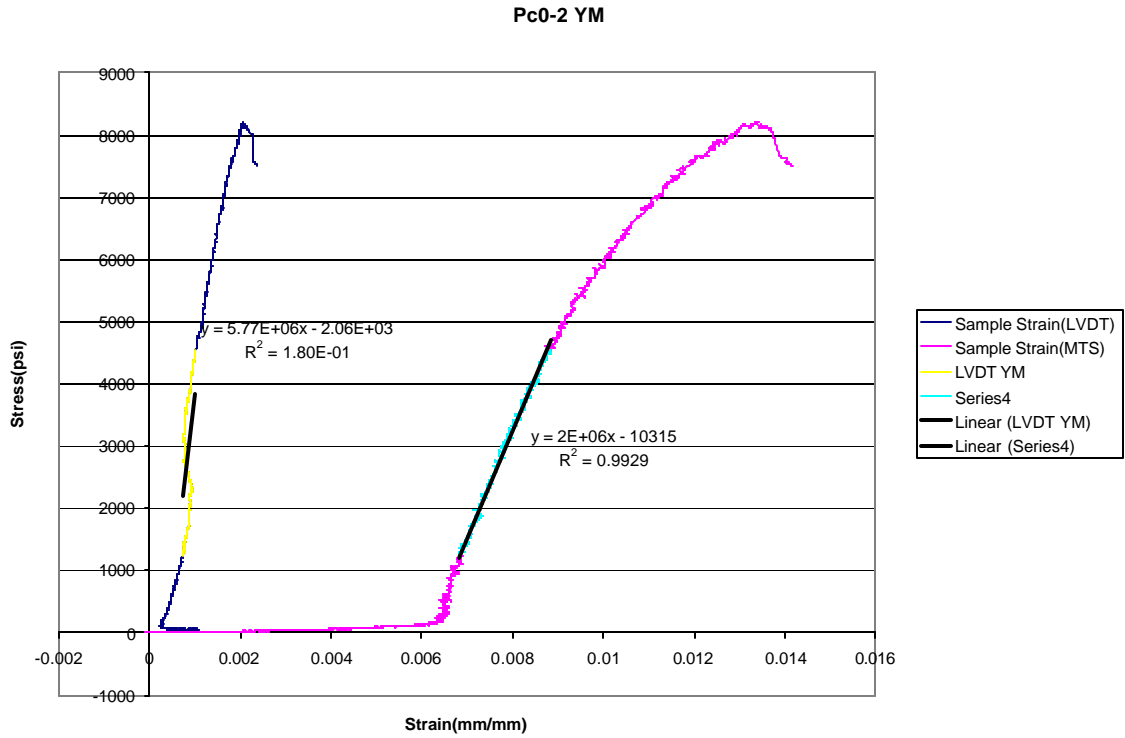




Figure B5—Plot of compressive Young’s modulus for Type 1 slurry at 1500-psi confining pressure.

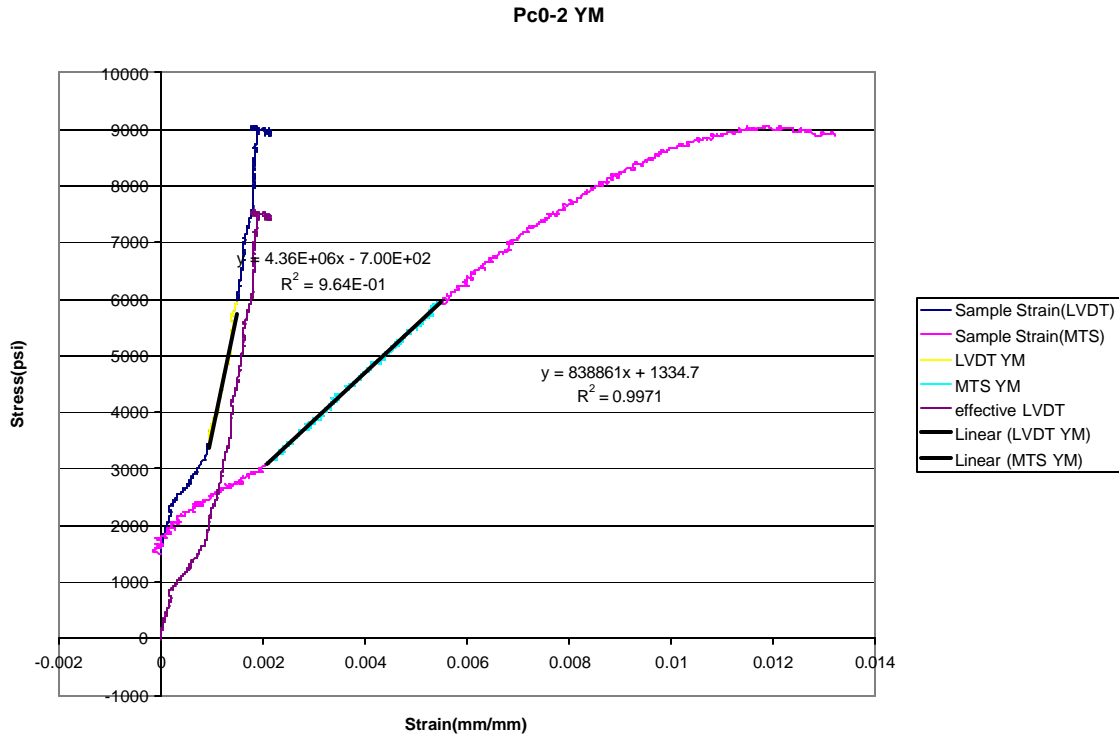




Figure B6— Plot of compressive Young’s modulus for Type 1 slurry at 5000-psi confining pressure.

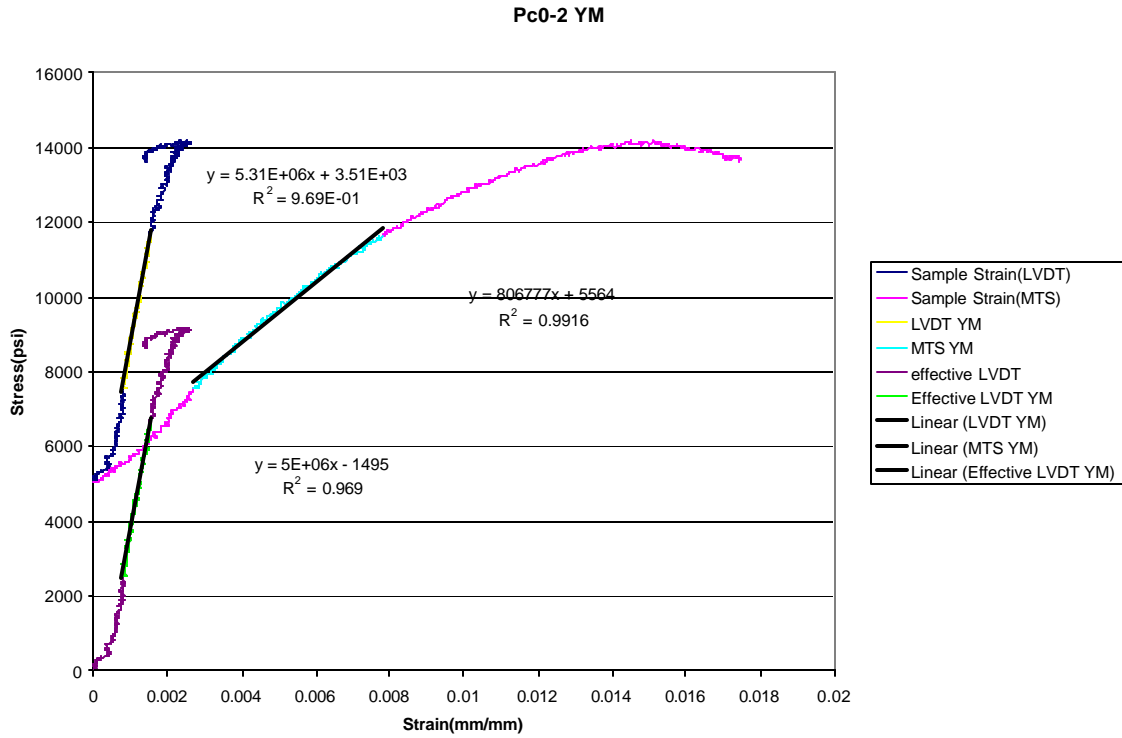




Figure B7— Plot of compressive Young’s modulus for 12-lb/gal foam slurry at 0-psi confining pressure.

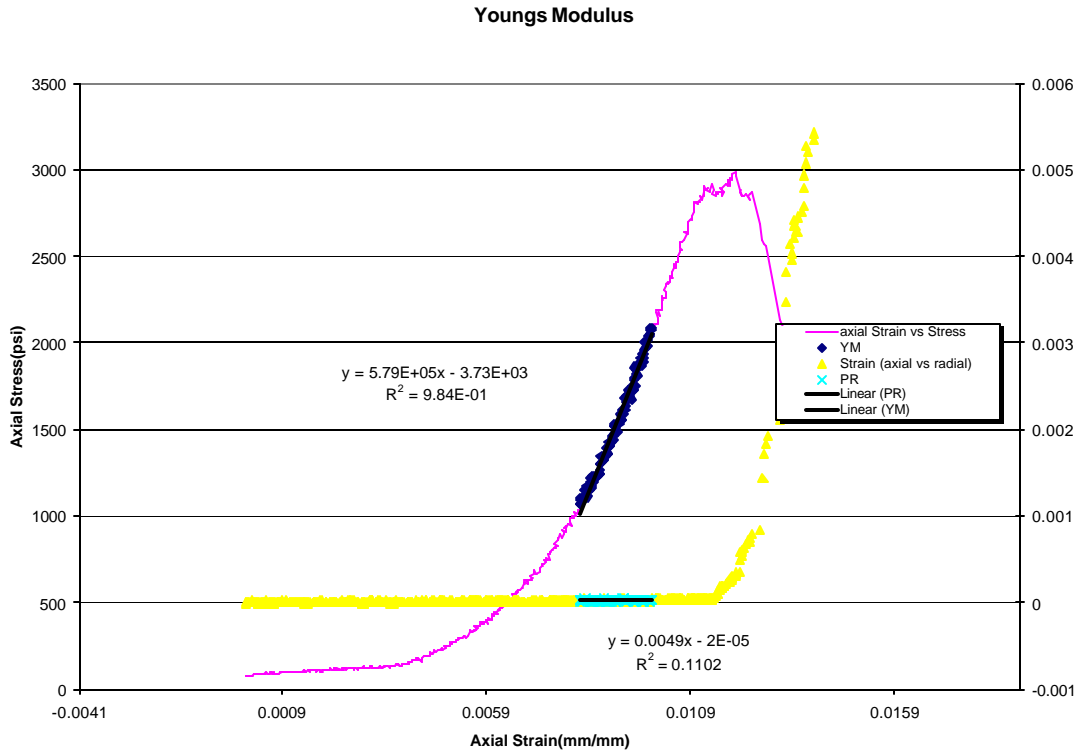




Figure B8— Plot of compressive Young’s modulus for 12-lb/gal foam slurry at 500-psi confining pressure.

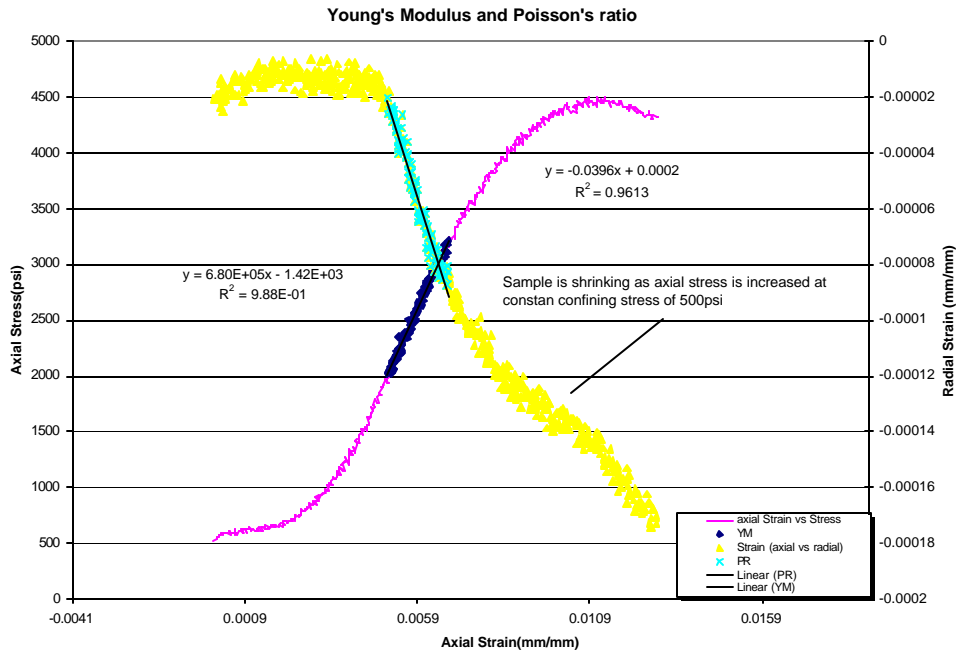


Figure B9— Plot of compressive Young’s modulus for 12-lb/gal foam slurry at 1000-psi confining pressure.

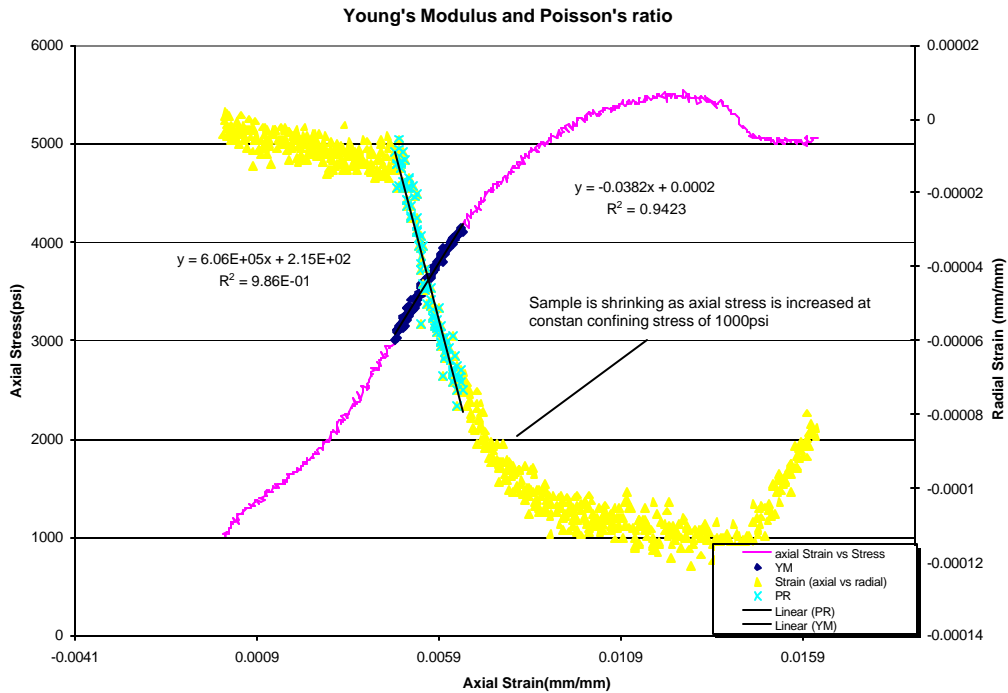




Figure B10— Plot of compressive Young's modulus for bead slurry at 0-psi confining pressure.

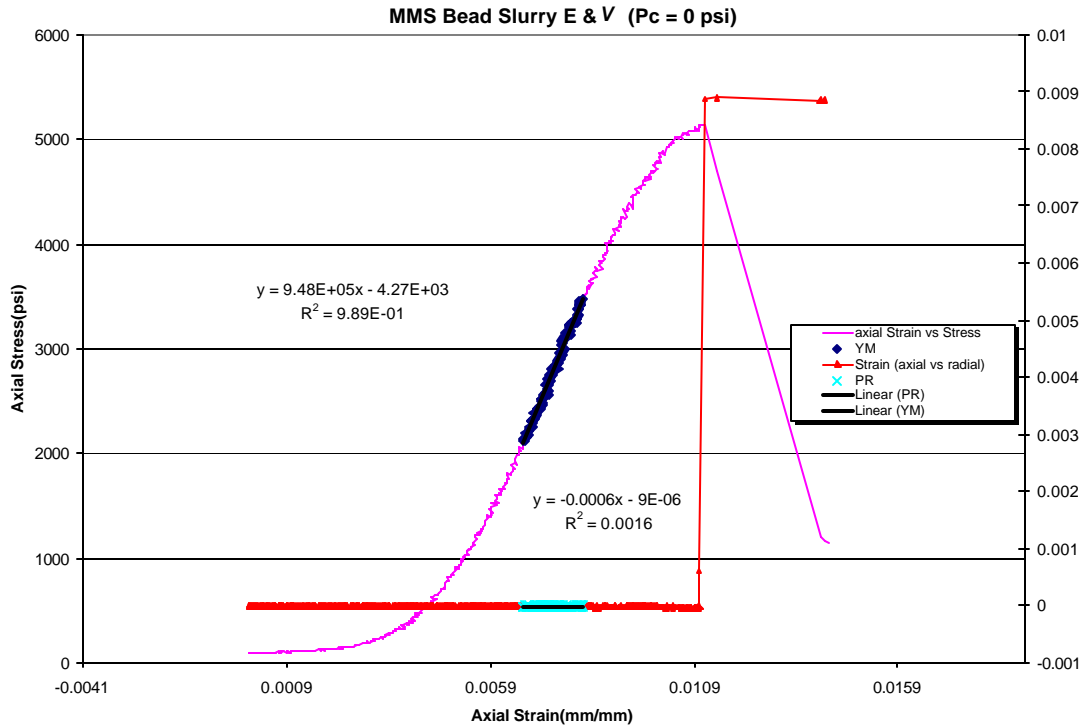




Figure B11— Plot of compressive Young’s modulus for bead slurry at 500-psi confining pressure.

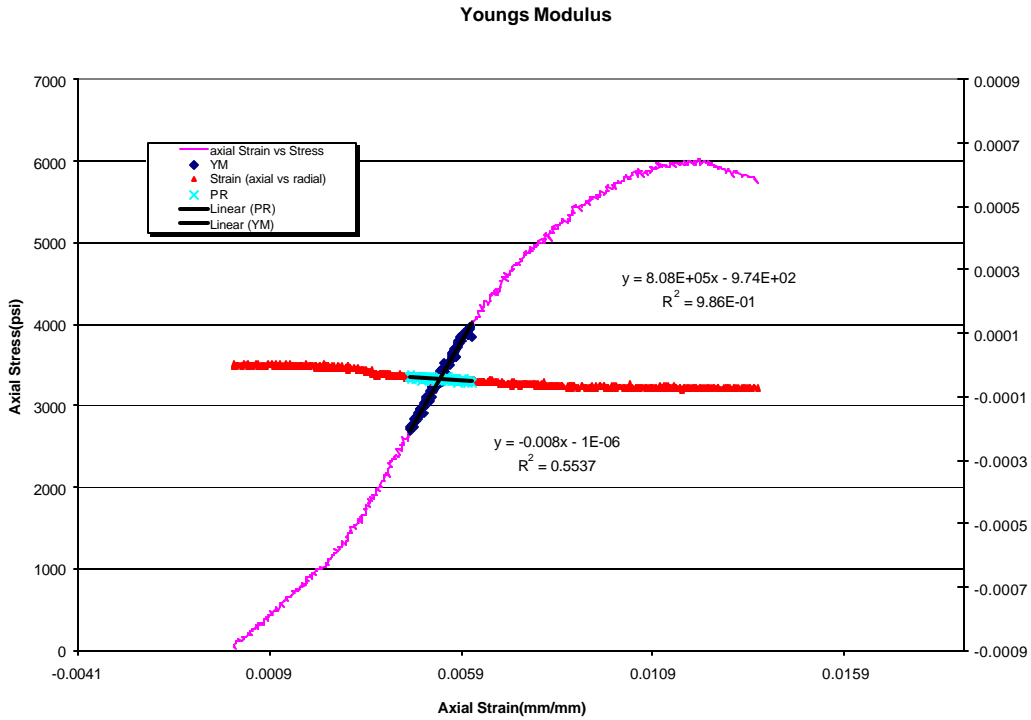


Figure B12— Plot of compressive Young’s modulus for bead slurry at 1000-psi confining pressure.

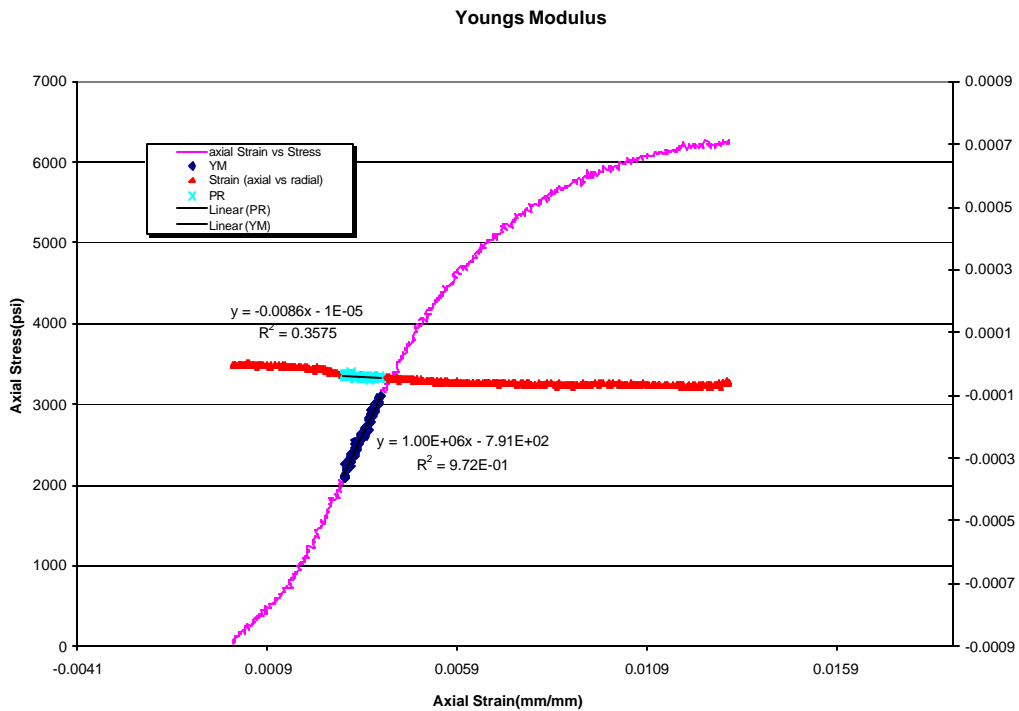




Figure B13— Plot of compressive Young’s modulus for latex slurry at 0-psi confining pressure.

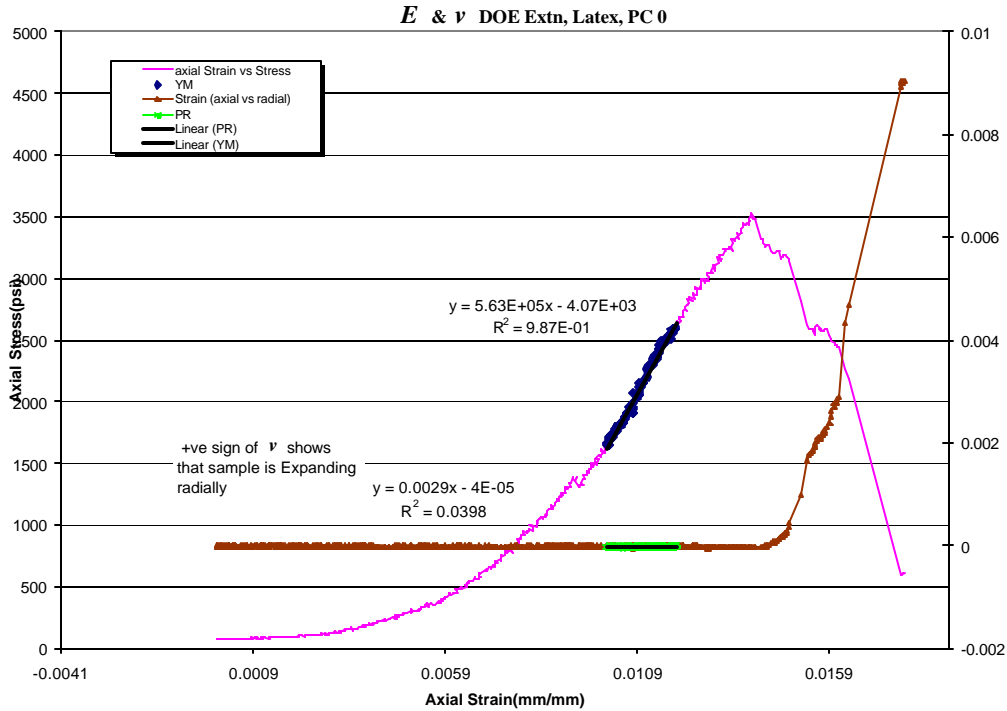


Figure B14— Plot of compressive Young’s modulus for latex slurry at 250-psi confining pressure.

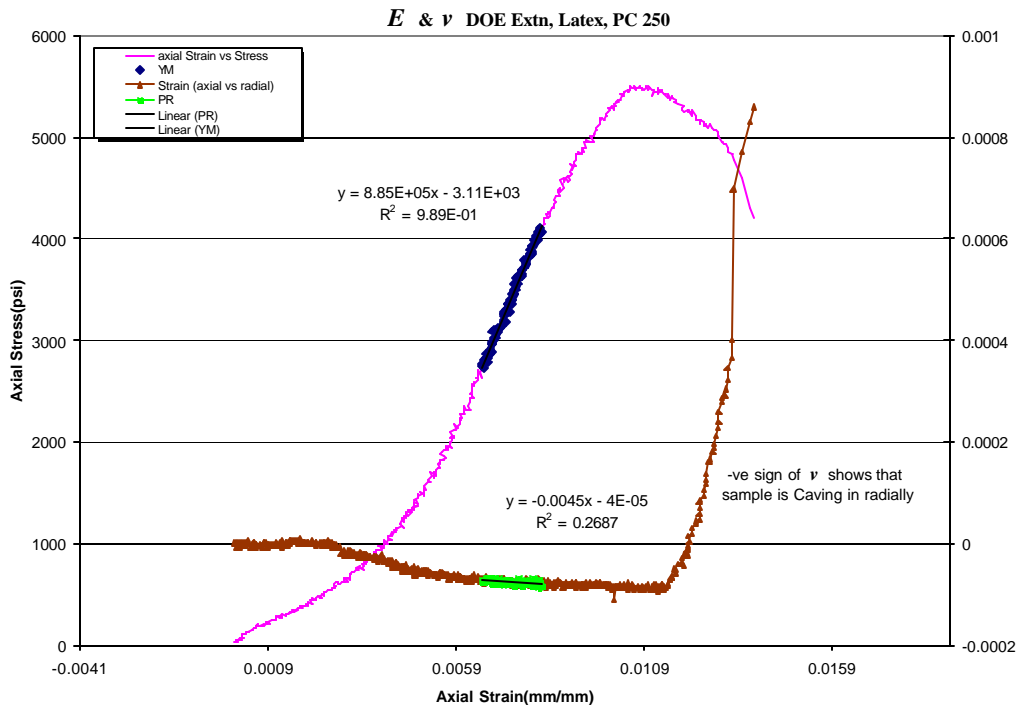




Figure B15— Plot of compressive Young’s modulus for latex slurry at 500-psi confining pressure.

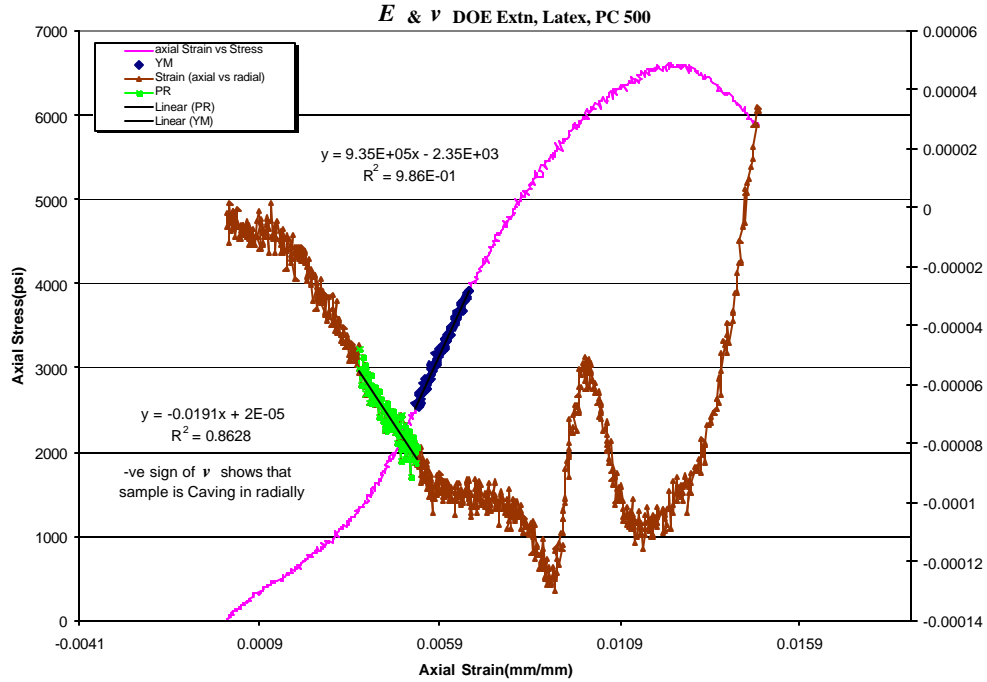


Figure B16— Young’s modulus measurements for Type 1 slurry at 500-psi confining stress and a 100-psi/min load rate.

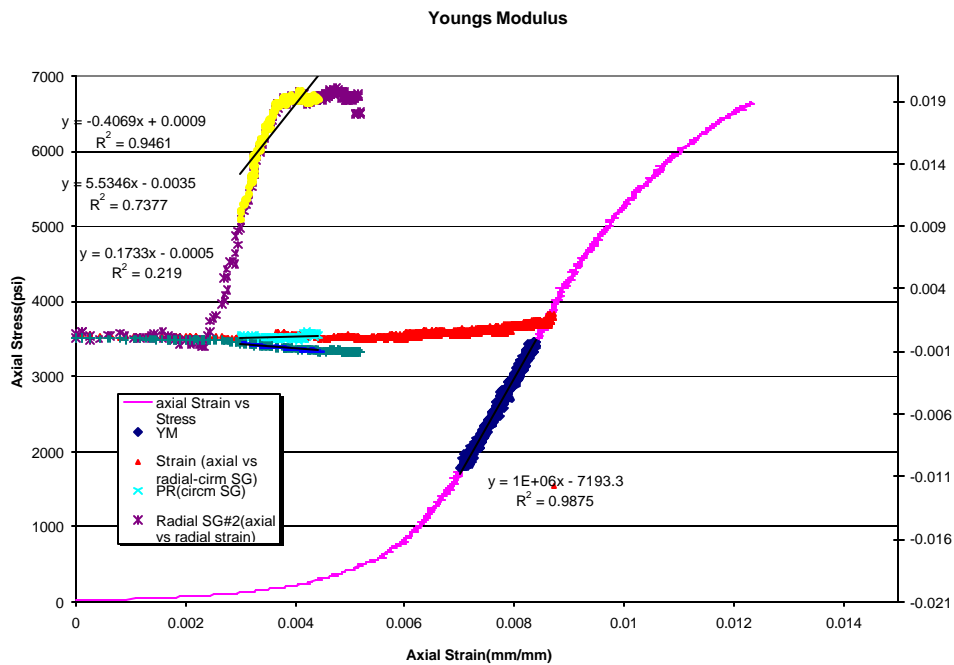




Figure B17—Young’s modulus measurements for Type 1 slurry at 500-psi confining stress and a 250-psi/min load rate.

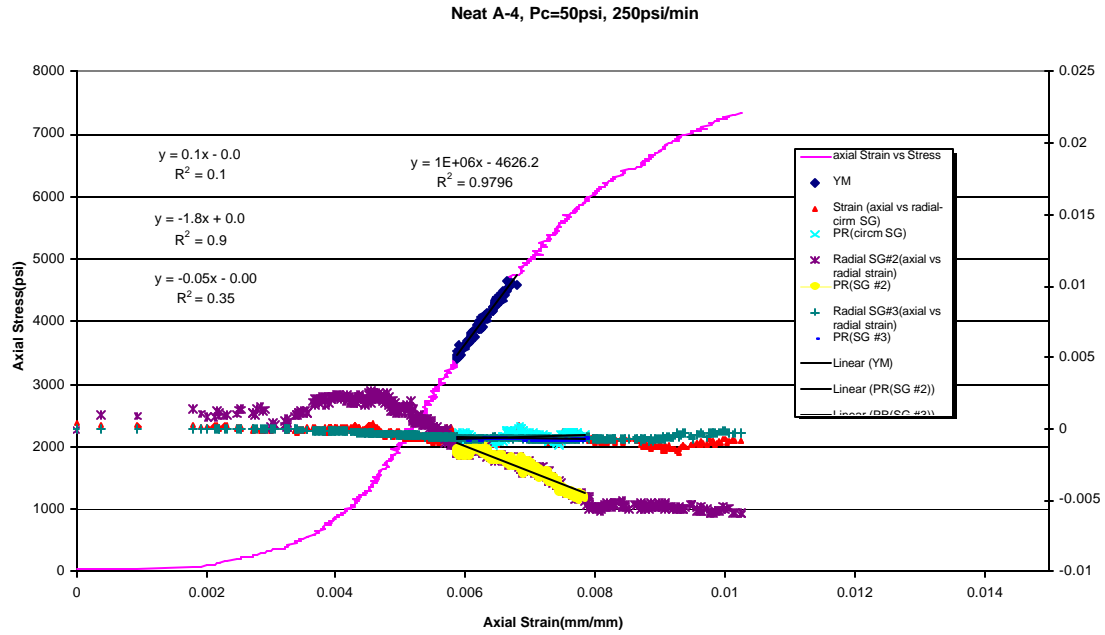




Figure B18—Young’s modulus measurements for Type 1 slurry at 500-psi confining stress and a 500-psi/min load rate.

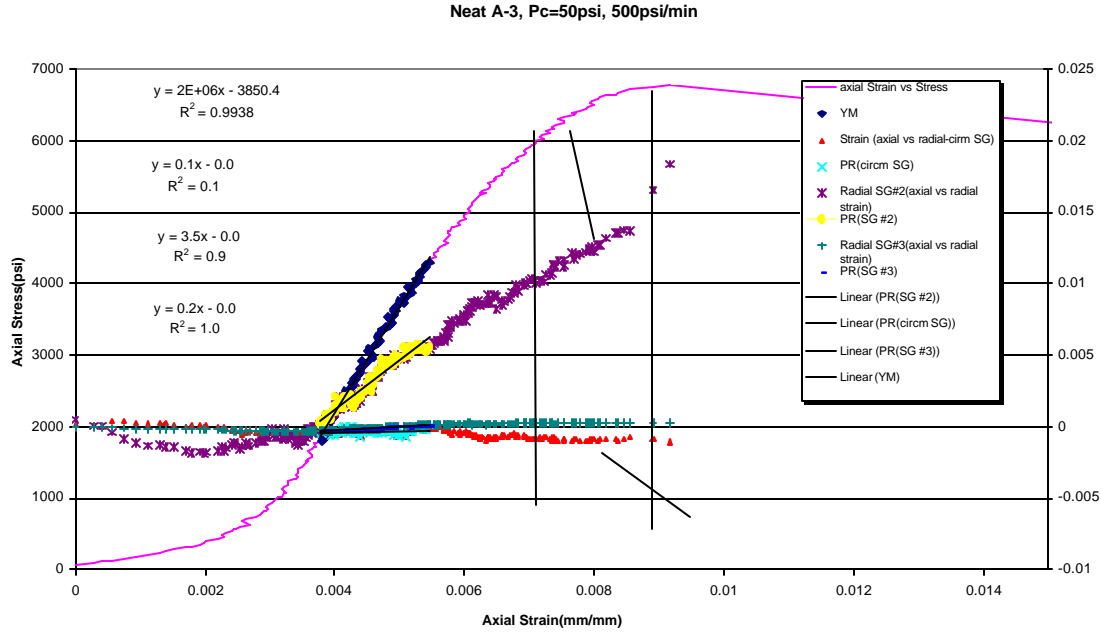


Figure B19—Hydrostatic cycling data for bead slurry showing anelastic strain.

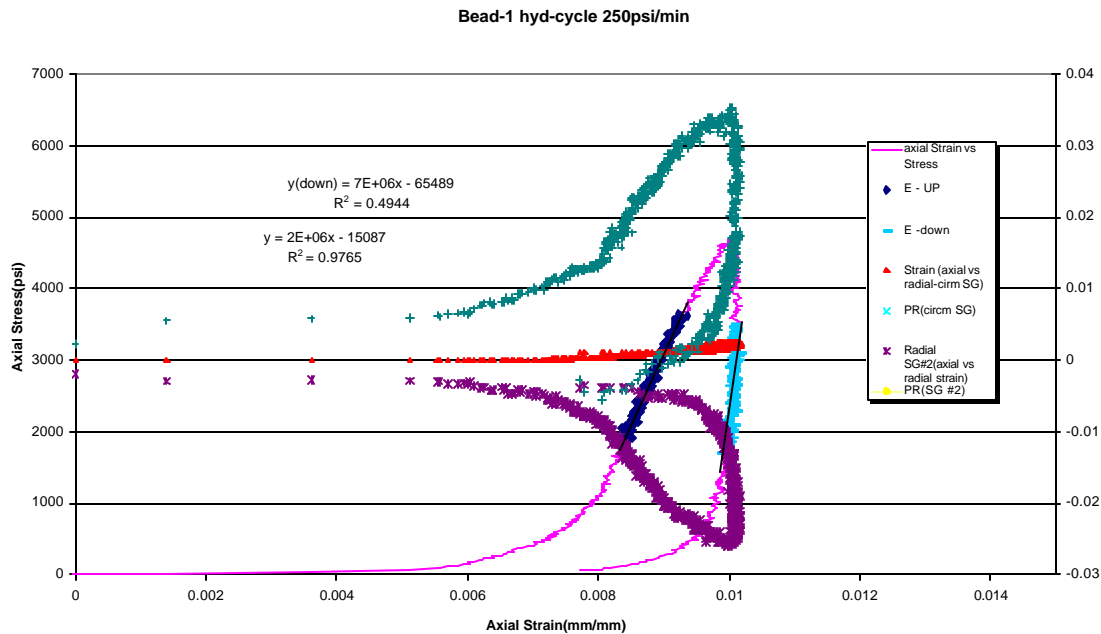




Figure B20— Hydrostatic cycling data for Class H slurry showing anelastic strain.

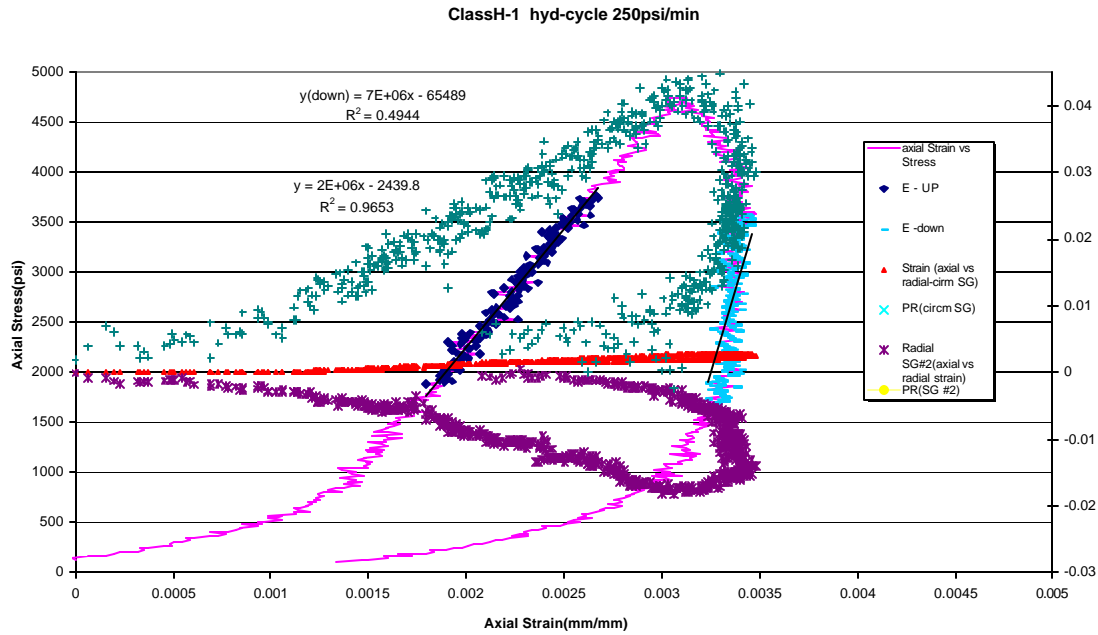


Figure B21— Hydrostatic cycling data for 12-lb/gal foam slurry showing anelastic strain.

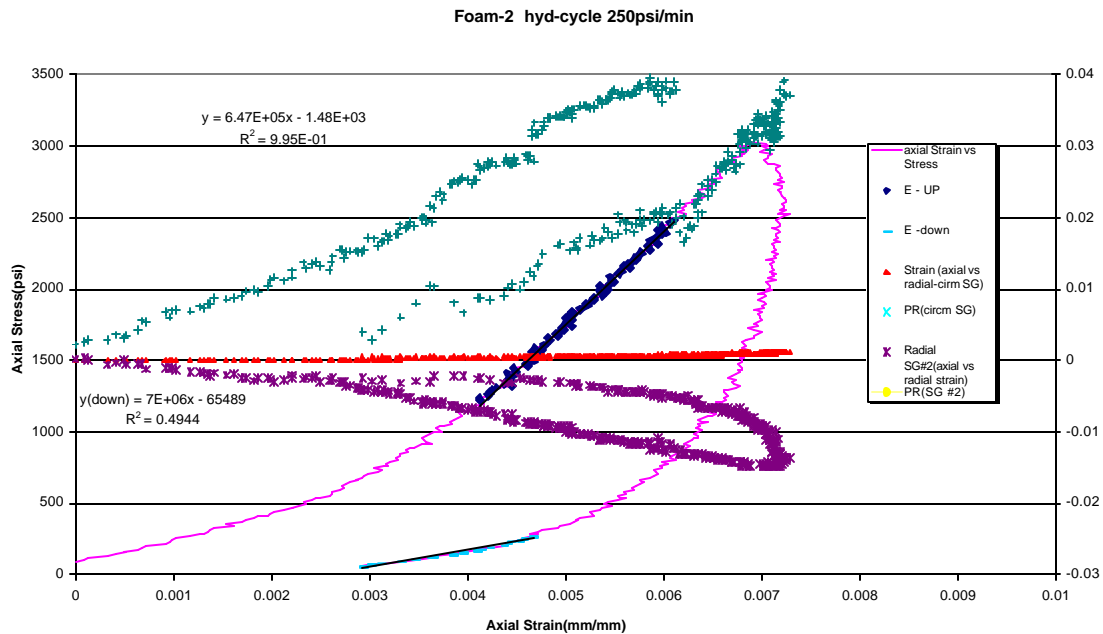




Figure B22— Hydrostatic cycling data for Type 1 slurry showing anelastic strain.

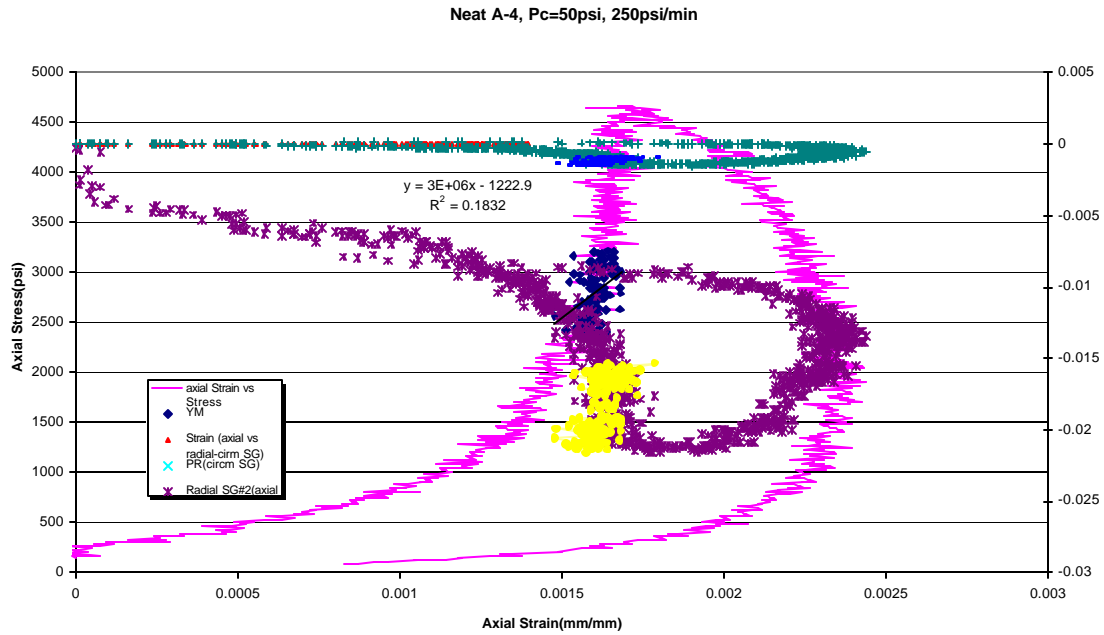


Figure B23— Hydrostatic cycling data for sodium metasilicate (SMS) slurry showing anelastic strain.

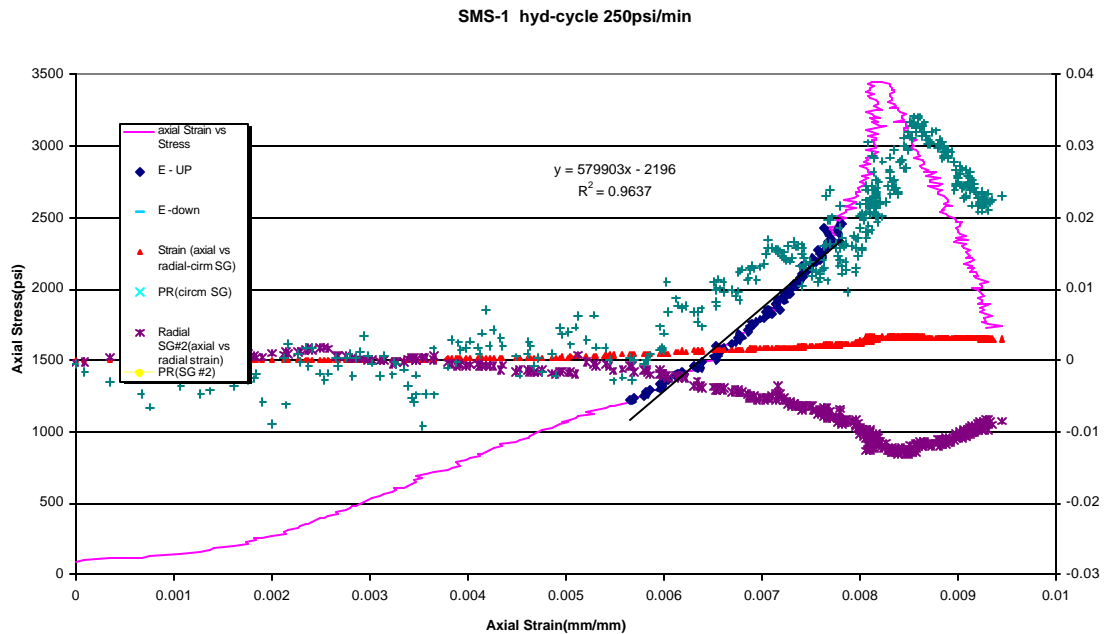




Figure B24— Anelastic strain failure load for neat Type 1 slurry at a load rate of 250 psi/min and confining pressure of 500 psi.

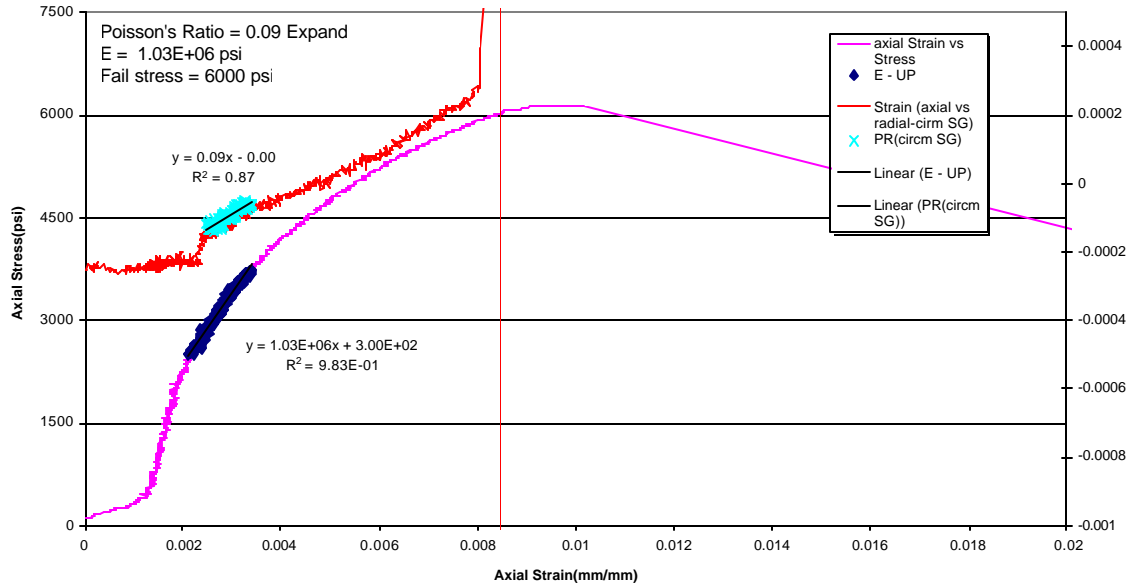


Figure B25— Anelastic strain failure load for foam slurry at a load rate of 250 psi/min and confining pressure of 500 psi.

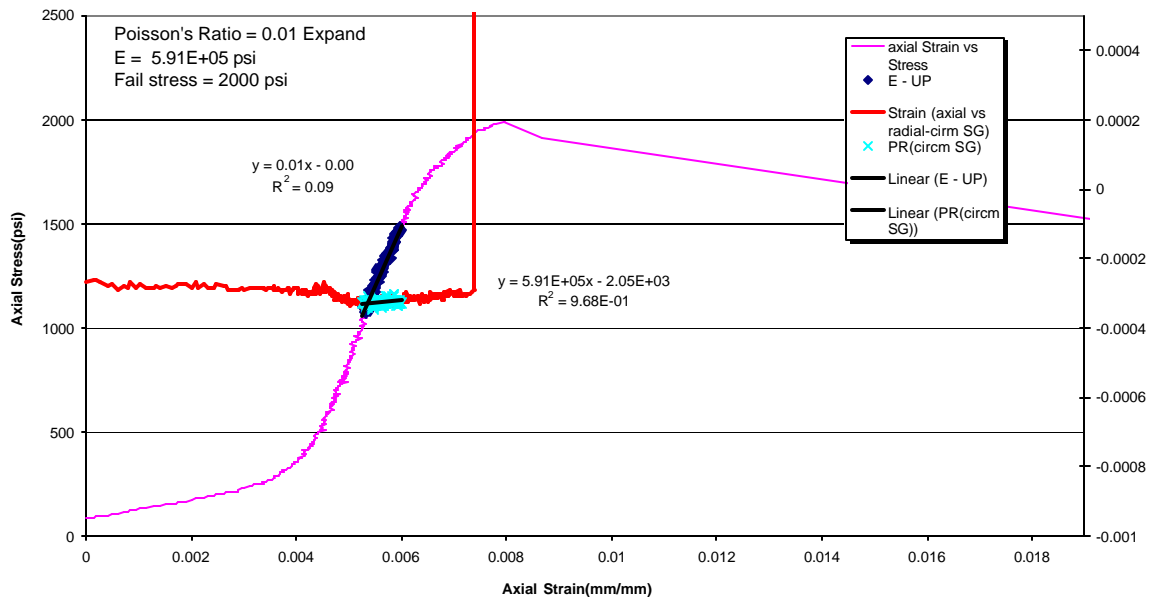




Figure B26— Anelastic strain failure load for bead slurry at a load rate of 250 psi/min and confining pressure of 500 psi.

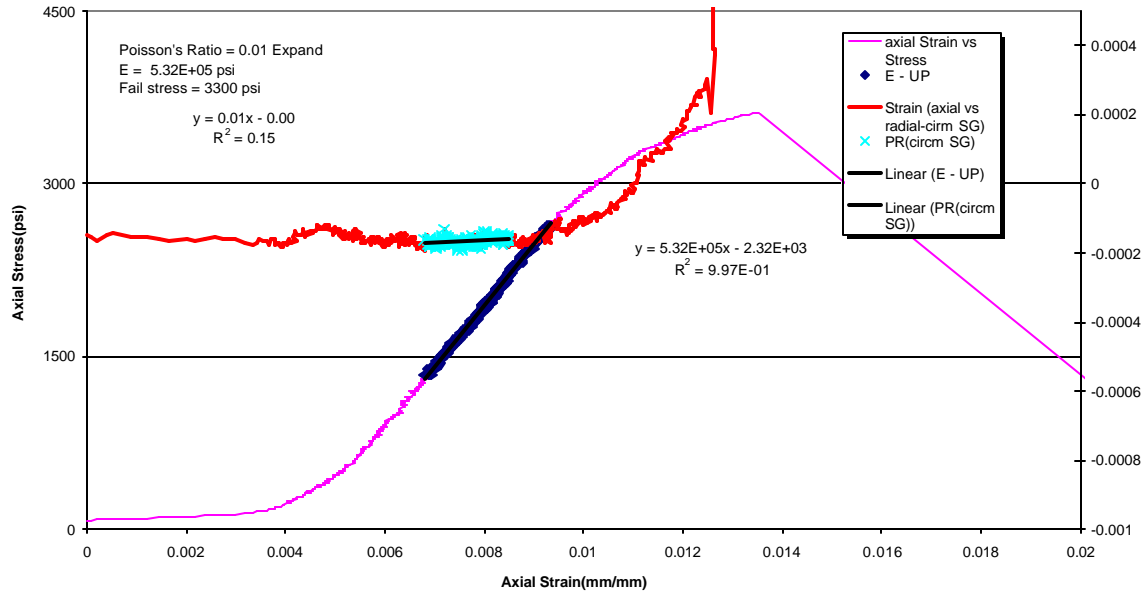


Figure B27—Anelastic strain failure load for latex slurry at a load rate of 250 psi/min and confining pressure of 500 psi.

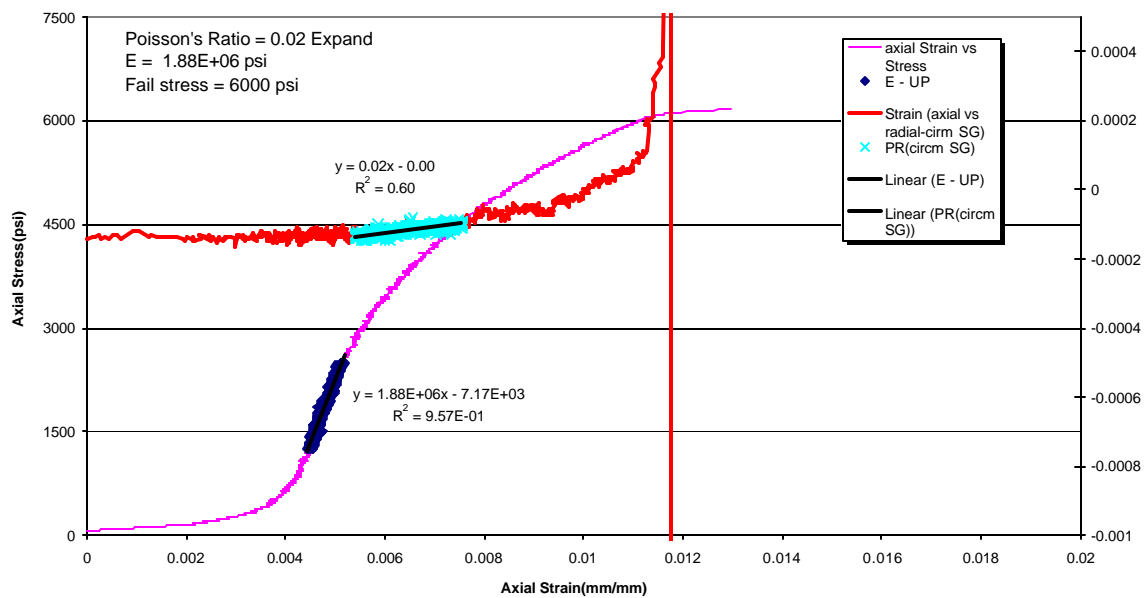




Figure B28—Anelastic strain, cycled to 25% of failure load, for Type 1 slurry at a load rate of 250 psi/min and confining pressure of 500 psi.

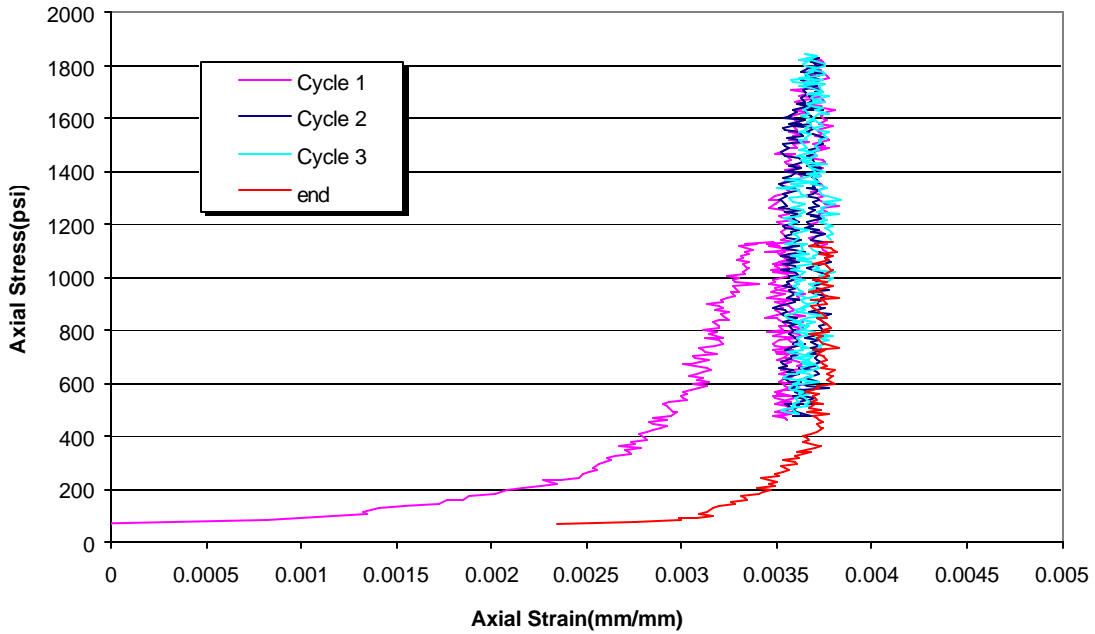


Figure B29—Anelastic strain, cycled to 25% of failure load, for foam slurry at a load rate of 250 psi/min and confining pressure of 500 psi.

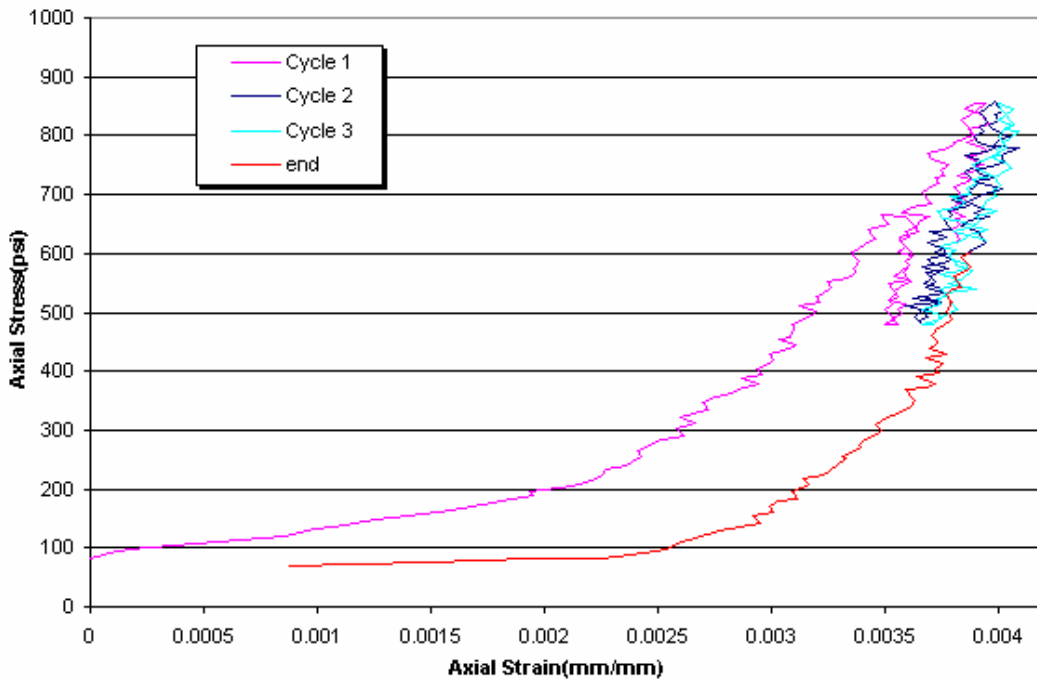




Figure B30—Anelastic strain, cycled to 25% of failure load, for bead slurry at a load rate of 250 psi/min and confining pressure of 500 psi.

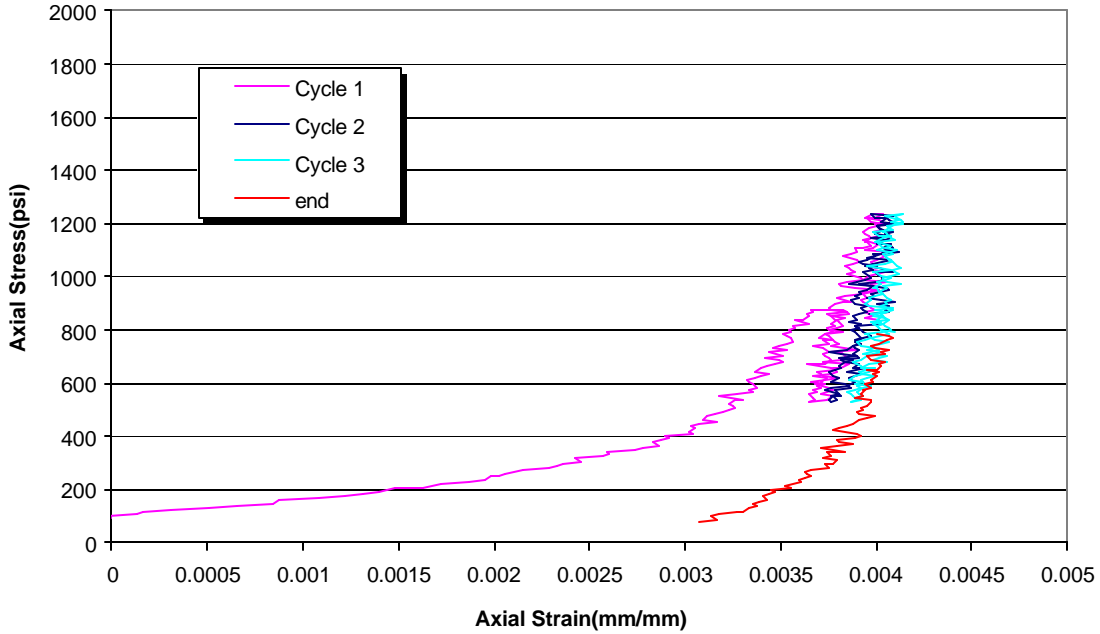


Figure B31—Anelastic strain, cycled to 25% of failure load, for latex slurry at a load rate of 250 psi/min and confining pressure of 500 psi.

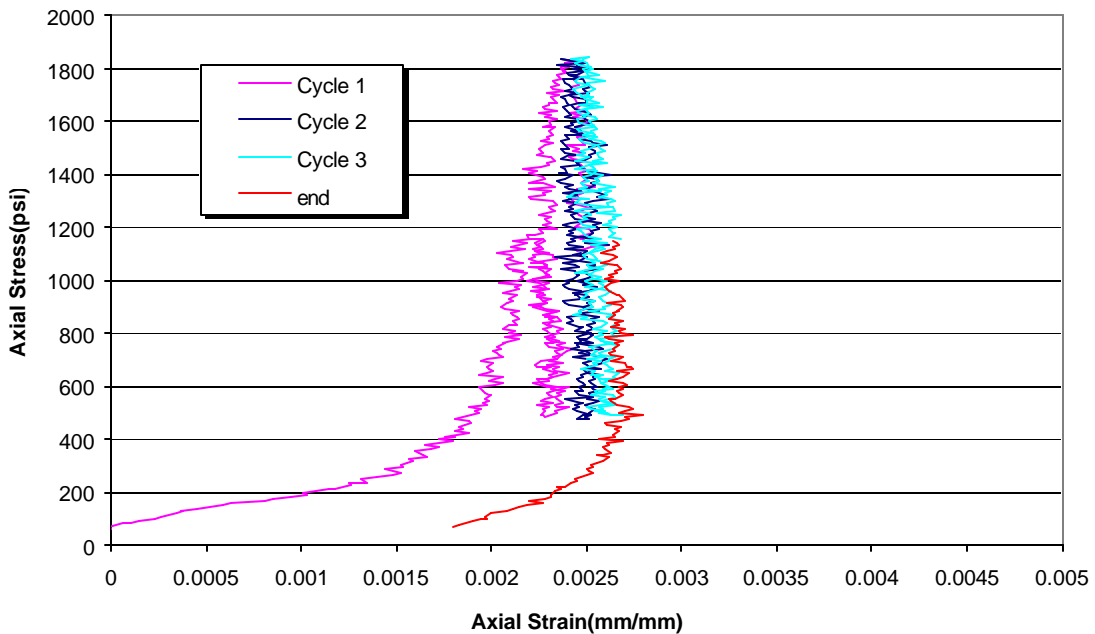




Figure B32—Anelastic strain, cycled to 50% of failure load, for Type 1 slurry at a load rate of 250 psi/min and confining pressure of 500 psi.

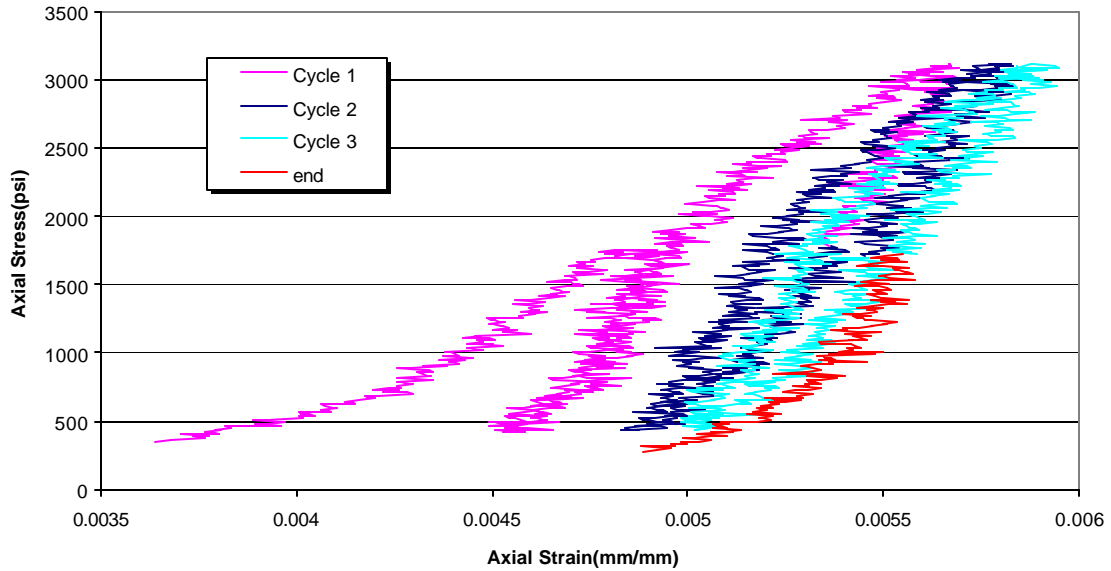


Figure B33—Anelastic strain, cycled to 50% of failure load, for latex slurry at a load rate of 250 psi/min and confining pressure of 500 psi.

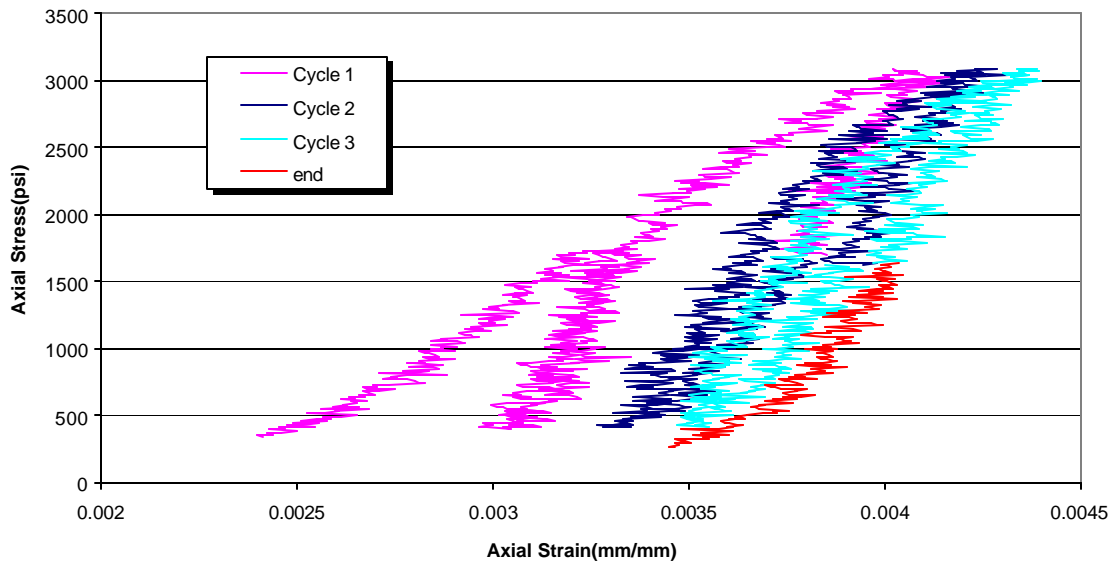




Figure B34—Anelastic strain, cycled to 50% of failure load, for bead slurry at a load rate of 250 psi/min and confining pressure of 500 psi.

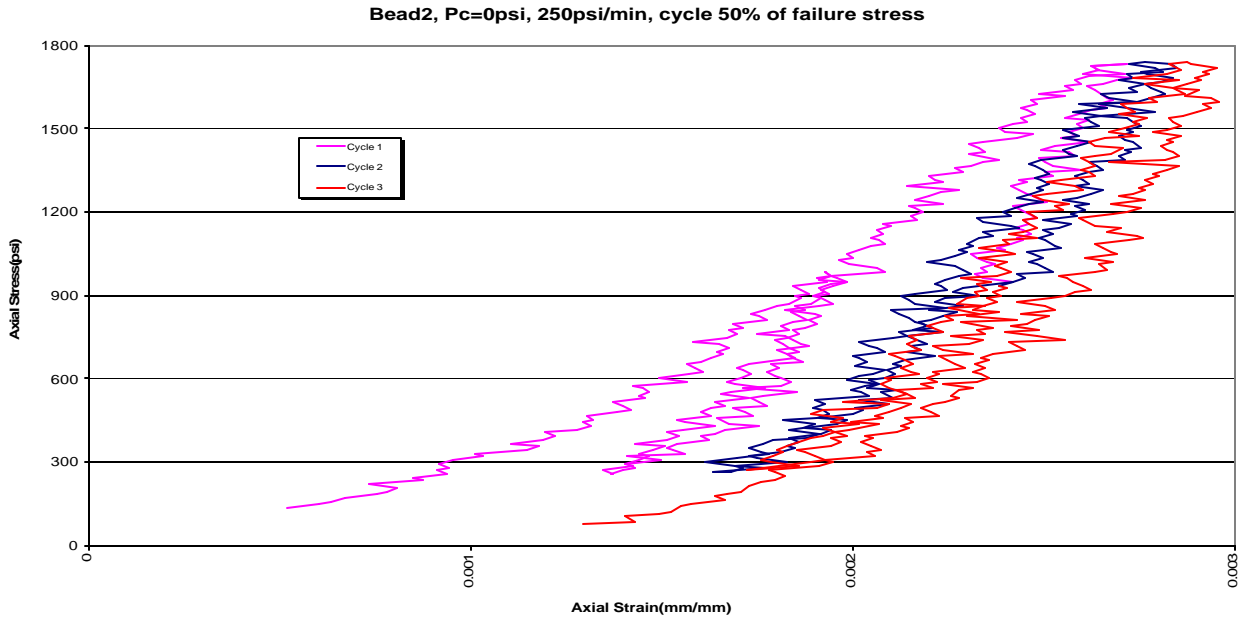


Figure B35—Anelastic strain, cycled to 50% of failure load, for foam slurry at a load rate of 250 psi/min and confining pressure of 500 psi.

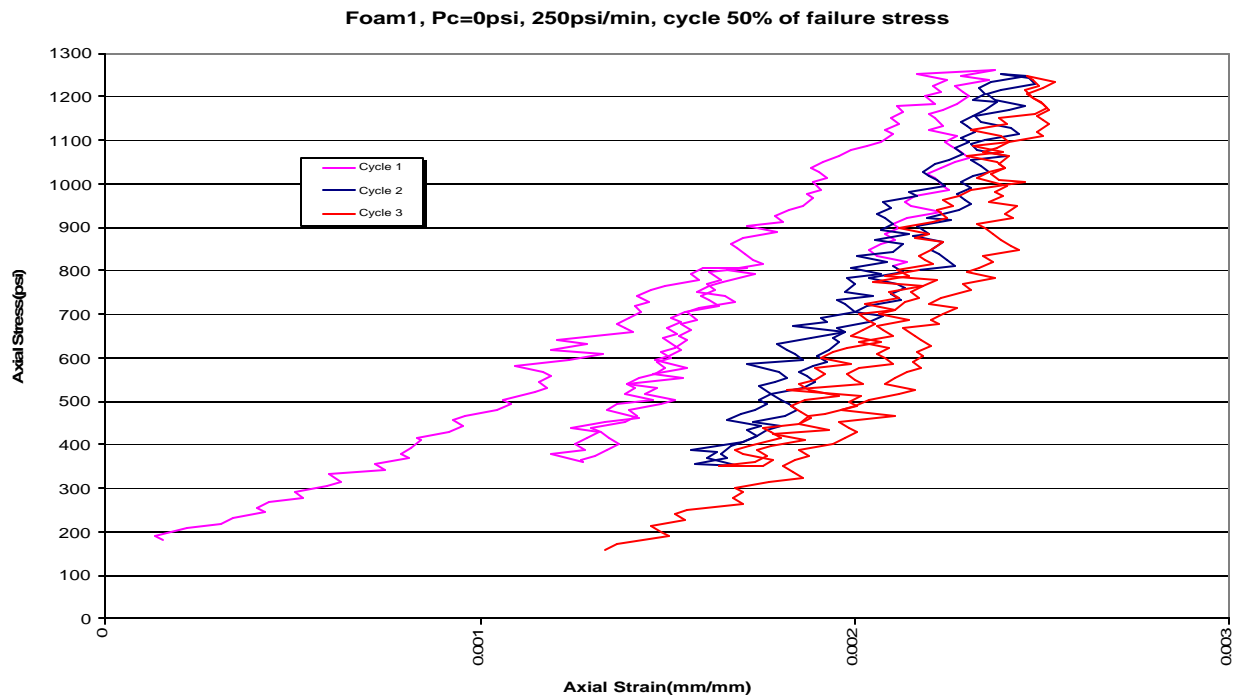




Table B1—Chronicle of 8ft Permeability Model Testing (mD)

Slurry #	Days Tested										
	1	7	14	23	37	44	51	60	63	65	66
1	0	0	0	0	0	0	0	0	0	0	0
2	0	0	0	0	0	0	0.107	0.12	0.116	0.05	0.05
3	33	71	72	70	71	71	*	*	*	*	*
4	26	57	60	42	30	30	*	*	*	*	*
5	0	0	0	0	0	0	0	0	0	0	0
6	0	0	0	0	0	0	0	0	0	0	0
7	0	0	0	0	0	0	0	0	0	0	0
8	0	0	0	0	0	0	0	0	0	0	0

Slurry #	Days Tested										
	67	71	73	78	79	80	84	85	86	87	88
1	0	0	0	0	0	0	0	0	0	0	0
2	0.05	0	0.05	0.03	0.03	0.02	0	0	0	0	0
3	*	*	*	*	*	*	*	*	*	*	*
4	*	*	*	*	*	*	*	*	*	*	*
5	0	0	0	0.03	0.03	0.03	0.02	0.02	0.02	0.02	0.02
6	0	0	0	0	0	0	0.02	0.02	0.02	0.02	0.02
7	0	0	0	0	0	0	0.02	0.02	0.02	0.02	0.02
8	0	0	0	0	0	0	0	0	0	0	0

Slurry #	Days Tested							
	99	100	101	105	106	107	108	113
1	0	0	0	0	0	0.09	0.08	0.11
2	0	0	0	0.23	0.217	1.3	1.24	1.71
3	*	*	*	*	*	*	*	*
4	*	*	*	*	*	*	*	*
5	0	0	0	0	0	0	0	0
6	0.02	0.02	0.02	0	0	0.01	0	0
7	0.6	0.8	0.8	0.74	0.87	2.75	*	*
8	3.1	3.51	3.51	3.51	*	*	*	*

Day 1 Thru 44 - 100 PSI	Day 51 - 200 PSI	Day 60 Thru 73 - 300 PSI	Day 78 Thru 88 - 400 PSI	
Day 88 Thru 113 - 500 PSI				



Table B2—Chronicle of second set of 8ft Permeability Model Testing (mD)
Days Tested

Slurry #	1	2	3	4	7	8	9	10	11	14	15
1	2.41	3.05	3.81	4.7	5.08	5.59	5.59	5.71	5.71	5.71	5.84
2	0	0	1.23	1.23	1.23	1.15	1.22	1.21	1.22	1.22	1.27
3	0	0	0	0	0	0	0	0	0	0	0
4	0	0	2.29	1.4	1.4	1.52	1.4	1.4	1.4	1.4	1.27
5	0	0	0	0	0	0	0	0	0	0	0
6	6.73	4.82	8	8.63	9.65	9.52	9.52	9.65	9.65	8.89	9.01
7	0.89	0.76	1.78	2.03	2.41	2.29	2.67	2.67	2.67	2.67	2.67
8	0	0	0	0	0	0	0	0	0	0	0
9	0	0	0	0	0	0	0	0	0	0	0
10	0	0	0	0	0	0	0	0	0	0	0

Days Tested

Slurry #	16	17	18	21	22	23	24	25	28	29	30
1	5.84	5.84	5.59	5.46	5.46	#	#	#	#	#	#
2	1.27	1.28	1.22	1.13	1.18	1.18	1.24	1.28	1.28	1.27	1.27
3	0	0	0	0	0	0	0	0	0	0	0
4	1.4	1.27	1.27	1.4	1.4	1.27	1.02	1.14	1.4	1.27	1.4
5	0	0	0	0	0	0	0	0	0	0	0
6	8.89	8.89	8.89	8.89	8.89	9.01	10.16	10.16	9.9	9.52	9.65
7	2.67	2.54	2.54	2.54	2.54	2.54	2.92	2.92	2.92	2.92	2.79
8	0	0	0	0	0	0	0	0.38	0.38	0.38	0.38
9	0	0	0	0	0	0	0	0	0	0	0
10	0	0	0	0	0	0	0	0	0	0	0

Days Tested

Slurry #	31	32	37	39	43	45	50	56	60	66	71
1	#	#	#	#	#	#	#	#	#	#	#
2	1.26	1.11	1.29	1.27	1.24	1.26	1.27	1.26	1.27	1.27	1.27
3	0	0	0	0	0	0	0	0	0	0	0
4	1.4	1.4	1.4	1.27	1.27	1.27	1.27	1.4	1.4	1.4	1.4
5	0	0	0	0	0	0	0	0	0	0	0
6	9.9	9.9	9.9	10.79	12.44	13.97	15.62	17.52	18.28	25.77	27.04
7	2.92	2.92	2.79	3.05	3.05	2.29	2.92	2.92	2.92	3.17	3.17
8	0.63	0.63	0.51	0.51	0.51	0.51	0.51	0.51	0.51	0.51	0.51
9	0	0	0	0	0	0	0	0	0	0	0
10	0	0	0	0	0	0	0	0	0	0	0

All tested at 100psi
denotes no longer testing



Compositions for Table B2

Slurry # 1: Type 1 + 20% Gel @ 12 ppg
Slurry # 2: Type 1 + 18% Gel @ 12.5 ppg
Slurry # 3: Type 1 + 16% Gel @ 13 ppg
Slurry # 4: Type 1 + 3% SMS @ 12.5 ppg
Slurry # 5: Type 1 + 2.5% SMS @13 ppg
Slurry # 6: 65:35 Type1:Poz + 16% Gel@12ppg
Slurry # 7: 65:35 Type1:Poz+ 12% Gel@12.5ppg
Slurry # 8: 65:35 Type1:Poz + 10% Gel@13ppg
Slurry # 9: TXI LW + 2% SMS @ 12 ppg
Slurry#10: TXI LW neat @ 13 ppg

Table B3—Chronicle of third set of 8ft Permeability Model Testing (mD)

Slurry #	Days Tested										
	1	2	3	5	8	10	12	15	18	20	23
1	7.36	6.86	7.11	6.86	6.73	6.73	3.55	5.71	7.11	6.6	4.57
2	8.63	6.35	10	5.84	6.09	7.49	3.94	5.71	7.24	6.6	6.09
3	2.29	3.05	3.17	3.17	3.3	3.3	0.89	2.92	3.55	3.81	3.43
4	0	0	0	0	0	0	0	0	0	1.27	1.27
5	0	0	0	0	0	0	0	0	0	0	0
6	0	0	0	0	0	0	0	0	0	0.38	0.38
7	5.97	5.97	6.86	7.24	6.73	6.98	4.7	5.84	7.11	6.98	6.22
8	32.1	34.2	36.2	35	35.6	35.8	31.2	x	x	x	x
9	50.5	53.3	57.4	56.8	56.8	57	50.3	x	x	x	x
10	35.9	36.2	37.8	37.5	38.1	38.1	35	x	x	x	x

Slurry #	Days Tested										
	26	28	30	33	39	44	54	60	69	73	82
1	6.73	5.71	6.60	6.60	6.86	6.86	6.6	3.68	3.55	3.3	2.41
2	6.09	6.35	6.09	6.60	6.86	6.6	6.86	6.98	7.62	7.11	7.62
3	6.86	5.33	6.35	8.63	12.70	8.00	9.27	15.87	18.79	19.81	x
4	1.27	1.52	2.03	4.57	16.00	13.94	14.47	4.57	6.6	8.76	21.58
5	0	0	0	0	0	0	0	0	0	0	0
6	0.63	0.51	0.51	0.51	0.51	0.51	0.51	1.02	0.63	0.63	0.51
7	6.47	6.73	6.60	7.11	7.36	6.22	4.95	7.74	8.38	8.63	10.28
8	x	x	x	x	x	x	x	x	x	x	x
9	x	x	x	x	x	x	x	x	x	x	x
10	x	x	x	x	x	x	x	x	x	x	x



Slurry #	Days Tested									
	92	113								
1	3.3	3.3								
2	9.14	12.32								
3	X	X								
4	X	X								
5	0	0								
6	0.63	0.51								
7	19.14	X								
8	X	X								
9	X	X								
10	X	X								

Compositions for Table B3

Slurry # 1: Type 1 + 2% SMS @ 13.4 ppg
Slurry # 2: Type 1 + 2% SMS @ 13 ppg
Slurry # 3: TXI LW + 3% SMS @ 11 ppg
Slurry # 4: TXI LW + 3% SMS @ 11.5 ppg
Slurry # 5: 65:35 Type1:Poz + 6% Gel @13.5 ppg
Slurry # 6: 50:50 Type1:Poz + 6% Gel @ 13.4 ppg
Slurry # 7: 50:50 Type1:Poz + 8% Gel @ 12.8 ppg
Slurry # 8: 50:50 Type1:Poz + 10% Gel @ 12.4 ppg
Slurry # 9: TXI "H" + 12% Gel @ 12 ppg
Slurry #10: TXI "H" + 8% Gel @ 12.5 ppg

¹ API Recommended Practice 10B: “Recommended Practice for Testing Well Cements,” 22nd Edition, American Petroleum Institute, Washington, D.C., December 1997.

² ASTM C469, Standard Test Method for Static Modulus of Elasticity (Young’s Modulus) and Poisson’s Ratio of Concrete in Compression.

³ “Standard Test Method for Splitting Tensile Strength of Cylindrical Concrete Specimens,” ASTM C496-96, West Conshohocken, PA, 1996.